Studies on Synthesis, Characterization and Catalytic Activity of Nano-Crystalline Sulfated Zirconia

A Thesis

Submitted to Bhavnagar University,

for the degree of

DOCTOR OF PHILOSOPHY

in

CHEMISTRY

by

MANISH KUMAR MISHRA

Under the Guidance of

Dr. R. V. Jasra

&

Dr. (Mrs.) Beena Tyagi

Silicates and Catalysis Discipline,

Central Salt & Marine Chemicals Research Institute
Bhavnagar-364 002, Gujarat.

April 2007

CANDIDATE'S STATEMENT

I hereby declare that the work incorporated in the present thesis is original and has not been submitted to any University/Institution for the award of a Diploma or a Degree. I further declare that the results presented in the thesis and the considerations made therein, contribute in general to the advancement of knowledge in Chemistry and in particular to entitled **"Studies on Synthesis, Characterization and Catalytic Activity of Nano-Crystalline Sulfated Zirconia"**.

Signature of the candidate

Manish Kumar Mishra

केन्द्रीय नमक व समुद्री रसायन अनुसंधान संस्थान
गिजुभाई बधेका मार्ग, भावनगर- ३६४ ००२

CENTRAL SALT & MARINE CHEMICALS RESEARCH INSTITUTE
(Council of Scientific &Industrial Research)
CSMCRI **Gijubhai Badheka Marg, Bhavnagar 364 002, Gujarat, India**

Dr. R. V. Jasra
Dy. Director & Head,
Silicates & Catalysis Discipline

CERTIFICATE BY THE GUIDE

This is to certify that the contents of this thesis entitled **"Studies on Synthesis, Characterization and Catalytic activity of Nano-Crystalline Sulfated Zirconia"** is the original research work of ***Manish Kumar Mishra*** carried out under our supervision. We further certify that the work has not been submitted either partly or fully to any other University or Institution for the award of any degree.

R. V. Jasra
(Ph. D Guide)

Beena Tyagi
(Co-Guide)

☎ (O) 0278-2567760 / 2568923 : Fax: 0278-2567562 / 2566970
E-mail: salt@csmcri.org Website: www.csmcri.org

dedicated to

MAA VAISHNODEVI

&

my parents

ACKNOWLEDGEMENT

This doctoral research could not have been conducted were it not for several key people who offered advice, inspiration and encouragement.

I would like to take this opportunity to express my gratitude to my guide, Dr. R. V. Jasra and co-guide Dr. (Mrs.) Beena Tyagi, for their guidance, inspiration and encouragement throughout this work. Their profound knowledge, enormous enthusiasm, and keen insights in material chemistry and catalysis have, and will continue to be, a great source of inspiration for me.

Special thanks go to my co-guide Dr. (Mrs.) Beena Tyagi, not only for sharing with me her vast material chemistry knowledge and encouraging me to pursue my Ph.D., but also for being a constant enthusiastic resource.

I profusely thank Dr. P. K. Ghosh, Director, CSMCRI, for allowing me to carryout research work in the institute.

Many thanks go to all my wonderful seniors and colleagues in our research institute for their assistance and friendship. I deeply appreciate the help I obtained from my seniors Priti, Yogi, Chintan and Jince at the initial, and sometimes difficult, stage when I began this work. I truly enjoyed the valuable discussions and friendship with Vivek, Mukesh, Srinivasan and Surender.

I would also like to acknowledge the important technical assistance of Dr. (Mrs.) P. Bhatt, for her XRD analysis, Mr. Vinod Agrawal for IR analysis, Mr. Vinod Boricha for his NMR analysis, Sunil, Prasanth and Ranjith for surface characterization.

I am grateful to my friends, Shobhit Singh, Jagan, KK, and colleagues, Kalpesh and Jinka, and the staffs of Silicates and Catalysis, P. G. M. Pillai, B. B. Parmar and J. M. Parmar for all the support they provided in due course of my research.

Finally, special gratitude goes to my family. My parents instilled in me the values of perseverance and responsibility, which were essential when working under pressure. The highest gratitude goes to my grand mother, whose constant enthusiasm, hopeful disposition, timely encouragement and deep faith in God has motivated me to persevere and properly prioritize my life. To my grand father, who instilled in me a strong work ethic and the value of common sense. Word "thank you" only scratch the surface of my gratitude for you both. I am heartily thankful to my wife for her invaluable moral support during my research.

Manish Kumar Mishra

Contents

Page No.

Introduction

1.1 Acid catalysis

Most of organic transformations are based on acid-base catalysis finding a wide range of applications in chemical industries. Acid catalysis is an important area in organic synthesis and is of fundamental industrial importance. It has a vital role in petrochemical industries, where it is used to upgrade oil by different acid catalyzed organic reactions such as isomerization, cracking and alkylation of hydrocarbons **[1]**. Besides it, acid catalysis has a wide range application in large-scale polymerization processes **[2]**, hydration reaction process for production of ethanol **[3, 4]** and dehydration reaction process for production of ethylene **[5]** at industrial scale. The acid catalyzed organic transformations for the synthesis of fine chemicals, pharmaceutical intermediates, flavors and fragrances, dyes and other important chemicals are also largely carried out in industries **[6- 8]**.

The acid catalyzed reactions are largely carried out by using homogeneous liquid acids like HF, H_2SO_4, $AlCl_3$ and $FeCl_3$ etc. HSO_3F/SbF_5 is known as liquid super acid and is used commercially in industrial processes and organic synthesis **[9]**. These homogeneous catalysts, however, have some disadvantages such as they are required in more than stoichiometric amount to attain maximum conversion. For example, for acylation of aromatics using $AlCl_3$ catalyst, the catalyst is used in more than stoichiometric ratio (1.5- 2.0 mol of $AlCl_3$ for 1 mol of aromatic substrate) to achieve maximum conversion of the aromatic compounds. They are corrosive to reaction system and a very careful handling is required. Use of homogeneous acid catalysts, in some reactions, give some undesired by-products, which need an extra separation step in the process. As well as these catalysts are not reusable and recoverable from reaction mixture after reaction, as either they form complex molecule with product or they are highly soluble in reaction mixture resulting into the hazardous waste influent. This also leads to the formation of hazardous inorganic acids as by-products. The disadvantages of homogeneous catalysts, environmental restrictions and requirement of non-polluting, atom-efficient and economic catalytic process inspired the need to find the alternative of the liquid acids.

1.2 Solid acids

The work on solid acids was started since 1970s **[10a]** to replace the use of conventional acid catalysts. Solid acids were found to be alternative to the homogeneous acids as they are non-corrosive, required in small catalytic amount, easy to separate, reuse and ecofriendly. Solid acid catalysts such as transition metal oxides, zeolites, ion-exchange resins and acid treated clays were reported to have potential for solving the drawbacks of liquid acids **[11]**. In 1979, Hino et al. **[10a]** reported that the transition metal oxides treated with sulfuric acid showed enhanced acidity than their pure oxides. Their acidity was found higher than that of anhydrous or concentrated sulfuric acid and these were called solid super acids. A solid super acid is defined as a solid material, which shows an acid strength higher than the acid strength of 100% sulfuric acid ($-H_0$ = 11.9) **[12]**. Superacids are advantageous as they can perform at lower temperatures and form reaction intermediates unattainable with conventional liquid acid catalysts. These are able to catalyze the reactions characteristics of very strong acid catalysts. The different liquid and solid super acids with acid strength ($-H_0$) are given in figure 1.

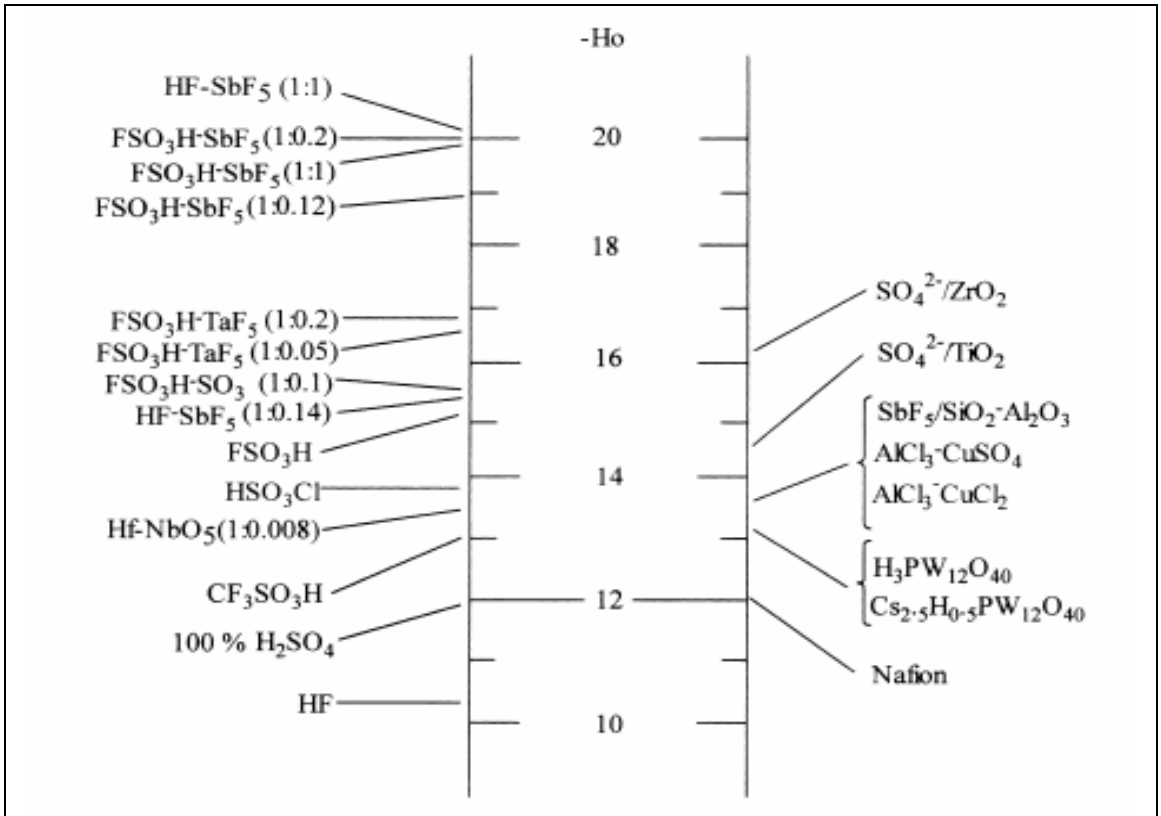

Figure 1. Acid strengths of liquid and solid super acids.

According to a review on industrial processes **[10b]**, 127 processes were found catalysis based and 115 processes are solid acid catalyzed. Use of solid acids makes a reaction more regio- and stereoselective. The selectivity can be controlled by varying the acidic strength, type of acidity (Bronsted or Lewis acid sites) and texture of solid acids, which can be tuned by varying synthetic methods and parameters during the synthesis. Recently **[13]**, various types of solid acids have been developed and categorized. The first group of solid acids consists of metal oxides and mixed oxides containing small amount of anions. The second group is metal oxides, mixed oxides, graphite, metal salts, etc. treated with antimony fluoride or aluminum chloride. The third group comprises perfluorinated polymer sulfuric acid (Nafion). The fourth group is zeolite and the fifth group is heteropolyacids. The sixth group is simple mixed oxides. The different groups of solid acids are summarized in Table 1. Arata et al. **[13, 14]** studied the acidic properties of various sulfated metal oxides as solid super acids belonging to first group of solid acids and found the order of acidity (with their $-H_0$) as follows:

SO_4/SnO_2 ($-H_0 = 18.0$) > SO_4/ZrO_2 ($-H_0 = 16.1$) > SO_4/HfO_2 ($-H_0 = 16.0$) > SO_4/TiO_2 ($-H_0 = 14.6$) > SO_4/Al_2O_3 ($-H_0 = 14.6$) > SO_4/Fe_2O_3 ($-H_0 = 13.0$) > SO_4/SiO_2 ($-H_0 = 12.2$).

Table 1. Groups of solid acids.

S. No.	Group	Solid acids
1	I	Sulfate promoted metal oxides, e.g., SO_4^{--}-ZrO_2, SO_4^{--}-TiO_2, etc.
2	II	SbF_5 or $AlCl_3$, supported on high surface area solids such as metal oxides, mixed oxides, graphite, metal salts, etc.
3	III	Polymeric superacid, Nafion H.
4	IV	Zeolites.
5	V	Heteropoly acids.
6	VI	Mixed metal oxides.

1.3 Sulfated-Zirconia

The zirconium oxide or zirconia is a useful material having wide applications as catalyst **[15]**, catalyst support **[16- 18]**, refractory material **[19]**, ceramic material **[20]**, ceramic biomaterial **[21]**, solid electrolyte for fuel cells **[22]**, sensor materials **[23]** and in electronic devices **[24]**. The zirconia mixed with other oxides **[25- 29]** or promoted with metal atoms **[30- 32]** has been reported as important catalytic materials. The zirconia itself possesses less acidity, but the modification with anionic species such as sulfate **[13, 14]**, tungstate **[33]**, phosphate **[34]**, borate **[35]**, etc. generates considerably enhanced surface acidity. The zirconia modified with sulfate species is called sulfated-zirconia and is a well-known solid super acid ($-H_0 = 16.1$). In 1962, Holm and Baily **[36]** found superior catalytic performances of a Platinum containing sulfated-zirconia gel compared to commercial Pt/ chloride alumina catalyst for skeletal isomerization of *n*-alkanes. The detail study about this material did not appear until 20 years. In 1979, Arata and coworkers **[10a, 37]** reported the presence of extremely strong acidity in sulfate treated zirconia and found a potential catalytic activity for the isomerization of *n*-butane at room temperature. The higher catalytic activity of sulfated-zirconia for skeletal isomerization of *n*-butane at low temperature shows the presence of superacidity, since the reaction does not take place in presence of 100 % sulfuric acid at ambient temperature. Later, sulfated-zirconia has been studied widely for alkylation **[38- 42]**, isomerization **[43- 54]** and cracking reactions of alkanes **[55]** to upgrade oil in the petroleum industry. Besides petroleum industries, sulfated-zirconia has been widely used to catalyze various reactions like alkylation **[56- 66]** and acylation of aromatics **[67- 74]**, esterification **[75- 81]**, etherification **[82, 83]**, isomerization of terpines and epoxides **[84- 88]**, nitration **[89]**, oligomerization [**90, 91**], etc. and also being tried to use in other industrially important acid catalyzed organic reactions to replace the conventional homogeneous acid catalysts to make green and economic process. Therefore, it has a promising future in the chemical industries. Reviews on the wide range applications of sulfated-zirconia for different organic reactions are available in literature **[92, 93]**.

Sulfated-zirconia is very important and potential solid acid catalyst as both types of acid sites, Bronsted as well as the Lewis sites, are present (Figure 2) on its surface **[37, 38, 94- 96]**. The sulfate species are bonded with zirconium atom as bidentate

chelating ligand **[97, 98]** and in presence of water molecule; the sulfate group behaves like ionic sulfate and generates Bronsted acid sites on the surface. The desorption of water molecule converts the ionic sulfate to covalently bonded sulfate group, which generates Lewis acid sites on zirconium atom by reducing the electronic density at zirconium atom. The required site can be predominantly populated by changing the reaction conditions, so it is capable to conduct both Bronsted and Lewis acid catalyzed reactions.

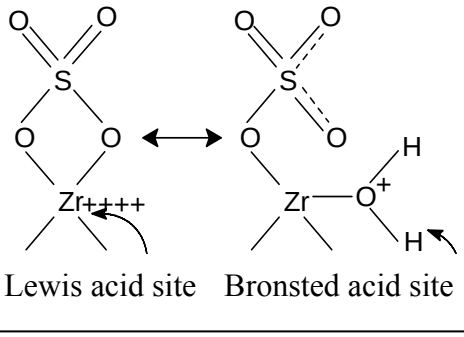

Figure 2. The schematic presentation of Bronsted and Lewis sites on the surface of the sulfated-zirconia.

1.4 Significance of nano-crystalline material

The synthesis of nano-crystalline materials is promising in catalysis, as nano-crystalline materials have improved catalytic activity because of large surface-to-volume ratio and changes in geometrical and electronic properties of the material. Nano-crystalline materials possess different properties than polycrystalline materials having large crystallite size, which are associated with size-dependent effects or high surface reactivity. Nano-crystalline materials have large number of surface atoms and also more corners and edges, which provides increased number of active sites available for a catalytic reaction resulting to increased catalytic activity. The higher number of surface atoms also helps in stabilization of metastable crystalline phase **[99]**. Nano-crystalline material facilitates the approach of the molecular orbitals of catalytic species and the molecular orbitals of reactant molecule lowering the activation energy of the catalytic reaction. The effect of nano-crystalline catalytic materials on the catalytic activity and selectivity has been observed. The nano-crystallites significantly increase the turn over numbers (TON), which is attributed to rate acceleration due to (1) the increase in coordinatively unsaturated edge sites, (2) the more favorable energy relationship between the molecular orbitals of the catalytic species and the reactant molecule to be activated, (3) a higher concentration of anion vacancies and defect sites on the crystallite surface,

(4) the higher electrical conductivity and ion mobility of nano-crystallite surface, (5) a higher degree of crystallographic strain, (6) alteration of the concentration of the crystallographic plane in the nano-crystallites **[100]**. Besides, the enhanced catalytic properties, nano-crystalline materials exhibit increased strength/hardness, improved toughness, reduced elastic modulus and ductility, enhanced diffusivity, higher specific heat, enhanced thermal expansion coefficient (CTE), and superior soft magnetic properties in comparison with conventional polycrystalline materials **[101- 104]**. The synthesis of nanocrystalline materials by different methods are reported in literature such as precipitation method, sol-gel method, gas phase synthesis, thermolysis, high energy ball milling, hydrothermal precipitation, etc **[105]**, among which, the sol-gel method is well known to synthesize nano-crystalline metal oxides. Because of the unique and enhanced catalytic properties of a nano-crystalline material, the synthesis of nano-crystalline sulfated-zirconia is promising in the field of catalysis.

1.5 Synthesis of nano-crystalline sulfated-zirconia

Though, sulfated-zirconia has been reported to be a solid super acid, its catalytic activity is strongly dependent on the synthetic methods and parameters that affect the structural, textural and acidic features of the catalyst, which are responsible for the catalytic activity. Many studies have been done on the synthesis of the sulfated-zirconia to study the effect of the synthetic methodology and parameters on the physico-chemical and catalytic properties of the sulfated-zirconia **[38, 92- 95, 106- 122]**. In order to synthesize a good catalyst in terms of better textural, structural and catalytic features, it is important to choose an appropriate method and optimize the synthetic parameters. The synthetic parameters such as type of precursor, concentration of the precursor, type of precipitating agent, type of sulfating agent, method of sulfate loading, drying temperature and method of drying, calcination temperature, etc. are major parameters affecting the properties of the sulfated-zirconia catalyst **[93]**.

The methods reported in literature to synthesize sulfated-zirconia are conventional precipitation method and sol-gel method, however, the sol-gel method is advantageous due to its ability to produce homogeneity in the physical properties and therefore, widely used. Some other routes such as thermal degradation or thermolysis of

zirconium sulfate have also been attempted to synthesize sulfated-zirconia **[123- 125]**. The one pot synthesis of sulfated-zirconia by thermolysis was reported by Arata et al. **[123]** using zirconium sulfate as starting material. The synthesis of sulfated-zirconia by thermolysis method was not found appropriate due to lack of reproducibility in properties and control on sulfur content. To synthesize nano-crystalline sulfated-zirconia, both the precipitation **[126]** as well as sol-gel methods **[70, 113, 127, 128]** have been used, however, the sol-gel method is most commonly used to synthesize nano-crystalline sulfated-zirconia.

1.5.1 Precipitation method

The precipitation method is the classical method for the synthesis of sulfated-zirconia **[14, 94]**. Synthesis of sulfated-zirconia by precipitation method involves the hydrolysis of the inorganic salts of the zirconium such as zirconium chloride **[129, 130]**, zirconium oxychloride **[131, 132]**, zirconium nitrate **[133]**, zirconium oxynitrate **[106]**, etc., in aqueous medium by hydrolyzing agent such as aqueous ammonia or urea **[106]** to zirconium hydroxide followed by sulfation with a suitable sulfating agent. Sulfuric acid, ammonium sulfate, hydrogen sulfide, ammonium sulfide, sulfur dioxide, sulfur trioxide, etc. are used as sulfating agents, but mostly sulfuric acid is used for sulfation **[95]**. The different methods of sulfation are reported such as wet impregnation method either by percolation method, which is the wet impregnation of zirconium hydroxide by passing the solution of sulfating agent through the zirconium hydroxide **[37]** or by immerging method, pouring the zirconium hydroxide in solution of sulfating agent **[14]** and gaseous impregnation of zirconium hydroxide with H_2S or SO_2 **[95]** followed by oxidation. The sulfated-zirconium hydroxide thus obtained is dried and calcined at required temperature, wherein; phase transformation of zirconium hydroxide from amorphous to crystalline phase and stabilization of sulfate ions take place.

Generally, the amorphous zirconium hydroxide is sulfated before crystallization by thermal treatment, however, sulfation of crystalline zirconia after calcination has also been reported **[38]**. The sulfation of amorphous zirconium hydroxide was found to give higher catalytic activity and acidity as compared to crystalline zirconia **[38]**. The method of sulfation and the sulfating agent are crucial factors in controlling the sulfur content of

the catalyst and therefore, the physico-chemical properties of the catalyst such as crystalline phase, crystallinity and acidity **[107]**. The sulfur content and the nature of sulfate binding with zirconium atom influence the strength and type of acidity in the catalyst. The effect of sulfating agent and sulfur content on the properties of sulfated-zirconia would be discussed in next section of this chapter. Generally, the sulfur content can be varied and controlled by impregnating the zirconium hydroxide in the sulfuric acid solution of required concentration and by calcination temperature, but these are not appropriate methods, as these methods do not give reproducibility in results.

Farcasiu et al. **[107]** synthesized sulfated-zirconia with controlled sulfur content by controlled impregnation of zirconium hydroxide, obtained by the precipitation of zirconyl nitrate, with sulfuric acid. In controlled impregnation, the zirconium hydroxide is covered with an H_2SO_4 solution of required concentration (0.5 M) containing the amount of acid intended to be adsorbed, making sure that the entire solid was covered followed by drying. Sulfation by controlled impregnation method resulted into similar structural, textural properties and catalytic activity as done by standard methods used for sulfation such as percolation, immerging or gaseous impregnation method. By this method, the sulfur content in the catalyst can be controlled by varying the concentration of the sulfuric acid used; instead of changing the calcination temperature as well as wasting of sulfuric acid can be avoided.

The synthesis of nano-crystalline zirconia using precipitation method has been studied and reported in literature **[126, 134]**, however, the synthesis of nano-crystalline sulfated-zirconia using precipitation method has not been reported.

1.5.2 Effect of synthetic parameters of precipitation method

The synthetic parameters significantly influence the physico-chemical properties and therefore, the catalytic activity of sulfated-zirconia. The most important parameters affecting the properties of sulfated-zirconia are precursor, hydrolyzing agent, pH of the solution, sulfating agent, concentration of sulfating agent, drying method and temperature, and calcination temperature.

There has been observed the remarkable effect of the type of precursor used in synthesis of sulfated-zirconia on the textural, structural and therefore on the catalytic

performance of the catalyst **[92, 93]**. The effect of the zirconium precursor **[133]** used was observed mainly on the crystal phase of the zirconia, for example, the synthesis from zirconium chloride precursor ($ZrCl_4$) results to either tetragonal or monoclinic form after calcination at the temperature in range of 400- 700 ºC, depending on the final pH and the rate of addition of ammonium hydroxide. However, using zircony chloride precursor ($ZrOCl_2$), only tetragonal phase of zirconia is obtained after calcination at similar temperature, irrespective of the preparation conditions.

The type of hydrolyzing agents also shows a significant effect on the textural properties of the sulfated-zirconia catalyst **[94, 106]**. Aqueous ammonia has been reported to be best hydrolyzing agent giving higher surface area (97 m^2/g) after calcination at 600 ºC, using zirconium chloride precursor **[106]**.

The pH of the solution is important parameter influencing the surface properties, structure and size of crystallites and catalytic activity **[108]**. The sulfated-zirconia synthesized at higher pH (> 9) has been reported to be possessing higher surface area. The crystalline phase of zirconia formed after calcination has also been observed to be affected by the pH of the solution. The transformation from tetragonal to monoclinic phase ratio is also affected by the pH of the solution. Tetragonal phase increases with increase of pH giving purely tetragonal phase at pH of 9.0 **[108]**.

The effect of the type of various sulfating agents has been observed in the sulfated-zirconia as the difference in sulfur content and surface area **[109]**. The effects of different sulfating agents such as sulfuric acid, ammonium sulfate, hydrogen sulfide, ammonium sulfide, sulfur dioxide, sulfur trioxide, sulfur trioxide, hydrogen sulfide, etc. have been studied by Sohn et al. **[95]**. The presence of sulfur species was found to be responsible for the differences in catalytic properties of the sulfated-zirconia from pure zirconia. The sulfur in higher oxidation state of +6 was found to be responsible for enhanced acidity and catalytic activity of sulfated-zirconia. The sulfation with sulfuric acid and ammonium sulfate resulted to catalytically active sulfated-zirconia, while on reduction with hydrogen; the activity of the catalyst was diminished. The sulfation using hydrogen sulfide, ammonium sulfide, sulfur dioxide, sulfur trioxide, sulfur trioxide, hydrogen sulfide gave catalytically inactive catalyst and showed similar activity after oxidation with oxygen as in sulfated-zirconia synthesized using sulfuric acid or

ammonium sulfate. According to Sohn et al. the oxidation state of sulfur is important and influences the acidity and catalytic activity of sulfated-zirconia and not the sulfating agent **[95]**.

The sulfation with sulfuric acid has shown to give higher sulfur content (1.4 wt.%) and surface area (104 m^2/g) after calcination (620 ºC), while sulfation with $(NH_4)_2SO_4$ gives lower sulfur content (0.81 wt.%) and lower surface area (95.3 m^2/g) after calcination at similar temperature **[109]**. The sulfation using other sulfating agents such as $(NH_4)_2S_2O_3$ and $(NH_4)_2S$ were found to give comparatively lower sulfur content (0.45 wt.% and 0.16 wt.% respectively) and lower surface area (45 m^2/g).

The sulfur content has been found to influence the physical properties such as crystallinity, crystallite size, surface area, acidity and type of acid sites and catalytic activity of the sulfated-zirconia catalyst **[51]**. The sulfur content has been reported to be dependent of the sulfating agent used **[109]**, therefore, the sulfating agent affects the catalytic properties of the sulfated-zirconia catalyst.

Morterra et al. **[135]** observed the effect of the sulfur content on the type of acid sites. In dehydrated sample, the surface having < 0.8 S per nm^2 has higher Lewis acidity. The sulfur atom higher than this value results to higher Bronsted sites. Therefore, the relative amount of the Lewis and Bronsted acid sites is decided by the sulfur content and the nature of the sulfate species on the surface. Zhang et al. **[136]** found that the increase in Bronsted acidity with increase of sulfur content has been observed upto a certain maximum after which the amount of Bronsted acidity remains constant. The percentage of Bronsted acidity increases from 0 to 98 % with increase of sulfur from 0 to. 9.87 wt.% and the percentage of Bronsted acidity remain steady on further increase in sulfur content (13.6 wt.%). Higher sulfur content increases the crystallization temperature and makes it slower **[111]**. The sulfur content can be varied and controlled by changing the calcination temperature and by controlled impregnation of sulfate in oxide **[51, 137]**.

The sulfate species on the surface of sulfated-zirconia has been found in different form. Generally, the sulfate is attached to zirconium atom at the surface as bidentate chelating ligand **[97, 98]**, which transform in ionic and covalent forms in presence and absence of water molecule respectively. However, higher sulfur content gives pyrosulfate and higher pyrosulfate species on the surface **[135, 137- 139]**.

Farcasiu et al. **[51]** studied the effect of the sulfur content on the properties and catalytic activity of sulfated-zirconia prepared by precipitation route followed by controlled impregnation of zirconium hydroxide with sulfuric acid. The sulfur content of the sulfated zirconia calcined at 610 ºC increases with an increase of the quantity of sulfuric acid solution (0.1 N). The ratio of retained sulfate after calcination and the impregnated sulfate initially decreases then increases. The surface area of the final catalysts increases with increase in sulfur content showing maximum surface area ~135 m^2/g at sulfur content of 3 wt.%. The content of sulfur less than 5.6 wt.% in the samples resulted into purely tetragonal phase after calcination while higher content of sulfur gave minor amount of monoclinic phase along with major tetragonal phase. At higher sulfate loading, most of sulfates are present in bulk rather than surface resulting into decrease of the surface area and crystallinity due to migration of sulfate inside the particle. The sample having 3 wt.% sulfur content after calcination at 610 ºC showed maximum activity for isomerization of methylcyclopentane to cyclohexane and it was concluded that the catalyst with higher sulfate near the bulk, not necessarily on the surface, showed maximum activity and tetragonal phase.

Sulfation with SO_3 has been found successful to generate superacidity **[54]** while that with SO_2 and H_2S is unable to give superacidity but oxidation of the catalyst after sulfation results into enhanced acidity **[95]**.

The thermal treatment of the sulfated zirconium hydroxide brings crystallization of zirconium hydroxide to crystalline zirconia and stabilization of the sulfate on the surface of oxide. Thermal treatment leads to dehydroxylation reaction resulting to crystal formation, during this period the sulfate comes from bulk on the surface and get stabilized by chemical bonding with zirconium atom through oxygen atom. The extra sulfate is lost as sulfur dioxide **[140]**. The thermal treatment thus reduces the number of surface hydroxy and sulfur content in the sample, which affects acidity and the ratio of Bronsted to Lewis acidity in the sample **[141]**. At higher temperature (above 600 ºC), some of sulfates decompose to form SO_2 and surface area decreases **[130, 137]**. The optimum calcination temperature required to develop crystallinity in the sample depends on the source and concentration of sulfating agent. The sulfated-zirconia was found to be

crystallized at 550 ºC, when was sulfated with sulfuric acid, and at 600 ºC, when was sulfated with ammonium sulfate.

Tran et al. **[110]** studied the effect of calcination temperature on the acidic and catalytic properties of the sulfated-zirconia catalyst. They also observed the effect of calcination temperature on the type of acid sites. The remarkable effect of calcination temperature was found on the sulfur content retained in the sulfated-zirconia catalyst after calcination compare to other physical properties. Sulfur content was found to be decreasing from 2.5 to 1.0 wt.% with increase of the calcination temperature from 500 to 700 ºC. The activities of the sulfated-zirconia samples were compared for both *n*-butane and propane transformations. The Lewis acidity increases at the expanse of the Bronsted acidity with increase of calcination temperature. The acid strength is decreased at higher calcination temperature and therefore the activity of the catalyst is lower. The concentrations of Lewis and Bronsted acid sites were found practically to be identical in the samples calcined at 600 ºC and at higher calcination temperatures, the Lewis acidity increases at the expense of the Bronsted acidity. The decrease in the acid strength and the number of protonic sites with increase of calcination temperature were found responsible for decreasing the activity of the sulfated-zirconia catalysts.

The precipitation method has some disadvantage like irreproducibility of the physical properties as it involves number of steps and it is very difficult to control the parameters and to perform each step with accuracy. This method does not provide homogeneity in properties of the catalyst.

1.5.3 Sol-gel method

Sol-gel technique brought a new approach to synthesize nano-crystalline material having better physical and chemical properties with homogeneity in appropriate way **[142- 148]**. Sol-gel technique is an emerging synthetic method to synthesize nano-crystalline metal oxides with high porosity and specific surface area. Sol-gel process **[142]** involves two steps, first is the hydrolysis of precursor to hydroxide, which is in the form of small colloidal particles of 0.1-1 μm dimension suspended in solvent medium, called Sol and second is the formation of gel from condensation or polymerization of the sol particles resulting into the formation of three dimensional continuous polymeric oxide

network entraining the solvent. Gel is a state where solid and liquid states are dispersed in each other and is a solid network containing liquid component trapped inside like water in the pores of a sponge. Sol-gel chemistry involves two reaction steps:

1. Hydrolysis- The hydrolysis of metal alkoxide precursor with water results to hydroxide by elimination of alcohol.

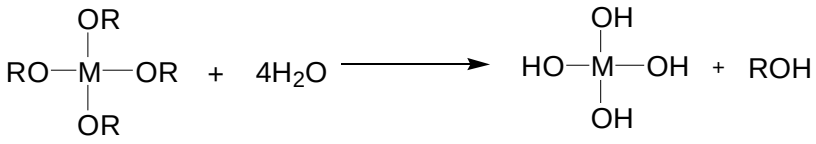

2. Condensation- The resulting metal hydroxide molecules undergo condensation by either self polymerization of hydroxides eliminating water molecules, called dehydrolysis, or by polymerization with metal alkoxide molecules by elimination of alcohol molecules, known as dealcoholysis. The polymerization results to metal-oxygen-metal bond formation and to formation of three dimensional gel networks.

(i) Dehydrolysis;

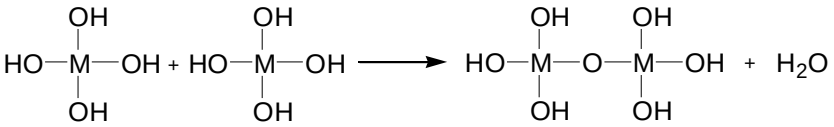

(ii) Dealcoholysis;

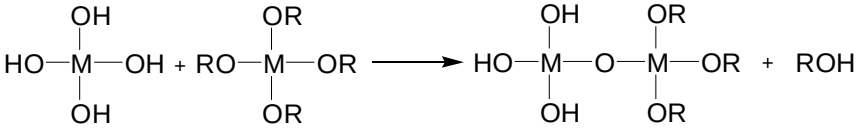

In sol-gel process, the precursor may be inorganic salt or a metalorganic compound dissolved in solvent medium. Generally, metalorganic compounds (metal alkoxides) dissolved in solvent (alcohol) are most commonly used. Sulfated-zirconia has been synthesized by sol-gel route mostly using zirconium propoxide in *n*-propanol/isopropanol or zirconium butoxide in butanol/isobutanol. The hydrolyzing agents used are aqueous ammonia, urea, water and acidified water depending upon pH of the medium of hydrolysis required. The gel is dried by different methods such as thermal, supercritical and freeze drying resulting into dried gel. The dried gel thus obtained is

sulfated with sulfuric acid or ammonium sulfate solution to provide sulfate ions. The sulfated hydrous zirconia is calcined at required temperature to crystallize the material.

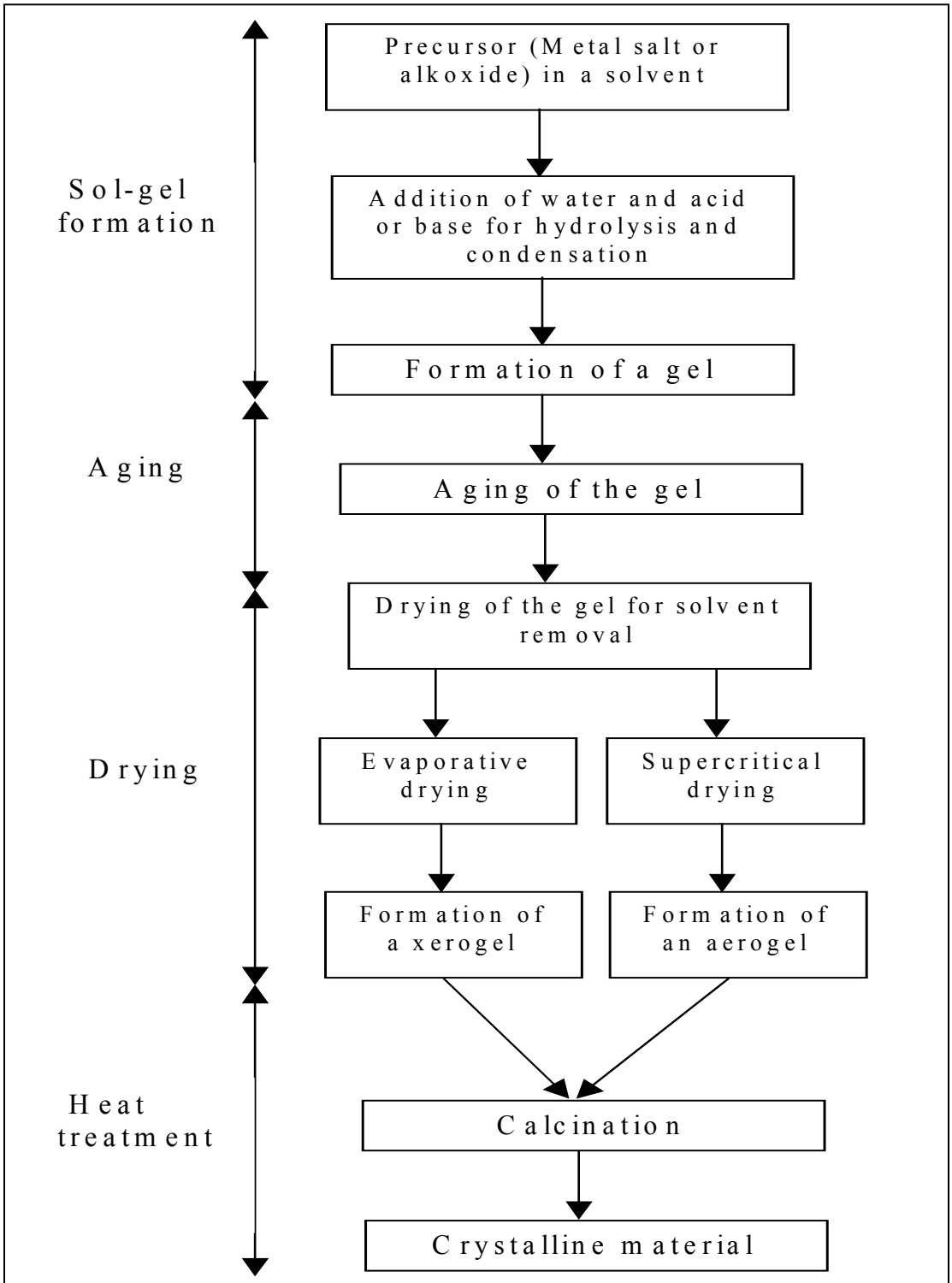

Figure 3. Schematic diagram of sol-gel method.

The sol-gel technique has been excessively used by different researchers **[111-122]** to synthesize sulfated-zirconia and the effect of sol-gel parameters on the properties of sulfated-zirconia have been studied and optimized (Table 2).

Ward et al. **[111, 112]** reported a more effective and appropriate one-step synthesis of sulfated-zirconia by sol-gel technique using zirconium alkoxide as precursor. The sulfuric acid was mixed with zirconium propoxide and propanol solution and water nitric acid mixture was added dropwise to form a cogel. Supercritical drying of the cogel with carbon dioxide to remove alcohol resulted into high surface area (122 m^2/g) aerogel. The aerogel was calcined at 600 ºC to crystallize it. This method changed the two-step sol-gel method (first step is hydrolysis and second step is sulfation) in one-step as sulfuric acid was introduced during hydrolysis. It was first one-step synthesis of sulfated-zirconia by sol-gel technique.

The preformed sol, with different particle size (10- 100 nm), was also used as precursor rather than zirconium propoxide by Ward et al **[143]**. The sol was transformed into gel by adding aqueous solution of ammonium hydroxide. After aging for 2- 3 hours, gel was dried at 110 ºC for 3 hours under vacuum. The dried sample was calcined at 500 ºC and then sulfated with aqueous solution of ammonium sulfate by impregnation method. The preformed sol was also used to get sulfated-zirconia cogel by adding ammonium sulfate in sol and hydrolyzing with ammonium hydroxide.

Tichit et al. **[113]** also reported one-step sol gel synthesis of sulfated-zirconia. They synthesized sulfated-zirconia by two methods; one as previously used by Ward et al. **[111, 112]** and second was the prehydrolysis of the zirconium propoxide with sulfuric acid by adding concentrate sulfuric acid in propoxide-propanol solution followed by complete hydrolysis with distilled water.

Li et al. **[116]** prepared sulfated-zirconia by sol-gel method with successive heat treatment at different steps of synthesis. 5 wt.% zirconium propoxide solution in *iso*-propanol was used as precursor. Water was added dropwise to the alkoxide-alcohol solution for several h and the sample was kept at 50 ºC for 24 hours under stirring and then at 70 ºC for 6 hours. The solvent was removed by evaporation at 90ºC over a time of 30 min. The sample was dried at 130 ºC for 16 hours in oven. Thus obtained material was called xerogel. The xerogel was pretreated at 385 ºC in flow of He. This heat treatment

before calcination was found suitable to get high surface area and to remove isopropyl alcohol from solid network. This heat treatment decreases the bulk volume and surface area. The xerogel was immersed in 0.5N H_2SO_4 for 15 min followed by filtration and drying at 130 ºC for 16 hours. The sulfate treated material was calcined at 600 ºC for 1 hour in flow of oxygen.

Table 2. Studies on the synthesis of sulfated-zirconia using sol-gel methods.

S. No.	Researchers	Sol-gel method	Study	Ref.
1	Ward et al.	One-step	Supercritical drying with CO_2, effect of effect of mode of addition of sulfuric acid, sulfate content and activation temperature on physicochemical and catalytic properties.	**[111, 112]**
2	Tichit et al.	One-step and two-step	Effect of mode of addition of sulfuric acid on physicochemical and catalytic properties.	**[113]**
3	Morterra et al.	One-step	Synthesis and characterization of physical, crystallographycal, morphological and catalytic properties.	**[114, 115]**
4	Li et al.	Two-step	Effect of water/ alkoxide ratio, pH of hydrolysis medium and the strength of sulfuric acid on physicochemical and catalytic properties.	**[116]**
5	Bedilo et al.	One-step and two-step	High temperature supercritical drying, effect of preparative variables on textural properties, sulfur content on catalytic activity.	**[117]**
6	Armendariz et al	One-step and two-step	Effect of concentration of sulfuric acid used in sulfation and calcination temperature on properties.	**[118]**
7	Parvulescu et al.	Colloidal sol-gel	Synthesis of sulfated-zirconia by colloidal sol-gel method, effect of template during gelification	**[119]**
8	Signoretto et al.	Two-step sol-gel	Effect of use of modifiers such as acetic acid, acetyl acetone, 2-methylpentane-2, 4-diol on the physicochemical properties	**[120]**
9	Melada et al.	One-step	Effect of method of drying, water/ alkoxide ratio, acid catalyst amount during hydrolysis, sulfur content on physicochemical properties.	**[121, 122]**

Parvulescu et al. **[119]** prepared sulfated-zirconia in two ways using zirconyl chloride, first one by colloidal sol-gel technique and second by impregnation of zirconium hydroxide. In colloidal sol-gel technique, the aqueous solution of the salt was hydrolyzed with aqueous ammonia to zirconium hydroxide precipitate, which was peptized with sulfuric acid or acetic acid-sulfuric acid mixture. In impregnation method, either as such precipitated zirconium hydroxide or preheated precipitated zirconium hydroxide at reflux temperature (90 ºC) was impregnated with sulfuric acid. The colloidal sol-gel preparation showed higher amount of retained sulfur after calcination and mono and polynucleate sulfate species as well as supported H_2SO_4 were observed on the surface.

Signoretto et al. **[120]** prepared sulfated-zirconia by sol-gel method followed by supercritical drying of the alcogel to aerogel starting from zirconium propoxide and using three modifiers namely acetic acid, acetyl acetone, 2-methylpentane 2, 4-diol to control hydrolysis rate. They studied the effect of modifiers on the morphology of the catalyst and also the porosity. The sulfated-zirconia synthesized by using acetic acid modifier showed microporous structure and the acetyl acetone modifier gave mesoporous material having pore size in range of 70 to 200 Å. The use of 2-methylpentane 2, 4-diol resulted to macroporous material.

The studies on the synthesis of nano-crystalline zirconia using sol-gel method are excessively reported in literature and have been found to be producing smaller crystallites compare to precipitation method **[126, 134, 144]**. The synthesis of sulfated-zirconia using sol-gel method is widely reported, however, the studies on the nano-crystalline sulfated-zirconia have not been much focused. As the sol-gel synthesis produces nano-crystalline zirconia support; therefore, the nano-crystalline sulfated-zirconia by sulfation of the nano-crystalline zirconia can also be synthesized. The synthesis of nano-crystalline sulfated-zirconia by sol-gel method has also been reported **[122, 127, 128]**. Ardizzone at al. **[128]** reported the synthesis of nano-crystalline sulfated-zirconia having crystallite size in range of 15- 17 nm, using sol-gel method in basic, acidic and neutral medium.

1.5.4 Effect of synthetic parameters of sol-gel method

The sol-gel process involves two reaction steps, hydrolysis and condensation. Any parameter that influences either or both reactions can impact on the properties of the product obtained. Livage et al. **[145]** revealed the effect of rate of hydrolysis and condensation on the properties of final product. The fast hydrolysis results to linear polymeric gel giving highly porous material while, the slow or controlled hydrolysis was found to be forming highly branched gel. Following are the important parameters influencing the physico-chemical properties of sulfated-zirconia.

1.5.4.1 pH effect

The pH of the medium has been found to be considerably affecting the textural properties of the material. For example, the rate of hydrolysis and condensation of tetraethyl orthosilicate (TEOS) varies as a function of pH **[146]**. The figure 4 shows that the rate of hydrolysis in acidic medium is higher than the condensation, while in basic medium, the condensation is faster. Further, the decrease in the acidity of the medium lowers the rate of hydrolysis as well as condensation and the rate of hydrolysis and condensation increase with basicity of the medium.

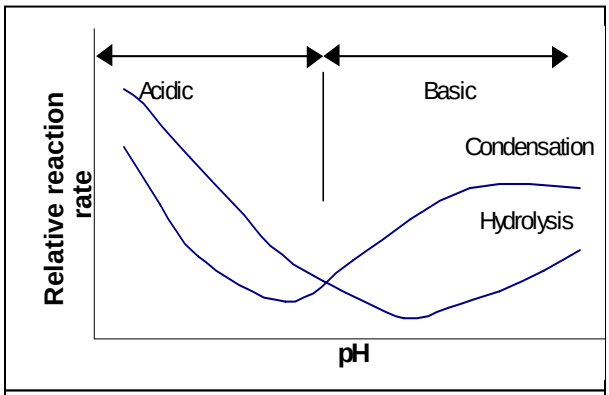

Figure 4. Schematic diagram of effect of pH on relative rates of hydrolysis and condensation on gel structure.

The role of pH on gel morphology can be explained by considering both hydrolysis and condensation reactions **[147]**. Hydrolysis is first order in H_2O and is favored under acid conditions; its rate relative to that of condensation is enhanced by either an increase in the concentration of water or a decrease in the pH. Under acidic conditions, which are favorable to hydrolysis, the rate of hydrolysis is faster than condensation and therefore, the gel is the result of a colloidal rather than a polymerization reaction resulting into weekly branched linear gel. At a higher pH, condensation reactions occur before hydrolysis is complete results to highly branched gel and colloidal

aggregates. The drying and heat treatment of these materials have different surface properties and pore structures.

Preformed sols as precursor are an attractive alternative in sol-gel synthesis **[148]**. The sol particles are stabilized by pH adjustment, thus pH of the solution, which can be changed by the addition of either acid or base, is the single most important parameter in obtaining a gel from preformed sols. The size and concentration of sol particles also affect the gel quality.

Li. et al. **[116]** studied the effect of pH on textural properties of sulfated-zirconia synthesized by sol-gel method and found to be affecting the surface area and pore volume. In order to understand the effect of pH on the surface areas of the resulting materials, a series of studies were performed in which the pH was varied through the addition of either HCl or NH_4OH. It shows that the BET surface area of the resulting xerogels increases with an increase in the pH. The pore volume of the xerogels also increases with increasing pH, while the average pore diameter remains almost constant (Table 3). The maximum surface area and pore volume were observed at pH of 8.3, there were not any significant increase in surface area and pore volume between pH of 8.3 and 11.2.

Table 3. Effect of pH on the textural properties of sulfated-zirconia **[116]**.

S. No.	pH	BET (m^2/g)	Pore volume (cm^3/g)	Average pore diameter (nm)
1	2.7	146	0.15	3.6
2	8.3	202	0.39	3.4
3	11.2	220	0.41	3.5

Bokhimi et al. **[127]** studied the effect of pH on the crystalline phase of sulfated-zirconia, synthesized by sol-gel method at different pH using hydrolysis initiators such as hydrochloric acid, acetic acid and ammonium hydroxide. The crystalline phases were observed to be dependent of the hydrolysis initiator used for the synthesis. The sample synthesized by using acetic acid had mainly tetragonal zirconia

crystalline phase, but in the samples synthesized using hydrochloric acid or ammonium hydroxide, the produced phase was mainly monoclinic at 800 ºC.

A study on the effect of acid amount during hydrolysis on the properties of sulfated-zirconia was done by Minesso et al. **[149]**. The sulfated-zirconia xerogels were prepared using one-step and two-step sol-gel methods varying the molar ratio of nitric acid and zirconium propoxide ($R = HNO_3/Zr(OC_3H_7)_4$) from 0 to 0.8 in closed and open vessels. The influence of molar ratio, R, was studied on gel time and the physical properties of the sulfated-zirconia. The strong effect of the HNO_3 addition on the gelation rate and on the properties related to the surface and bulk structures of the sulfated zirconia xerogels were observed. At low R (≤ 0.6), the gelation time was observed to be shorter (2- 10 min.) and on increasing there was longer gelation time (2- 210 hours). Moreover, the physical appearance of the resultant products was also influenced by the amount of acid used. Low stoichiometric ratios ($R \leq 0.6$) induced the rapid formation of a white precipitate. The increase in the acid amount resulted in the formation of opaque and cloudy gels. At high R values (≥ 0.6), the gels became clear and transparent. The gelation was completely suppressed when the acid concentration was sufficiently high ($R \geq 1$). The acid amount was also observed to be affecting the textural properties of the sulfated-zirconia. The surface area of the sulfated-zirconia samples significantly decreased on increasing the nitric acid amount. At lower HNO_3/alkoxide molar ratio ($R \leq 0.6$), the surface area was in range of 113- 80 m^2/g, which gradually decreased on increasing nitric acid amount. The samples prepared by using lower R (< 0.6) showed the presence of mesopores. At higher HNO_3 concentrations (HNO_3/alkoxide molar ratio > 0.6), the mesopores gradually disappeared and the samples were mainly characterized by a microporous structure with a very low pore volume. A shift toward a smaller pore size with the addition of nitric acid concentration was also reported by Bedilo et al. **[117]** for the sulfated-zirconia aerogels. The amount of acid has also been observed to be influencing the crystalline phase in the sulfated-zirconia. The samples synthesized at R =0, showed a prevalent presence of the tetragonal phase, as well as a small amount of the monoclinic phase. The monoclinic phase completely disappeared in the samples prepared with intermediate values of R (0.68), whereas it became the main crystalline phase for the sample with the largest amount of HNO_3 (R = 0.8).

1.5.4.2 Effect of precursor and modifiers

The precursor, mostly metal alkoxides, of the material to be synthesized has been observed to be influencing the properties of the material. The rate of hydrolysis and condensation depend on the reactivity of the metal alkoxide, which depends on the structure of the metal alkoxide (partial positive charge or electropositive nature of metal atom, size of alkoxide group, and coordination number of the metal atom). Longer and bulkier alkoxide groups decrease the rate of hydrolysis and condensation as the propoxide shows higher reactivity than butoxide **[150]**.

Signoretto et al. **[120]** synthesized sulfated-zirconia by sol-gel method from zirconium propoxide using three modifiers namely acetic acid, acetyl acetone, 2-methylpentane 2, 4-diol to control the rate of hydrolysis and condensation reactions. They studied the effect of modifiers on the morphology of the catalyst and also the porosity. The sulfated-zirconia synthesized by using modifier showed gradual increase in porosity with acetic acid, acetyl acetone and 2-methylpentane 2, 4-diol resulting to microporous, mesoporous and macroporous materials.

1.5.4.3 Amount of water

The amount of water used during hydrolysis and the rate of water addition also influence gel characteristics. The hydrolysis ratio (h), the moles of water per mole of metal alkoxide [$M(OR)_m$], has remarkable effect on the sol-gel chemistry.

i) If $h < 1$; an infinite network seldom forms due to the low functionality of the precursor towards condensation. Because of less M-OH group for cross-linking, gelation time is decreased.

ii) If $1 < h < m$; polymeric gel is formed.

iii) If $h > m$; cross-linked polymers, particulate gels are formed.

Li et al. **[116]** studied the effect of water/alkoxide molar ratio on the physical properties of the sulfated-zirconia synthesizing by two-step sol-gel technique. The water-alkoxide ratio was found to be affecting the surface areas of the sulfated-zirconia, which significantly increase with increasing water/alkoxide ratios. The sample synthesized at the ratio of 4 had lower surface area (121 m^2/g), while the surface area at the ratio of 40

was 202 m^2/g. The pore size distribution was also observed to become much sharper with an increase in the water/alkoxide molar ratio.

Armendariz et al. **[118]** also studied the effect of water/alkoxide molar ratio on the properties of sulfated-zirconia synthesized by one-step sol-gel technique varying the ratio from 1 to 4. The effect of ratio was observed on the gelation time as the gelation time decreased with increase of the ratio. The water/alkoxide molar ratio influences the crystallization temperature of the sulfated-zirconia. The crystallization temperature increases with increase of ratio. At the ratio of 1, the crystallization temperature was found to be 407- 623 ºC, while at R = 4, it was 423- 700 ºC. The surface area was also found to be slightly increasing with increasing the water/alkoxide ratio and maximum surface area (88 m^2/g) was found at the water/alkoxide molar ratio of 4. The catalytic activity of the sulfated-zirconia catalysts was also found to be affected by the R value. The catalyst synthesized at higher ratio of 4 was found highly active for *n*-hexane isomerization.

Bianchi et al. **[76]** have also studied the effect of water/alkoxide molar ratio on the physical properties of the sulfated-zirconia synthesized by one-step sol-gel technique. The water/alkoxide ratio was found to be affecting the surface state and the catalytic properties of the sulfated-zirconia catalyst. The increase in the water/alkoxide ratio in the sol–gel synthesis provokes a parallel increase in both the O/Zr and O/S atomic ratios, i.e. in the total O-atom surface amount. The ratio was found to be influencing the catalytic activity of the sulfated-zirconia catalysts for esterification reaction. The activity of the catalysts decreased with increase of ratio due to presence of higher amount of chemisorbed water molecules on the surface of zirconia as the water molecules compete with the reactant molecules for the active sites to be adsorbed.

Melada et al. **[122]** also observed the effect of water/alkoxide ratio on the surface area and retained sulfur content in sulfated-zirconia prepared by one-step sol-gel technique. The water/alkoxide ratio was found be an important parameter in the development of a high surface area (140 m^2/g) and in the sulfur content (3 wt.%) after calcination at 550 ºC.

The rate of hydrolysis has been reported to be controlled by using some agents to replace the alkoxide groups. Hamouda et al. **[151]** studied the effect of controlled

hydrolysis of precursor on the properties of sulfated-zirconia. The sulfated-zirconia samples were synthesized by one-step sol-gel method by adding acetic acid as water source and to control the rate of hydrolysis. The sulfated-zirconia samples were synthesized by two methods; first sulfuric acid and acetic acid was added in alkoxide followed by stirring for 1 h and second the sulfuric acid was added in alkoxide and stirred for 1 hour then acetic acid was added. The sample prepared by second method had higher sulfur content (0.74 wt.%) but lower surface area (51 m^2/g) after calcination at 600 ºC and higher in catalytic activity for *n*-hexane isomerization. This result indicates that sulfate groups are probably more strongly bound to the zirconia if sulfuric acid was mixed with alkoxide before hydrolysis.

1.5.4.4 Effect of temperature and solvent

Temperature and solvent have been reported to affect the sol-gel transformation step during the synthesis of silica from tetraethyl orthosilicate and therefore, the properties of the final product **[152]**. Varying the reaction temperature, the relative rates of hydrolysis and condensation can be changed. Solvent can change the nature of the alkoxide through solvent exchange or affect the condensation reaction. For the synthesis of microsized uniform silica particles, long chain alcohols as solvent have been used to control the hydrolysis and condensation rate and to reduce the polarity of the system (modified seed growth), as well as to stabilize large particles **[153]**. A gel can also be prepared without solvent using ultrasound irradiation to homogenize the reaction mixture **[154]**.

1.5.4.5 Aging

Aging is the time period between the formation of a gel and the removal of solvent. As long as pore remains filled with solvent, the gel is not static and undergoes many transformations **[142, 150]**. Longer aging leads to a more cross-linked network resulting to higher surface area.

1.5.4.6 Drying

The drying of the gel is an important step in sol-gel method to remove the trapped solvent in side the pores of gel and has been found to be affecting the textural properties of the sulfated-zirconia. There are different methods of drying of gel such as thermal, supercritical and freeze drying. The simple thermal drying is mostly used to dry the gel resulting into the dried gel having collapsed pores and reduced the surface area. The liquid-vapour interface formed in side the pores collapses the pores and therefore, oxide network during thermal evaporation of solvent. The dried gel having sintered pores and lower surface area is called xerogel. In order to avoid this problem, supercritical and freeze drying methods have been used and found appropriate way to remove solvent without changing texture of the pores. The supercritical drying has been done at low temperature using some supercritical gases like CO_2 and at high temperature where solvent itself is used as supercritical fluid. At low temperature supercritical drying **[111, 112]**, the supercritical fluid is introduced in pores replacing the solvent and then the supercritical fluid is taken out from the pores without disturbing the texture of the pores. At high temperature supercritical drying, the supercritical condition is established to convert the solvent into supercritical fluid and then supercritical fluid is drained from pores without changing the texture of pores **[117]**. The supercritical drying avoids the liquid-vapour interface inside the pores. The supercritical drying of gel results into high surface area porous aerogel. The freeze drying of the gel is done in freeze dryer **[76, 155]**. The gel is frozen by liquid nitrogen in the freeze drier to remove the solvent under vacuum.

Melada et al. **[121]** studied the effect of oven drying at 100 ºC and high temperature supercritical drying (at above the supercritical conditions of *n*-propanol, P = 60 bar, T = 250 ºC) on the physical and catalytic properties of sulfated-zirconia synthesized by one-step sol-gel method. The samples were calcined at 470, 550 and 630 ºC for 5 hours. The surface area of the xerogel was found to be about three times larger than the surface area of the aerogel, but the xerogels showed a sharp and continuous decrease in surface area with the temperature while the aerogels showed slight decrease in the surface area. The crystallinity of the aerogels was found to be higher than the crystallinity of the xerogels. The xerogels were amorphous up to around 500 ºC and at

higher temperatures; they crystallize to the tetragonal form, showing a minor monoclinic phase. The aerogels appear to be crystalline even at the lowest temperature (470 ºC) and the crystal phase composition is unaffected by the calcination treatment, the only effect being a slight increase in the crystallite size. The difference between the highest temperature aerogels and xerogels is the major presence of the monoclinic component in the aerogels. The formation of the monoclinic form attributed to the high ratio of water/alkoxide (water/alkoxide molar ratio = 14:1) and by the high pressure adopted in the supercritical evaporation procedure. The catalytic activity of sulfated-zirconia obtained from calcination of xerogel for *n*-butane isomerization was higher than that of aerogel.

1.5.4.7 Effect of sulfation method

The sulfation method has been found to be affecting the physicochemical and catalytic properties of the sulfated-zirconia synthesized by sol-gel method. Generally, the gel is sulfated by immerging into the required amount and concentration of sulfuric acid solution followed by filtration and drying. The method is used in two-step sol-gel technique and also called as ex-situ sulfation. The in-situ sulfation is the promotion of sulfate ion to the gel during hydrolysis by adding sulfuric acid in either alkoxide or through hydrolyzing water in one-step sol-gel method. Ward et al. **[112]** studied the effect of sulfation method on the physical, structural and catalytic properties of the sulfated-zirconia synthesized by sol-gel technique.

The sulfated-zirconia catalyst prepared by impregnation of dried aerogel followed by calcination at 600 ºC was found to be having significantly decreased surface area (25 m^2/g), while the catalyst synthesized by sulfation of calcined aerogel had higher surface area (108 m^2/g). The sample prepared by one-step sol-gel method followed by calcination at 600 ºC had higher surface area than two-step samples. They reported that the precrystallized zirconia sample, obtained by sol-gel method, at 500 ºC (tetragonal) could be sulfated to get an active catalyst. High hydroxy content on the surface of the sample is the activity-determining factor, which allowed for successful sulfate impregnation. The dried as well as calcined both samples, obtained from sol-gel method were found suitable for sulfate promotion as they were having higher surface hydroxy

content. The calcined sample of zirconia (400 ºC) obtained from precipitation method, on sulfation did not give catalytically active catalyst and therefore, it was earlier opinion that an amorphous sample should be used for sulfation to get better activity **[10a, 137, 140]**.

Tichit et al. **[113]** also reported the effect of sulfation method on the properties of sulfated-zirconia synthesized by sol-gel method. Two different protocols were studied in which sulfuric acid was introduced either with the hydrolysis water or in the zirconium alkoxide solution and were compared with sulfated-zirconia synthesized by two-steps by post-sulfation of zirconium hydroxide obtained either by the sol-gel method or by precipitation of inorganic salts. The sulfated-zirconia sample synthesized by addition of sulfuric acid in alkoxide before hydrolysis in one-step sol-gel method had highest specific surface area (108 m^2/g), broader pore size distribution than the surface areas of other samples having narrower pore size distribution, while the sulfur content was similar in all samples after calcination at 650 ºC. The isotherm in the former sample was of type IV, while in others of type II. The effect of sulfuric acid addition in alkoxide or in-situ sulfation on the textural properties was explained by occurrence prehydrolysis of alkoxide induced by the trace amounts of water present in concentrated sulfuric acid. The sulfated-zirconia samples synthesized by the one-step method were the most active catalysts for the hydroconversion of *n*-hexane. Moreover, the sample prepared by adding sulfuric acid through the hydrolysis water exhibited enhanced activity for *n*-hexane conversion.

Armendariz et al. **[118]** also noticed the effect of mode of sulfuric acid addition during hydrolysis on the texture of the sulfated-zirconia synthesized by one-step sol-gel method. Hydrolysis of alkoxide with acidified water results to narrow distribution of mesopores in sulfated-zirconia and the sample, synthesized by hydrolysis of alkoxide and sulfuric acid mixture, by water possesses wide range of large mesopores.

The sulfur content has been observed to be affecting the physicochemical and catalytic properties of the sulfated-zirconia synthesized by sol-gel method. Ward et al. **[111]** studied the effect calcination temperature on sulfur content. The thermal treatment brings sulfates on the surface of zirconia and generates Bronsted acid sites. A minimum density of sulfate in the sulfated-zirconia catalyst (which was obtained from aerogel having 20 mol % sulfate, after calcination at above 500 ºC) was found, which was

observed to be needed to generate higher acidity and therefore, higher catalytic activity for isomerization of *n*-butane. Higher sulfate density (which was obtained from aerogel having 20 mol % sulfate, after calcination at below 500 ºC) retarded the crystallization and increased calcination temperature required to generate maximum catalytic activity.

Li et al. **[116]** observed the effect of strength of sulfuric acid on the textural and catalytic properties of the sulfated-zirconia catalysts synthesized by sol-gel method. Effect of acid strength on the physical properties of sulfated-zirconia was studied by using the different concentrations of sulfuric acid for sulfation ranging from 0.05 to 2.0 N. The results showed that a maximum in the surface area (186 m^2/g) is obtained when zirconia was sulfated using 0.5 N H_2SO_4. A sharp decrease in surface area was observed when the strength of H_2SO_4 was increased to 2.0 N resulting to lower surface area of 40 m^2/g. The sulfur loading increased with the strength of the sulfuric acid. This large sulfur concentration results in a higher concentration of the sulfate group on the surface. This higher concentration of sulfate groups makes the catalyst thermally more resistant to sintering and results to catalytically more active tetragonal phase of zirconia. The catalytic activity of the sulfated-zirconia samples for isomerization of *n*-butane was found to be gradually increasing with strength of sulfuric acid. Optimized amount of sulfuric acid, to get a catalyst of higher surface area and higher activity for isomerization of *n*-butane, was 0.5 N H_2SO_4.

Cutrufello et al. **[156]** also studied the effect of normality of the sulfuric acid used in the sulfation step on the properties of sulfated-zirconia synthesized by sol-gel method. A systematic change in the concentration of the sulfuric acid showed that the optimum acid concentration was 0.25 N showing the highest crystallinity, highest specific surface area (171 m^2/g) and maximum activity for *n*-butane isomerization. An increase in the concentration of the sulfuric acid above 0.25 N resulted in a decrease in both crystallinity and surface area. The sulfur content was found to be increasing from 1.08 to 8.42 wt.% with increase of concentration from 0.05 to 2.0 N of sulfuric acid solution.

1.5.5 Advantages of sol-gel technique over conventional precipitation method

Sol-gel technique has brought a new approach for synthesis of nano-crystalline sulfated-zirconia, providing high purity because of purity of precursor, homogeneity at molecular level, controlled porosity and well-defined pore size distribution with high surface area. The advantage of the sol-gel method for synthesis of sulfated-zirconia includes the ability to vary physical characteristics such as surface area, pore size, pore volume, crystal forms and catalytic behavior by changing the synthetic parameters **[111-122]**. Sol-gel synthesis results to the zirconia having higher surface area and higher hydroxyl content, which are responsible for stabilization of catalytically active and thermally stable tetragonal crystal form as well as the higher loading of sulfate **[119]** on the surface (higher sulfur content). The sol-gel method has been found advantageous for synthesis of nanocrystalline materials compare to conventional precipitation method due to ease of control of homogeneity of physicochemical properties in sol-gel method. It is a low temperature synthesis and can be done at room temperature. The sol-gel synthesis gives nano-crystalline, mesoporous material with high surface area, higher concentration of anionic vacancies **[126]** and predominantly pure tetragonal phase **[157]**. It involves less number of synthetic steps and preparative variables like precursor concentration, molar ratio of precursor and water, pH, gelation time, drying method and activation temperature, so it is easy to control steps and to maintain the preciseness during synthesis. In sol-gel technique, several components can be introduced in single step. The comparative study of the properties of the sulfated-zirconia catalysts, synthesized by precipitation and sol-gel techniques, has shown the better textural and catalytic properties of the catalyst prepared by sol-gel method **[70, 113]**.

1.6 Structural models for sulfated-zirconia and mechanism for generation of acid sites

The sulfate provided to zirconium oxide network after sulfation remains in the bulk of oxide network. Thermal treatment brings the sulfate ions on the surface of zirconia during crystallization. The surface sulfates are stable and are chemically bound

with zirconium atom through oxygen. The surface sulfates are responsible for the generation of acidity and the type of acidity is determined by the nature and bonding of surface sulfate species. To understand the generation of superacidity, it is important to know the structure of sulfate. IR and X-ray photoelectron spectroscopy are helpful tools to do this. Tanabe and coworkers **[97, 98]** proposed structure of sulfate species on the zirconia surface as chelating bidentate ligand (Scheme 1). In presence of water molecules, sulfate behaves like an inorganic sulfate complex as hydrogen bonding between water molecule and sulfate group partially ionize the S=O double bond and decrease the bond order from 2 to 1.5. The dehydration of sulfated-zirconia shows structural transformation and sulfate species becomes like an organic sulfate with stronger covalent character to S=O double bond. This structure is responsible for the superacidity because inductive effect of S=O double bond increases electron deficiency at zirconium atom **[98, 111]**.

Lavalley and coworkers **[138]** proposed a different structural model for surface sulfate species (Scheme 2). They suggested the sulfate having one S=O double bond and three bonding to zirconium atom through oxygen atom. The dehydrated sulfated-zirconia has two types of sulfate species. At lower content of sulfate (< 2 wt.%), sulfate has one S=O double bond and three S-O bonds connecting to zirconium atom. At higher content of sulfate (> 2 wt.%), sulfates are found as most active pyrosulfate species on the surface of zirconia. They reported effect of water on surface sulfate species with evidence by IR spectra. They postulated that hydrated sulfate species are more ionic. Morterra et al. **[137]** also supported Lavalley's model.

Tanabe's Model

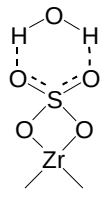

Hydrated Structure

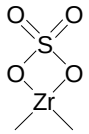

Dehydrated structure

Scheme 1

Lavalley's Model

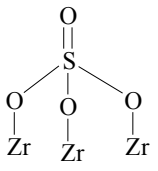

Dehydrated structure of sulfate species at low sulfur content

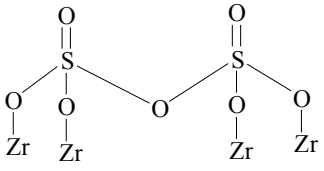

Dehydrated structure of sulfate species at high sulfur content

Scheme 2

Kumbhar et al **[158]** proposed the structural model of surface sulfate species having two S=O double bond bonded with zirconium atom through two oxygen atoms (Scheme 3).

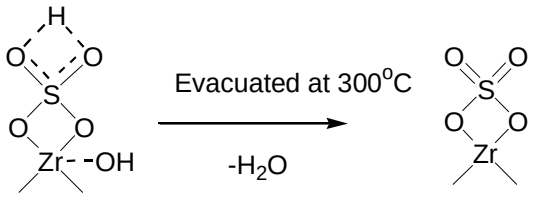

(i) Hydrated Structure (ii) Dehydrated structure

Scheme 3

Chen et al. **[140]** have proposed a possible mechanism for the generation of the acid sites on the surface of S-ZrO_2. This mechanism suggests the formation of acid sites to be a two-step chemical reaction between the superficial hydroxyl groups and the sulfate anions.

1. $Zr(OH)_4n + xH_2SO_4 = Zr_n(OH)_{4n-2x}(SO_4)x + 2xH_2O$.
2. $Zr_n(OH)_{4n-2x}(SO_4)_x = Zr_nO_{2n-x}(SO_4)_x + (2n-x)H_2O$.

The first chemical reaction is the reaction between hydroxyl group and sulfate group, which occurs during the impregnation with sulfates and the subsequent drying. The second step occurs during calcination of the sample. Yamaguchi **[11]** has proposed a possible scheme for the formation of acid sites (Scheme 4). This structure is essential for the catalysis of reactions. It has further been suggested that such a structure is most probably developed at the edge or corner of the metal oxide surfaces. It is revealed by the fact that the first doses during a stepwise loading of the acid on microcrystalline ZrO_2 selectively form sulfate groups on crystal defects such as corners and edges **[137]**.

Morterra et al. **[141]** have observed the surface sulfates to exhibit a highly covalent character in a dehydrated sulfated-zirconia sample. It has also been observed that the adsorption of basic molecules, like pyridine, on the central metal cation causes a large shift in the IR band for S=O double bond from 1370 to 1330 cm^{-1} **[97]**. These observations suggest that the highly covalent surface sulfates have lesser covalent character, in presence of basic molecules. The partial rehydration of the catalyst initially

converts the surface sulfates to a lesser covalent form and then into ionic form **[141]**. This results to the transformation of the strong Lewis sites to Bronsted acid sites. The subsequent decrease in the catalytic activity towards *n*-butane isomerization suggests that the strong Lewis sites associated with these highly covalent sulfates are catalytically active. The covalent sulfates in structure of the Yamaguchi model (Scheme 4) exhibit a strong electron attracting ability from a basic molecule and hence generate superacidic sites.

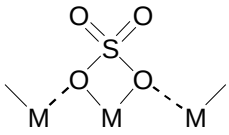

Scheme 4

Another model (Scheme 5) has been proposed by Arata et al. **[159]** for the structure of the active site. They described the formation of Bronsted sites as a result of the uptake of water molecules as a weak Lewis base on the Lewis acid site supporting by the IR studies.

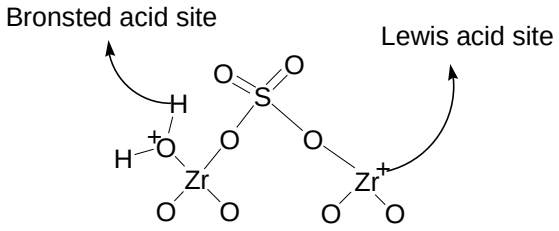

Scheme 5

Clearfield et al. **[96]** proposed a model (Scheme 6) to explain the formation of Bronsted sites. The bisulfate ion, which is predominant species in sulfuric acid, displaces a Zr-OH-Zr bridge during chemisorption on the surface of hydrated zirconia. On heating, either the bisulfate ion reacts with an adjacent hydroxyl group or two adjacent hydroxyl groups can react with each other, eliminating water. The former results in to the generation of Lewis-type acidity, whereas the latter leads to the formation of a Bronsted-type site.

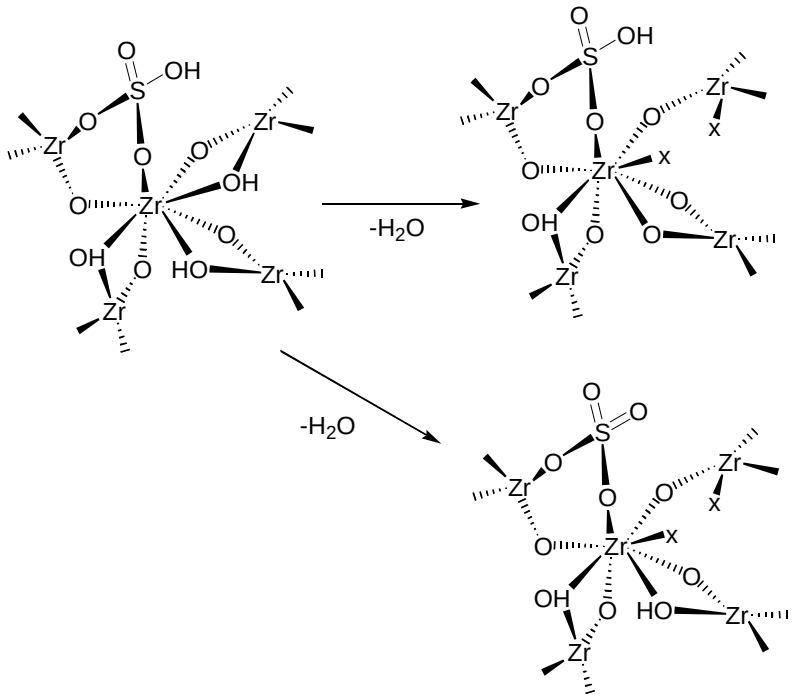

Scheme 6

Kustov et al. **[160]** has also explained the mechanism of the generation of Bronsted acidity. The treatment of hydrous zirconia with sulfuric acid results in the elimination of the terminal Zr-OH species due to their substitution by bisulfate anions **[161]** enhancing the acid strength of the bridging ZrOH groups. They proposed structures of an ionic form with a proton forming a multicenter bond with the SO_4^{--} anion and a covalent form with hydrogen-bonded hydroxyl groups (Scheme 7). They have also explained the generation of Lewis acid sites, which was attributed to the increase of the electron-accepting properties of three-coordinate zirconium cations via the inductive effect of sulfate anions, which withdraw electron density from the zirconium cation.

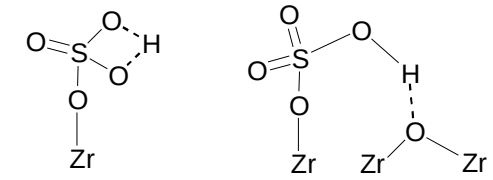

Scheme 7

Babou et al. **[162]** have proposed that the interaction of the zirconia support with sulfuric acid solution results in the trapping of the protons and sulfate ions by the surface hydroxy groups. Dehydration results in the loss of water molecule (Scheme 8), leading to the formation of the structure (A). Further dehydration at higher temperatures (> 200 ºC) liberates second water molecule giving the structure (B).

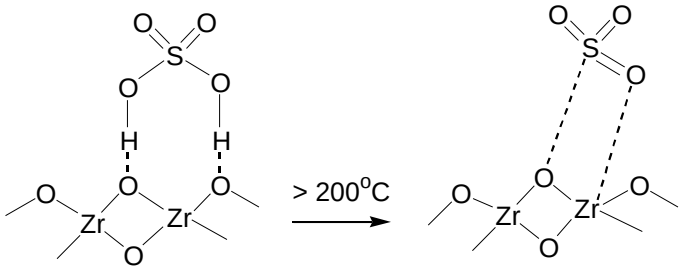

Scheme 8

1.7 Type of surface acidity

The type of acidity present on the surface of sulfated-zirconia has been studied by different researchers by using different techniques. Initially, there were conflictions about the type of acidy, whether it was Bronsted or Lewis. Yamaguchi et al. **[97, 106, 163]** reported the presence of only Lewis sites while Sohn et al. **[95]** and Hino et al. **[37]** reported the presence of both type of acidity on the surface of sulfated-zirconia. Presence of both the Lewis and Bronsted types of acidity on the surface of sulfated-zirconia has also been observed by different researchers **[38, 94, 96]**. The presence of Bronsted acid sites on the surface and their importance for catalytic activity are strongly demonstrated by some reports **[164, 165]**. The type of acidity and strength of the acid sites present on the surface of zirconia are strongly influenced by the synthesis method and synthetic parameters **[37, 112, 118, 119, 121, 166, 167]**. The synthesis method and structure of surface sulfate species and thus acidity have also been found to be dependent on each other **[111]**.

Morterra and coworkers **[135, 137, 141]** and Pinna et al. **[168]** have proposed that the Bronsted acid sites are the most labile form and it is not irreversibly lost on thermal activation above 650 ºC, but gets transformed into Lewis acid sites. Lewis acidity

is generally showed by the sulfates located in the crystal defects such as edges and corners of crystals. The higher concentration of sulfuric acid results into Bronsted acidity and the sulfates are in the form of polynuclear pyrosulfate **[137]**.

Fogash et al. **[169]** have revealed the presence of Bronsted and Lewis acid sites with different acid strengths proved by microcalorimetric and FT-IR studies of ammonia adsorption on the catalyst. The microcalorimetric study gave the initial heat of adsorption of ammonia in range of 150- 165 kj/mol, which was attributed to the presence of strong Bronsted and Lewis site. IR spectroscopy showed the presence of NH_4^+ ions, which are formed by adsorption of ammonia on the Bronsted sites. It revealed the existence of Bronsted acidity in association with the Lewis type acid sites.

Lunsford et al. **[170]** have proved the existence of both types of acid sites on the surface by ^{13}P MAS NMR spectroscopy using trimethyl phosphine as a probe molecule. The signals at -3.4 ppm and -33 ppm were assigned for the adsorbed trimethyl phosphine molecules at Bronsted and Lewis sites.

Babou et al. **[162]** observed from IR studies of adsorbed bases, such as butane (C_4H_{10}), carbon monoxide (CO), water (H_2O) and pyridine (C_5H_5N), the presence of two types of Lewis site, one Lewis type site associated with the zirconia support and the other due to the presence of surface sulfates and one type of Bronsted site exist at the surface of sulfated-zirconia. The IR study of the sulfated-zirconia adsorbed with pyridine showed two types of Lewis sites, one of them was associated with the coordinatively unsaturated zirconium atoms showing the band at 1444 cm^{-1} and another type of Lewis site was assigned by the band at 1459 cm^{-1}, which was attributed to presence of sulfate. The band at 1542 cm^{-1} was attributed to adsorbed pyridine at Bronsted sites. The study supported the presence of both the sites in the sulfated-zirconia.

The FT-IR study using pyridine as basic probe to study the distribution of Bronsted and Lewis acidity in the sulfated-zirconia catalysts has been widely used **[92, 97, 162, 171- 177]**.

The mechanism of the generation of the acidic sites, Bronsted and Lewis sites, has been described by several authors **[170, 178, 179]** considering the model of sulfated-zirconia proposed by Clearfield et al. **[96]**. The model (Scheme 6) explains the formation of Bronsted and Lewis sites more clearly. The surface sulfates are found as bisulfates

having a -OH group, the bisulfate groups and surface hydroxy groups act as Bronsted sites. Lewis sites are the electron deficient zirconium atoms connected with sulfate group and the coordinatively unsaturated zirconium atoms. The neighboring Lewis sites withdraw electrons from the bisulfate group and hydroxy groups weakening the S-O-H bond and O-H bond respectively, which enhance the strength of Bronsted acidity. It has been reported **[178]** that the stronger Lewis sites by their electron attracting nature generate stronger Bronsted sites and therefore, higher acidity. However, the proportion of Bronsted sites has been found to be higher (2/3 of total acid sites) than Lewis sites (1/3).

1.8 Characterization of sulfated-zirconia

Characterization of the catalysts is an important study to evaluate their physicochemical properties and the catalytic activity using different instrumental techniques. The characterization of sulfated-zirconia catalysts involves the examination of textural, structural and catalytic properties. The textural properties include the surface area, pore volume, pore size, pore shape and pore size distribution. Structural properties are the crystal phase, crystal structure, crystallinity, crystallite size and structure of surface sulfate species. Besides these, the elemental analysis to get sulfur content, the thermal analysis of the catalyst, measurement of total acidity and type of surface acidity are also important for complete evaluation of the catalyst.

1.8.1 Structural properties (Crystal phase, crystallinity, crystallite size, structure and nature of surface sulfate species)

Powder X-ray diffraction study

The lattice planes in a crystal are designated as (*hkl*) and characterized by Miller indices *h*, *k* and *l*, which are reciprocals of the intersections between the lattice plane and the three crystallographic axes that span the unit cell of the crystal. The incident X-ray beam (S_o) and the lattice planes have to be oriented in a certain angle (θ) to allow diffraction. Beams reflected at parallel lattice planes in the distance (d_{hkl}) interfere and give an intensity maximum, which occurs as peak in X-ray diffractogram, if their path

difference $2d_{hkl}$ is an integer of wavelength (λ). This condition has been described as Bragg's law **[180]**,

$n. \lambda = 2. d_{hkl}. \sin\theta$

The X-ray diffractogram is the pattern obtained by plotting the intensity of the diffraction lines versus the angle 2θ. In powder samples with randomly oriented crystallites, the same amount of the crystallites has the right orientation for the diffraction for all lattice planes. If, instead, a certain pattern is preferred, the intensity of some reflections is lowered or increased. Information about the lattice parameters is available from peak position. The sharpness of the diffraction lines is determined from their intensity together with their breadth, which is called the full width at half maximum (FWHM). The breadth of the peak is increased with decreasing crystallite size. The XRD pattern of the sample shows the intensity of X-ray diffracted by different plane of the crystals at different angles.

The crystal phase identification is based on the comparison of the set of reflections of the specimen with that of pure reference phases or with database. The Powder Diffraction File (PDF) is the base most commonly used. The crystallinity (%) of the phases is calculated by comparing the areas of the characteristic peaks of the phases. The percent composition of each phase was calculated from the peak areas, hw, where h and w are the height and the half width of the X-ray diffraction pattern at the characteristic peaks **[181]**.

$$\% \text{ Composition of phase A} = \frac{(hw) \text{ of phase A} \times 100}{(hw) \text{ of phase A} + (hw) \text{ of phase B}}$$

X-ray diffraction line broadening analysis is used to determine crystallite size of the crystalline phase using Scherrer formula **[182]**,

$\text{Crystallite size} = K. \lambda / W. \cos\theta$

Where, K = shape factor, λ = wavelength of X-ray radiation used, W = difference of broadened profile width of the experimental sample (W_b) and standard profile width of the reference sample (W_s), θ = angle of diffraction.

1.8.2 FT-IR study

FT-IR spectroscopic study (1400- 400 cm^{-1}) leads to a great deal of information, e.g., the presence of various groups, structure, hydrogen bonding, etc. The interaction of IR radiation with molecule results to variation in the dipole moment and therefore, the vibrational energy level of the molecule, which are quantized. The activation of the molecule leads to different mode of vibrational motions such as stretching (symmetric and asymmetric) and bending and promotes the molecule in higher vibrational energy level. The energy of the stretching vibrational motion is higher than that of the bending vibration and the asymmetrical stretching motion (asymmetrical stretching frequency) is higher in energy than the symmetrical stretching (asymmetrical stretching frequency). The transition in vibrational energy levels of the molecule gives IR spectrum, which is the graph between the wave number and the % transmittance or absorbance.

The structure of the surface sulfates and the nature of bonding between sulfate and zirconia surface is studied by FT-IR spectroscopy **[98]**. The FT-IR spectra of sulfated-zirconia show the IR bands for sulfate group between 1250- 996 cm^{-1}, for asymmetric and symmetric stretching vibrations of partially ionized S=O double and S-O single bonds **[98]**. The bands at ~1020 and ~930 cm^{-1} are attributed to the asymmetric and symmetric stretching mode of vibrations of S-O bonds respectively. The asymmetric and symmetric stretching mode of vibrations of partially ionized S=O bonds are characterized by the bands in range of 1090- 1040 cm^{-1}. The S=O bond is characterized by the band at ~1400 cm^{-1}, which is attributed to asymmetric stretching vibration of S=O bond. However, in hydrated sulfated-zirconia, the sulfate is bonded with water molecule by hydrogen bonding and therefore, S=O bond is partially ionized and does not show the band at ~1400 cm^{-1}. The adsorbed water molecule gives a broad peak at ~3400 cm^{-1}, attributed to the ν_{O-H} stretching mode and at 1631-1635 cm^{-1}, attributed to δ_{O-H} bending mode of water molecule **[111]**. The in-situ heating of the sample to evacuate the adsorbed water molecules in DRIFT (diffused reflectance infra-red spectroscopy) study shows the band ~1400 cm^{-1}. The value of $\nu_{S=O}$ shifts towards lower or higher wave number depending upon the type of sulfate. Morterra et al. **[135]** reported the $\nu_{S=O} \leq 1400$ cm^{-1} for the isolated sulfates in the samples having lower sulfur content ($S \leq 0.8$ wt.%) and in the samples having higher sulfur content ($S \geq 0.8$ wt.%) the pyrosulfates are characterized b

higher value of the $\nu_{S=O}$ ($\geq$ 1400 cm^{-1}). The shifting of $\nu_{S=O}$ towards lower wave number has also been reported to be due to interaction of the base molecules, such as pyridine, with Lewis sites reducing the bond order of S=O bond of the sulfate **[97]**.

1.8.3 Textural properties (N_2 adsorption desorption isotherm study)

Sulfated-zirconia is a heterogeneous catalyst. Heterogeneous catalysts are porous and having large surface area. The determination of surface area, pore volume, pore size, pore size distribution, porosity and pore shape is an important requirement in catalyst characterization. The area of a rough surface is called as external surface area and the area of the pore walls is an internal surface area. These properties are most often determined by using gas adsorption method, called Physisorption, which gives adsorption isotherm. The adsorption isotherm is the relationship between the amount of the gas adsorbed and the relative pressure at constant temperature. The first step in interpretation of a physisorption isotherm is to observe the shape of isotherm, which tells the qualitative nature of the surface coverage and the way of pore filling. Surface area is most often determined by BET-method (Brunauer-Emmett-Teller method) **[183]** from physisorption isotherm data using BET equation,

$$\frac{P/P_o}{n^a(1 - P/P_o)} = \frac{1}{n_m^a . c} + \frac{c - 1}{n_m^a . c}\frac{P}{P_o}$$

Where P/Po = relative pressure,

n^a = volume of gas adsorbed,

n_m^a = volume of gas adsorbed in monolayer formation,

c = constant, indicates the shape of isotherm and order of magnitude of the adsorbent-adsorbate interaction.

The samples are degassed under vacuum at 120 ºC for 4 hours, prior to measurement, to evacuate the physiosorbed moisture. Nitrogen (at 77 K) is generally used as most suitable adsorbate. IUPAC classification **[183]** has classified the isotherms in four types as shown in figure 5(a). Type I is reversible isotherm, showing steady adsorption after certain relative pressure (P/Po). It is characteristic of microporous materials (pore size < 2 nm). Type II is also reversible isotherm and is showed by non-

porous or macroporous materials (pore size > 50 nm). Isotherm shows unrestricted monolayer-multilayer adsorption upto high P/Po. Type III isotherms are found in the systems, in which the overall adsorbent-adsorbate interactions are weak in comparison with relatively strong adsorbate-adsorbate interactions and shows unrestricted monolayer-multilayer adsorption. Type IV isotherm is completely different from others and is having a hysteresis loop and the plateau at high P/Po. This type of isotherm is given by mesoporous materials. The first part of the isotherm shows monolayer formation and initial multilayer formation on the wall of mesopores. The knee of the isotherm represents the completion of monolayer and start of multilayer. However, at certain P/Po, there is a sharp increase in adsorption, which shows the capillary condensation in mesopores. The pore volume is calculated by BJH- method (Barrett, Joyner and

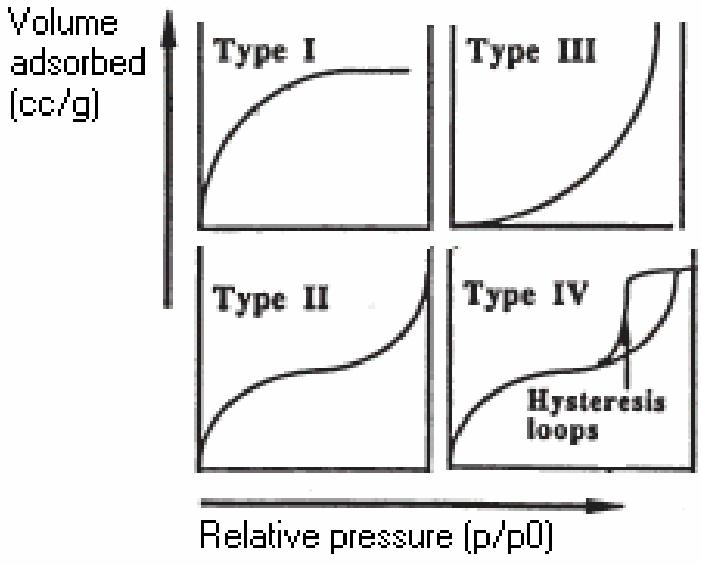

Figure 5(a). Types of isotherms.

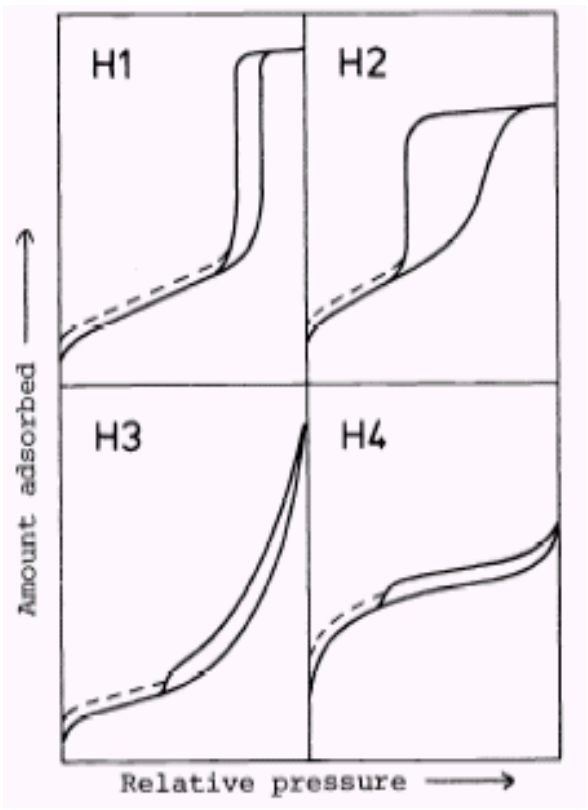

Figure 5(b). Types of hysteresis.

Halenda method) **[183]**. The procedure involves notional emptying of the pores by a stepwise reduction of P/Po. The hysteresis loops are informative tool to know the shape, size of mesopores and their distribution. IUPAC classification categorizes the hysteresis (Figure 5b) into four groups **[183]**. Type H1- represents narrow distribution of relatively uniform mesopores. Type H2- shows complex pore structure. Type H3 and H4 show unlimited adsorption at high relative pressure, indicating the absence of well-defined mesopores. Type H3 hysteresis is obtained in layer structure, showing narrow slit shape pores.

1.8.4 Measurement of acidity and type of acidity

Sulfated-zirconia has both type of acid sites, Bronsted and Lewis acid sites, on the surface. In assaying acidity, probes are needed to measure the acidity (number of sites and strength of sites) and type of acid sites on the surface. The acidity includes both an intensive and an extensive factor **[184]**. Intensive factor is the strength of each type of acid sites and extensive factor is the total number of acid sites including Bronsted and Lewis acid sites. The combination of both factors gives total acidity of the catalyst **[184]**. To obtain the extensive factor, a base is adsorbed on all types of sites. The amount of adsorbed base directly gives total number of sites. The intensive factor is obtained by measuring heat of reaction between base and acid sites. The acidity, type of acid sites and their population on the surface of the solid acid catalyst is measured by three methods,

i. Chemical method, ii. Thermochemical method and iii. Spectrochemical method

1.8.4.1 Chemical method

Chemical method involves the chemical reactions between probe base molecule and the acid sites on the surface.

(a) Using Hammett indicators

The use of Hammett indicators has been reported as one of the chemical method for acidity measurement of sulfated-zirconia **[37]**. Hammett indicators are weak base and have characteristic colour, when get protonated. A series of Hammett indicators (H_0) ranging from –18 to + 4 are used. The small quantity of the activated catalyst is added to

a dilute solution of indicators until one of an adjacent pair shows the acid colour and the other the basic colour. The H_0 of the surface is taken as falling between these two H_0 values. This method gives a rough idea of acidity.

(b) By Titration method

Titration method has also been used to examine acidity. It expresses the acidity as the surface concentration of sites having strength greater than the pKa values of a series of the indicators. First time Johnson **[185]** used this technique in nonaqueous media. The dilute benzene solution of n-butylamine was added in the benzene suspension of the catalyst, on which an indicator showed its acid colour. The end point was taken when the acid colour was completely discharged from butter yellow. Thus a total acidity was obtained. Benesi **[186]** advanced the titration method by producing acid site distribution curves. A complete set of Hammett indicators was employed with aliquots of the catalyst equilibrated with increasing amount of 0.07 M n-butylamine in benzene. A small quantity of the equilibrated catalyst to vials containing dilute benzene solution of various indicators was added to determine the extent of neutralization. The end point was taken from that vial where only a few particles had indication of acid colour of the indicator. This process was repeated with a series of indicators of increasing pKa. This method gives total acidity but do not quantify Bronsted and Lewis sites.

(c) By Catalytic test reactions

Using a catalytic test reaction, either acidity (Bronsted and Lewis acidity) of the catalyst can be evaluated in terms of (wt.%) conversion. The chosen reaction should be known that whether it is catalyzed by Bronsted or Lewis acid. Thus it gives a rough idea about the acidity and the type of the more populated acid site on the surface. For example, dehydration reaction of alcohols are Bronsted acid catalyzed, therefore higher conversion of alcohol to alkene shows presence of dominant Bronsted acid sites on the surface.

1.8.4.2 Thermochemical method

Thermochemical method is used to get the intensive factor (strength of acid sites) by thermal programmed desorption of basic molecule and microcalorimetry. Both methods employ base molecules to examine interactions between surface acid sites and probe base molecules. Generally, basic molecule such as ammonia and pyridine are widely used as probe molecules.

Thermal programmed desorption has been found more effective tool to assess the total number and strength of acid sites **[187]**. The catalyst is activated at required temperature, and then is saturated with probe molecule in vapour form under well-defined adsorption condition. Excess gas is flushed out and the sample is heated in flow of an inert gas. By a thermocouple, the temperature of the catalyst and the composition of the effluent gas may be monitored by adsorption/titration, thermal conductivity, flame ionization or mass spectroscopy. Mass change during heating can also be measured by microbalance.

Microcalorimetry is used to measure the heat evolved during adsorption giving the extent of interaction between sites and base molecules and therefore, the strength of the sites **[188]**. Microcalorimeters are typically connected to volumetric systems with sensitive pressure measurement device for accurately measuring adsorbed amounts. Differential heat of adsorption is obtained by admitting small mount of adsorbate to the adsorbent.

1.8.4.3 Spectroscopic method

FT-IR spectroscopy has been found as most useful instrumental method for acidity measurement and quantification of Bronsted and Lewis sites using a weak basic probe molecule such as ammonia **[114, 169, 187]** or pyridine **[92, 97, 162, 171- 177]**. The FT-IR study using pyridine is most common method to study of surface acidity and distribution of Bronsted and Lewis sites. The base molecules get adsorbed chemically with Bronsted and Lewis sites forming the positively charged species. FT-IR spectra of sulfated-zirconia adsorbed with pyridine show the bands in range of 1400 – 1700 cm^{-1} for adsorbed pyridine at Bronsted and Lewis sites. The pyridine adsorbed at Bronsted sites gives the characteristic bands at 1640, 1607, 1540 and 1490 cm^{-1} **[189]** and the pyridine

adsorbed at Lewis sites gives bands at 1604, 1574, 1490, and 1445 cm^{-1} **[190]**. The band at 1445 cm^{-1} is for pyridine adsorbed at Lewis sites and the band at 1540 cm^{-1} shows the adsorbed pyridine at Bronsted sites. The area of the peak of the band at 1445 and 1540 cm^{-1} give the amount of pyridine adsorbed at Lewis and Bronsted sites respectively and therefore, the amount of Lewis and Bronsted sites. The FT-IR study of the sample adsorbed with basic probe molecule at higher temperature gives the amount of stronger sites.

Besides, the ammonia and pyridine, other weak base probe molecules such as benzene, CD_3CN, CO, etc. have also been used in FT-IR spectroscopic study to estimate the acidity of sulfated-zirconia. Kustov et al. **[160]** used IR spectroscopy to study the acidic properties of sulfated-zirconia. The Bronsted acidity was estimated using benzene. The band shift of OH groups towards low frequency due to hydrogen bonding with benzene molecules was considered as the measure of acid strength of Bronsted sites. Larger the shift, stronger is the acid sites. They found a shift of 200 cm^{-1} in sulfated-zirconia compare to non-sulfated zirconia (100 cm^{-1}) showing the enhancement in acidity after sulfation.

Adeeva et al. **[191]** using FT-IR spectroscopy in presence of CD_3CN as base observed the shift of the OH band towards the lower frequency ($\Delta\nu_{O\text{-}H}$ = 430 cm^{-1}). The shift of OH band towards lower frequency shows the significantly higher acidity of the sulfated-zirconia. Adeeva et al. also estimated Lewis acidity by FT-IR study of sulfated-zirconia after adsorption of carbon monoxide, which showed a band at 2200 cm^{-1}. The shift of the band towards lower frequency shows the acidic strength of the Lewis sites.

NMR-spectroscopy, using a probe molecule such as aniline, trimethyl phosphine, has also been used to assess the acidity of the sulfated-zirconia catalysts **[192, 193]**. Coster et al. **[192]** studied the acidic properties of sulfated-zirconia using trimethyl phosphine as base molecule by carrying out the ^{13}P MAS NMR. The downfield shift was used to measure the acidic strength. The down field shift of ^{13}P MAS NMR lines revealed the presence of stronger Lewis sites in the sulfated-zirconia. However, the Bronsted acidity by ^{13}P MAS NMR study could not be assessed as the lines for the trimethyl phosphine molecule adsorbed with Bronsted sites was also found at same location. Riemer **[194, 195]** reported a ^{1}H MAS NMR study of Bronsted acid strength of sulfated-

zirconia. ^{1}H chemical shift were correlated with the acid strength of surface hydroxy groups. The sulfated-zirconia shows a signal at 5.85 ppm, while a main signal at 3.86 ppm along with a weaker signal at 1.60 ppm is found in the pure zirconia. The downfield shift of the signal for sulfated-zirconia shows higher acidic strength of Bronsted sites.

1.8.5 Thermal analysis

Thermogravimetric analysis (TGA) and differential thermal analysis (DTA) are performed using simultaneous DSC/TGA to study the decomposition pattern and stepwise and total weight loss in the samples. Samples are scanned in given temperature range (50-1000 ^{o}C) with certain heating rate under flow of an inert gas (N_2).

1.8.6 Elemental analysis

As sulfur content decides the acidity as well as the type of acid sites on the surface, sulfur analysis is an important characterization to evaluate the acidity of the catalyst. Percentage of total sulfur retained in sulfated zirconia samples after calcination are analyzed by elemental analyzer and by Inductive Couple Plasma-OES (ICP) analysis.

1.9 Applications of sulfated-zirconia in acid catalyzed reactions

Sulfated-zirconia is having both type of acidity, Bronsted as well as Lewis, on the surface. This is advantageous point about sulfated-zirconia as it can catalyze both type of reactions viz. Bronsted and Lewis catalyzed reactions. The presence of super acidity on the surface is helpful in attaining the reaction intermediates; those are generally not formed in low acidity and also it is capable to catalyze a reaction at low temperature. Since 1979, sulfated-zirconia and promoted sulfated-zirconia (with Ni, Mn, Fe, Pt, etc.) have been receiving much attention, among other solid acids such as clays, zeolites, heteropolyacids and ion exchange resins, due to their superior catalytic activity for hydrocarbon conversions **[14, 94]**. Sulfated-zirconia has numerous applications in oil refinery and petrochemical industries. Sulfated-zirconia gained more popularity among other zirconia based solid acids due to its high activity for isomerization of lower alkanes even at low temperatures. The application of sulfated-zirconia has been reported in literature in many large-scale industrial processes, especially in petroleum industry for

alkylation **[38- 42]**, isomerization **[43- 53]** and cracking reactions **[54, 55]**. Besides it, a number of industrially important organic transformations using sulfated-zirconia have been reported in literature such as alkylation of aromatics, alkylation of alkane with alkenes for gasoline production, acylation of aromatics, isomerization of terpines, etherification, esterification, Fischer-Tropsch reaction, carbonylation etc.. Here few industrially important organic transformations reported to be catalyzed by sulfated-zirconia are given.

1.9.1 Alkylation

Alkylation reactions have been employed industrially for the past 7 decades to produce high-octane gasoline blend stocks, chemical commodities, intermediates and detergents. Alkylation is the electrophilic substitution reaction of aromatics or olefins with alkylating agents in presence of an acid. It is one of the methods for C-C bond formation by substitution on aromatic ring or olefins by alkyl or aryl group. Various solid acid catalysts such as zeolites, sulfated zirconia, clays, silica-alumina, ion-exchange resins and γ-alumina **[195- 200]** are reported in literature for alkylation reactions. Sulfated-zirconia has been found as good catalyst for a number of alkylation reactions. Alkylating agents, generally used, are alkyl halides, alkyl alcohols, aryl halides, aryl alcohols, aryl alkyl ethers, dialkyl ethers, alkenes, etc. The use of halides is avoided because of production of HCl as byproduct in reaction. Alkylation has been reported as Bronsted acid catalyzed reaction. Few examples of alkylation reactions reported on sulfated-zirconia are given below.

1.9.1.1 Alkylation of aromatics with aryl halides

Alkylation of aromatics is an important reaction to synthesize alkyl or aryl substituted aromatics. Sulfated-zirconia has been reported for benzylation of benzene and toluene using benzyl chloride as good solid acid catalyst **[56, 57]** used sulfated-zirconia for the preparation of benzyl toluene by the benzylation of toluene using different alkylating agents such as benzyl chloride, benzyl alcohol and benzyl ether (Figure 6). Though, sulfated-zirconia is an active catalyst for the benzylation of aromatics, the effect of substituents in the substrate and alkylating agent also has been found to be affecting

the reactivity and selectivity. The aromatic substrates having electron donating groups such as alkyl, alkoxy, hydroxy, etc. and alkylating agents having electron attracting groups like halogens on ortho or para positions are more reactive.

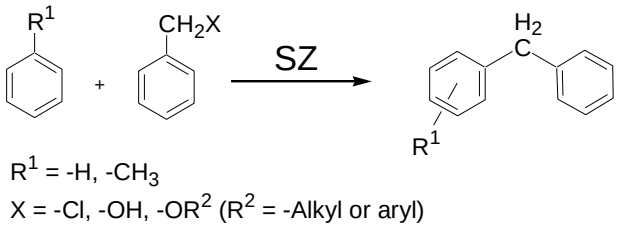

Figure 6. Alkylation of aromatics with benzylating agents using sulfated-zirconia **[56, 57]**.

1.9.1.2 Alkylation of phenols

Alkylation of phenols is an industrially important reaction to synthesize alkylated phenols. Alkylated phenols like *tert.*-butylated hydroxytoluene (BHT) are a well known antioxidant and the basic raw material for the manufacture of oil-soluble phenol-formaldehyde resins. Different types of solid acids used for the butylation of p-cresol include ion-exchange resins, sulfated zirconia, clays, silica-alumina and γ-alumina **[197- 200]**. The *tert.*-butylation of *p*-cresol is generally carried out using *iso*-butylene as alkylating agent, but it has not been found suitable due to the problem of handling and the possibility of a consecutive self polymerization of *iso*-butylene lowering the selectivity of *tert.*-butylated hydroxytoluene. Yadav et al. **[58]** reported the tertiary butylation of *p*-cresol with isobutylene over sulfated-zirconia studying the kinetic parameters, effects of various parameters such as partial pressure of *iso*-butylene, catalyst loading, particle size, and temperature on the rates of reaction (Figure 7).

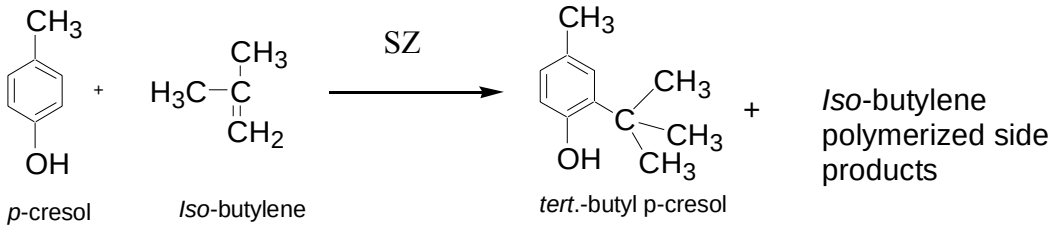

Figure 7. Alkylation of *p*-cresol with *iso*-butylene using sulfated-zirconia **[58]**.

The *tert.*-butanol and methyl *tert.*-butyl ether (MTBE) were found as best alternative of the *iso*-butylene (Figure 8). Yadav et al. **[59]** used a sulfated-zirconia catalyst (UDCaT-1) for tertiary butylation of *p*-cresol using methyl *tert.*-butyl ether as alkylating agent at 100 ºC. This catalyst showed good conversion (45 %) and good selectivity for 2-*tert.*-butyl *p*-cresol (97 %).

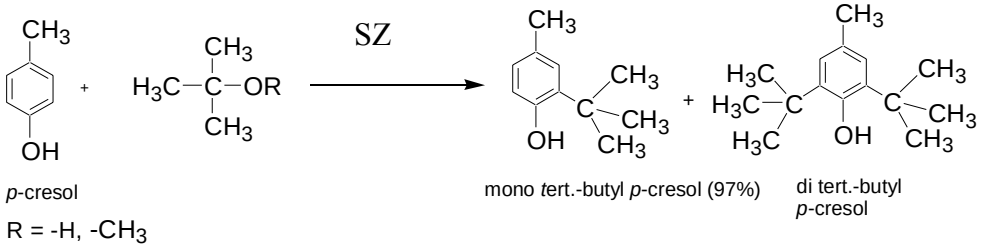

Figure 8. Alkylation of *p*-cresol with *tert.*-butyl alcohol/ methyl *tert.*-butyl ether using sulfated-zirconia **[59]**.

Yadav et al. **[60]** also studied the alkylation of catechol, resorcinol, and anisole with methyl *tert.*-butyl ether over sulfated-zirconia (Figure 9) showing remarkable activity and selectivity of the desired products (4-*tert.*-butyl substituted). The selectivity of the desired product from *tert.*-butylation of catechol and anisole was higher (88 and 70 % respectively) with sulfated-zirconia, while resorcinol results to single product.

Yadav et al. **[61]** studied the alkylation of 4-methoxyphenol with methyl *tert.*-butyl ether over different solid acid catalysts at 150 ºC and 150 psi. Sulfated-zirconia showed lesser activity for the reaction but the selectivity of the desired product (2-*tert.*-butyl hydroxyl phenol) was comparatively higher (85 %) than other catalysts (Figure 10). Vapour phase tertiary butylation of phenol has also been done over sulfated-zirconia using tertiary butyl alcohol as alkylating agent at 200 ºC **[62]**. The conversion of the phenol and the selectivity of the desired product were found excellent with same catalytic activity on repeated use of the catalyst.

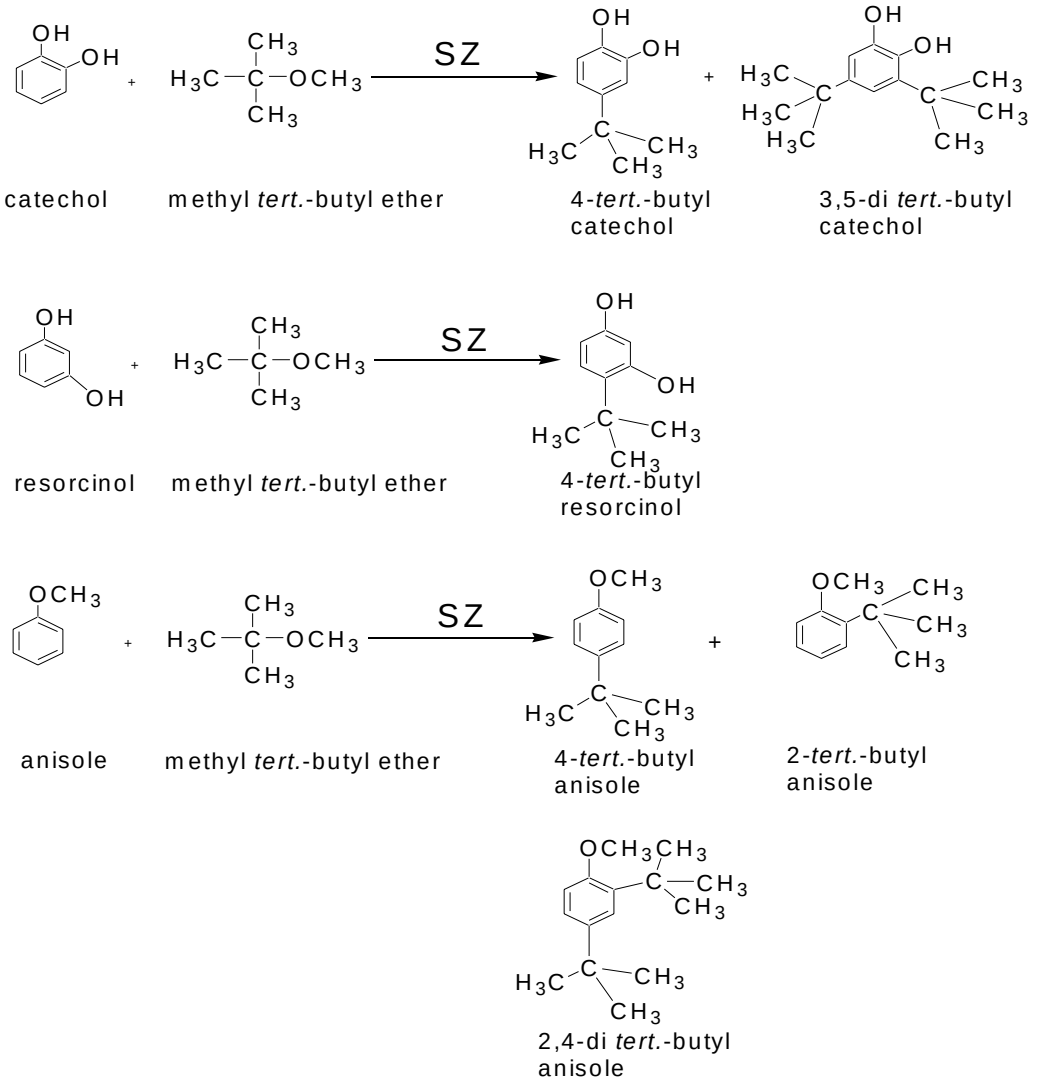

Figure 9. Alkylation of catechol, resorcinol and anisole with methyl *tert.*-butyl ether using sulfated-zirconia **[60]**.

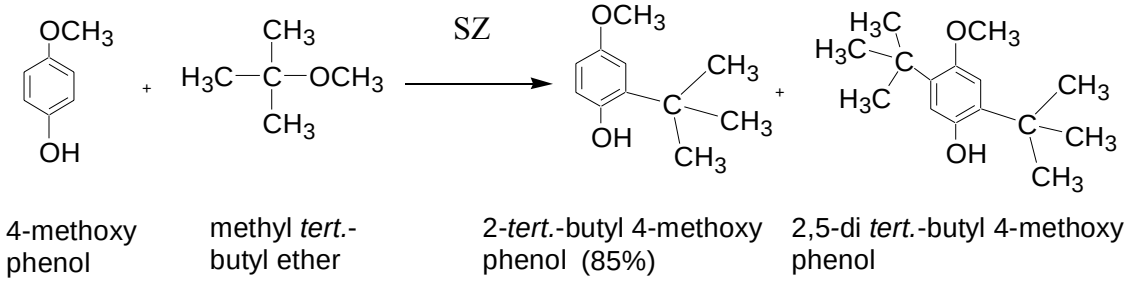

Figure 10. Alkylation of 4-methoxyphenol with methyl *tert.*-butyl ether using sulfated-zirconia **[61]**.

1.9.1.3 Alkylation of o-xylene with styrene

Phenyl xylene ethane is an ingredient of corrosion protective coating of chlorinated rubbers and chlorine containing synthetic resin, as high-energy fuel for jets, turbojets, rockets, missile engines and high stability lubricants. Sulfated-zirconia has been used for the synthesis of phenyl xylene ethane by alkylation of *o*-xylene with styrene **[63]**. Sulfated-zirconia showed similar activity as Nafion-H and cation exchange resin (65 % conversion of *o*-xylene) but the selectivity of desired product (phenylxylylethane) was higher (100 %) in case of sulfated-zirconia (Figure 11).

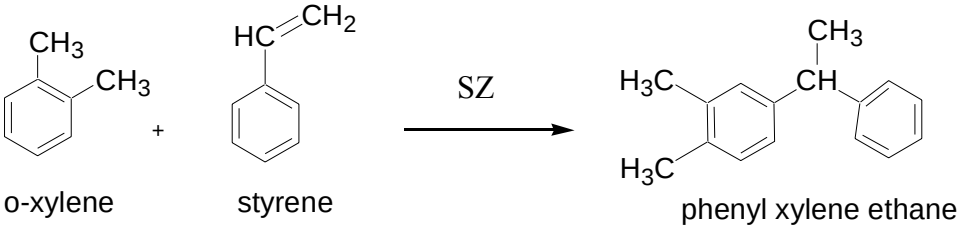

Figure 11. Alkylation of *o*-xylene with styrene using sulfated-zirconia **[63]**.

1.9.1.4 Alkylation of alkanes with alkenes

Alkylation of alkanes with olefins is an industrially important process for production of highly branched paraffins (C_8, mainly trimethylpentanes) used for the production of reformulated gasolines. The high octane number, relatively low volatility, clean burning characteristics, and complete absence of sulfur and nitrogen make alkylate an excellent blending component for reformulated gasoline. Sulfated-zirconia has been found superior to zeolite catalysts for alkylation of *iso*-butane with 1-butene (Figure 12) resulting to 90- 100 % conversion of *iso*-butane at 650 ºC **[38]**. There are two side reactions along with alkylation, oligomerization of alkenes and cracking of alkanes. Low temperature avoids the cracking of alkanes and high acidity inhibits oligomerization of alkenes. Das et al. **[39]** reported the catalytic activity of sulfated-zirconia for alkylation of isobutane with 1-butene in gas phase with excellent conversion of isobutane and selectivity of desired product (2, 2, 4- trimethylpentane).

Clark et al. **[40]** employed carbon dioxide as supercritical solvent for supercritical alkylation of *iso*-butane with 1-butene at temperature (50 ºC) lower than the critical temperature of *iso*-butane (135 ºC) and found 20 % conversion of *iso*-butane at a

space velocity of 0.25 g of 1-butene/ g of catalyst/ hour, a feed CO_2/ *iso*-butane/ olefin molar ratio of 86:8:1, 155 bar. The alkylation of *iso*-butane with 2-butene over sulfated-zirconia has also been studied giving 60- 100 % conversion of *iso*-butane and 69 % selectivity of trimethyl pentane at 150- 250 ºC **[41, 42]**.

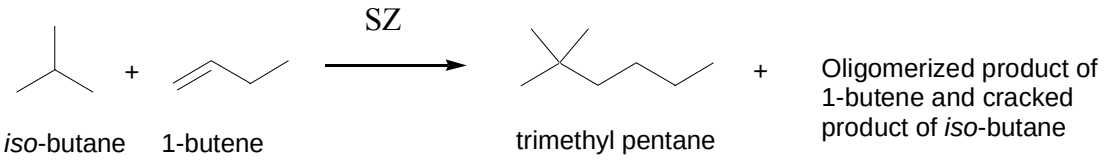

Figure 12. Alkylation of *iso*-butane with 1-butene using sulfated-zirconia **[38]**.

1.9.1.5 Alkylation of aromatics with alkenes

The alkylation of toluene with ethylene to produce ethyltoluenes (Figure 13) is a reaction of significant industrial interest, especially because the polymer poly (*para*-methylstyrene), produced from the *p*-ethyltoluene raw material, has significant property advantages over polystyrene.

Ginosar et al. **[64]** reported the alkylation of toluene with ethylene over solid acid catalysts such as microporous zeolites and mesoporous sulfated-zirconia in liquid, near-critical liquid, and supercritical conditions using propane as the supercritical cosolvent. The sulfated-zirconia exclusively resulted to alkylation (100 %), whereas the zeolites led to both alkylation and cracking/disproportionation activities. The reaction phase had no effect on the activity of the sulfated-zirconia and product selectivity. Alkylation of benzene with higher alkenes such as decene and dodecene is commercially important to produce linear alky benzenes. Sulfated-zirconia has been reported for alkylation of benzene with linear olefins **[65]**.

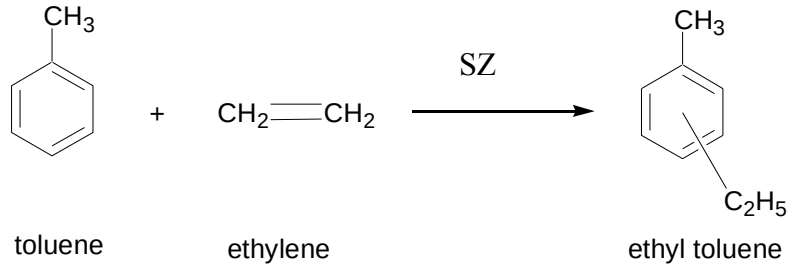

Figure 13. Alkylation of toluene with ethylene using sulfated-zirconia **[64]**.

1.9.1.6 Trans alkylation

Sulfated-zirconia has been used for trans alkylation of di-isopropylbenzene with benzene and substituted benzenes giving 60 % conversion of di-isopropylbenzene at 200 ºC after 2 hours **[66]**. Trans alkylation of di-isopropylbenzene with benzene gives cumene, which is an intermediate in phenol production (Figure 14).

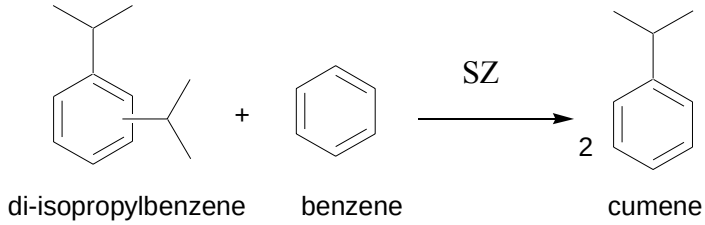

Figure 14. Trans alkylation of di-isopropylbenzene with benzene using sulfated-zirconia **[66]**.

1.9.2 Acylation

Acylation is an important reaction to synthesize different type of aromatic ketones finding use as drug intermediates, fine chemicals, flavors, fragrances, pesticides, dyes, etc. industrially important chemicals. Acylation is the electrophilic substitution by acyl group in presence of an acid, involving a carbocation intermediate. Sulfated-zirconia has been reported as active catalyst for acylation of aromatics. Acylating agents, generally used, are acid anhydrides, acid halides and carboxylic acids. Acylation has been reported as Lewis acid catalyzed reaction. Some acylation reactions reported on sulfated-zirconia are given below.

1.9.2.1 Acylation of aromatics with different acylating agent

Acylation of benzene with *p*-chlorobenzoyl chloride results to *p*-chlorobenzophenone, which is useful as fine chemical and drug intermediate for synthesis of Cytrazin. Yadav et al. **[67]** reported the acylation of benzene with *p*-chlorobenzoyl chloride over sulfated-zirconia with good yield (80- 90 %) and 100 % selectivity of the desired product (*p*-chloro benzophenone). Acylation of benzene with *p*-chlorobenzoyl chloride was tried with different solid acid catalysts such as dodecatungstophosphoric acid, clay, Amberlite, Amberlyst-15, Indion-130, Filtrol-24 clay, and sulfated zirconia.

Sulfated-zirconia was one among other solid acids to be active giving 100 % selective of *p*-chlorobenzophenone (Figure 15).

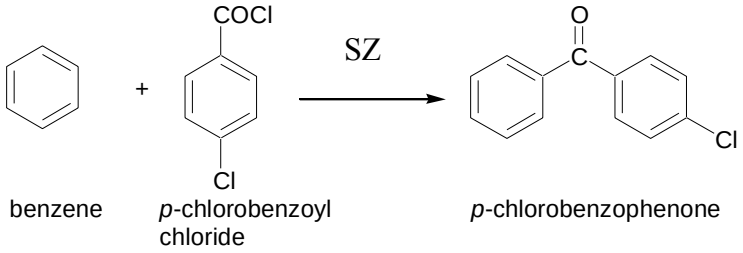

Figure 15. Acylation of benzene with *p*-chlorobenzoyl chloride using sulfated-zirconia **[67]**.

Acylation of benzene and toluene are important reactions for synthesis of acetophenone and *p*-methyl acetophenone respectively finding application as perfume, pharmaceutical, solvent, etc. Hino et al. **[68]** reported vapour phase acylation of benzene and toluene with acetic acid to synthesize acetophenone (25 %) and *p*-methyl acetophenone (45 %) respectively.

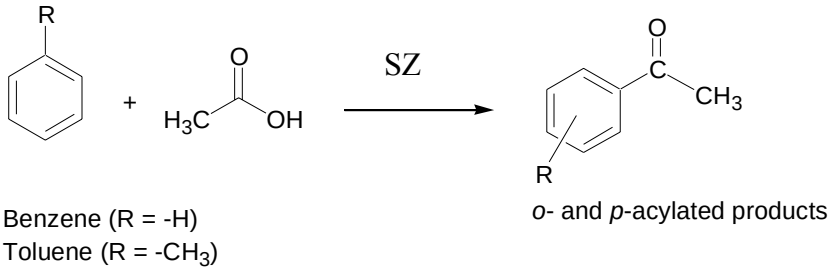

Figure 16. Acylation of benzene and toluene with acetic acid using sulfated-zirconia **[68]**.

The acylation of different aromatic substrates (anisole, *o*-xylene, *m*-xylene and *p*-xylene) with acid anhydrides (Figure 17) over sulfated-zirconia has been reported with good yield of respective ketones **[69]**. Deutsch et al. **[70]** studied the effect of different acylating agents on the rate of acylation of aromatics. Acetic anhydride and benzoic anhydride were found to be reacting faster than benzoyl chloride.

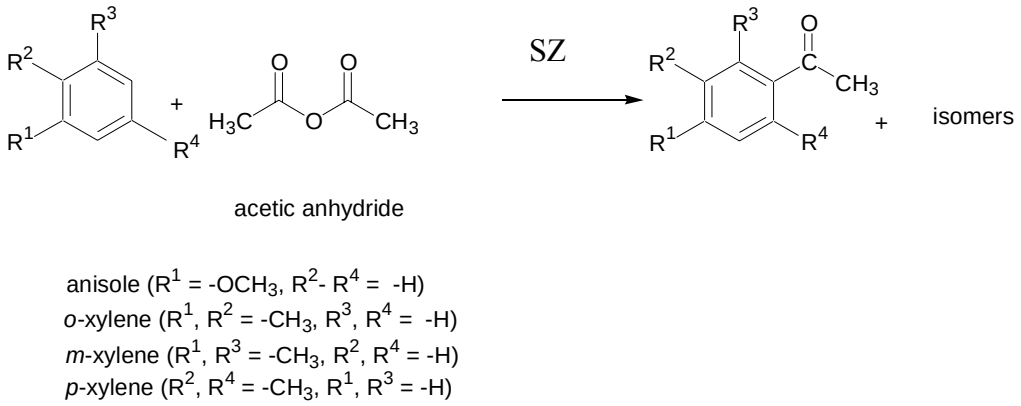

Figure 17. Acylation of different aromatics with acetic anhydride using sulfated-zirconia **[69]**.

Trunschke et al. **[71]** reported the benzoylation of anisole with benzoic anhydride over sulfated-zirconia with higher yield of *p*-acylated product studying the deactivation and regeneration of the catalyst.

Acylation of benzo- 15-crown-5 (B15C5) crown ether by acetic anhydride (Figure 18) in the absence of solvent was reported with 70 % yield of acylated product in 2 hours **[72]**. The acylated product is a key intermediate for a variety of technological products such as complexants for the separation of radioactive cations, ionophore antibiotics and phase transfer catalysts.

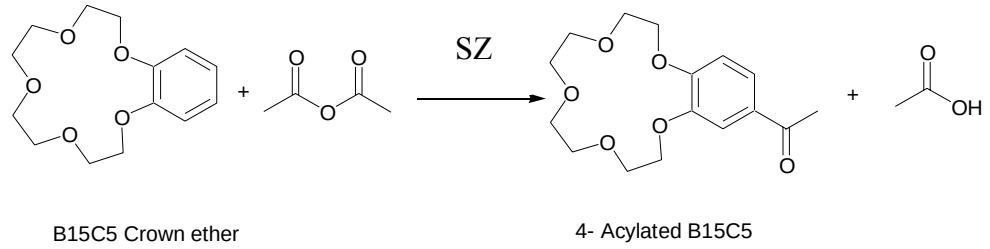

Figure 18. Acylation of benzo- 15-crown-5 (B15C5) crown ether with acetic anhydride using sulfated-zirconia **[72]**.

Deutsch et al. **[73]** studied the acylation of different aromatic compound on sulfated-zirconia using acetic anhydride, benzoic anhydride and benzoyl chloride as acylating agent and the reactivity of the aromatic compounds (Figure 19). The reactivity decreases in the following order: anisole > mesitylene > 3-chloroanisole ~ *m*-xylene ~ 2-

chloroanisole > toluene for benzoylations on sulfated-zirconia. The sulfated-zirconia was found to be highly active for benzoylation of anisole resulting to 95 % yield of ketonic product.

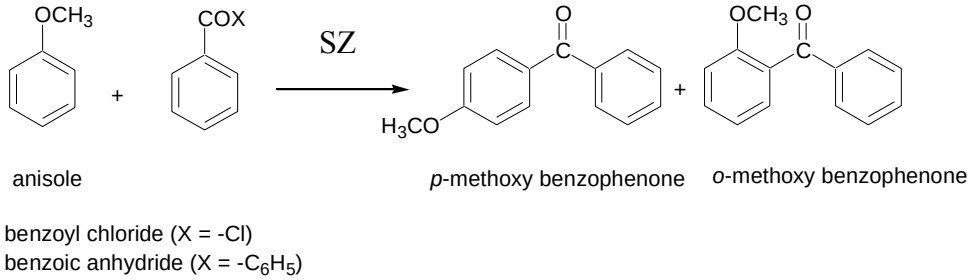

Figure 19. Benzoylation of anisole with benzoyl chloride and benzoic anhydride using sulfated-zirconia **[73]**.

1.9.2.2 Acylation of phenols

2, 4-dihydroxy acetophenone is an important compound and finds application as drug intermediate (allergy therapeutic agents), perfumes, fine chemical, cosmetics (UV-screening), food preservatives and in spectrophotometric determination of iron. Sulfated-zirconia has been reported for acylation of resorcinol with acetic acid giving 6 % conversion of resorcinol with 43 % selectivity of resorcinol acetophenone **[74]**. The reaction (Figure 20) involves O-acylation of phenol followed by Fries rearrangement to give C-acylated product (2, 4-dihydroxy acetophenone).

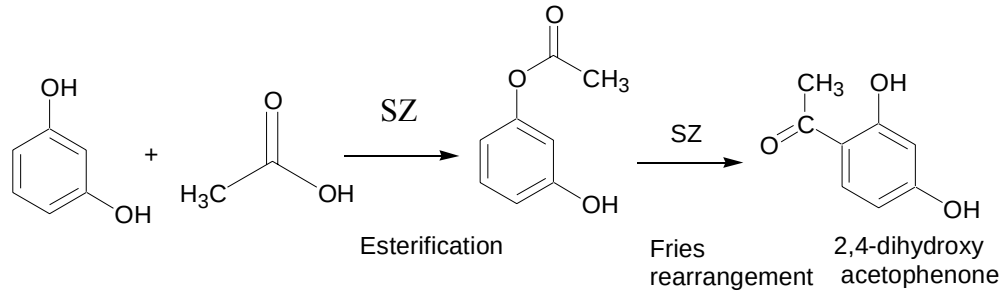

Figure 20. Acylation of resorcinol with acetic acid using sulfated-zirconia **[74]**.

1.9.3 Isomerization

Sulfated-zirconia has been found as an excellent catalyst for isomerization reactions and to catalyze a number of isomerization reactions of industrial importance. Isomerization is reported as Bronsted acid catalyzed reaction. Few isomerization reactions reported on sulfated-zirconia are given below.

1.9.3.1 Isomerization of n-alkanes to branched alkanes

It is an industrially important reaction for production of high octane branched hydrocarbons from straight chain hydrocarbons for blending with gasoline. Isomerization of *n*-alkanes to branched alkanes requires super acidity under mild conditions. Yamaguchi **[11]** reported the higher activity of sulfated-zirconia for isomerization of *n*-butane at ambient temperature (Figure 21).

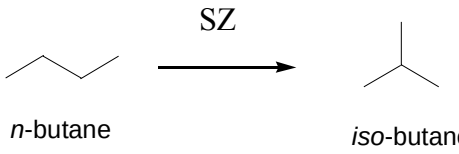

Figure 21. Isomerization of *n*-butane to *iso*-butane using sulfated-zirconia **[11]**.

Isomerization of *n*-alkanes by sulfated-zirconia and modified sulfated-zirconia has been studied by many researchers **[43, 48]**. However, sulfated-zirconia shows low selectivity and rapid deactivation due to coking of catalytic sites. The use of platinum increases the stability of the catalyst towards deactivation and also increases the selectivity. The isomerization of higher straight chain hydrocarbons (C > 10) to branched products with conversion of 60- 80 % and selectivity of 60 % has also been studied **[49]**. Grau et al. **[50]** reported sulfated-zirconia for hydroisomerisation-cracking of *n*-octane to light paraffins.

Farcasiu et al. **[51]** have reported the sulfated-zirconia for isomerization of methyl cyclopentane to cyclohexane at 65 ºC and found that the catalysts, having sulfur content of around 3 wt.%, were more active (Figure 22).

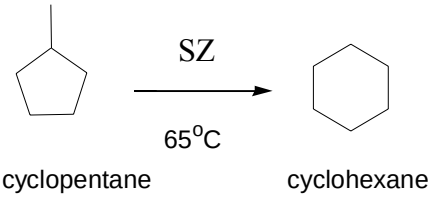

Figure 22. Isomerization of methyl cyclopentane to cyclohexane using sulfated-zirconia **[51]**.

Suh et al. **[52]** reported the isomerization of *n*-butene over microporous sulfated-zirconia with higher selectivity (~20 %) of *iso*-butene at 450 ºC. The micropores (5 Å) of sulfated-zirconia were observed to be resulting to the high selectivity of *iso*-butene. Other products such as propene and pentene were formed by the oligomerization-cracking reactions.

Funamoto et al. **[53]** reported isomerization of *n*-butane over sulfated-zirconia under supercritical condition. At atmospheric pressure, isomerization of light alkanes over solid acid catalysts results to fast deactivation of catalyst due to coke formation on the active sites. In supercritical condition of reactant and product, for the isomerization of *n*-butane over sulfated zirconia at optimized condition (215 ºC, 4.0 MPa), no significant deactivation of the catalyst was found.

Li et al. **[54]** synthesized catalytically active sulfated-zirconia catalysts by gaseous sulfation of crystalline zirconia with gaseous SO_3 for isomerization of *n*-butane. They observed the higher catalytic activity of sulfated-zirconia prepared by sulfation of crystalline zirconia with gaseous sulfur trioxide compare to sulfated-zirconia prepared by conventional sulfation with sulfuric acid due to the presence of labile sulfate species resulting to higher Bronsted acid sites on the surface.

1.9.3.2 Isomerization of epoxides to aldehydes

This is a commercially important reaction to prepare perfumery aldehydes and their acetals. It involves the acid catalyzed epoxide ring-opening step. The selectivity of the desired product is very low and it depends on the nature of the catalyst. Yadav et al. **[84]** reported sulfated-zirconia for epoxide ring opening of 1, 2-epoxyoctane showing 20 % conversion to a number of products such as 1-octanal, methyl hexyl ketone, furan, 2-

octanene-1-ol, 3-octene-1-ol (cis), 3-octene-1-ol (trans) and the products of aldol condensation (Figure 23).

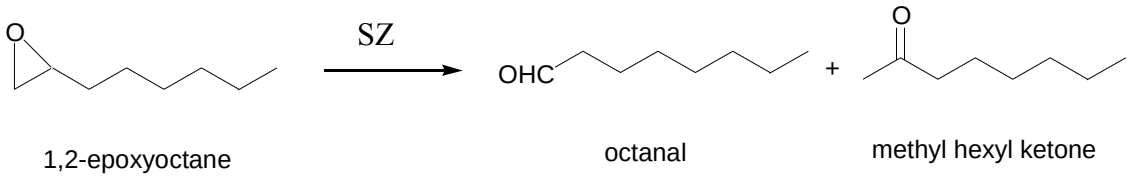

Figure 23. Isomerization of 1, 2-epoxyoctane using sulfated-zirconia **[84]**.

1.9.3.3 Isomerization of terpines

Sulfated-zirconia has been found as an active catalyst for isomerization of various terpines for preparing perfumery chemicals. Yadav et al. and Chuah et al. **[85, 86]** have reported the isomerization of isopulegol from citronellal with sulfated-zirconia giving 97 % conversion and 52- 65 % selectivity (Figure 24). Tanabe et al. **[87]** reported the isomerization of terpinolene over sulfated-zirconia with 65 % conversion and 78 % selectivity. Grzona et al. **[88]** studied the isomerization of α-pinene over sulfated-zirconia.

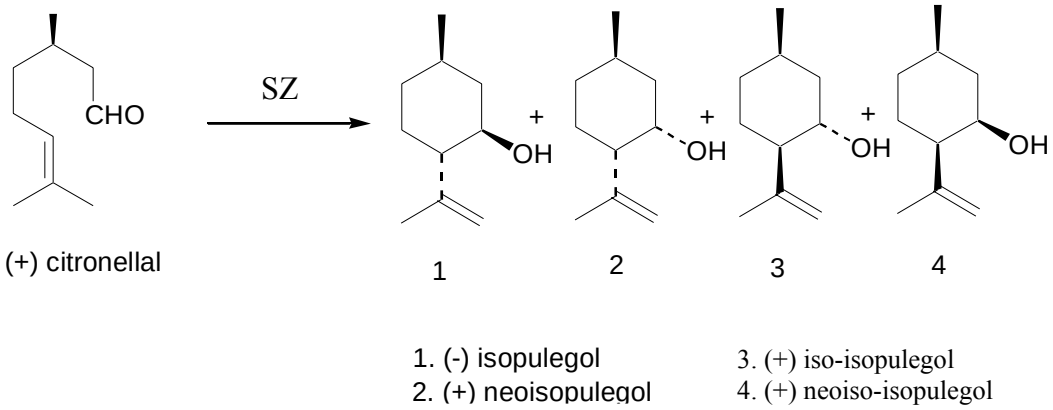

Figure 24. Isomerization of (+) citronellal to (-) isopulegol using sulfated-zirconia **[85, 86]**.

1.9.4 Esterification

Esters are having pleasant smell, so they are widely employed as flavour and perfumery chemicals. Sulfated-zirconia has been tested for a number of esterification reactions **[75- 78]**. Yadav et al. **[79]** reported the sulfated-zirconia as an active solid acid catalyst for esterification of phenethyl alcohol and cyclohexanol with acetic acid (Figure 25).

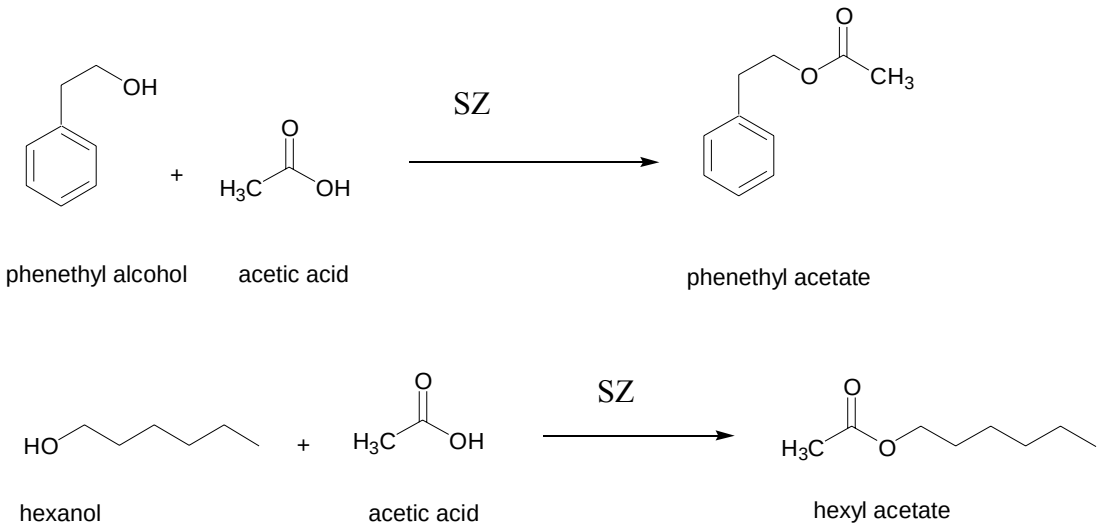

Figure 25. Esterification of phenyl alcohol and hexanol with acetic acid using sulfated-zirconia **[79]**.

The sulfated-zirconia has been reported an active solid acid catalyst for the esterication of 2-ethylhexanol with phthalic anhydride to dioctyl phthalate (Figure 26), which is an industrially important plasticizer **[80, 81]**.

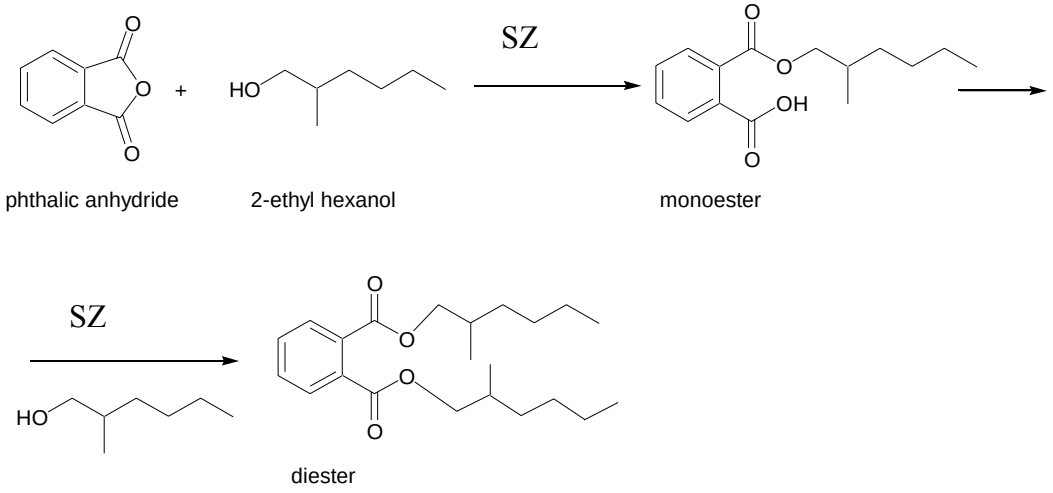

Figure 26. Esterification of phthalic anhydride with 2-ethyl hexanol using sulfated-zirconia **[80, 81]**.

1.9.5 Etherification

Sulfated-zirconia has been found to be active for the etherification reactions to produce ethers of industrial importance. The methyl *tert.*-butyl ether is gasoline oxygenate, which is produced by etherification of *tert.*-butyl alcohol with methanol (Figure 27). The side reactions, along with etherification, are dehydration of *tert.*-butanol to *iso*-butene and formation of dimethyl ether, whish reduce the selectivity of methyl *tert.*-butyl ether. Quiroga et al. **[82]** carried out etherification of *iso*-butene with methanol using sulfated-zirconia at 90- 110 ºC to produce methyl *tert.*-butyl ether.

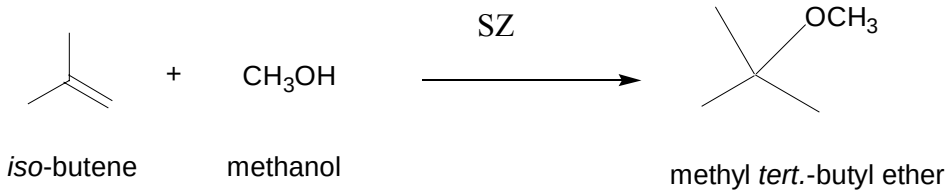

Figure 27. Etherification of *iso*-butene with methanol using sulfated-zirconia **[82]**.

The tetrahydropyranylation is an etherification reaction, which is generally used to protect hydroxyl groups in organic synthesis. Reddy et al. **[83]** reported tetrahydropyranylation for protection of hydroxyl groups with 3, 4-dihydro-2H-pyran (DHP) over sulfated-zirconia under solvent free conditions at low reaction times showing excellent yield of the product ranging from 82- 96 % with 100 % selectivity (Figure 28).

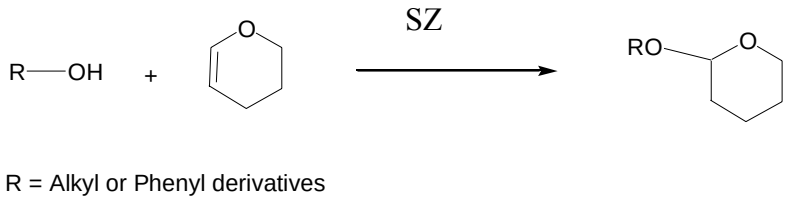

Figure 28. Tetrahydropyranylation of hydroxy compounds with 3, 4-dihydro-2H-pyran using sulfated-zirconia **[83]**.

1.9.6 Nitration

The para-nitrated products of substituted benzene are of industrial interest, which is generally prepared by nitration of substituted benzene with a mixture of nitric acid and sulfuric acid. The use of solid super acids avoids the problem of spent acid

disposal and increase para selectivity. Sulfated-zirconia has been used to nitrate chlorobenzene (Figure 29) with nitric acid and acetic anhydride mixture giving 100 % conversion and high para selectivity of 77 % **[89]**.

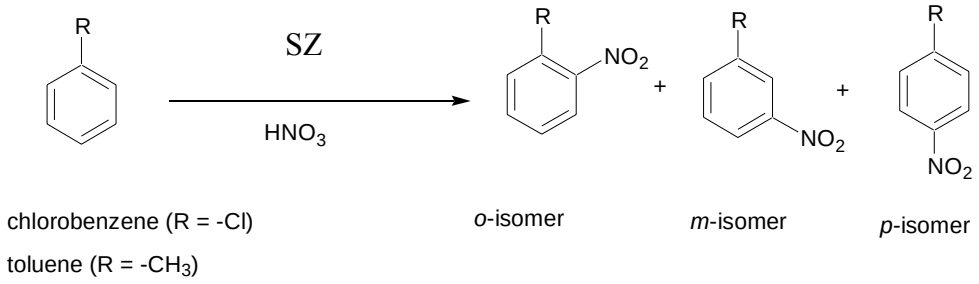

Figure 29. Nitration of aromatics using sulfated-zirconia **[89]**.

1.9.7 Oligomerization

Oligomerization is industrially important acid catalyzed reaction. The products of oligomerization of hexene and heavier olefins are important for synthetic fuel producers to reduce refinery complexity, as well as to produce good quality middle distillates and lubricating oils. Akio et al. **[90]** reported the oligomerization of 1-decene over sulfated-zirconia. A. de Klerk **[91]** studied the oligomerization of 1-hexene and 1-octene over different solid acid catalysts such as amorphous silica-alumina, sulfated-zirconia, MCM-41, and the zeolites ZSM-5, Y and Omega to identify the catalyst properties required for higher olefin oligomerization. Sulfated-zirconia was found to be active solid acid catalyst for oligomerization showing higher selectivity of (C_{12}) desired product (80- 90 %).

Summary of present work

The present thesis consists of six chapters having below discussed contents.

The first chapter of the thesis contains acid catalysis, advantages of solid acid catalysts over conventional homogeneous acid catalysts, introduction of sulfated-zirconia, synthesis methods, effect of synthetic parameters on physicochemical and catalytic properties, structural models of the surface sulfate species, generation of acidity, type of acidity, characterization techniques and applications in different acid catalyzed organic transformations.

The second chapter discusses the synthesis and characterization of a series of nano-crystalline sulfated-zirconia by two-step sol-gel technique using zirconium propoxide as a precursor with varying synthetic parameters. The effect of the synthetic parameters namely precursor concentration, hydrolyzing agents, stirring mode, drying temperature, time and calcination temperature on the physical and catalytic properties of the catalysts are studied. The nature of sulfate species having S$^{+\cdots}$O ionic structure and S=O covalent structure is ascertained by FT-IR spectroscopy. Presence of S=O covalent structure is semi-quantified by DRIFT spectroscopy at different temperatures and is correlated with the catalytic activity for benzylation of toluene. The amount of bulk sulfur and the nature of sulfate species on the surface are observed to have significant influence on the catalytic activity of the samples. The activity of the catalysts prepared is studied for the benzylation of toluene with the benzyl chloride as a benzylating agent.

The third chapter extends the synthesis of nano-crystalline sulfated-zirconia using two-steps as well as one-step sol-gel technique in acidic, basic and neutral medium studying the effect of mode addition of sulfuric acid during hydrolysis in one-step and two-step synthesis, water to alkoxide molar ratio, pH of hydrolysis medium on the textural, structural, acidic and catalytic properties of sulfated-zirconia. The catalytic performance is studied by acylation of anisole and veratrole with acetic anhydride as an acylating agent. The reaction conditions such as reaction temperature, reaction time, molar ratio of reactants and substrate to catalyst weight ratio for acylation were optimized.

The fourth chapter describes the study on the isomerization of longifolene to isolongifolene with nano-crystalline sulfated-zirconia samples, synthesized by the one-

and two-steps sol-gel method. The detailed study on the optimization of reaction parameters such as reaction temperature, substrate/catalyst weight ratio and reaction time is done. The kinetic study of the isomerization reaction is studied to determine the order of reaction, rate constant and activation energy. The further isomerization of isolongifolene to tetraline derivative and other products with nano-crystalline sulfated-zirconia was also studied. The physico-chemical properties of sulfated-zirconia responsible for the further isomerization of isolongifolene were investigated.

The fifth chapter consists of the application of the nano-crystalline sulfated-zirconia, synthesized by one-step and two-step sol-gel methods, for the synthesis of the 7-substituted 4-methyl coumarins such as 7-amino 4-methyl coumarin and 7-hydroxy 4-methyl coumarin from activated phenols namely *meta*-amino phenol and *meta*-hydroxy phenol respectively and ethyl acetoacetate. The detail study of the reaction to optimize the reaction parameters such as temperature, reactants molar ratio, substrate/catalyst weight ratio and solvent effect is done to obtain the maximum conversion. The microwave assisted synthesis of 7-hydroxy 4-methyl coumarin is also discussed.

The sixth chapter of the thesis comprises of the conclusions and summary of the work done for the synthesis and characterization of the nano-crystalline sulfated-zirconia using sol-gel technique and their catalytic performance in different acid catalyzed reactions studied.

Chapter 2

Structural, Textural, and Catalytic Properties of Nano-crystalline Sulfated Zirconia Prepared by Two-step Sol-Gel Technique

2.1 Introduction

The physicochemical properties such as structural, textural and therefore, the catalytic properties of sulfated-zirconia are affected by the method of synthesis and synthetic parameters, which has been widely studied by different research groups **[38, 92-95, 106- 122]**. There are several synthetic parameters influencing the catalytic properties of sulfated-zirconia, however the effects of synthetic parameters particularly the zirconia precursor **[106]**, the sulfation procedure **[95]**, and the calcination treatment **[110, 201]** on catalytic activity has been thoroughly discussed in the literature. It is important to select an appropriate method and to optimize the synthetic parameters to synthesize a good catalyst of improved catalytic properties. The sol-gel method has been found to be appropriate route to synthesize purely nano-crystalline, high surface area porous material and is advantageous due to the ease of control of homogeneity and physical properties **[142]**. The sol-gel technique has been widely used for the synthesis of sulfated-zirconia **[111- 122]**. Sulfated-zirconia synthesized by the sol-gel technique shows improved properties showing nano-crystalline predominantly tetragonal phase **[157]**, higher sulfur content **[119]**, higher concentration of anionic vacancies **[126]**, and improved catalytic activity **[70, 113]**. The studies show that the sol-gel parameters such as precursor concentration, drying, and calcination temperature significantly affect the important properties of sulfated-zirconia **[111- 115, 120]**. The most of the sol-gel parameters have been studied and found to have a significant influence on the variation of the physicochemical and catalytic properties. However, the effects of physical perturbation on the structural and textural and thus the catalytic activity of sulfated zirconia have not yet been studied. The physical perturbation during the hydrolysis and condensation steps can influence the structural, textural and catalytic properties of sulfated-zirconia.

In this chapter, a series of sulfated-zirconia samples were synthesized by a two-step sol-gel technique using zirconium propoxide as a precursor, aqueous ammonia as hydrolyzing agent and sulfuric acid (1N) as sulfating agent. The effect of different synthetic parameters such as concentration of precursor, mode of physical perturbation, drying temperature, and calcination temperature on the structural (crystallinity, nature of surface sulfate group and average crystallite size), textural (surface area and pore size

distribution) and catalytic properties of sulfated-zirconia catalysts for benzylation of toluene with benzyl chloride was studied.

2.2 Experimental

2.2.1 Materials

Zirconium propoxide [$Zr(OC_3H_7)_4$] (70 wt. % solution in *n*-propanol) was procured from Sigma-Aldrich, USA, concentrated H_2SO_4, *n*-propanol, aqueous ammonia (25 %), toluene and benzyl chloride were from s.d. Fine Chemicals, India, and were used as such without any further purification.

2.2.2 Catalyst synthesis

Sulfated-zirconia samples were synthesized by using a two-step sol-gel technique. The zirconium propoxide in *n*-propanol was hydrolyzed by drop wise addition of distilled water at pH 7 or aqueous ammonia at pH 9- 10 at room temperature under continuous stirring. Two concentrations of the zirconium propoxide of 70 and 10 wt. % in *n*-propanol were used for synthesis and 1:4 molar ratio of zirconium propoxide to water was used for hydrolysis. During the hydrolysis and condensation, the effect of physical perturbation on the properties of the catalysts was studied and was carried out by ultrasonication or magnetic stirring. Ultrasonication was performed by an ultrasonicator (Cole Parmer model 8891) having 47 kHz sound wave frequency for 30 to 120 min. Magnetic stirring was done by a magnetic stirrer (Mirak Thermolyne) at around 1100 rpm for 2 to 8 h. The gel was filtered and dried at room temperature and then at 80 or 110 ºC for 12 h to remove the solvent from the pores of the gel. The dried gel was powdered (170 mesh) and sulfated with concentrated H_2SO_4 by pouring the powdered dried gel in concentrated H_2SO_4 solution (1N) under stirring for 30 min. (15 ml H_2SO_4 solution (1N) was taken for sulfation of 1 gm powdered dried gel). The sulfated gel was filtered and dried at room temperature and then at 110 ºC for 12 h to completely evaporate the water from the gel. Samples were calcined at different temperatures ranging from 400 to 600 ºC for 3 h in a muffle furnace in static air atmosphere.

The synthesis parameters, studied during the synthesis of all the sulfated-zirconia samples, are summarized in Table 1. The samples are named as SZ, which stands for sulfated-zirconia, numbers 1-14 are serial number of laboratory experiments. MS and US represent magnetic stirring and ultrasonication respectively.

Table 1. Synthetic parameters of sulfated-zirconia samples.

Sample	Zr. Propoxide Conc. (wt %)	Hydrolyzing agent	Stirring mode and time (h)	Drying Temp. (°C)	Calcination Temp. (°C)
SZ-1	70	(H_2O + NH_3) mixture	MS (2)	RT (25)	600
SZ-2	70	(H_2O + NH_3) mixture	MS (2)	80	600
SZ-3	70	(H_2O + NH_3) mixture	MS (8)	110	600
SZ-3	70	(H_2O + NH_3) mixture	MS (8)	110	500
SZ-4	10	Aq. NH_3	MS (8)	110	500
SZ-7	10	Aq. NH_3	US (1/2)	110	600
SZ-6	10	Aq. NH_3	US (1)	110	600
SZ-11	10	Aq. NH_3	US (2)	110	600
SZ-14	70	Aq. NH_3	US (2)	110	600

2.2.3 Catalyst characterization

The sulfated-zirconia samples were characterized by XRD, FT-IR, DRIFT, N_2 adsorption desorption isotherm, Thermal analysis and elemental sulfur analysis.

2.2.3.1 X-ray Powder Diffraction studies

The identification of the crystalline phase formed and measurement of the crystallinity of the phase in sulfated-zirconia and pure zirconia were carried out by X-ray powder diffractometer (Philips X'pert) using CuKα radiation (λ = 1.5405 Å). The samples were scanned in 2θ range of 0 to 70° at a scanning rate of 0.4 degree/second. Crystallite size of the tetragonal phase was determined using XRD data from characteristic peak (2θ) 30.5° for the (111) reflection of maximum intensity using the Scherrer formula **[182]**,

Crystallite size = K.λ /W.cosθ

Where, K is shape factor and is equal to 0.9 and W is the difference of broadened profile width of experimental sample (Wb) and standard profile width of reference silicon sample (Ws).

The tetragonal and monoclinic phases present in the samples were quantified **[202]** by comparing the areas of the characteristic peaks of the tetragonal phase (2θ at 30.5º for the (111) reflection) and the monoclinic phase (2θ at 28.6º and 31.6º for $(11\bar{1})$ and (111) reflection, respectively). The percent composition of each phase was calculated from the areas, *hw*, where h and w are the height and the half width of the characteristic peaks as given below,

% tetragonal = [(*hw*) tetragonal/ Σ (*hw*) tetragonal and monoclinic] X 100

% monoclinic = [(*hw*) monoclinic/ Σ (*hw*) tetragonal and monoclinic] X 100

2.2.3.2 FT-IR Studies

The structure of sulfur species present on the surface of oxide and nature and bonding of sulfate group with the zirconia surface before and after calcination at different temperatures were studied by FT-IR spectrophotometer (Perkin-Elmer GX spectrophotometer). The spectra were recorded in the range 400-4000 cm^{-1} with a resolution of 4 cm^{-1} as KBr pellets.

Diffuse Reflectance FT-IR (DRIFT) Studies

Diffuse reflectance FT-IR (DRIFT) studies of the sulfated-zirconia samples were done to observe the effect of *in-situ* heating on the nature of the surface sulfate group and to access the Lewis acid sites present in the sample, which could not be observed by recording FT-IR spectra at room temperature. DRIFT study was carried out using an FT-IR spectrophotometer equipped with The Selector DRIFT accessory (Graseby Specac, P/N 19990 series) incorporating an environmental chamber (EC) assembly (Graseby Specac, P/N 19930 series) connected with an automatic temperature controller (Graseby Specac, P/N 19930 series) for heating and water circulator for cooling. The sulfated-zirconia sample was mixed with KBr (~1 wt.%) and the spectra

were recorded. The reference spectrum was recorded with KBr. The spectra were recorded at room temperature and after in situ heating at different temperatures from 150 to 450 ºC with heating rate of 25 ºC/min, keeping the samples at each temperature for 30 min, at 1 atm pressure under flow of dry N_2 (30 cm^3/min). Typically, 30 scans were co-added at a resolution of 4 cm^{-1}.

2.2.3.3 N_2 adsorption-desorption isotherm studies

Textural properties such as specific surface area, pore volume, pore size and pore size distributions of sulfated-zirconia and pure zirconia samples were determined from N_2 adsorption-desorption isotherm studies at liquid nitrogen temperature (77 K) by ASAP 2010, Micromeritics, USA. Surface area and pore size distribution in the samples were determined using the BET equation and BJH method **[183]** respectively. Before the analysis, the samples were degassed under vacuum at 120 ºC for 4 h to evacuate the physiosorbed moisture.

2.2.3.4 Thermal Analysis

Thermogravimetric analysis (TGA) and differential thermal analysis (DTA) were performed using simultaneous DSC/TGA (TA Instruments, model SDT 2960). Samples were exposed in the temperature range of 25-900 ºC with a heating rate of 10 ºC/min under air flow (100 cm^3/min).

2.2.3.5 Sulfur Analysis

Percentage of sulfur retained in sulfated zirconia samples after calcination was analyzed by a CHNS/O elemental analyzer (Perkin-Elmer, 2400).

2.2.3.6 Catalytic Activity

The catalytic activity of the sulfated zirconia samples was tested by carrying out the benzylation of toluene with benzyl chloride in liquid phase batch reactor. In a double neck round bottom flask, toluene (20 mmol) and benzyl chloride (20 mmol) were taken and the preactivated catalyst, at 450 ºC for 2 h, was added to the reaction mixture with

toluene to catalyst weight ratio 10. The reaction was carried out at 110 ºC, maintained in oil bath, in N_2 atmosphere under continuous stirring of reaction mixture at 600 rpm by magnetic stirrer. The reaction was monitored by analyzing the reaction mixture using gas chromatography (HP6890) having a HP50 (30 miter long) capillary column with a programmed oven temperature from 50 to 200 ºC, a 0.5 cm^3/min flow rate of N_2 as carrier gas and FID detector. The conversion of toluene was calculated by using weight percent method; the initial theoretical weight percent of toluene was divided by initial GC peak area percent to get the response factor. Final unreacted weight percent of toluene remaining in the reaction mixture was calculated by multiplying response factor with the area percentage of the GC peak for toluene obtained after the reaction.

The conversion was calculated as follows:

Response factor = Initial theoretical weight percent of toluene/ Initial GC peak area percent of toluene before reaction.

Final unreacted weight percent of toluene = Response factor X Final GC peak area percent of toluene after reaction.

$$\text{Conversion (wt \%) of toluene} = \frac{100 \text{ X [Initial wt\% - Final wt\%]}}{\text{Initial wt\%}}$$

$$\text{Selectivity of } p\text{-benzylated toluene (wt. \%)} = \frac{100 \text{ X [GC peak area\% of } p\text{-benzylated toluene]}}{\sum \text{ Total GC peak area \% for all the products}}$$

The kinetic study of benzylation of toluene with benzyl chloride was performed over one of the sulfated-zirconia samples, SZ-14, which showed maximum activity, to get the optimum time for the maximum conversion. The kinetic study shows that the reaction is completed within 4 h. Therefore, the reaction with other sulfated-zirconia catalysts was carried out for 4 h.

2.2.3.7 Regeneration study

The regeneration of spent catalyst was done by washing with acetone to remove the adsorbed reactants and products followed by activation at 450 ºC for 2 h in static air

atmosphere. The catalytic activity of the regenerated catalyst was tested by carrying out the benzylation of toluene with benzyl chloride under similar reaction condition as was done with fresh catalyst.

2.3 Results and Discussion

2.3.1 Structural Properties

2.3.1.1 Crystalline Phase

X-ray diffraction patterns of pure zirconia (ZrO_2) samples before calcination (dried at 110ºC) and after calcination at temperatures of 400, 450, 500 and 600 ºC are given in Figure 1.

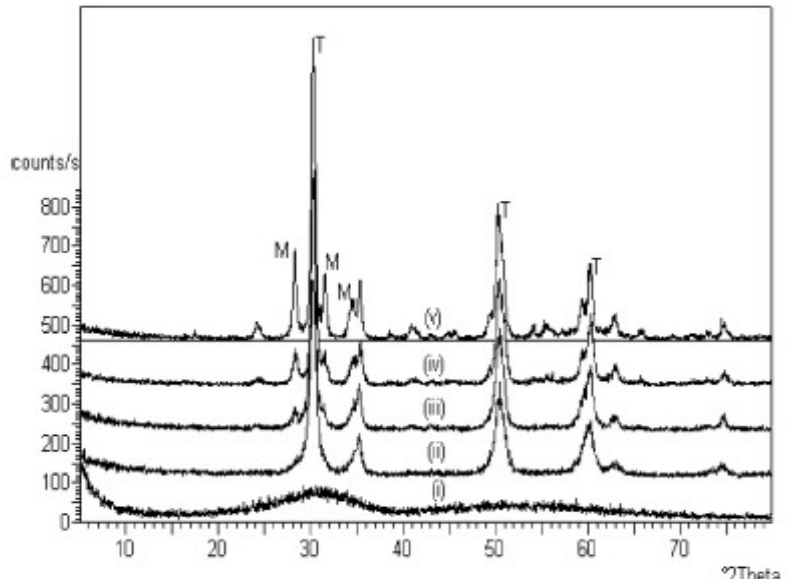

Figure 1. X-ray diffraction patterns of ZrO_2 samples (i) before calcination (110 ºC) and after calcination at (ii) 400, (iii) 450, (iv) 500 and (v) 600 ºC.

The sample before calcination was amorphous in nature. The sample, calcined at 400 ºC, was crystalline and showed purely tetragonal phase, whereas the samples calcined at above 400 ºC had monoclinic phase also along with tetragonal phase. Percent compositions of crystalline phases in samples at different calcination temperatures are

given in Table 2. The monoclinic phase gradually increased from 4 to 29 % with an increase in the calcination temperature from 450 to 600 ºC. It clearly indicates the transformation of tetragonal crystalline phase to monoclinic crystalline phase at higher calcination temperatures showing significant influence of calcination temperature on the formation of the phases. The dried zirconium hydroxide sample at 110 ºC was amorphous in nature and crystallinity developed on thermal treatment at higher temperatures. On heat treatment amorphous $Zr(OH)_4$ first transformed to a metastable tetragonal and then to a monoclinic crystalline phase. The transformation of tetragonal to monoclinic phase occurs due to the loss of hydroxyl groups by the dehydroxylation. The hydroxy groups have been reported to be responsible for stabilization of the tetragonal phase **[157]**. Therefore, the dehydroxylation resulted to transformation of tetragonal to monoclinic phase giving a mixture of both tetragonal and monoclinic phases of zirconia at higher calcination temperature.

Figure 2a and 2b shows the XRD patterns of sulfated-zirconia samples calcined at 450, 500 and 600 ºC. The sample, calcined at 450 ºC, was amorphous. The samples, calcined at 500 ºC, were crystalline and had predominantly the tetragonal phase. With increase of calcination temperature, the monoclinic phase started to increase. Table 2 shows the percent composition of crystalline tetragonal and monoclinic phases in samples at different calcination temperatures. In sulfated-zirconia, crystallization of an amorphous sample to a crystalline phase occurs at higher temperature (450 ºC) than that of pure sample (400 ºC). The reason of increase in crystallization temperature in sulfated-zirconia samples is the presence of SO_4^{--} ions, which requires higher thermal energy for the removal of hydroxyl groups for dehydroxylation during crystallization **[126]**. Dehydroxylation of the amorphous phase at 500 ºC generated mainly tetragonal zirconia. Calcination of pure zirconium oxide at higher temperatures (between 500 to 600 ºC) generated the monoclinic phase, however, the transformation of tetragonal to monoclinic phase in sulfated-zirconia samples has been found at higher temperature, which is attributed to the presence of sulfate groups resisting the dehydroxylation of the sample.

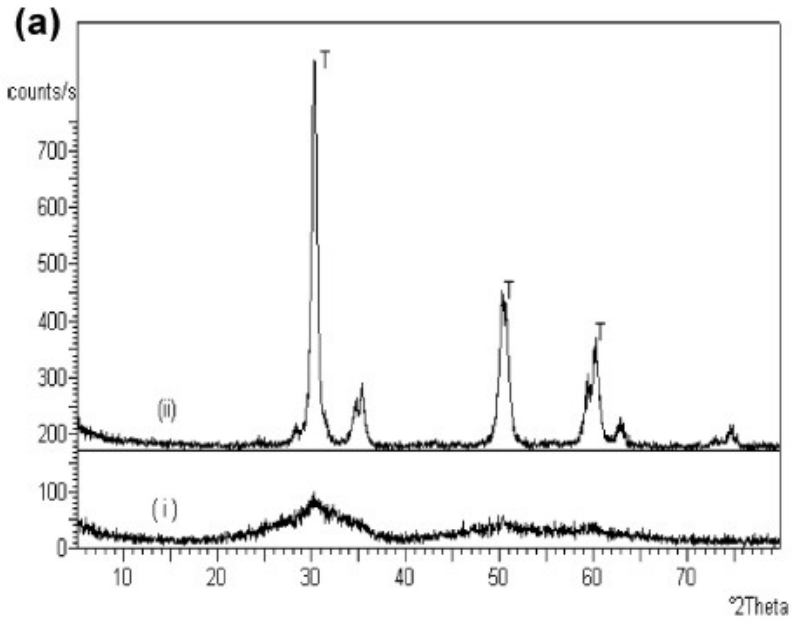

Figure 2a. X-ray diffraction patterns of SZ-4 samples after calcination at (i) 450 and (ii) 500 ºC.

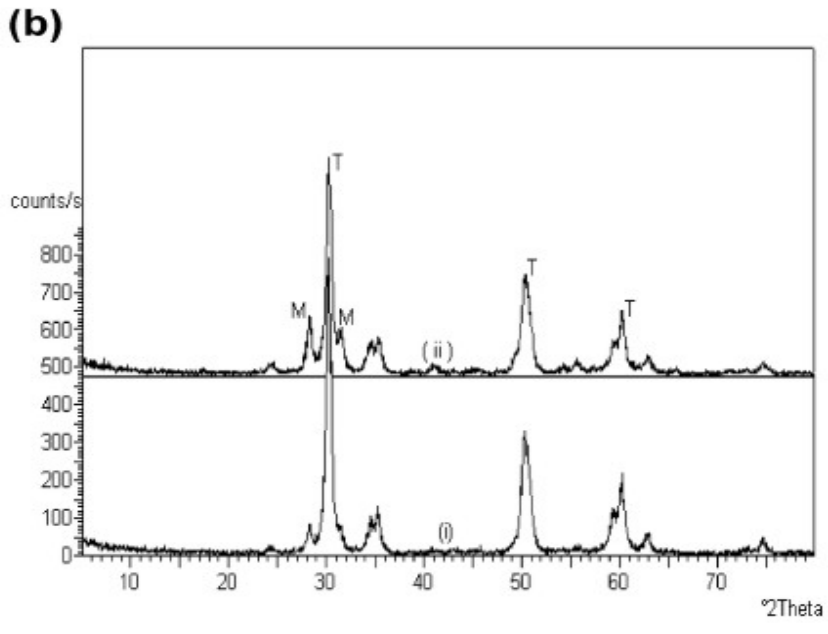

Figure 2b. X-ray diffraction patterns of SZ-3 samples after calcination at (i) 500 and (ii) 600 ºC.

The effect of synthetic parameters such as physical perturbation and drying temperature showed remarkable effect on the formation of crystalline phase and crystallinity of the phase. The effect of physical perturbation during synthesis has been seen on the crystalline phase. The sulfated-zirconia samples, SZ-6, SZ-7, SZ-11 and SZ-14 were prepared using ultrasonication. Table 2 shows the presence of predominantly tetragonal phase in all samples, prepared by ultrasonication method, even after calcination at 600 ºC. While, at same calcination temperature (600 ºC), the samples prepared using magnetic stirring, SZ-3, gave monoclinic phase also (22 %) along with tetragonal phase. The higher thermal stability of the tetragonal phase in samples prepared using ultrasonication as compared to conventional stirring probably is due to higher loading and proper dispersion of sulfate ions on zirconium oxide surface during ultrasonication, which is also confirmed by a higher sulfur content retained (0.78- 1.91 wt.%) in these samples (Table 4). The sulfur content affects crystallization and therefore, calcination temperature.

Effect of drying temperature of gel, before calcination, was also found to be affecting the calcination temperature and formation of phase. Table 2 and Figure 3a and 3b show that the samples initially dried, before calcination, at 80 or 110ºC have only tetragonal phase after calcination at 600 ºC, whereas the sample initially dried at room temperature, SZ-1, showed predominantly a monoclinic phase (89 %) after calcination at 600 ºC. The drying of gel at room temperature could not remove the solvent (*n*-propanol) completely, which is present with precursor and also formed during the hydrolysis of the alkoxide. The presence of *n*-propanol filled inside the gel pores affected sulfate loading, as sulfate ions could not go inside the pores during the sulfation process and therefore, forms the monoclinic phase at lower calcination temperature.

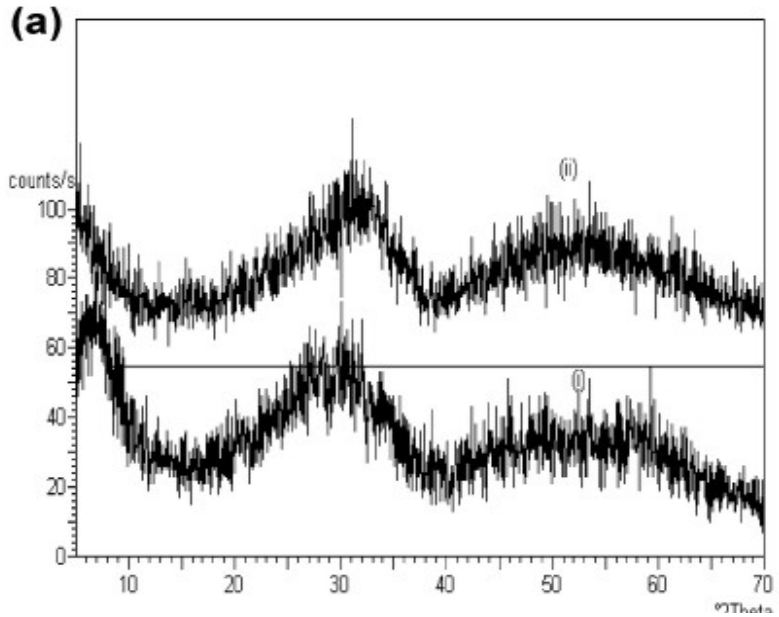

Figure 3a. X-ray diffraction patterns of amorphous sulfated-zirconia samples before calcination (i) SZ-1 dried at 25 ºC and (ii) SZ-2 dried at 80 ºC.

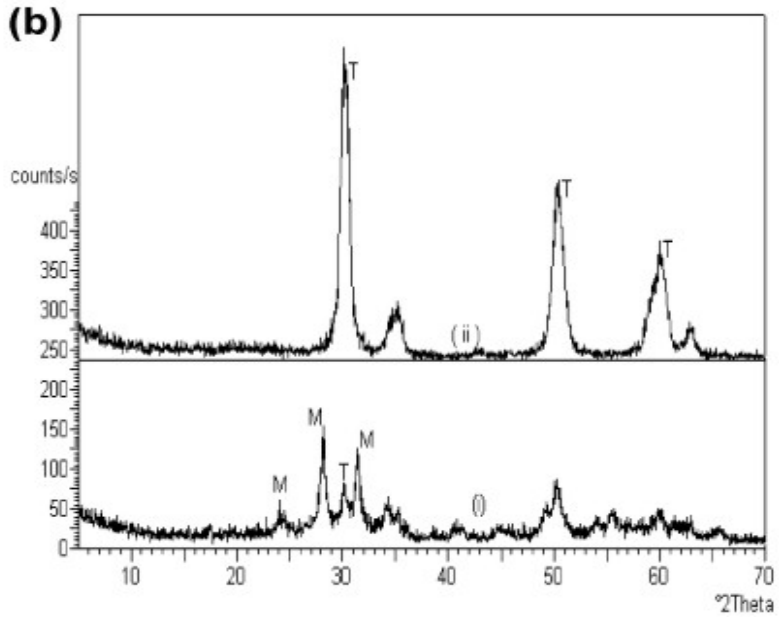

Figure 3b. X-ray diffraction patterns of crystalline sulfated-zirconia samples (i) SZ-1 and (ii) SZ-2 after calcination at 600 ºC.

2.3.1.2 Crystallite Size

Crystallite sizes of the tetragonal phase were determined from X-ray diffraction data using Scherrer formula. Table 2 shows the crystallite sizes of sulfated-zirconia as well as pure zirconia. All the samples, prepared by the sol-gel technique, are nano-crystalline (10-23 nm). The crystallite size of tetragonal phase of pure zirconia samples (ZrO_2) increases progressively from 13 to 23 nm with an increase in calcination temperature (400-600 ºC), which shows the sintering of zirconia crystallites with temperature forming larger crystallites. The presence of sulfate in the zirconia samples reduces the crystallite size, as crystallite size of sulfated-zirconia was found smaller than that of pure zirconia.

Table 2. Crystalline phase and crystallite size of sulfated and pure zirconia samples.

Sample	Calcination Temp. (ºC)	Phase (%)		Crystallite size (nm)
		T	M	
SZ-1	600	11	89	
SZ-2	600	100	0	10
SZ-3	600	78	22	16
SZ-3	500	94	6	17
SZ-4	500	99	1	15
SZ-7	600	96	4	13
SZ-6	600	96	4	12
SZ-11	600	100	0	13
SZ-14	600	100	0	15
ZrO_2	400	100	0	13
ZrO_2	450	96	4	18
ZrO_2	500	83	17	20
ZrO_2	600	71	29	23

T = Tetragonal phase, M= Monoclinic phase

The concentration of precursor showed to be slightly affecting the crystallite size. Slightly lower crystallite sizes were observed in the samples, prepared by using 10 wt.% solution of the precursor, either stirred by conventional (15 nm) or ultrasonication methods (13 nm) than the samples, prepared by using 70 wt.% solution of the precursor, either stirred by conventional (16-17 nm) or ultrasonication methods (15 nm). The samples prepared by ultrasonication (SZ-6, SZ-7, SZ-11, SZ-14) were found to be of

slightly smaller crystallite size (12-15 nm) than those synthesized by magnetic stirring (15-17 nm). The sample SZ-2 was found to be the only exception having a low crystallite size (10 nm), prepared by using higher concentration (70 wt.%) with conventional stirring.

The detail study on characterization of structural, textural and catalytic features of the sulfated-zirconia samples was carried out with the crystalline sulfated-zirconia samples showing higher or 100% tetragonal crystalline phase.

2.3.1.3 FT-IR Studies

The FT-IR spectra of pure and sulfated-zirconia samples calcined at 600 ºC are given in Figure 4. The FT-IR spectra of sulfated-zirconia samples dried at room temperature and 110ºC show the IR bands of the SO_4^{--} ions at 1220-1214, 1130-1128, 1060-1054, and 996 cm^{-1}, for asymmetric and symmetric stretching frequencies of partially ionized S=O double and S-O single bonds **[98]**.

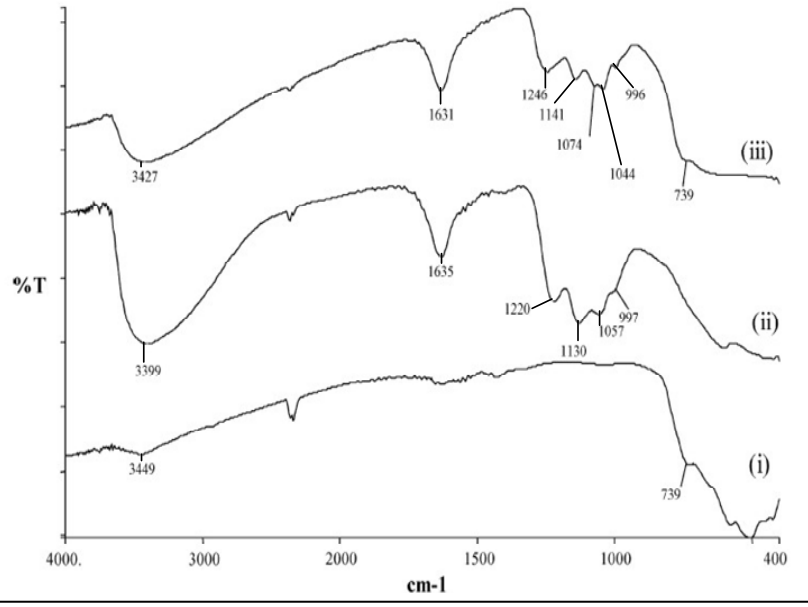

Figure 4. FT-IR spectra of (i) pure zirconia, (ii) sulfated-zirconia after drying at 110ºC and (iii) sulfated-zirconia after calcination at 600ºC.

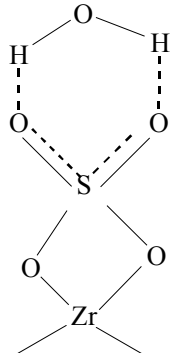

Scheme 1

The IR spectra of the sulfated-zirconia samples, after calcination, show the IR bands at 1246-1220, 1142-1138, 1049-1044 and 996 cm^{-1}, which are characteristic of inorganic chelating bidentate sulfate groups and thus showing the presence of chelating bidentate sulfate group on the surface of zirconia as shown in Scheme 1. Before calcination the sulfate ions are free, either trapped inside the pores or on the surface of the zirconium hydroxide. On calcination, free sulfate ions undergo strong bond formation with zirconia surface. The strong bond formation between sulfate group and zirconia surface after calcination is evident from the shifting of IR bands toward higher wave numbers. A broad peak at around 3400 cm^{-1} is attributed to the ν_{O-H} stretching mode of water bonded with zirconia surface and the surface sulfate groups and the broadness of the peak is due to the hydrogen bonding effect of water with surface sulfates **[111]**. The band at 1631-1635 cm^{-1} is attributed to δ_{O-H} bending mode of water associated with zirconia surface and the surface sulfate groups **[111]**.

The sulfated-zirconia samples after drying at ambient temperature, 80 or 110 ºC show similar IR spectra. After calcination at 600 ºC, the sample, which was initially dried at ambient temperature, showed a broad peak at 1130 cm^{-1} (figure 5), however, the samples, dried at 80ºC or 110 ºC, showed the characteristic peaks of bidentate chelating sulfate (Figure 4 and 5). It clearly indicates the role of drying temperature, for evaporation of solvent during drying of the gel, on the nature and bonding of sulfate group. The presence of solvent (propanol) before sulfation may affect the bonding of sulfate ions with the zirconium atom.

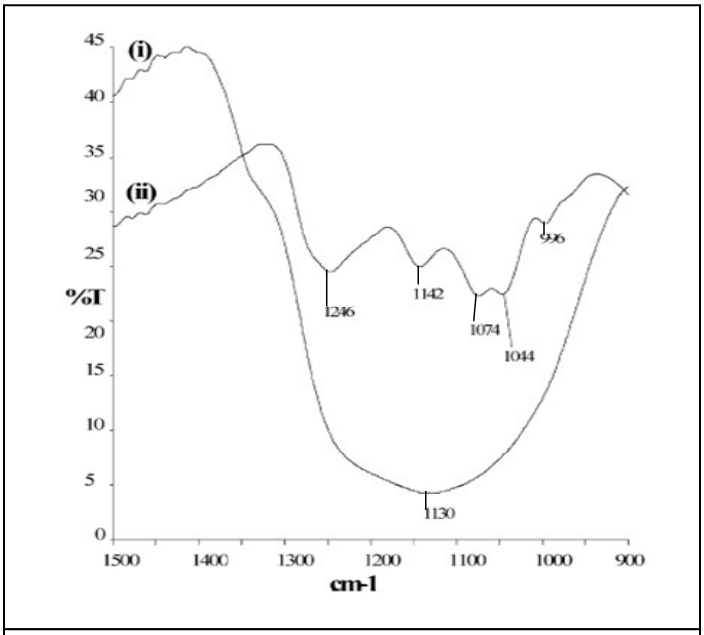

Figure 5. FT-IR spectra of sulfated-zirconia sample after calcination at 600 ºC (i) SZ-1 (dried at RT) and (ii) SZ-2 (dried at 80 ºC).

2.3.1.4 Diffuse Reflectance FT-IR Studies

The DRIFT spectra of sulfated-zirconia samples calcined at 600 ºC, recorded after *in-situ* heating at different temperatures from 150- 450 ºC are shown in figure 6. All sulfated-zirconia samples, at ambient temperature, showed a weak to medium band at around 1401 cm^{-1}, which is assigned to asymmetric stretching ($\nu_{S=O}$) of S=O double bond indicating the presence of covalently bonded surface sulfates having S=O bonds as shown in Scheme 2. This structure is responsible for the formation of the Lewis acid sites on the surface by attracting the electron density form the zirconium atom. The *in-situ* heating of the samples at 150 ºC shows the increase in the intensity of peak at 1401 cm^{-1}, which gradually increases with temperature from 250 to 450 ºC. The broad peaks at 3400 cm^{-1} and at 1630 cm^{-1} were decreased after heating at 150 ºC, showing the removal of adsorbed water molecules. This spectral change shows the structural transformation from Bronsted acid sites (Scheme1) to Lewis acid sites (Scheme 2) on the removal of molecular water from the samples. The peak area of the $\nu_{S=O}$ band was calculated to quantify the amount of Lewis acid sites in the samples. The peak area of the $\nu_{S=O}$ band gradually increases with temperature from room temperature to 450 ºC (Figure 7), which shows the sensitivity of the surface sulfates towards the molecular water in sulfated-zirconia samples **[111, 203]** and causes transformation of Bronsted acid sites to Lewis acid sites. The higher peak area of the $\nu_{S=O}$ band at 450 ºC shows the presence of more covalently bonded surface sulfates presenting the higher Lewis acid sites. The peak area of the $\nu_{S=O}$ band has been correlated with the total sulfur content present in the catalysts and the catalytic activity of the catalysts for the benzylation of toluene, which is explained in later section.

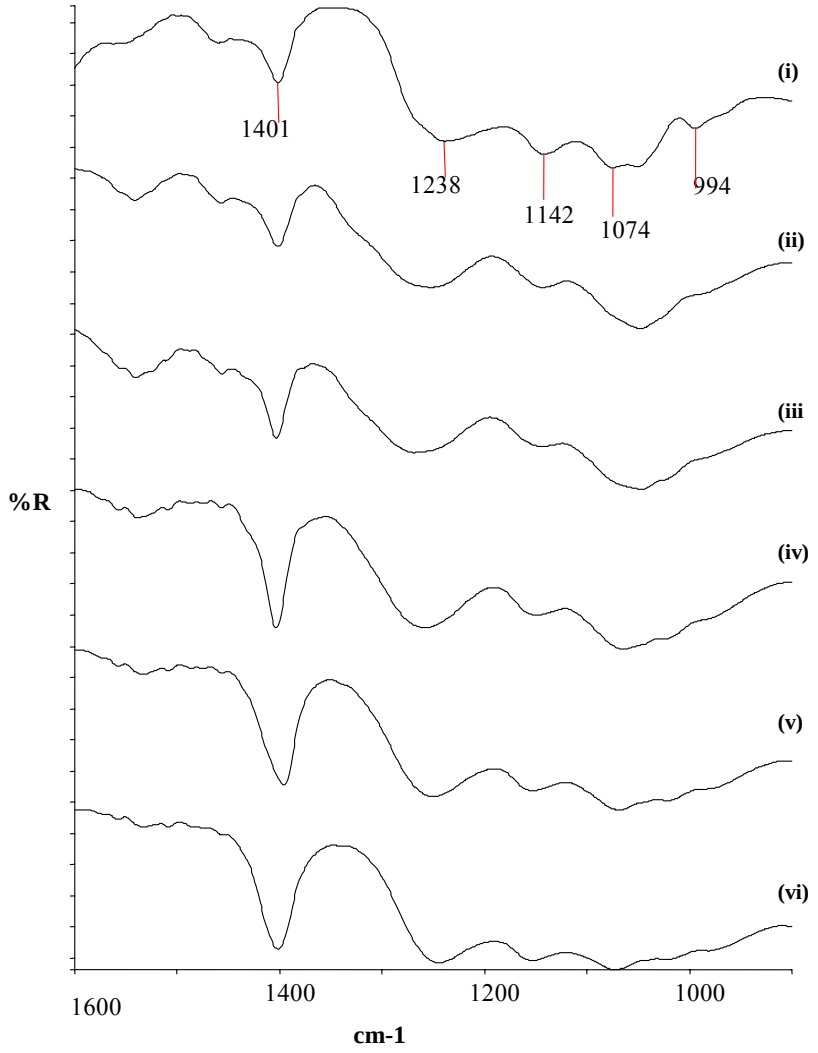

Figure 6. DRIFT spectra of calcined sulfated-zirconia samples after *in-situ* heating at (i) RT, (ii) 150, (iii) 250, (iv) 300, (v) 400 and (vi) 450 ºC.

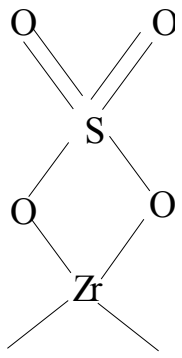

Scheme 2

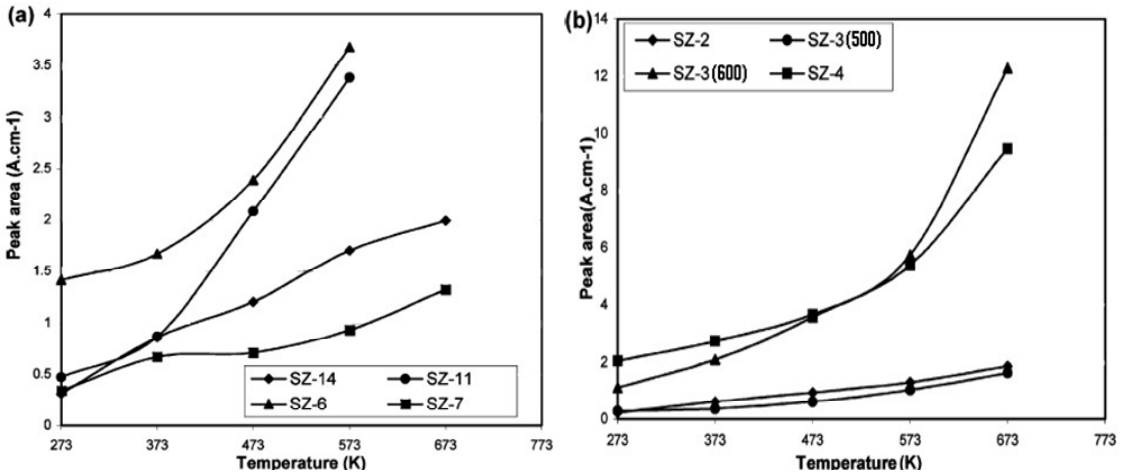

Figure 7. Variation of peak area of the band at 1401 $cm^{-1}$with temperature in the sulfated-zirconia samples synthesized by **(a)** ultrasonication and **(b)** mechanical stirring.

2.3.2 Textural Properties

Figure 8 shows the N_2 adsorption desorption isotherm of pure zirconia, calcined at 600 ºC, which was measured at liquid nitrogen temperature (77 K). The isotherm is of type III, which is shown by the nonporous materials. The low surface area (6-9 m^2/g) and pore volume (0.043 cm^3/g) of the pure zirconia sample (Table 3), calcined at 600 ºC, and also shows the nonporous nature.

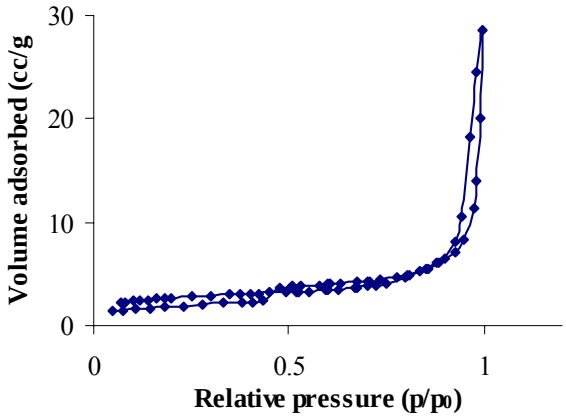

Figure 8. N_2 adsorption isotherm at 77 K for pure zirconia calcined at 600ºC.

N_2 adsorption desorption isotherms for amorphous sulfated-zirconia samples calcined at 450 ºC indicates the presence of mesopores (Figure 9a). Presence of large mesopores was also confirmed by its low surface area (25-41 m^2/g) and higher pore volume (0.084 cm^3/g). The crystalline sulfated-zirconia samples, calcined at 500-600 ºC, show N_2

adsorption desorption isotherms of type IV (Figure 9b), which is characteristic of mesoporous materials.

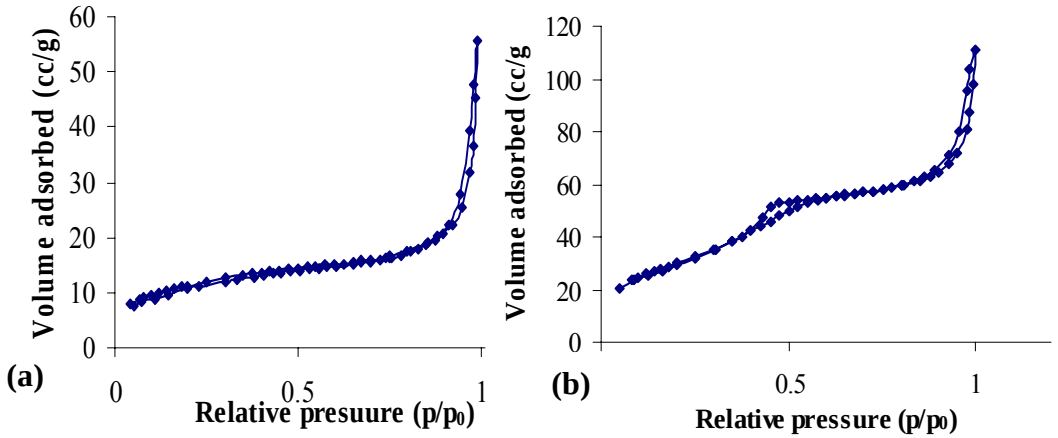

Figure 9. N_2 adsorption isotherms of **(a)** amorphous sulfated-zirconia sample calcined at 450 ºC and **(b).** crystalline sulfated-zirconia sample calcined at 500- 600 ºC.

However, there is a large increase in adsorption at higher relative pressure (P/Po), which shows the presence of larger size mesopores in these solids. The inflection point observed in the N_2 adsorption isotherm at around (P/Po) 0.4 shows the capillary condensation within the mesopores after the formation of monolayer. However, this inflection in all the samples was not sharp, indicating that the pores are not of uniform size and have broad distribution. All samples show hysteresis of H2 or H3 type. The materials having complex pore structure generally show H2 hysteresis. H3 hysteresis does not have any limiting adsorption at high relative pressure and indicates absence of any well-defined pore structure in the material.

The surface area of the samples was calculated from the adsorption isotherm using the BET equation. The surface area of different samples is given in Table 3. The crystalline sulfated-zirconia samples show higher surface area (71-116 m^2/g) than amorphous sulfated-zirconia (25-41 m^2/g) and pure zirconia (6-9 m^2/g). The surface area increases with increasing calcination temperature but after certain calcination temperature it decreases, which may be due to sintering of pores at higher temperature. The pore size distribution (Figure 10) in all the samples was found broad ranging from 20 to 100 Å. N_2

adsorption desorption isotherm and adsorption data show that the crystalline sulfated-zirconia samples have high surface area as well as defined mesoporosity.

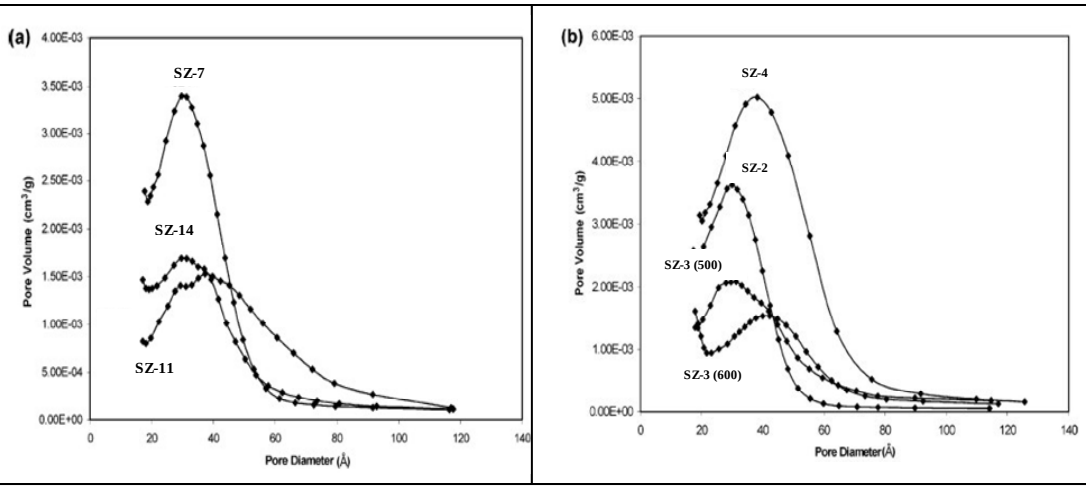

Figure 10. The pore size distribution in sulfated-zirconia samples, synthesized by **(a)** ultrasonication and **(b)** conventional stirring.

Table 3. Textural properties of sulfated and pure zirconia.

Sample	BET Surface area (m^2/g)	BJH adsorption Pore volume (cm^3/g)	BJH adsorption Pore size (Å)
SZ-2 (450)	41	0.084	98
SZ-2 (600)	116	0.131	44
SZ-3 (600)	71	0.106	61
SZ-3 (500)	85	0.130	59
SZ-4 (500)	86	0.126	51
SZ-7 (600)	110	0.175	58
SZ-6 (600)	107	0.155	63
SZ-11 (600)	64	0.081	45
SZ-14 (600)	85	0.136	73
Z-2 (600)	9.5	0.043	264

The effect of the concentration of the precursor and mode of stirring was not found to be showing any significant effect on the textural properties, however, the time of ultrasonication had shown slight effect on surface area as the surface area was found to be higher in samples prepared in 30 min (110 m^2/g) than those prepared in 2 h (64 m^2/g).

2.3.3 Thermal Analysis

During the calcination of dried zirconium hydroxide gel at 500 ºC, the observed weight loss of pure zirconia sample was found to be 24 wt %. This weight loss is almost equal to the theoretically calculated weight loss (22.6 wt %) during transformation of the zirconium hydroxide to zirconia by the dehydroxylation reaction.

$$Zr(OH)_4 \longrightarrow ZrO_2 + 2H_2O$$

The weight loss increased with increasing the calcination temperature. It increased to 33% at 600 ºC, which might be due to loss of water by dehydroxylation during the transformation of tetragonal to monoclinic phase of zirconia.

The weight loss (weight of the sample before calcination – weight of the sample after calcination) observed in all sulfated-zirconia samples, after calcination at 500 and 600 ºC, was 28- 32 wt %, which is due to loss of excess water in sample remained and formation of oxide from hydroxide by dehydroxylation during calcination and not due to loss of sulfur.

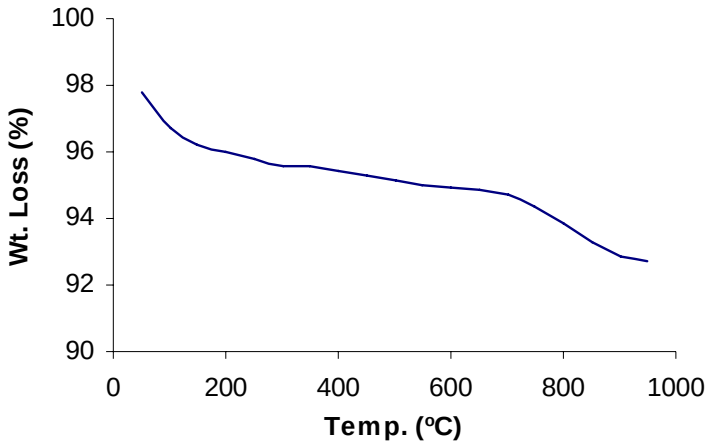

Figure 11. TGA graph of the sulfated-zirconia sample calcined at 600 ºC.

The thermal analysis (TGA) of the samples showed weight loss at ~200 and 725 ºC (Figure 11). An endothermic peak at 40 ºC and exothermic peaks at 340 ºC and at higher temperatures 900 ºC were observed (DTA is not given in the figure). The initial first step weight loss at lower temperature at around 200 ºC is due to the water loss and

the second step weight loss at higher temperature at around 400 ºC is observed for tetragonal to monoclinic transformation and the weight loss at temperatures higher than 700 ºC is because of sulfur loss.

2.3.4 Sulfur Analysis

The percentage of sulfur in sulfated-zirconia samples retained after calcination at 500 and 600 ºC are given in Table 4. The amount of sulfur retained after calcination in the sulfated-zirconia samples was observed to be affected by the synthetic parameters such as concentration of the precursor, mode and duration of stirring during synthesis. The sample SZ-14 (600), synthesized by ultrasonication retained higher sulfur (1.91 wt.%) in comparison to the samples prepared by conventional stirring. The duration of ultrasonication was also found to be affecting the sulfur loading. In the samples SZ-7, SZ-6 and SZ-11, prepared by ultrasonication, the retained sulfur after calcination increased from 0.78 to 1.77 wt.% with increasing the ultrasonication time from 30 to 120 min keeping other conditions same. Ultrasonication assisted preparation of sulfated-zirconia may be causing higher dispersion of sulfate ions over the zirconia resulting in higher loading of sulfur **[203]**. The samples prepared by ultrasonication contained higher sulfur amount but the nature of the sulfur species on the surface was found to be similar i.e. inorganic bidentate chelating sulfate, as in other samples.

Table 4. Amount of sulfur (wt%) and S atom/ nm^2 in sulfated-zirconia samples after calcination at 500 and 600ºC.

Sample	Sulfur (wt%)	S/ nm^2
SZ-2 (600)	1.18	0.6
SZ-3 (600)	0.87	0.8
SZ-3 (500)	1.35	0.9
SZ-4 (500)	0.93	0.7
SZ-7 (600)	0.78	0.4
SZ-6 (600)	0.99	0.6
SZ-11 (600)	1.77	1.7
SZ-14 (600)	1.91	1.4

The total sulfur content was correlated with covalently bonded sulfur, which represents Lewis acid sites and quantified by peak area of the $\nu_{S=O}$ band (Figure 12). The

correlation shows that the samples having < 1.0 wt.% sulfur content have higher Lewis acid sites, whereas the samples with 1.0- 2.0 wt.% or > 2.0 wt.% sulfur content have less Lewis acid sites and higher Bronsted acid sites. Further, S atom per nm^2 in the sulfated-zirconia samples were also calculated (Table 4) and correlated with the catalytic activity of the samples for benzylation of toluene and therefore Bronsted and Lewis acidity, which will be discussed in next section.

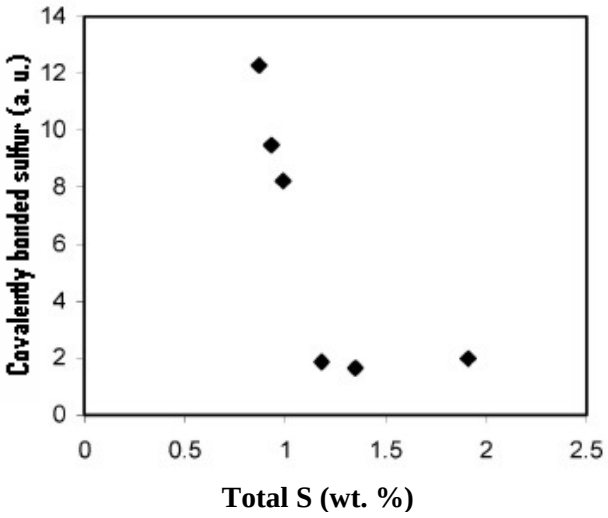

Figure 12. Relation of covalently bonded sulfur and total sulfur**.**

2.3.5 Catalytic Activity

The conversion of toluene and the selectivity of the *p*-benzyl toluene for the benzylation of toluene with benzyl chloride over different sulfated-zirconia samples under similar reaction conditions are given in Table 5.

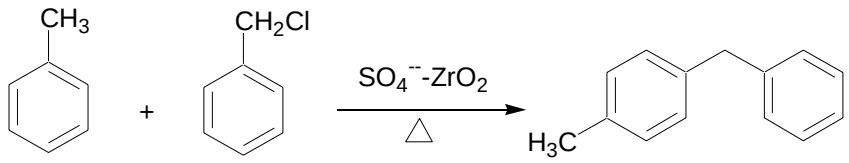

The sample, SZ-14, prepared by ultrasonication method showed higher catalytic activity among all the samples and gave maximum conversion of toluene (68 %) after 4 h

with 100 % selectivity of the *p*-benzyl toluene. The higher catalytic activity of the sample SZ-14 is attributed to higher sulfur content (1.91 wt.%) in the sample, which generates higher Bronsted acid sites. The concentration of the precursor used for synthesis of sulfated-zirconia, was observed to be affecting the activity of the samples. The samples, SZ-3 (500), SZ-3 (600) and SZ-14 (600), prepared by using higher concentration (70 wt.%) of the precursor showed higher activity in comparison to the samples, prepared by using a lower (10 wt.%) concentration of the precursor whether the samples were prepared by ultrasonication or magnetic stirring.

Table 5. Kinetic study of benzylation of toluene with benzyl chloride on SZ-14.

Reaction Time (h)	Conversion (wt.%)	Selectivity (%) for *p*-benzyl toluene
0.5	46	100
1	48	100
2	51	100
3	56	100
4	68	100
5	66	100
6	67	100

(20 mmol toluene, 20 mmol benzyl chloride (Molar ratio = 1:1), 0.1 g catalyst, Reaction Temperature = 110 ºC)

Table 6. Benzylation of toluene with benzyl chloride on sulfated-zirconia samples.

Catalyst	Conversion (wt.%)	Selectivity (%) for *p*-benzyl toluene
SZ-3 (600)	61	100
SZ-3 (500)	27	100
SZ-4 (500)	30	100
SZ-7 (600)	17	100
SZ-6 (600)	17	100
SZ-11 (600)	53	100
SZ-14 (600)	68	100

(20 mmol toluene, 20 mmol benzyl chloride (Molar ratio = 1:1), 0.1 g catalyst, Reaction Temperature = 110 ºC, Reaction Time = 4 h)

The catalytic activity of the sulfated-zirconia samples was correlated with the total sulfur retained in the sample, covalently bonded sulfur and surface area. The surface areas (Table 3) of these samples were not found to be showing any correlation with wt.% conversion. The samples SZ-11 and SZ-14, prepared by ultrasonication, had lower surface area (64 and 85 m^2/g respectively) but they showed higher catalytic activity (53 and 68 % respectively), therefore, surface area alone could not determine the catalytic activity. The amount of sulfur and the nature of the sulfur bound with the zirconia surface had been found to be determining the catalytic activity of the samples. Figure 13a shows the relation of wt.% sulfur with wt.% conversion. There is a linear correlation of wt.% conversion for benzylation of toluene with wt.% sulfur, which shows that the activity of the samples increases with sulfur content due to increase in Bronsted acidity in the samples, which shows that the benzylation is a Bronsted acid catalyzed reaction.

The effect of total sulfur content was correlated with the activity of the samples by total wt.% sulfur per unit surface area, which was calculated by dividing wt.% sulfur retained in the sample with surface area of the sample. The total wt.% sulfur per unit surface area was plotted against wt.% conversion for benzylation of toluene (Figure 13b). The plot is clearly showing that the catalytic activity of the samples increases with increase in the sulfur per unit area of the sample.

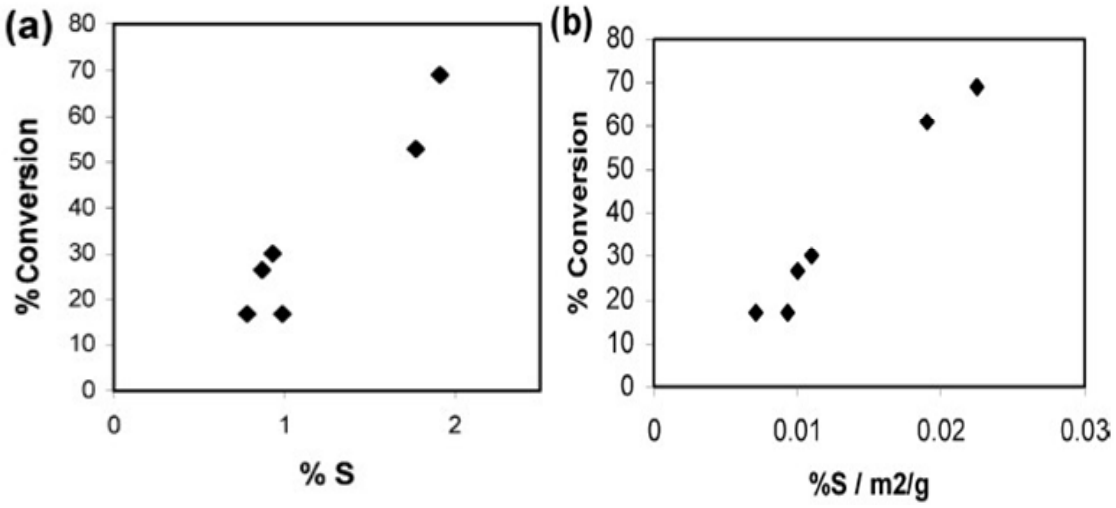

Figure 13(a). Correlation of catalytic activity with sulfur content and **(b)** with sulfur per unit surface area.

The nature of sulfur species was correlated with the activity of the samples by plotting a graph (Figure 14) between wt.% conversion and the peak area of $\nu_{S=O}$ band (covalently bonded sulfur, which generates Lewis acid sites). The activity of the samples was found to be decreasing with increase in covalently bonded sulfur (the peak area of $\nu_{S=O}$ band). Both correlations show that the catalytic activity of the sulfated zirconia samples increase linearly with increasing total sulfur content of the sample (Figure 13b) and decrease with increasing covalently bonded sulfur. It indicates that the covalently bonded sulfur species is not participating in catalysis of benzylation of toluene and the sulfur species other than covalently bonded sulfur are responsible for providing catalytically active sites. These sulfur species are having structure as shown in Scheme 1, which generates Bronsted acid sites. Therefore, the Bronsted acid sites, generated by the ionic form of sulfur, are responsible for higher catalytic activity for the benzylation of toluene and not the Lewis acid sites.

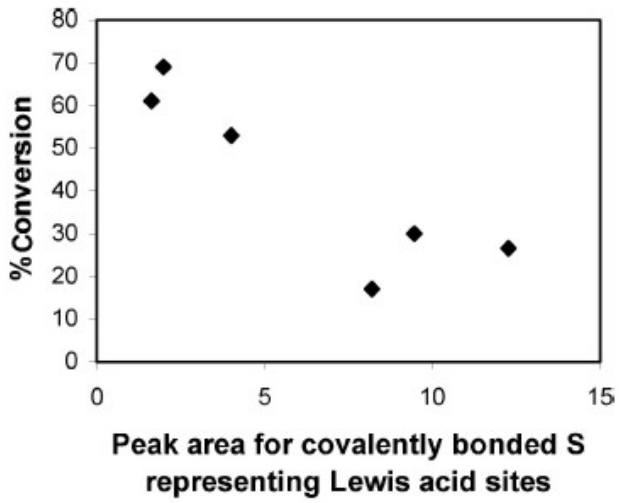

Figure 14. Correlation of covalently bonded sulfur representing Lewis acid sites with catalytic activity for benzylation of toluene.

The S atom per nm^2 in the sulfated-zirconia samples was also correlated with the activity of the samples for benzylation of toluene (Figure 15). The correlation shows that the samples with > 0.8 S per nm^2 gave higher activity for benzylation of toluene (53-

68 %) due to higher Bronsted acidity. The samples with < 0.8 S per nm^2 showed lesser activity for benzylation giving lower conversion of toluene (17- 30 %), which is attributed to lesser Bronsted acidity. These results show the similarity with the observation of Morterra et al. **[135]**, who also found that the lower sulfur content in the sulfated-zirconia (< 0.8 S atom per nm^2) gives more Lewis acid sites and the higher sulfur content (> 0.8 S atom per nm^2) generates more Bronsted acid sites.

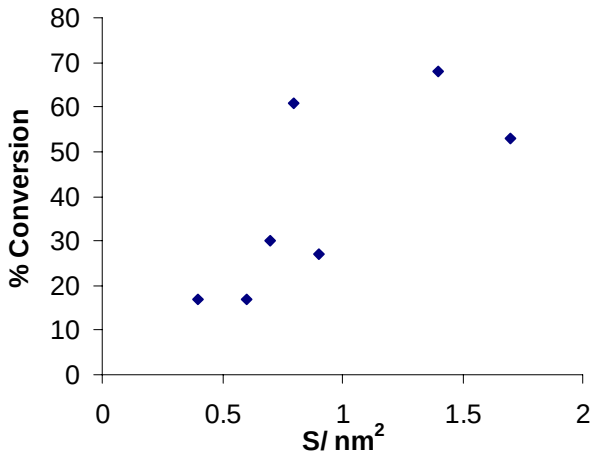

Figure 15. Correlation of S/ nm^2 with catalytic activity for benzylation of toluene.

The study is in accord to the observation of Babou et al. **[162]**, who also reported the higher catalytic activity of the sulfated-zirconia catalysts, having ionic form of surface sulfate species in presence of water, for isomerization of *n*-butane. This observation is in contrast with the observations of Morterra et al. **[141]** that the surface sulfate in ionic configuration is catalytically inactive sulfur species.

2.3.6 Regeneration study

For regeneration study, the catalyst SZ-14 was selected, which had shown highest activity for benzylation of toluene. The spent catalyst was regenerated by washing with acetone to remove the adsorbed reactants and products followed by activation at 450 ºC for 2 h. The regenerated catalyst showed decreased activity than fresh catalyst as the conversion of toluene decreased (35 %). It shows that the catalyst is

not regenerated by this method. The surface area of the regenerated catalyst (SZ-14) was also measured; it showed a decrease from 85 to 77 m^2/g.

2.4 Conclusions

The sol-gel technique has been found to be an appropriate route to synthesize nano-crystalline sulfated-zirconia catalyst having a low crystallite size (< 20 nm) giving predominantly tetragonal phase, which was found thermally stable at higher temperature. The effect of drying of the gel before calcination is an important step to remove the solvent completely in order to generate purely tetragonal phase and higher sulfur loading. The effect of various synthetic parameters on the structural, textural and catalytic properties of sulfated-zirconia has been observed. Ultrasonication provides higher sulfur loading to the samples and also results to lower crystallite size as compared to conventional mechanical perturbation during the synthesis. The amount of sulfur retained and the nature of the sulfur species bound with the zirconia surface play a significant role in determining the catalytic activity of a sample as well as the type of acidity on the surface. The catalyst having lower sulfur loading (< 1.0 wt.%) exhibits higher covalently bonded sulfur species, which generates Lewis acid sites on the surface and the catalyst containing higher sulfur amount (> 1.0 wt.%) possesses ionic sulfur species and shows Bronsted acidity. The ionic sulfur species was found catalytically active for benzylation of toluene. The covalently bonded sulfur species was found highly sensitive in nature towards molecular water and in presence of water molecule the covalently bonded sulfur species was converted to ionic sulfur species. Ultrasonication assisted preparation of sulfated-zirconia samples with higher concentration of the precursor was found to be resulting to higher loading and dispersion of sulfur and thus gives higher catalytic activity for the benzylation of toluene.

Chapter 3

(I)

Structural, Textural and Catalytic Properties of Nano-crystalline Sulfated Zirconia prepared by One-step and Two-step Sol-Gel Technique

3.1 Introduction

The sol-gel technique has been found to be most common and appropriate route for the synthesis of nano-crystalline sulfated-zirconia with improved structural, textural and catalytic properties. The sol-gel synthesis of sulfated-zirconia has been reported by one-step and two-step methods. One-step sol-gel method involves the hydrolysis of precursor and sulfation simultaneously in single step giving alcogel **[111, 112, 114, 115, 121, 122]**. Two-step sol-gel method is two-step synthesis, which involves the hydrolysis of precursor in first step giving gel followed by sulfation in second step **[113, 116- 118, 120]**. One-step synthesis takes place in acidic medium as sulfuric acid is added during sol-gel reactions and two-step synthesis may be in either acidic **[112]** or basic **[117]** or neutral medium **[116]**. Ward et al. **[111, 112]** reported first time one-step synthesis of sulfated-zirconia by sol-gel technique using zirconium alkoxide as precursor. The sulfuric acid was mixed with zirconium propoxide and *n*-propanol solution and water nitric acid mixture was added drop wise to form cogel.

In the present study, the synthesis of sulfated-zirconia by sol-gel technique has been extended from two-step to one-step sol-gel technique. Sulfated-zirconia catalysts were synthesized by one-step and two-step sol-gel methods. The first part of the chapter is the synthesis and characterization of the sulfated-zirconia catalysts studying the effect of one-step and two-step sol-gel methods on structural and textural properties. The second part is the study of catalytic behavior of sulfated-zirconia catalysts for acylation of anisole and veratrole**.** The reaction conditions, such as reaction temperature, time, molar ratio of substrates and substrate to catalyst wt. ratio and the regeneration of spent catalyst were studied. The aim of present study was to study the effect of sol-gel parameters such as the way of addition of sulfuric acid in alkoxide, water to alkoxide molar ratio, pH of the synthesis medium and calcination temperature on the physicochemical and catalytic properties of the sulfated-zirconia catalysts.

3.1.1 Experimental

3.1.1.1 Material

Zirconium propoxide (70 wt.% solution in *n*-propanol) was procured from Sigma Aldrich, USA, *n*-propanol, aqueous ammonia (25%), concentrate sulfuric acid

and pyridine were from s.d. Fine chemicals, India. All the chemicals were used as such without any further purification.

3.1.1.2 Catalyst synthesis

The sulfated-zirconia samples were synthesized by sol-gel technique using one-step method in acidic medium and two-step method in basic as well as neutral medium. The zirconium propoxide (40 ml) was used as a precursor after dilution (30 wt.%) with *n*-propanol (52.3 ml), distilled water or liquid ammonia as hydrolyzing agent and concentrate sulfuric acid as a sulfating agent. By one-step sol-gel method, three samples were synthesized. One sample was synthesized as follows; concentrate H_2SO_4 (36N, 1.02 ml) was added in distilled water (6.4 ml, water to alkoxide molar ratio = 4), which was used as hydrolyzing agent. The acidified water was added drop wise to zirconium propoxide (30 wt.% solution in *n*-propanol) under continuous stirring. After 3 h aging at room temperature the resulting gel was filtered and dried initially, at room temperature, followed by drying at 110 ºC for 12 h and calcination at 600 ºC for 2 h in static air atmosphere. The sample was designated as SZO1, where O denotes one-step technique.

The second sample by one-step sol-gel method was synthesized by adding H_2SO_4 (36N, 1.02 ml) in zirconium propoxide (30 wt.% solution in *n*-propanol) followed by addition of distilled water (water to alkoxide molar ratio = 4) drop wise under continuous stirring. The gel was kept for aging for 3 h at room temperature, followed by drying at 110 ºC for 12 h and calcination at 600 ºC for 2 h in static air atmosphere. The sample was designated as SZO2.

The third sample was synthesized by adding H_2SO_4 (36N, 1.02 ml) in zirconium propoxide (30 wt.% solution in *n*-propanol) followed by addition of distilled water drop wise under continuous stirring till the solution got solidified due to gel formation, which consumed 4.2 ml of water (water to alkoxide molar ratio = 2.7). The gel was kept for aging for 3 h at room temperature, followed by drying at 110 ºC for 12 h and calcination at 600 ºC for 2 h in static air atmosphere. The sample was further calcined at higher temperatures of 700 and 800 ºC for 2 h in static air atmosphere to study the effect of calcination temperature on the structural, textural and catalytic properties of the sample. The samples, thus synthesized, were designated as SZO2 (600), SZO2 (700) and SZO2 (800), where the values in parenthesis denote the calcination temperature. [The sample SZO2 is different from the sample SZO2

(600) in the use of the water to alkoxide molar ratio for hydrolysis. The sample SZO2 was synthesized by using water to alkoxide molar ratio of 4, while the sample SZO2 (600) was synthesized by hydrolyzing the zirconium propoxide by using lesser quantity of water (water to alkoxide molar ratio = 2.7) just sufficient to form the gel].

In two-step method, two samples were synthesized; in neutral and basic medium. In basic medium; the zirconium propoxide (30% solution in *n*-propanol) was hydrolyzed by adding liquid ammonia drop wise till pH reached 9- 10 under continuous stirring and in neutral medium, the zirconium propoxide (30 wt.% solution in *n*-propanol) was hydrolyzed by adding distilled water (6.4 ml, water to propoxide ratio = 4) drop wise. After 3 h aging at room temperature under stirring, the gel was filtered and dried at room temperature followed by drying at 110 ºC for 12 h. The dried gel was meshed (170 mesh) and sulfated with sulfuric acid by pouring the powdered gel in 1N sulfuric acid solution (15 ml per gm of zirconium hydroxide) under stirring for 30 min and filtered. The sulfated samples were dried at 110 ºC for 12 h. The dried samples were then calcined at 600 ºC for 2 h in static air atmosphere. The samples, thus synthesized, were designated as SZTB and SZTN respectively, where T denotes two-step technique, B and N denotes basic and neutral medium.

3.1.1.3 Catalyst Characterization

3.1.1.3.1 X-ray Powder Diffraction studies

The structural properties such as the crystalline phase formed and the crystallite size of the phase in sulfated-zirconia samples were measured by X-ray powder diffractometer (Philips X'pert) using CuKα radiation (λ = 1.5405 Å). The samples were scanned in 2θ range of 0 to 70º at a scanning rate of 0.4 degree/second.

Crystallite size of tetragonal phase was determined from the characteristic peak (2θ) 30.5º for the (111) reflection with d-spacing of 2.9 Å using the Scherrer formula **[182]**,

Crystallite size = K.λ /W.cosθ

Where, K is shape factor and is equal to 0.9 and W is the difference of (Wb) broadened profile width of experimental sample and (Ws) standard profile width of reference silicon sample.

3.1.1.3.2 FT-IR Spectroscopic Studies

The nature of surface sulfates in the samples after calcination was studied by FT-IR spectroscopic study (Perkin-Elmer GX spectrophotometer). The spectra were recorded in the range 400-4000 cm^{-1} with a resolution of 4 cm^{-1} as KBr pallets.

3.1.1.3.3 DRIFT studies

The diffuse reflectance IR (DRIFT) study of the sulfated-zirconia samples was done to observe the effect of *in-situ* heating on the nature of surface sulfate species and for quantification of Lewis acidity in the samples by *in-situ* heating of the samples at 450 ºC using FT-IR spectrophotometer equipped with 'The Selector' DRIFT accessory (Graseby Specac, P/N 19900 series) and Automatic Temperature Controller (Graseby Specac, P/N 19930 series). Typically, 30 scans were recorded at a resolution of 4 cm^{-1} under dry N_2 flow (30 cm^3/min).

3.1.1.3.4 FT-IR Spectroscopic Studies of the samples adsorbed with pyridine

The Bronsted and Lewis acidity of the sulfated-zirconia samples was measured by FT-IR study of the samples adsorbed with pyridine. The sample (0.2 g) was activated at 450 ºC for 2 h. The activated sample was cooled in desiccator under vacuum and was exposed to pyridine (25 ml) for 1 h. The FT-IR study of the pyridine adsorbed samples was carried out using an FTIR spectrophotometer equipped with The Selector DRIFT accessory (Graseby Specac, P/N 19900 series) incorporating an environmental chamber (EC) assembly (Graseby Specac, P/N 19930 series). The heating was done by using an automatic temperature controller (Graseby Specac, P/N 19930 series) connected with the environmental chamber. The spectra of the samples were recorded in the range of 400-4000 cm^{-1}. The spectra were recorded at room temperature and after in situ heating at different temperatures from 150 to 450 ºC with heating rate of 25 ºC /min, keeping at each temperature for 15 minutes under dry N_2 flow (30 cm^3/min).

3.1.1.3.5 N_2 adsorption-desorption isotherm studies

Textural properties such as specific surface area, pore volume, pore size and pore size distributions of the samples were determined from N_2 adsorption-desorption isotherms at liquid nitrogen temperature 77 K (ASAP 2010, Micromeritics, USA). Surface area and pore size distribution were determined using the BET equation and

BJH method **[183]** respectively. Before the analysis, the samples were degassed under vacuum at 120 ºC for 4 h to evacuate the physiosorbed moisture.

3.1.1.3.6 Bronsted acidity by cyclohexanol dehydration

The assessment of Bronsted acidity present in the sulfated-zirconia samples was done by dehydration of cyclohexanol to cyclohexene as a model test reaction, which is a Bronsted acid catalyzed reaction. The dehydration of cyclohexanol to cyclohexene with sulfated-zirconia samples was carried out in vapor phase using a fixed bed glass reactor. The sample (0.5 g) was packed in a glass reactor bed and *in-situ* activated at 450 ºC for 2 h under flow of N_2 or air (15 cm^3/min). The effect of the *in-situ* activation of the samples, under N_2 and air, on their activity was studied. The temperature of the reactor was brought down to reaction temperature of 175 ºC and cyclohexanol (5 ml) was delivered by syringe pump injector (Cole Parmer, 74900 series) with a flow rate of 0.042 cm^3/min under flow of N_2 (15 cm^3/min).

The vapor of reaction mixture was condensed by condenser and collected after 1 h. The reaction mixture was analyzed by gas chromatography (HP6890) having a FID detector, a HP50 (30 miter long) capillary column with a programmed oven temperature from 50 to 200 ºC and a 0.5 cm^3/min flow rate of N_2 as carrier gas. The conversion of cyclohexanol was calculated on the basis of its weight percent; the initial theoretical weight percent of cyclohexanol was divided by initial GC peak area percent to get the response factor. Final unreacted weight percent of cyclohexanol remaining in the reaction mixture was calculated by multiplying response factor with the area percentage of the GC peak for cyclohexanol obtained after the reaction.

The conversion of cyclohexanol was calculated as follows:

Response factor = Initial theoretical weight percent of cyclohexanol/ Initial GC peak area percent of cyclohexanol before reaction.

Final unreacted weight percent of cyclohexanol = Response factor X Final GC peak area percent of cyclohexanol after reaction.

$$\text{Conversion of cyclohexanol (wt \%)} = \frac{100 \text{ X [Initial wt\% - Final wt\%]}}{\text{Initial wt\%}}$$

$$\text{Selectivity of cyclohexene (wt. \%)} = \frac{100 \text{ X [GC peak area\% of cyclohexene]}}{\sum \text{Total GC peak area \% for all the products}}$$

3.1.1.3.7 Thermal Analysis

Thermogravimetric analysis (TGA) was performed using SDTA851e, Mettler Toldeo. Samples were exposed in the temperature range of 50- 900 ºC with a heating rate of 10 ºC/min under nitrogen flow (100 cm^3/min).

3.1.1.3.8 Sulfur Analysis

Percentage of sulfur retained in sulfated-zirconia samples after calcination was analyzed by a CHNS/O elemental analyzer (Perkin-Elmer, 2400). The sulfur content on the surface of zirconia and total sulfur were also measured by Inductive Couple Plasma-OES (Perkin Elmer Instrument, Optima 200 DV). The total sulfur was measured by dissolving the sample (100 mg) in 40% HF solution (15- 20 drops) followed by addition of 5 wt.% boric acid solution making up to 100 ml, which was analyzed by ICP. The surface sulfur was measured by leaching out the surface sulfates by adding the sample (100 mg) in 0.1 N NaOH solution (100 ml) under stirring for 5 min. The solution was filtered by filter paper to separate the solid and concentrated HCl (2 ml) was added to acidify the solution and analyzed by ICP.

3.1.2 Results and Discussion

3.1.2.1 Structural Properties

3.1.2.1.1 Crystalline Phase and Crystallite Size

The X-Ray Diffraction pattern of sulfated-zirconia samples SZO1, SZO2, SZTB and SZTN, after calcination at 600 ºC (Figure 1) show the characteristic peaks of tetragonal phase at 2θ of 30.18, 35.3, 50.2 and 60.2, which indicate the presence of purely tetragonal crystalline phase in all samples. The samples are highly crystalline. The X-Ray Diffraction pattern of the sample SZO2 (600) also shows the characteristic peaks of tetragonal phase (Figure 2) indicating the presence of purely tetragonal crystalline phase, however, the sample was less crystalline at 600 ºC and the crystallinity of the samples increases with increasing the calcination temperature from 600 to 800 ºC (Figure 2). However, only tetragonal crystalline phase was observed even after calcination at 800 ºC. The stabilization of tetragonal phase at higher temperature is attributed to the presence of sulfate.

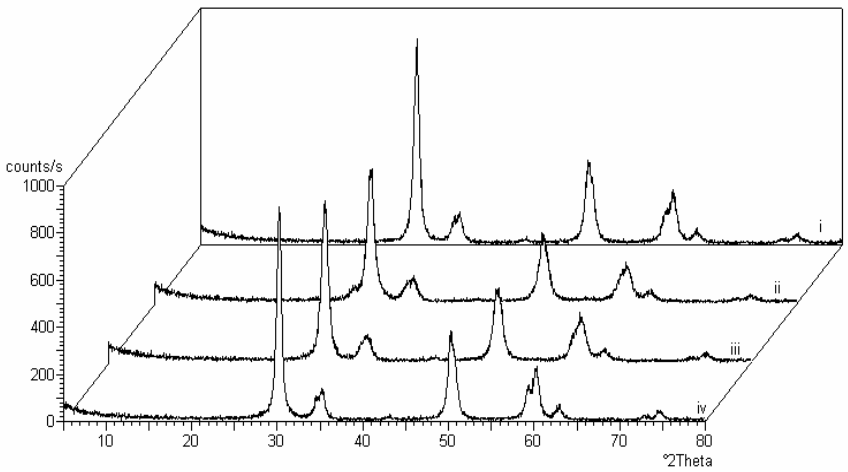

Figure 1. XRD pattern of: (1) SZO1, (2) SZO2, (3) SZTB and (4) SZTN, after calcination at 600ºC.

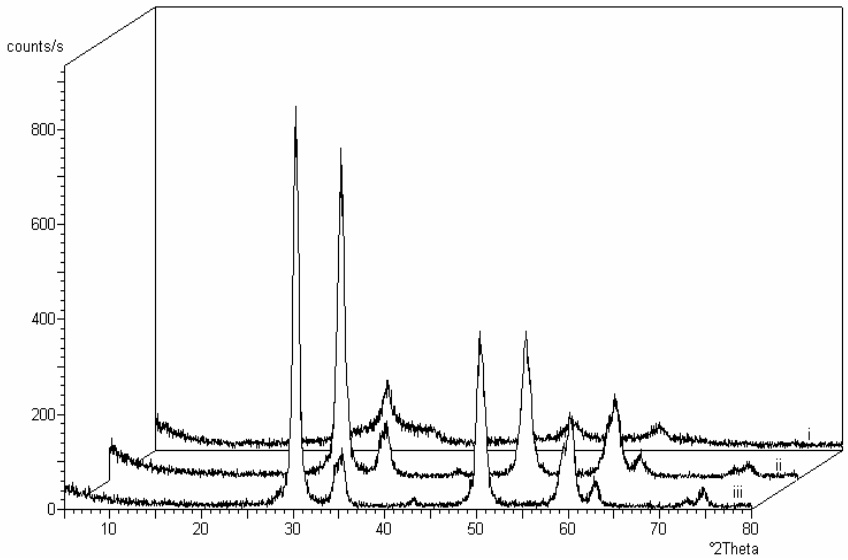

Figure 2. XRD patterns of sulfated-zirconia samples SZO2 (600) calcined at (i) 600, (ii) 700 and (iii) 800ºC.

The crystallite size of all samples was found in range of 9 to 16 nm, which shows that all sulfated-zirconia samples are nano-crystalline in nature (Table.1). Among the samples, synthesized by one-step sol-gel method, the sample SZO2 (600) has smaller crystallite size (9 nm) and in the samples, synthesized by two-step sol-gel method, the sample SZTB shows smaller crystallite size (11 nm). The crystallite size

of SZO2 (600) sample increases from 9 to 14 nm with increase of calcination temperature from 600 to 800 ºC. Thus the sulfated-zirconia samples, synthesized by one-step and two-step method, are having purely tetragonal phase and nano-crystalline.

Table 1. Crystalline phase and crystallite size of sulfated-zirconia samples.

Sample	Crystalline phase	Crystallite size (nm)	S (wt.%)[a] after calcination at 600 ºC
SZO1	T	14	1.3
SZO2	T	11	1.6
SZO2 (600)	T	9	3.0
SZO2 (700)	T	11	1.1
SZO2 (800)	T	14	0.6
SZTB	T	11	1.4
SZTN	T	16	1.3

T = Tetragonal phase.
[a]Measured by CHNS/O analysis.

The crystallinity of sulfated-zirconia samples, calcined at 600 ºC was observed to be related to sulfur content. The samples having sulfur content in the range of 0.6 to 1.6 wt.% were highly crystalline whereas higher sulfur content (3.0 wt.%) significantly lowers the crystallinity. The transformation of amorphous to crystalline phase i. e., crystallization, is dehydroxylation process involving the loss of hydroxyl groups to form crystallites **[157]**. The sulfate ions attached with hydroxyl groups resist the crystallization process. The higher thermal energy is required for the removal of hydroxyl groups for crystallization. This results into increase in calcination temperature required for crystallization **[126]**.

3.1.2.1.2 FT-IR studies

All sulfated-zirconia samples, synthesized by one-step and two-step sol-gel method after calcination at 600 ºC show similar IR-spectra; therefore, FT-IR spectrum of one of the sulfated-zirconia sample is given (Figure 3). It shows bands at 1250-1242, 1142, 1074, 1044 and 996 cm^{-1}, which are characteristics bands of inorganic chelating bidentate sulfates for asymmetric and symmetric partially ionized S=O

double bond and S-O single bond stretching mode **[98]**. The broad bands at around 3400 cm^{-1} and at 1639 cm^{-1} (not shown in the spectrum) are attributed to the presence of water molecules adsorbed with the surface sulfates and zirconia surface. The broadness of the peak is due to the hydrogen bonding **[111]**. The structure has partially ionized S=O bonds due to the presence of water molecule associated with sulfate group by hydrogen bonding **[98]**, which shows the ionic structure of sulfate species on the surface of zirconia as shown in Scheme 1. In hydrated sample, the sulfate is bonded with H_2O molecule through hydrogen bonding, which makes S=O bond partially ionic decreasing double bond character. The IR study shows that the structure of the surface sulfate is as an ionic chelating bidentate sulfate bonded with zirconium atom through two oxygen atoms and with water molecule by hydrogen bonding (Scheme 1). As all sulfated-zirconia samples, synthesized by one-step and two-step sol-gel method, show similar spectra, the sulfate species in all samples are of similar type.

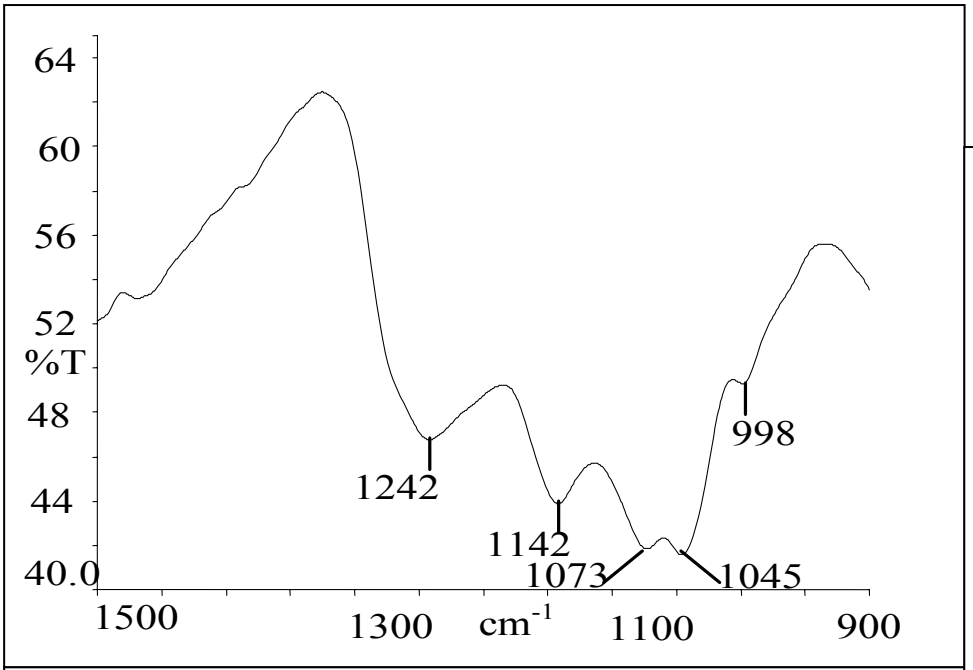

Figure 3. FTIR Spectra of sulfated-zirconia sample.

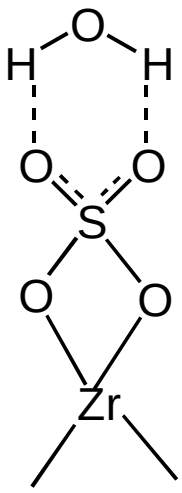

Scheme 1

3.1.2.1.3 DRIFT study

The effect of desorption of water molecule from surface sulfate species by *in-situ* heating of the sample was studied by diffuse reflectance IR (DRIFT) study after *in-situ* activation at 450 ºC. DRIFT spectrum (Figure 4) showed the presence of

additional band at 1405 cm^{-1}, which indicates the presence of S=O covalent bond in sulfate group (Scheme 2) and is responsible for generation of Lewis acid sites **[98]**. It clearly indicates the sensitivity of the sulfated-zirconia samples towards moisture. The removal of water molecules results into S=O covalent character responsible for the Lewis acid sites in sulfated-zirconia samples. The absorbance peak area of the band at 1405 cm^{-1} was measured to assess the Lewis acidity in the samples. It was observed in the range of 2.2–3.1 A cm^{-1} in all the samples. The low values of absorbance peak area of 1405 cm^{-1} indicate the presence of less Lewis acidity in the catalysts.

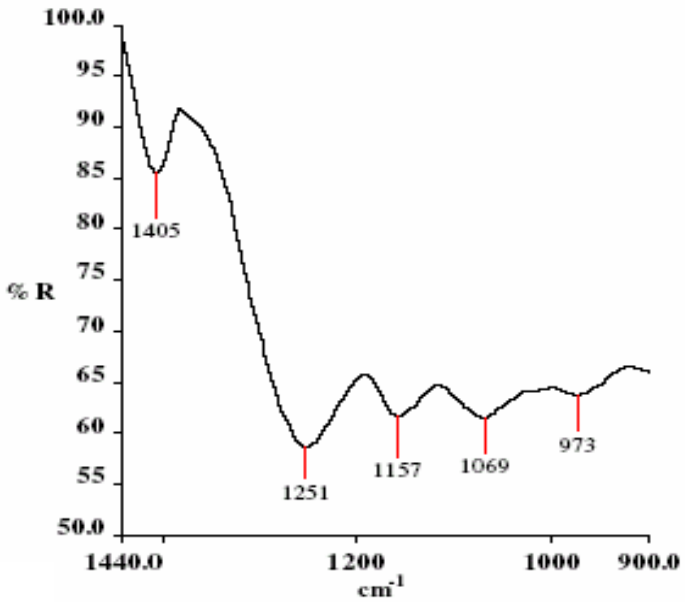

Figure 4. DRIFT spectra after in situ activation at 450 ºC.

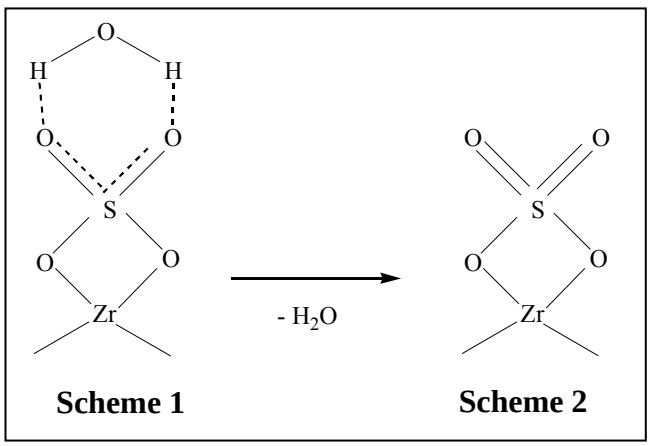

Scheme 1 **Scheme 2**

3.1.2.1.4 FT-IR Studies of the sulfated-zirconia samples adsorbed with pyridine at different temperature

FT-IR spectra of sulfated-zirconia samples adsorbed with pyridine at different temperatures from 150 to 450 ºC (Figure 5a- 5g) show bands in range of 1400- 1650 cm^{-1} for adsorbed pyridine at Bronsted and Lewis sites and a broad peak in OH region. The pyridine adsorbed at Bronsted sites gives the characteristic bands at 1640, 1607, 1540 and 1490 cm^{-1} **[189]** and the pyridine adsorbed at Lewis sites gives bands at 1604, 1574, 1490, and 1445 cm^{-1} **[190]**. The band at 1445 cm^{-1} is for pyridine adsorbed at Lewis sites and the band at 1540 cm^{-1} shows the adsorbed pyridine at Bronsted sites. The peak at 1490 cm^{-1} represents the total acidity in the sample.

All sulfated-zirconia samples showed the presence of both Bronsted and Lewis acid sites (Figure 5a- 5g). After *in-situ* heating at different temperature, the samples, calcined at 600ºC, retain pyridine at higher temperature of 450 ºC, which indicates the presence of significant amount of stronger Bronsted and Lewis acid sites. The samples, calcined at higher temperatures of 700 ºC showed less intensity of the peaks, which significantly decreased at 450 ºC. The sample, calcined at 800 ºC also showed less intensity of peaks, which were decreased only after 250 ºC, indicating the presence of weaker Bronsted and Lewis acid sites.

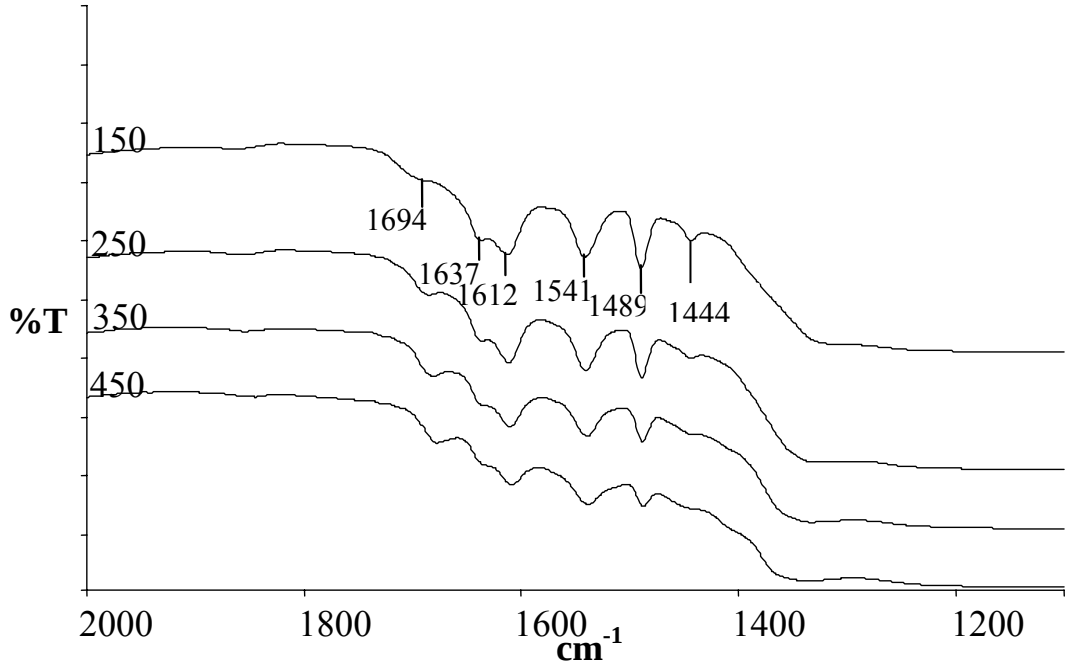

Figure 5a. FTIR spectra of pyridine adsorbed sulfated-zirconia sample SZO1 after desorption at (i) 150, (ii) 250, (iii) 350 and (iv) 450 ºC.

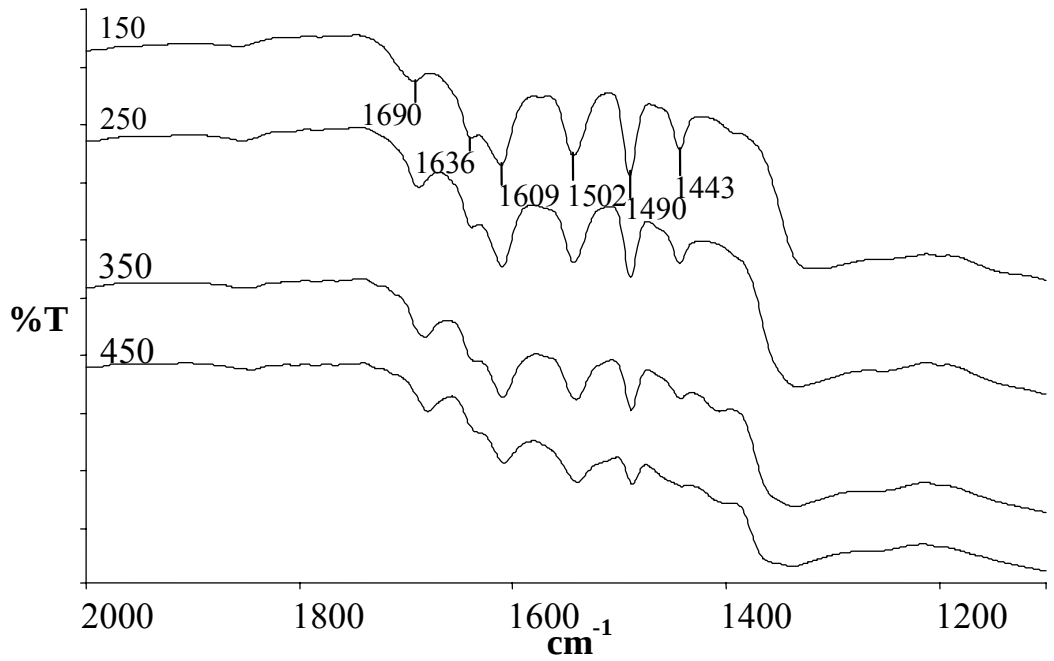

Figure 5b. FTIR spectra of pyridine adsorbed sulfated-zirconia sample SZO2 after desorption at (i) 150, (ii) 250, (iii) 350 and (iv) 450 ^{o}C.

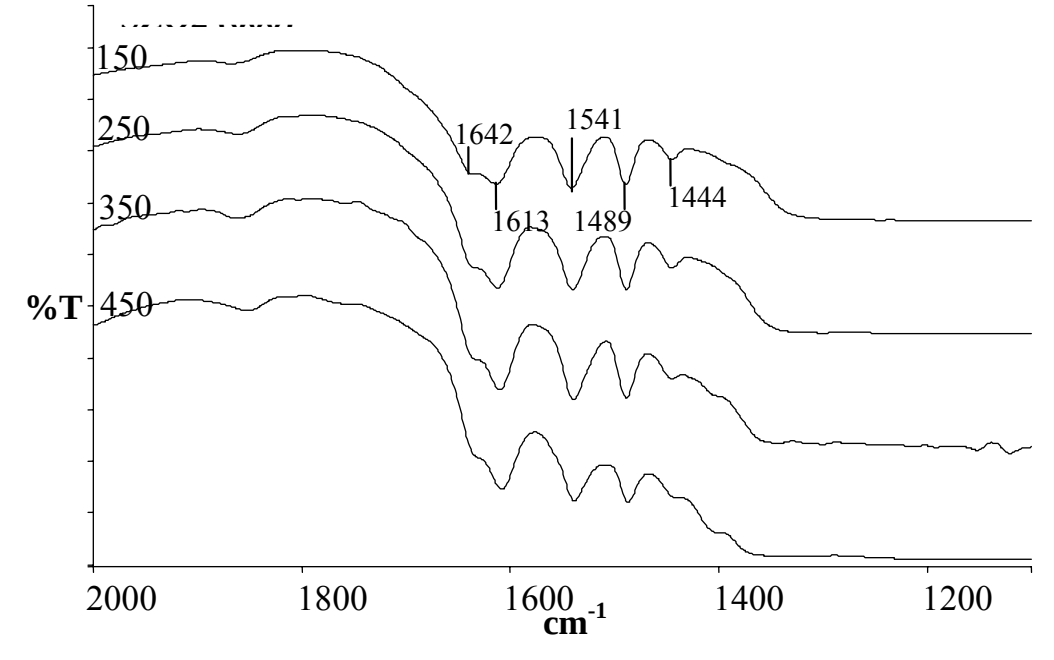

Figure 5c. FTIR spectra of pyridine adsorbed sulfated-zirconia sample SZO2 (600) after desorption at (i) 150, (ii) 250, (iii) 350 and (iv) 450 ^{o}C.

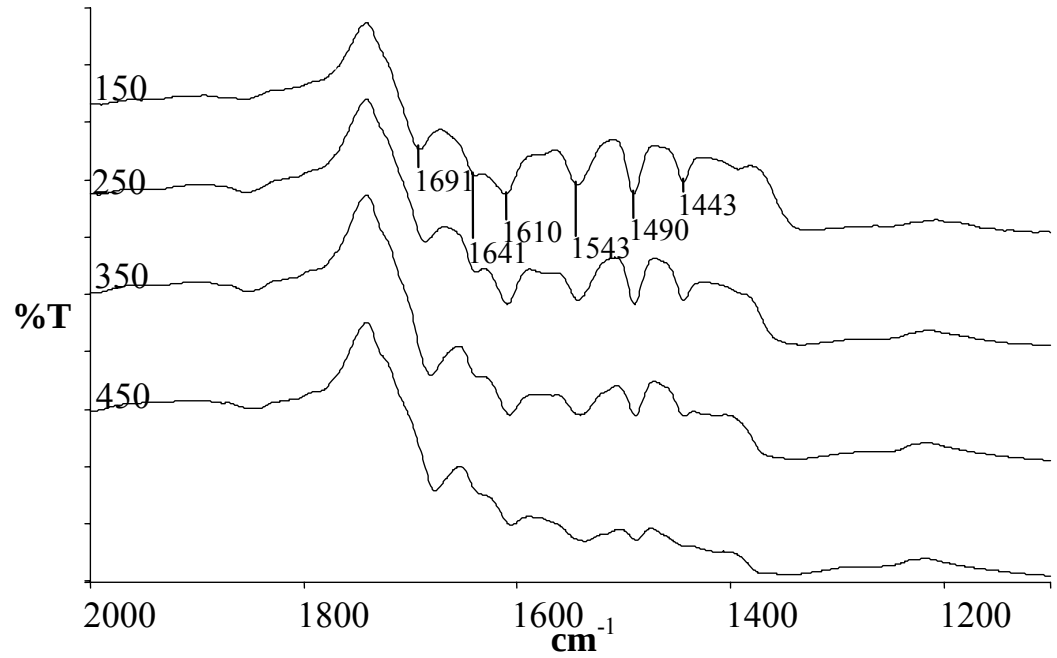

Figure 5d. FTIR spectra of pyridine adsorbed sulfated-zirconia sample SZO2 (700) after desorption at (i) 150, (ii) 250, (iii) 350 and (iv) 450 ^{o}C.

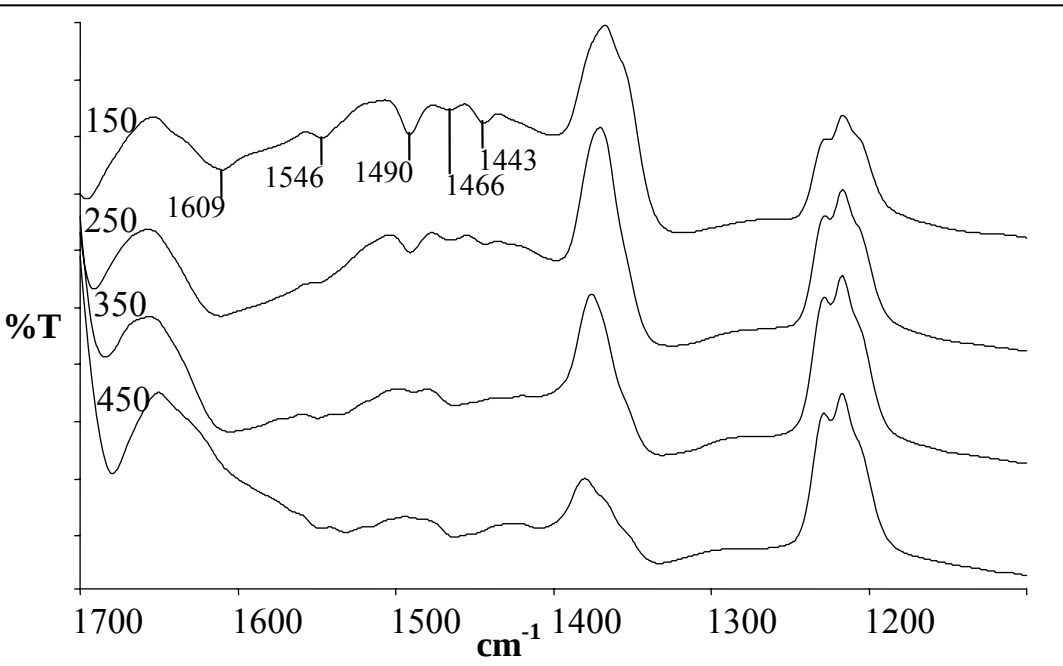

Figure 5e. FTIR spectra of pyridine adsorbed sulfated-zirconia sample SZO2 (800) after desorption at (i) 150, (ii) 250, (iii) 350 and (iv) 450 ^{o}C.

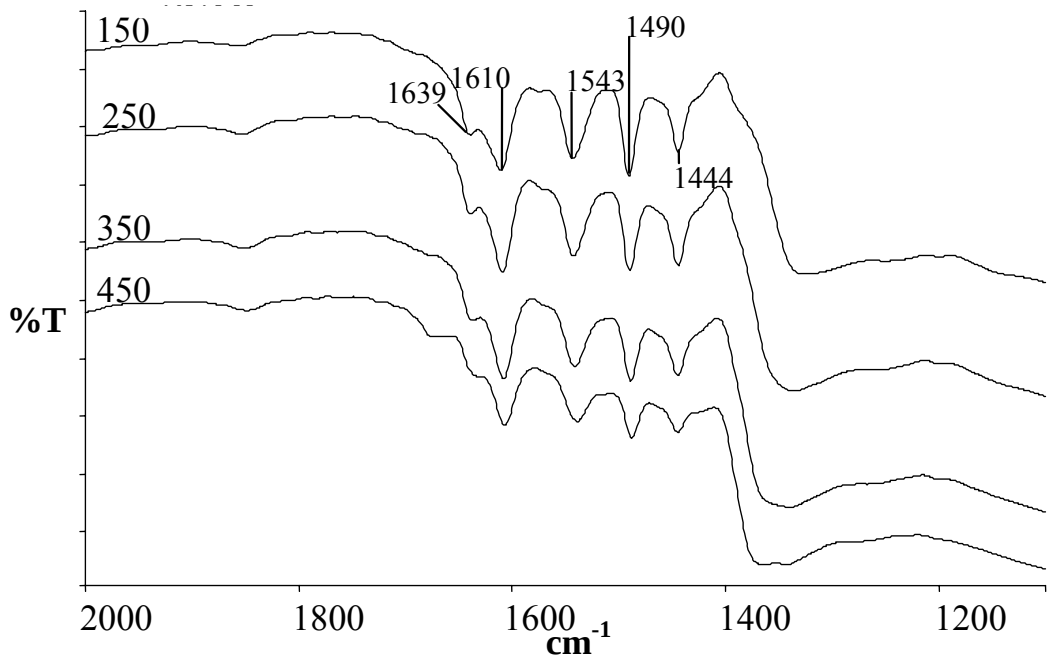

Figure 5f. FTIR spectra of pyridine adsorbed sulfated-zirconia sample SZTB after desorption at (i) 150, (ii) 250, (iii) 350 and (iv) 450 ^{o}C.

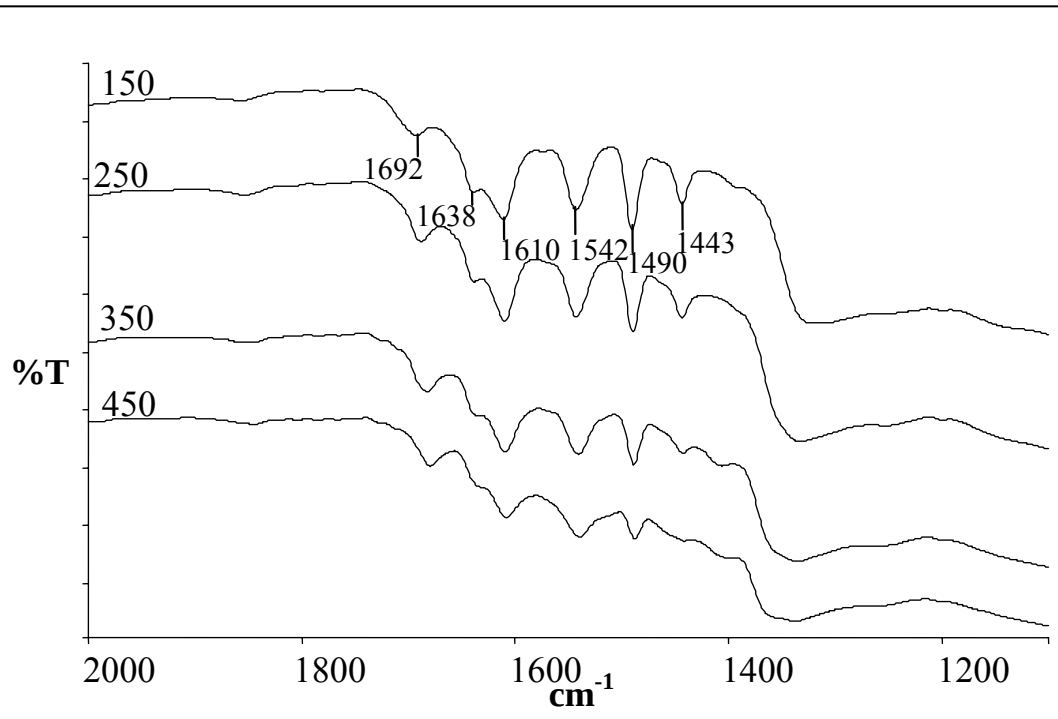

Figure 5g. FTIR spectra of pyridine adsorbed sulfated-zirconia sample SZTN after desorption at (i) 150, (ii) 250, (iii) 350 and (iv) 450 ^{o}C.

3.1.2.2 Textural Properties

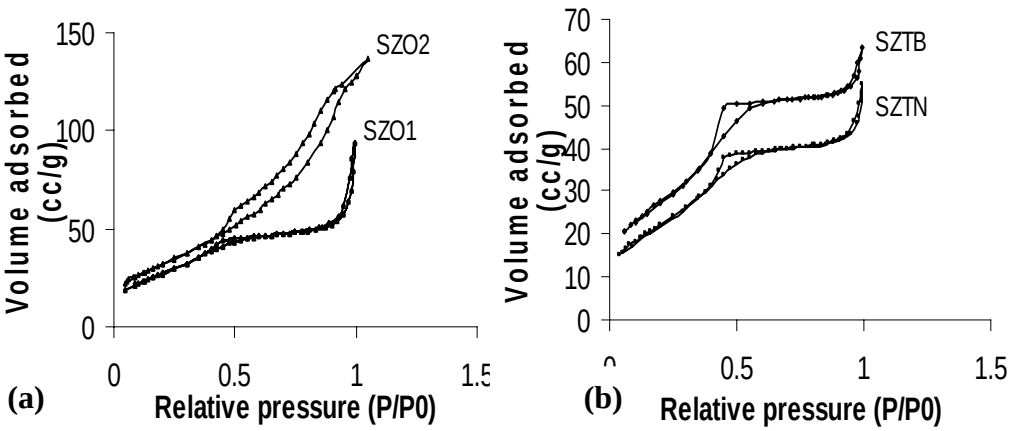

Figure 6. N_2-adsorption-desorption isotherms of sulfated-zirconia samples **(a)** SZO1, SZO2, (**b)** SZTB and SZTN calcined at 600 ºC.

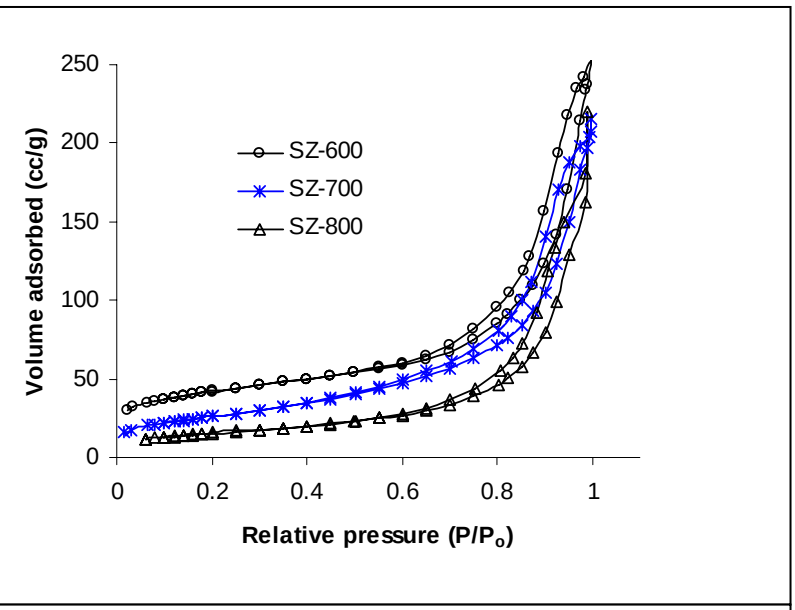

Figure 6 (c).N_2 Adsorption-desorption isotherms of the samples SZO2 calcined at (i) 600, (ii) 700 and (iii) 800 ºC.

N_2 adsorption-desorption isotherms of the sulfated-zirconia samples (Figure 6a, 6b and 6c), synthesized by one-step and two-step sol-gel method calcined at 600- 800 ºC, measured at 77 K are showing the isotherm of type IV, which is characteristic of mesoporous absorbents showing that the samples are mesoporous material. However, there is a large increase in adsorption at higher relative pressure (P/Po), which shows the presence of larger size mesopores in the samples. The

inflection point at relative pressure (P/Po) = 0.4, is not sharp in all the samples, which reflects that the pores are not of uniform size and have broad distribution. The samples SZO1, SZTB and SZTN have type H2 hysteresis, whereas, the samples SZO2, SZO2 (600), SZO2 (700) and SZO2 (800) show a broad hysteresis of type H3, reflecting the presence of large mesopores.

Table 2. Textural properties of sulfated-zirconia samples.

Sample	Surface area (m^2/g)	Pore volume (cm^3/g)	Pore size (Å)
SZO1	101	0.15	58
SZO2	118	0.19	62
SZO2 (600)	150	0.33	89
SZO2 (700)	96	0.28	120
SZO2 (800)	58	0.25	170
SZTB	101	0.09	35
SZTN	81	0.08	42

The surface area of the samples after calcination at 600 ºC (calculated from adsorption isotherm using BET equation) was in the range of 81-150 m^2/g (Table2). The samples, synthesized by one-step sol-gel method, have higher surface area, pore volume and pore size as compared to the samples, synthesized by two-step sol-gel method. Among the samples, synthesized by one-step sol-gel method and calcined at 600 ºC, the samples, SZO2 (600) has the highest surface area (150 m^2/g), pore volume (0.33 cm^3/g) and pore size (89 Å) and in the samples, synthesized by two-step sol-gel method, the sample SZTB has higher surface area (101 m^2/g). The surface area of SZO1 and SZTB is equal (101 m^2/gm), while there is large difference between pore volume and pore size. The surface area of the samples calcined at higher temperature (700 and 800 ºC) was found to be decreasing with temperature due to increase of crystallite size and sintering but the pore volume increased due to formation of larger pores by collapse of pores (Table 2). The surface area has been observed to be related with the crystallite size. The samples, SZO1, SZO2 (600) and SZTB, having smaller crystallite size (11- 14 nm), show higher surface area (101- 150 m^2/g) and the sample SZTN shows lower surface area (81 m^2/g) due to large crystallite size (16 nm). With increasing the calcination temperature from 600 to 800 ºC, the crystallite size of the samples SZO2 (600), SZO2 (700) and SZO2 (800) gradually increases (from 9 to 14

nm), which reduces the surface area (from 150 to 58 m^2/g). The pore size distribution (Figure 7a, 7b and 7c) was observed to be very broad (20- 80 Å) in the samples, synthesized by one-step sol-gel method adding sulfuric acid in alkoxide solution, than other samples (20- 60 Å).

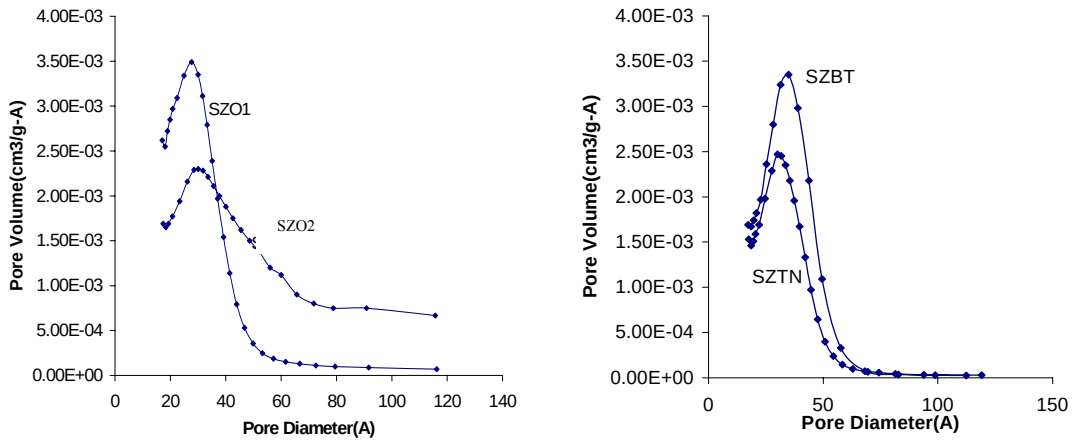

Figure 7. Pore size distribution in the samples, synthesized by **(a)** one-step and **(b)** two-step sol-gel method, calcined at 600 ºC.

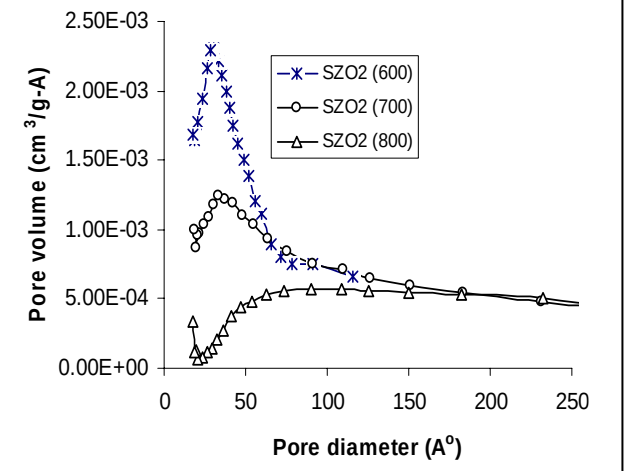

Figure 7c. Pore size distribution in the samples SZO2 (600), SZO2 (700) and SZO2 (800), synthesized by one-step sol-gel method, calcined at 600- 800 ºC.

3.1.2.3 Dehydration of cyclohexanol to cyclohexene

The results of the activity of the sulfated-zirconia samples, synthesized by one-step and two-step sol-gel method, for dehydration of cyclohexanol to cyclohexene test reaction are given in Table 4. The dehydration reaction is Bronsted acid catalyzed reaction; therefore the conversion value directly gives Bronsted acidity of the samples.

Table 3. Conversion (wt.%) of cyclohexanol and selectivity of cyclohexene with sulfated-zirconia samples, *in-situ* activated under different atmosphere.

Sample	Activation in flow of N_2	Activation in flow of air	Selectivity of cyclohexene (%)
	Conversion (wt.%)	Conversion (wt.%)	
SZO1	83	100	~100
SZO2	87	80	~100
SZO2 (600)	28	85	~100
SZO2 (700)	29	100	~100
SZO2 (800)	15	17	~100
SZTB	85	64	~100
SZTN	78	71	~100

(Cyclohexanol = 5 g, Catalyst = 0.5 g, Activation Temperature = 450 ºC, Reaction Temperature = 175 ºC, Reaction Time = 1 h)

All sulfated-zirconia samples, *in-situ* activated at 450 ºC in flow of nitrogen, were found to be active for dehydration of cyclohexanol showing the presence of significant amount of Bronsted acidity (Table 3). The samples SZO1, SZO2, SZTB and SZTN showed higher conversion of cyclohexanol (78- 87%) with 100% selectivity of cyclohexene showing the presence of higher Bronsted acidity in the samples. The samples SZO2 (600), SZO2 (700) and SZO2 (800), showed very low conversion of cyclohexanol (15- 29%). However, the *in-situ* activation of the samples SZO2 (600) and SZO2 (700) in flow of air significantly enhanced the conversion of cyclohexanol (85- 100% with 100% selectivity of cyclohexene) showing higher activity (Table 3). The lesser activity of the sample SZO2 (800), either activated in flow of nitrogen or air, for dehydration of cyclohexanol is attributed to lesser sulfur content (0.6 wt.%), which generates very less Bronsted acidity. The *in-situ* activation

of the sample SZO1 in flow of air also showed enhanced activity for dehydration of cyclohexanol (100%). It shows that the activation condition and particularly the different atmosphere (nitrogen and air) affect the activity of the samples.

The activation of the sample before the reaction is an important step in order to have maximum activity of the catalyst. In the sample, before activation, the surface acidity and therefore, activity is suppressed as the sulfates are in inactive hydrated form due to adsorbed water molecules by hydrogen bonding. Further, the acid sites are occupied by water molecule adsorbed by hydrogen bonding. The activation of sample (dehydration) brings the sulfates in active dehydrated form, which generates the surface acidity and further, the acid sites become free from adsorbed water molecules. Therefore, the activation of the catalyst before reaction is an essential step. The studies **[167, 178]** have shown the requirement of certain amount of hydration in the sulfate-zirconia catalysts in order to generate Bronsted and Lewis acid sites and higher acidity, however, the higher amount of water diminishes the activity of the catalyst. The lower catalytic activity of the hydrated sulfated-zirconia catalyst has been reported due to alteration of oxidation-reduction properties of surface sulfates **[167]**. The phenomenon of the activity of dehydrated form of sulfate and inactiveness of hydrated form of sulfates can be explained by the oxidation state of sulfur. In ionic form the oxidation state of sulfur is reduced (<+6), while in active dehydrated form of sulfate, the oxidation state of sulfur is higher (+6). The higher oxidation state of sulfur (+6) has been reported to be responsible for higher activity of sulfated-zirconia **[95]**.

The activation under air may be oxidizing the sulfur species to higher oxidation state and help in the desorption of the physically adsorbed water molecules in the catalyst. The higher conversion of cyclohexanol with the samples SZO1, SZO2, SZTB and SZTN (78- 85%), even after activation under nitrogen, shows that these samples could be activated under these conditions. The results show that all sulfated-zirconia catalysts are having higher Bronsted acidity; however, the method of activation of the catalyst plays an important role in order to attain maximum activity.

The presence of higher Bronsted acidity in the samples, SZO1, SZO2, SZTB and SZTN, is also evident from low values of absorbance peak area (2–3 A cm^{-1}) of $\nu_{S=O}$ band at 1405 cm^{-1} indicating weak Lewis acidity in the samples (Table 4).

Table 4. Absorbance peak area of the band at 1400 cm^{-1} (A cm^{-1}) in samples.

Sample	Absorbance peak area of the band at 1400 cm^{-1} (A cm^{-1})
SZO1	2.3
SZO2	2.2
SZTB	2.2
SZTN	3.1

3.1.2.4 Thermal Analysis

The weight loss in the sulfated-zirconia samples, calcined at 600- 800 ºC, was in range of 3.4- 4.3 wt.%, which is due to loss of excess water in sample remained, dehydroxylation and loss of sulfur at higher temperature (Figure 8a and 8b).

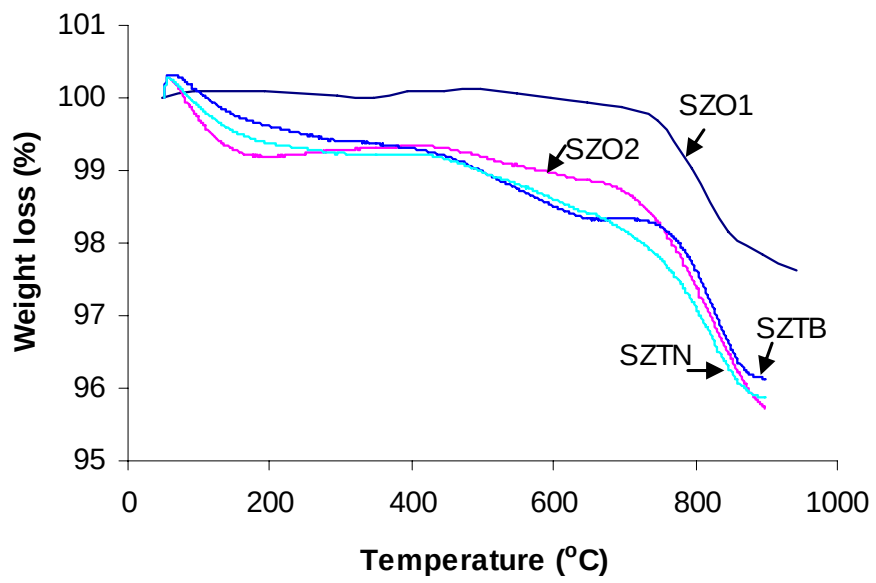

Figure 8a. TGA graphs of the sulfated-zirconia samples, synthesized by one-step and two-step sol-gel methods, calcined at 600 ºC.

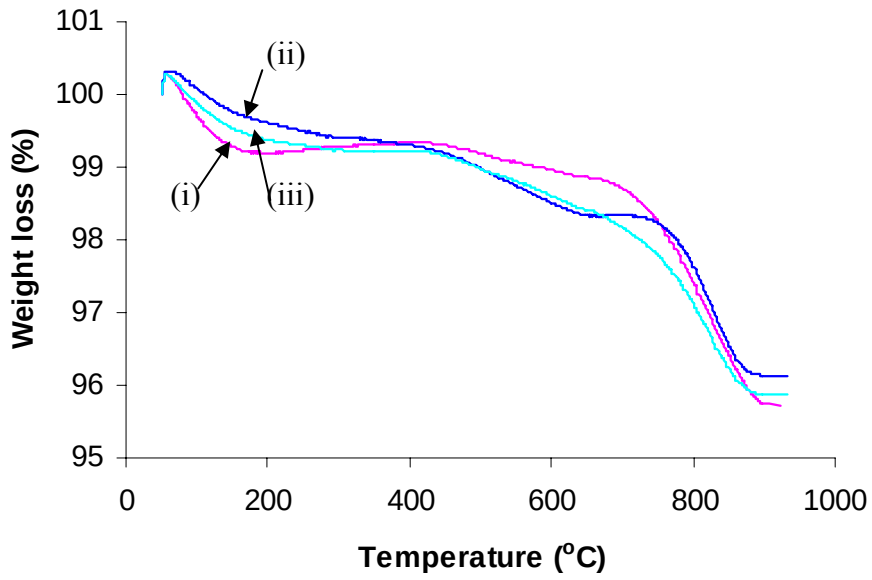

Figure 8b. TGA graphs of the sulfated-zirconia samples (i) SZO2 (600), (ii) SZO2 (700), and (iii) SZO2 (800).

3.1.2.5 Sulfur analysis

Table 5 shows the data of sulfur content in the sulfated-zirconia samples before and after calcination. It shows that the sulfur content in the samples after calcination at 600 ºC is in the range of 1.3 to 3.0 wt.% (measured by CHNS/O). The total sulfur content in the samples (1.1- 2.9 wt.%; measured by ICP) was found to be in the similar range (1.0- 2.6 wt.%) of the surface sulfur content, which shows that all sulfate species are present at or near the surface of zirconia.

Table 5. Sulfur content (wt.%) in sulfated zirconia samples after calcination at different temperature

Sample	Before calcination	After calcination		
	S (wt.%)[a]	Total S (wt.%)[a]	Total S (wt.%)[b]	Surface S (wt.%)[b]
SZO1	3.5	1.3	1.3	1.3
SZO2	3.8	1.6	-	-
SZO2 (600)	4.0	3.0	2.9	2.6
SZO2 (700)	4.0	1.1	1.2	1.1
SZO2 (800)	4.0	0.6	0.7	0.6
SZTB	4.4	1.4	1.1	1.0
SZTN	5.2	1.3	1.1	1.0

[a]Measured by CHNS/O analysis, [b]Measured by ICP analysis.

The higher sulfur content in the sample SZO2 (600) is attributed to *in-situ* sulfation by adding sulfuric acid in alkoxide, which retains more sulfates after calcination at 600 ºC. The addition of sulfuric acid in zirconium propoxide i. e., *in-situ* sulfation, may result to binding of sulfates with zirconium propoxide replacing the propoxide groups **[112]**. The hydrolysis with water forms sulfated zirconium hydroxide keeping the zirconium and sulfate bond intact and undergo polycondensation to form the gel. The sulfates are thus bonded with zirconium and are trapped in the gel network, which on calcination comes out from bulk on the surface consuming some thermal energy. After calcination at 600 ºC, the most of sulfates came out from bulk to surface. However, a very small fraction of sulfates could be lost due to insufficient amount of thermal energy at 600 ºC and retained most of sulfates on the surface showing higher sulfur content in the sample.

Further more, the less water (water/ alkoxide molar ratio = 2.7), used for the synthesis of SZO2 (600), could not hydrolyze the Zr-SO_4 bonds as the water was consumed in the hydrolysis of zirconium propoxide and therefore, the Zr-SO_4 bond remains intact. It has also been reported **[118]** that the hydrolysis at lower water to alkoxide molar ratio results to the gel having unhydrolyzed alkoxide groups attached with zirconium atoms, which are decomposed to carbon dioxide on calcination. The decomposition of the unhydrolyzed alkoxide groups resists the decomposition of sulfur species and retains more sulfur in the sample. The sample SZO2 was also synthesized by similar method as the sample SZO2 (600), however, the higher water to alkoxide ratio used for the synthesis of SZO2 was found to be responsible for the less sulfur content (1.6 wt.%) in the sample. The higher amount of water (water/ alkoxide molar ratio = 4), added for hydrolysis, hydrolyzes the Zr-SO_4 bonds. Thus, the most of sulfates become free in the gel network. These sulfates are easily lost during calcination at 600 ºC, retaining less sulfur in the sample.

The sulfur content in the samples SZO2 (600), SZO2 (700) and SZO2 (800) gradually decreases due to calcination at higher temperature decomposing the sulfates. The sulfur content was observed to be affecting the physicochemical properties and therefore, the catalytic properties of the samples. The higher sulfur content (3.0 wt.%) in the sample SZO2 (600) lowers the crystallinity giving smaller crystallite size (9 nm) and higher surface area (150 m^2/g). The sulfur content ranging from 0.6- 1.6 wt.% in the samples (SZO1, SZO2, SZO2 (700), SZO2 (800), SZTB and SZTN) results to higher crystallinity with slightly higher crystallite size (11- 16

nm) and lower surface area (81- 101 m^2/g). The sample SZO2 (800) having less sulfur content (0.6 wt.%) show higher crystallite size (14 nm), less surface area (58 m^2/g) and less acidity with weak Bronsted and Lewis acid sites. The effect of sulfur content on the catalytic properties of the sulfated-zirconia samples will be discussed for acylation of anisole and veratrole, in the second part of this chapter.

3.1.3 Conclusions

The synthesis of sulfated-zirconia catalysts by one-step and two-step sol-gel methods results to nano-crystalline mesoporous material having purely tetragonal phase. The sulfated-zirconia catalysts, synthesized by one-step sol-gel methods, were observed to show higher surface area, pore volume and pore size. Among the samples synthesized by one-step sol-gel method, the sample, synthesized by addition of sulfuric acid in alkoxide solution before hydrolysis shows higher surface area, pore volume and pore size. The higher sulfur content in the sample, synthesized by one-step sol-gel method by *in-situ* sulfation, by adding sulfuric acid in alkoxide solution, remarkably affects the physicochemical properties, acidity and catalytic activity of the sample. The *in-situ* sulfation in synthesis by one-step sol-gel method adding sulfuric acid in alkoxide results to the samples having higher surface area, pore volume and pore size but broad pore size distribution. The sulfated-zirconia catalysts, synthesized by one-step and two-step sol-gel methods, contain both stronger Bronsted and Lewis acid sites, which is reduced in the sample calcined at high temperature. All samples, synthesized by one-step and two-step sol-gel method, are highly active for dehydration of cyclohexanol showing the presence of significantly higher Bronsted acidity, however, the activity of the samples is affected by the activation condition.

Chapter 3

(II)

Acylation of Aromatic Ethers such as Anisole and Veratrole using Nano-crystalline Sulfated Zirconia prepared by One-step and Two-step Sol-Gel Technique

3.2 Introduction

Friedel-Crafts acylation of aromatic compounds to synthesize aromatic ketones is of commercial importance as fine chemicals, drug intermediates, fragrances and perfumery chemicals. An aromatic ketone is formed by reaction of an aromatic compound with an acylating agent such as acyl halide, acid anhydride, carboxylic acid or an ester, in the presence of acid. Generally, the reaction is carried out in presence of Lewis acids such as transition metal halides in more than stoichiometric amount. The use of these homogeneous catalysts in large amount on industrial scale is economically and environmentally unfavorable. The selectivity of the desired product is lesser as some times, the reaction leads to formation of variety of side products. The catalyst cannot be recovered from reaction mixture after completion of reaction as it forms complex molecule with the product, which gets hydrolyzed to hydroxides during water work up. To overcome the drawbacks of the conventional homogeneous catalysts, the heterogeneous catalysts such as zeolites, modified clays, ion exchange resins, heteropoly acid, supported ionic liquids, proton or Lewis acids on a support and Nafion or Nafion like composites, have been found best alternate and have been excessively reported in the literature for acylation of a number of aromatics **[204-213]**. Sulfated-zirconia has been studied for acylation of a number of aromatic compounds namely toluene, xylene, anisole, veratrole, naphthalene, etc. to synthesize different aromatic ketones **[67- 74]**.

The acylation of anisole and veratrole gives para-acylated products as major product, which finds usage as fine chemicals, drug-intermediates, sweetening agents and fragrances. Para-acylated anisole i.e., 4-methoxy acetophenone synthesized by is intermediate for the production of sodium salt of 2-(4-methoxy benzoyl) benzoic acid, which is a sweetening agent. Para acylated veratrole i.e., 3, 4-dimethoxy acetophenone is intermediate for the production of vesnarinone, which is a cardiotonic.

In the present chapter, the catalytic behavior of sulfated-zirconia catalysts, synthesized by one-step and two-step sol-gel methods, was studied for acylation of anisole and veratrole with acetic anhydride and the reaction conditions, such as reaction temperature, time, molar ratio of substrates, substrate to catalyst weight ratio and the regeneration of spent catalyst were studied.

3.2.1 Experimental

3.2.1.1 Material

Anisole, tridecane and acetic anhydride were procured from s.d. Fine chemicals, India and veratrole was from Spectrochem, India. All the chemicals were used as such without any purification.

3.2.1.2 Acylation of anisole and veratrole with acetic anhydride

The catalytic activity of the sulfated-zirconia samples, synthesized by one-step and two-step sol-gel methods, was studied for acylation of anisole and veratrole with acetic anhydride. In a 50 ml reaction tube of reaction station (12 Place Heated Carousel Reaction Station, RR99030, Radleys Discovery Technologies, UK), anisole or veratrole and acetic anhydride was taken in 1:2 ratio and tridecane (10 wt% of substrate) was used as internal standard. The catalyst activated at 450 ºC for 2 h and cooled under vacuum (substrate to catalyst ratio = 10) was added in the reaction mixture. The reaction was carried out at different temperatures in the range of 110 to 170 ºC by heating the reaction mixtures in different reaction tubes on reaction station under stirring for 5 min. to 3 h. The reaction tubes containing reaction mixture were taken out at different time intervals and the reaction mixture was filtered to separate the catalyst and was analyzed by gas chromatogram (HP6890) having a HP50 (30 miter long) capillary column with a programmed oven temperature from 50 to 200 ºC, a 0.5 cm^3/min flow rate of N_2 as carrier gas and FID detector.

The conversion of aromatic substrate (anisole/veratrole) was calculated by using weight percent method; the initial theoretical weight percent of aromatic substrate was divided by initial GC peak area percent to get the response factor. Final unreacted weight percent of aromatic substrate remaining in the reaction mixture was calculated by multiplying response factor with the area percentage of the GC peak for aromatic substrate obtained after the reaction.

Response factor = Initial theoretical weight percent of aromatic substrate/ Initial GC peak area percent of aromatic substrate before reaction.

Final unreacted weight percent of aromatic substrate = Response factor X Final GC peak area percent of aromatic substrate after reaction.

$$\text{Conversion of anisole or veratrole (wt \%)} = \frac{100 \text{ X [Initial wt\% - Final wt\%]}}{\text{Initial wt\%}}$$

$$\text{Selectivity of 4-methoxy acetophenone (wt. \%)} = \frac{100 \text{ X [GC peak area\% of 4-methoxy acetophenone]}}{\sum \text{Total GC peak area \% for all the products}}$$

$$\text{Selectivity of 3, 4-dimethoxy acetophenone (wt. \%)} = \frac{100 \text{ X [GC peak area\% of 3, 4-dimethoxy acetophenone]}}{\sum \text{Total GC peak area \% for all the products}}$$

3.2.1.3 Catalyst regeneration

The regeneration study of sulfated-zirconia catalyst was done with the spent catalyst, which was recovered from the reaction mixture by filtration. The used catalyst was washed with acetone to remove the adsorbed reactants and products and activated at 650 ºC for 4 h in flow of air. The catalyst was used for further reaction cycles under the optimized reaction conditions.

3.2.2 Results and Discussion

3.2.2.1 Acylation of anisole and veratrole with acetic anhydride over sulfated-zirconia samples

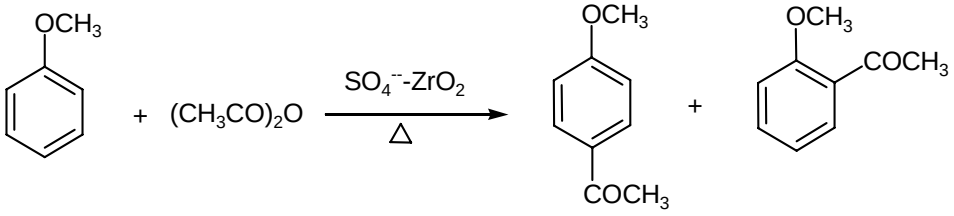

Anisole — Acetic anhydride — 4- Methoxy acetophenone — 2- Methoxy acetophenone

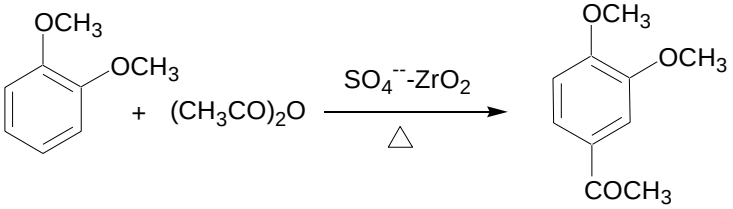

Veratrole — Acetic anhydride — 3, 4-Dimethoxy acetophenone

The catalytic activity of sulfated-zirconia samples, synthesized by one-step and two-step sol-gel method, for acylation of anisole and veratrole with acetic anhydride is given in Table 6a and 6b respectively. The reaction was initially carried out taking substrate to acylating agent molar ratio of 1:2 and substrate to catalyst weight ratio of 10 at 110 ºC for 3 h. The reaction conditions were then optimized in order to improve the conversion, which will be discussed in later section.

All four samples were found active for acylation reaction showing the conversion of anisole and veratrole in range of 25- 36 % and 29- 42 % respectively. However, the samples, synthesized by two-step sol-gel method, showed higher activity for acylation of anisole and veratrole. The sample SZTB showed maximum conversion of anisole (36 %) and veratrole (42 %). The acylation of anisole using sulfated-zirconia samples resulted to 4-methoxy acetophenone (98 %) and 2-methoxy acetophenone (2 %), while veratrole gave single acylated product, 3, 4-dimethoxy acetophenone (100 %). The conversion of veratrole was higher than the conversion of anisole due to highly activated aromatic ring in former.

Table 6a. Activity of the sulfated-zirconia samples for acylation of anisole.

Sample	Conversion of anisole (wt.%)	Selectivity (%) of 4-methoxy acetophenone	Selectivity (%) of 2-methoxy acetophenone
SZO1	25	98	2
SZO2	30	98	2
SZTB	36	98	2
SZTN	27	98	2

(10 mmol anisole, 20 mmol acetic anhydride (1:2), 0.1 g tridecane (internal standard), 0.1 g catalyst, Reaction Temperature = 110 ºC, Reaction Time = 3 h)

Table 6b. Activity of sulfated-zirconia samples for acylation of veratrole.

Sample	Conversion of veratrole (wt.%)	Selectivity (%) of 3,4-dimethoxy acetophenone
SZO1	29	100
SZO2	39	
SZTB	42	
SZTN	33	

(10 mmol veratrole, 20 mmol acetic anhydride (1:2), 0.1 g tridecane (internal standard), 0.1 g catalyst, Reaction Temperature = 110 ºC, Reaction Time = 3 h)

Effect of calcination temperature on the catalytic activity

The effect of calcination temperature on the structural, textural and acidic properties has already been discussed in previous section. The calcination temperature was observed to be affecting the activity of the sulfated-zirconia samples for acylation of anisole and veratrole also. The effect of calcination temperature on the catalytic activity of the samples was studied with the sample SZO2 calcined at 600- 800 ºC, viz., SZO2 (600), SZO2 (700) and SZO2 (800) at 110 ºC for 3 h.

The conversion of anisole and veratrole was found to be significantly increased in SZO2 (700) giving 35 % conversion of anisole with 98 % selectivity of 4-methoxy acetophenone (Figure 9). The conversion of veratrole with the sample SZO2 (700) increased to 60 % with 100 % selectivity of 3, 4-dimethoxy acetophenone. However, the sample SZO2 (800), calcined at still higher temperature (800 ºC) showed the decrease in the conversion of both anisole and veratrole (Figure 9).

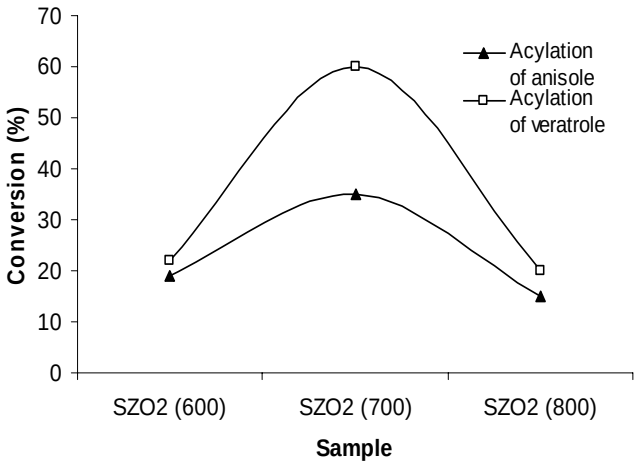

Figure 9. Effect of calcination temperature on the catalytic activity of sulfated-zirconia catalysts (calcined at 600, 700 and 800 ºC) for acylation of anisole and veratrole.

The results showed that the calcination temperature has significant effect on the activity of the sulfated-zirconia samples, which is related with the sulfur content retained and therefore the surface acidity of sulfated-zirconia. The higher sulfur content (3.0 wt.%) in the sample SZO2 (600) generates higher number of Bronsted acid sites as compared to Lewis acid sites, which is also evident by the FT-IR spectra after pyridine adsorption (Figure 5c) showing an intense peak at 1541 cm^{-1} (for Bronsted acid sites) and less intense peak at 1444 cm^{-1} (for Lewis acid sites). The

calcination at higher temperature (700 ºC) decreases the sulfur content (1.1 wt.%) in the sample SZO2 (700), which increase the amount of Lewis sites as can be clearly seen by FT-IR spectra (Figure 5d) showing intense peak at 1443 cm^{-1} (for Lewis acid sites). The increased amount of Lewis acid sites enhances the activity of the catalyst for acylation reaction. Further, the calcination at 800 ºC results to very less sulfur content (0.6 wt.%) in the sample, which generates less and very weak Bronsted and Lewis acid sites, which can also be seen by FT-IR spectra (Figure 5e) having weak peaks at 1546 and 1443 cm^{-1} and therefore, the catalyst showed lower catalytic activity. The study confirms that an optimum amount of sulfur (~1 wt.%) is required to generate reasonable amount of stronger Bronsted and Lewis acid sites and thus higher catalytic activity.

3.2.2.2 Effect of reaction temperature

The effect of reaction temperature on acylation of anisole and veratrole with sulfated-zirconia was studied to optimize the reaction temperature for achieving maximum conversion of aromatic substrate. The study was done by carrying out the reaction with SZO2 (700), which showed maximum activity for acylation reaction, at different temperatures ranging from 110 to 170 ºC for 3 h.

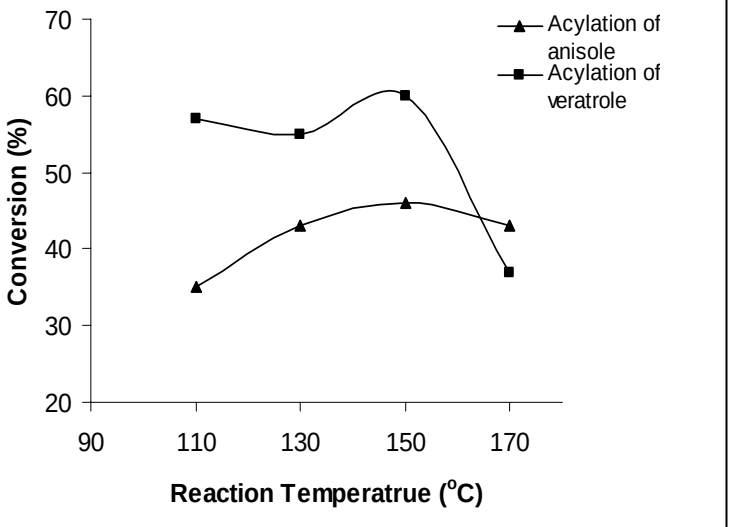

Figure 10. Variation of conversion (wt.%) of anisole and veratrole with reaction temperature.

Figure 10 shows the effect of the reaction temperature on the conversion of anisole and veratrole. The conversion of anisole as well as veratrole was found to be

gradually increased with increase in reaction temperature and showed maximum conversion of anisole (46 %) and veratrole (60 %) at 150 ºC, while selectivity remained constant. After 130 ºC, the conversion of anisole remained almost constant up to 170 ºC (43- 46 %) but conversion of veratrole significantly decreased at 170 ºC (37 %). The further study on acylation of anisole and veratrole was done at 150 ºC as optimized temperature.

3.2.2.3 Optimization of reaction time

The reaction time required to achieve maximum conversion of anisole and veratrole at 150 ºC was obtained by carrying out the reaction with SZO2 (700), under similar reaction conditions from 5 min. to 3 h. The data (Table 7) shows that the maximum conversion of anisole was achieved within 30 min. with 46 % conversion and 98 % selectivity of 4-methoxy acetophenone while veratrole showed maximum conversion (60 %) within 10 min. with 100 % selectivity of 3, 4-dimethoxy acetophenone. There is no further increase in conversion of anisole and veratrole at higher time and the selectivity of the acylated products remains steady with time. The kinetic data reveals that the acylation reaction is very fast with sulfated-zirconia catalyst. Although, the maximum conversion of anisole and veratrole was observed within 30 and 10 min. respectively, for the further study, the acylation of anisole and veratrole was carried out for 60 and 30 min. respectively.

Table 7. Conversion (wt.%) of anisole and veratrole with time.

Reaction time (minutes)	Conversion of anisole (wt.%)	Selectivity (%) of 4-methoxy acetophenone	Conversion of veratrole (wt.%)	Selectivity (%) of 3,4-dimethoxy acetophenone
5	37	98	46	100
10	35	98	60	100
15	36	98	59	100
30	46	98	59	100
60	46	98	60	100
120	45	98	60	100
180	46	98	60	100

(10 mmol anisole/ veratrole, 20 mmol acetic anhydride (1:2), 0.1 g tridecane (internal standard), 0.1 g catalyst, Reaction Temperature = 150 ºC)

3.2.2.4 Effect of aromatic substrate to acetic anhydride molar ratio

The effect of aromatic substrate to acetic anhydride molar ratio on the conversion of anisole and veratrole in acylation reaction was studied by carrying out the reaction with SZO2 (700) at 150 ºC for 60 and 30 min. respectively at different molar ratio in range of from 1:1 to 1:3.

The conversion of veratrole significantly increases from 42 to 61 % with increasing the amount of acetic anhydride from 1:1 to 1:3 molar ratio (Table 8); however, for anisole only slight variation in conversion (42- 48 %) was observed with increasing the molar ratio of anisole to acetic anhydride from 1:1 to 1:3. The selectivity of the acylated products of anisole and veratrole remains constant.

Table 8. Effect of substrate to acetic anhydride molar ratio on conversion of anisole and veratrole.

Molar Ratio	Conversion of anisole[a] (wt.%)	Selectivity (%) of 4-methoxy acetophenone	Conversion of veratrole[b] (wt.%)	Selectivity (%) of 3,4-dimethoxy acetophenone
1:1	42	98	42	100
1:2	46	98	59	100
1:3	48	98	61	100

(0.1 g tridecane (internal standard), 0.1 g catalyst, Reaction Temperature = 150 ºC, [a]Reaction Time = 60 min. and [b]Reaction Time = 30 min.)

3.2.2.5 Effect of aromatic substrate to catalyst weight ratio on conversion

The effect of substrate to catalyst weight ratio on acylation of anisole and veratrole was studied with SZO2 (700) by carrying out reaction at 150 ºC for 60 and 30 min. respectively, taking different ratio of substrate to catalyst by weight (5- 20 wt.%).

With increasing the substrate to catalyst weight ratio from 5 to 20, the conversion of anisole and veratrole was observed to be decreasing from 52 to 32 % and 66- 48 % respectively (Figure 11), while the selectivity of the acylated products remains steady. Thus the lower substrate to catalyst weight ratio gives higher conversion of anisole and veratrole.

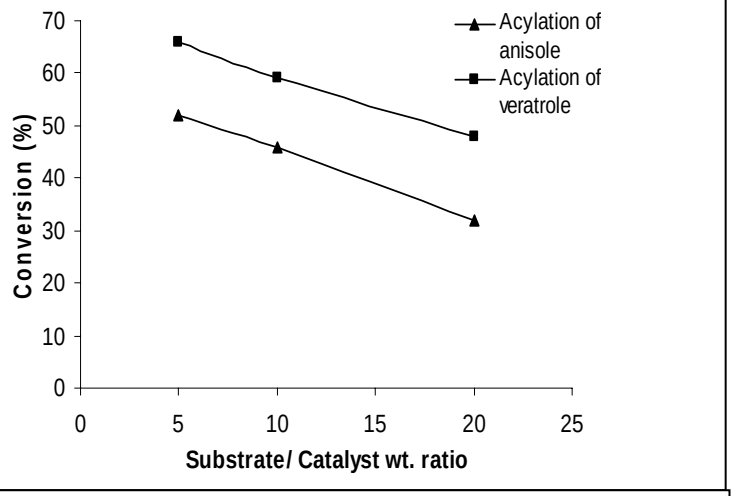

Figure 11. Variation of the conversion of anisole and veratrole with substrate/ catalyst wt. ratio.

3.2.2.6 Regeneration study

The regeneration study was carried out with the spent catalyst, SZO2 (700), separated from reaction mixture by filtration. The thermally regenerated catalyst SZO2 (700) showed similar conversion and selectivity for acylation of anisole and veratrole, under similar reaction conditions, as the fresh catalyst. Table 9 shows that the regenerated catalyst show similar activity till 4 reaction cycle.

Table 9. Conversion of anisole and veratrole with regenerated sulfated-zirconia catalyst.

Regeneration Cycle	Conversion of anisole[a] (wt.%)	Selectivity (%) of 4-methoxy acetophenone	Conversion of veratrole[b] (wt.%)	Selectivity (%) of 3,4-dimethoxy acetophenone
Ist	46	98	59	100
IInd	45	98	59	100
IIIrd	46	98	58	100
IVth	44	98	58	100

(10 mmol anisole/ veratrole, 20 mmol acetic anhydride (1:2), 0.1 g tridecane (internal standard), 0.1 g catalyst, Reaction Temperature = 150 ºC, [a]Reaction Time = 60 min. and [b]Reaction Time = 30 min.)

FT-IR spectra of regenerated catalyst (Figure 12a and 12b) is not showing any peak of adsorbed reactants or products in regenerated catalyst and therefore, the acid sites of the catalyst are not getting deactivated.

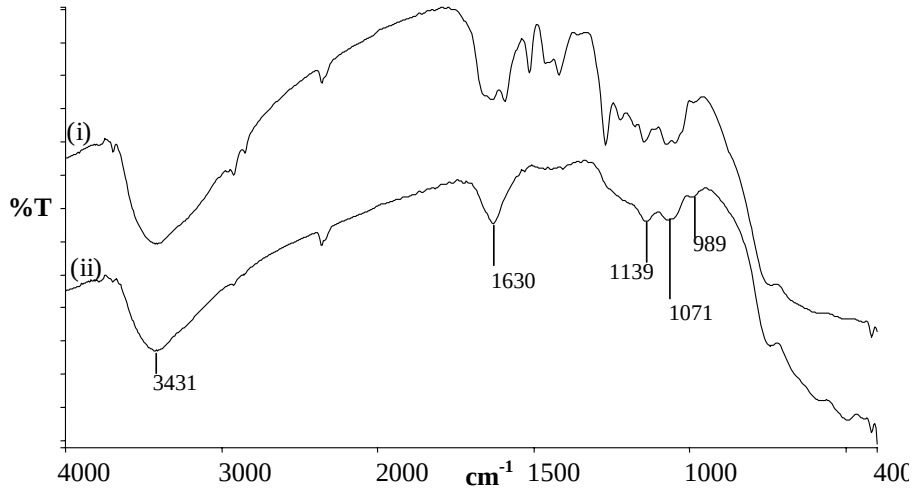

Figure 12a. FT-IR spectra of: (i) used and (ii) regenerated catalyst separated from reaction mixture of acylation of anisole.

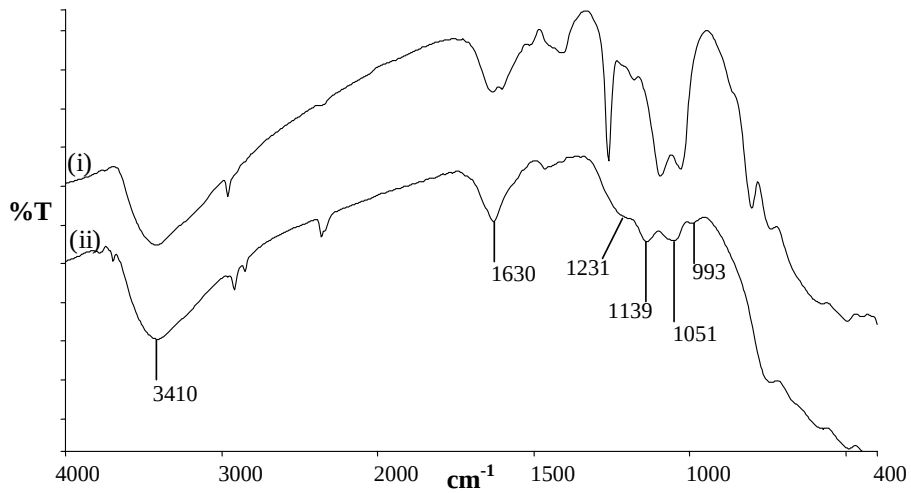

Figure 12b. FT-IR spectra of: (i) used and (ii) regenerated catalyst separated from reaction mixture of acylation of veratrole.

3.2.3 Conclusions

The sulfated-zirconia samples are catalytically active for acylation reaction showing good conversion for acylation of anisole and veratrole. The optimum sulfur content (~1 wt.%) is required to give higher activity in the sulfated-zirconia. The acylation reaction with sulfated-zirconia samples shows fast kinetics giving maximum conversion of anisole (46 %) and veratrole (59 %) within 30 and 10 min respectively. The reaction variables were observed to be affecting the conversion of anisole and

veratrole. The spent catalyst is easily regenerated by thermal regeneration method giving similar conversion and selectivity for acylation of anisole and veratrole till 4 reaction cycles without loss of activity.

Chapter 4

(I)

Isomerization of Longifolene to Isolongifolene with Nano-crystalline Sulfated Zirconia

4.1 Introduction

Sulfated-zirconia has been studied for various commercially important acid catalyzed organic transformations such as acylation, alkylation, isomerization, nitration, esterification, etherification, etc. **[92, 93]**. Sulfated-zirconia is an excellent catalyst for isomerization reactions and catalyzes a number of isomerization reactions. Isomerization is an acid catalyzed rearrangement reaction involving alkyl group or C-C bond or C=C bond shifting. Isomerization reaction has wide range applications in petrochemical, perfumery and fine chemical industries to synthesize number of valuable chemicals. Isomerization of *n*-alkanes to branched alkanes is an industrially important isomerization reaction for production of high octane branched hydrocarbons from straight chain hydrocarbons for blending with gasoline **[43, 44]**. Sulfated-zirconia is known as a potential catalyst for isomerization of *n*-alkanes at ambient temperature **[10a]**, which requires high temperature with conventional catalysts such as sulfuric acid. Therefore, it is known as super solid acid catalyst. The isomerization of *n*-butane to branched product over sulfated-zirconia has been extensively studied **[10a, 11, 43- 48, 53, 54]**. Sulfated-zirconia has also been found active for isomerization of higher *n*-alkanes to branched product **[49, 50]**, isomerization of cycloalkanes **[51]** and isomerization of alkenes **[52]**. Besides, hydrocarbon isomerization, there are only a few studies reported for isomerization of epoxides **[84]** and various terpines **[85, 87, 88]** for preparation of perfumery chemicals such as aldehydes and their acetals.

Terpines constitute a class of natural products that can be transformed into novel and valuable compounds of commercially importance for the production of fragrances, perfumes, flavors, and pharmaceuticals as well as useful synthetic intermediates. The catalytic transformations of terpines results into various valuable chemicals. These transformations comprise reactions such as isomerization, hydration, condensation, hydroformylation, hydrogenation, cyclization, oxidation, rearrangement, and ring contraction/enlargement.

Longifolene ($C_{15}H_{24}$), also known as decahydro-4, 8, 8-trimethyl-9-methylene 1-4-methanoazulene, is a tricyclic sesquiterpene. It is commercially important chemical having characteristic woody odor **[214]** and is used in perfumery industry to synthesize valuable products such as synthetic perfumes, flavoring agents, synthetic resin and

synthetic organic chemicals. It is naturally occurred in the plants of Pinus genus of Pinacea family such as Pinus *longifolia*, P. *roxburghii* and P. *sylvestris*. Indian turpentine, obtained from Pinus *longifolia*, which is found in Himalayas region, contains about 30 % by weight of the sesquiterpene longifolene. The molecule of longifolene has special chemical activity as it contains a reactive, polarisable double bond, which is very susceptible to electrophiles. Addition of an electrophile produces a carbocation, which is the intermediate species for rearrangement. The strained molecule of longifolene makes it more reactive **[215]**. The acid catalyzed isomerization of longifolene gives economically important isomerized product, known as isolongifolene, (2, 2, 7, 7-tetramethyltricyclo undec-5-ene). Isolongifolene finds perfumery applications as perfumery agent and intermediate compound for the synthesis of other perfumery chemicals. The acylated, hydroformylated and other products obtained by acid catalyzed reactions of isolongifolene are also extensively used in perfumery and pharmaceutical industries due to their woody amber odor **[216, 217]**.

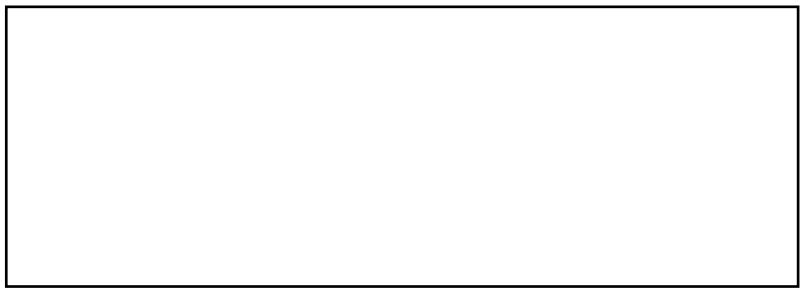

Generally, isolongifolene is synthesized by isomerization of longifolene using liquid acids like sulfuric acid/ acetic acid **[218]**, BF_3/ Et_2O **[219, 220]**, bromo-acetic acid **[221]** and by multi-step synthesis starting from camphene-carboxylic acid **[222]**. The isomerization of longifolene using liquid acids takes longer time (14 days) to be completed **[218]** and also gives other rearranged products such as tetraline and octalin derivatives as side products **[223]**. The formation of the other side product is attributed to the reactive nature of molecule and also it depends on the acidic strength and concentration of the catalyst. Bromoacetic acid catalyzed isomerization results to formation of allo-isolongifolene as major product (80%) and isolongifolene as minor product (20%) **[221]**. The efforts had been made to replace the homogeneous liquid acids

looking on their disadvantages by using solid acid catalysts like clays and silica gel for isomerization of longifolene to isolongifolene **[224, 225, 226]**. The isomerization of longifolene using these catalysts takes long time to be completed, 17 hours **[225]** to 36 hours **[224]**.

In the present chapter, the catalytic activity of nano-crystalline sulfated zirconia catalysts (SZO1, SZO2, SZTB and SZTN), synthesized by one-step and two-step sol–gel methods, (as described in Chapter 3) has been evaluated for isomerization of longifolene to isolongifolene. Various reaction parameters such as reaction temperature, substrate/catalyst weight ratio and reaction time have been optimized to get maximum conversion and selectivity. The kinetic study of the isomerization reaction is also studied to determine the order of reaction, rate constant and activation energy. The regeneration study of used catalyst was also done. The isomerization of longifolene was also done at large scale giving similar conversion and selectivity. The liquid phase, single step and solvent free isomerization of longifolene to isolongifolene with high catalytic conversion (>90%) and selectivity (~100%) within 15 min of the reaction and reusability of sulfated-zirconia catalyst up to ten cycles with similar activity and selectivity is novelty of the present work.

4.1.1 Experimental

4.1.1.1 Material

Zirconium propoxide (70 wt.% solution in *n*-propanol) was procured from Sigma Aldrich, USA, *n*-propanol, aqueous ammonia (25%) and concentrate sulfuric acid were from s.d. Fine chemicals, India. Longifolene raw material with purity of ~ 60 % was procured from Dhruv Aroma Chemicals, Vadodara, India. The raw material of longifolene was distilled to remove most of impurities and made it ~ 79 % pure. All other chemicals were used as such without any purification.

4.1.1.2 Catalyst synthesis

The sulfated-zirconia catalysts (SZO1, SZO2, SZTB and SZTN) were synthesized by sol-gel method using one-step method in acidic medium and two-step method in basic as well as neutral medium as described in Chapter 3.

4.1.1.3 Catalyst characterization

The sulfated-zirconia catalysts (SZO1, SZO2, SZTB and SZTN) were characterized by X-ray Powder Diffraction study, FT-IR Spectroscopy, DRIFT study, N_2 adsorption-desorption isotherm study, dehydration of cyclohexanol to cyclohexene as model reaction for assessment of Bronsted acidity, CHNS/O and ICP (Inductive Couple Plasma) for Sulfur Analysis. The description of the characterization techniques used to characterize the sulfated-zirconia samples is given in chapter 3.

4.1.1.4 Measurement of specific rotation

Specific rotation [α] of longifolene before and after isomerization was measured by Automatic Polarimeter (Digi Pol 781, Rudolph Instruments Inc.) using Na lamp (λ = 589 nm) in quartz cell (d = 100 mm) at 29 ± 1ºC.

4.1.1.5 Catalytic activity

4.1.1.5.1 Isomerization of longifolene

The catalytic isomerization of longifolene was carried out in liquid phase batch reactor. In a 25 ml round bottom flask equipped with a water condenser, longifolene (procured from Dhruv Aroma Chemicals, Vadodara and used after distillation, [α] neat = $+32.6^{o}$) and the catalyst, preactivated at 450 ºC for 2 h, was added in the flask. The flask was kept in an oil bath at required temperature. The reaction was carried out at atmosphere pressure under stirring at around 400 rpm using a magnetic stirrer. The samples from reaction mixture were drawn at regular intervals and analyzed with a Hewlett–Packard gas chromatogram (HP 6890) having a HP50 (30 miter long) capillary column with a programmed oven temperature from 50 to 200 ºC, a 0.5 cm^3/min flow rate of N_2 as carrier gas and FID detector. The conversion of longifolene was calculated on the basis of its weight percent; the initial theoretical weight percent of longifolene was divided by initial GC peak area percent to get the response factor. Final unreacted weight percent of longifolene remaining in the reaction mixture was calculated by multiplying response factor with the area percentage of the GC peak for longifolene obtained after the reaction.

The conversion was calculated as follows:

Response factor = Initial theoretical weight percent of longifolene/ Initial GC peak area percent of longifolene before reaction.

Final unreacted weight percent of longifolene = Response factor X Final GC peak area percent of longifolene after reaction.

$$\text{Conversion (wt \%) of longifolene} = \frac{100 \text{ X [Initial wt\% - Final wt\%]}}{\text{Initial wt\%}}$$

$$\text{Selectivity of isolongifolene (wt. \%)} = \frac{100 \text{ X [GC peak area\% of isolongifolene]}}{\sum \text{Total GC peak area \% for all the products}}$$

The product was identified by FT-IR (Perkin–Elmer GX), ^{1}H NMR spectroscopy (Bruker, Advance DPX 200MHz) and GC-MS analysis (Shimadzu GC MS-QP 2010).

4.1.1.5.2 Catalyst regeneration

The regeneration study of sulfated-zirconia catalyst was done on the spent catalyst (SZO2), which was recovered from the reaction mixture by filtration. The used catalyst was washed with acetone and activated at 450 ºC for 2 h. The catalyst was used for further reaction cycles. After every reaction cycle, recovered catalyst was thoroughly washed with acetone and activated at 450 ºC for 2 h.

4.1.2 Results and discussion

4.1.2.1 Physico-chemical properties of sulfated-zirconia catalysts

X-ray diffraction patterns of sulfated-zirconia samples (SZO1, SZO2, SZTB and SZTN) after calcination at 600 ºC (Figure 1, in Chapter 3) show peaks at 2θ = 30.18, 35.3, 50.2 and 60.2 for tetragonal crystalline phase. All the samples are highly crystalline and having purely tetragonal phase at 600 ºC. Crystallite size of the tetragonal phase of the sulfated-zirconia samples were in the range of 11–16 nm (Table 1, in Chapter 3) showing the nano-crystalline nature.

The FT-IR spectrum of the sulfated-zirconia sample shows (Figure 3, in Chapter 3) that the structure of the surface sulfate is as an ionic chelating bidentate sulfate bonded with zirconium atom through two oxygen atoms and with water molecule adsorbed with the sulfate by hydrogen bonding (Scheme 1, in Chapter 3).

The DRIFT study, after in situ activation at 450 ºC, of the sulfated-zirconia samples shows the presence of additional band at 1405 cm^{-1} (Figure 4, in Chapter 3), indicating the presence of S=O bond in sulfate group (Scheme 2, in Chapter 3), which is responsible for generation of Lewis acid sites **[98]**. The absorbance peak area of the band at 1405 cm^{-1} was measured to assess the Lewis acidity in the samples. The peak area of the $\nu_{s=o}$ band was observed in the range of 2.2–3.1 A cm^{-1} in all the samples. The low values of absorbance peak area of 1405 cm^{-1} indicate the presence of less Lewis acidity in the catalysts.

N_2 adsorption isotherms (Figure 6a and 6b, in Chapter 3) of the sulfated-zirconia samples, calcined at 600 ºC, measured at 77 K are showing the isotherm of type IV, which is characteristic of mesoporous absorbents showing that the samples are mesoporous material. However, there is a large increase in adsorption at higher relative pressure (P/Po), which shows the presence of larger size mesopores in the samples. The inflection point at relative pressure (P/Po) = 0.4, is not sharp in all the samples, which reflects that the pores are not of uniform size and have broad distribution. Three samples (SZO1, SZTB and SZTN) had hysteresis of type H2, except sample SZO2, which showed a broad hysteresis of type H3, reflecting the presence of large mesopores. The surface area was calculated from adsorption isotherm using BET equation. The surface area was in the range of 81–118 m^2/g (Table 2, in Chapter 3). The pore volume and pore size distribution were calculated by BJH method. The samples showed pore volume and average pore diameter in the range of 0.081- 0.19 cm^3/g and 35- 62 Å, respectively. The pore size distribution was observed to be very broad ranging from 20 to 120 Å (Figure 7, in Chapter 3).

All four samples of sulfated-zirconia, synthesized by one-step and two-step sol-gel methods, *in-situ* activated in flow of nitrogen showed good activity for dehydration of cyclohexanol to cyclohexene (Table 3, in Chapter 3) giving the conversion (wt.%) of cyclohexanol in the range of 78- 87 % with 100 % selectivity for cyclohexene. The

dehydration of cyclohexanol to cyclohexene is Bronsted acid catalyzed reaction, therefore, the higher activity of the samples for dehydration of cyclohexanol indicates that all the sulfated-zirconia catalysts have significantly higher amount of Bronsted acidity. The presence of higher Bronsted acidity in the samples is also evident from low values of absorbance peak area (2–3 A cm^{-1}) of the $\nu_{s=o}$ band at 1405 cm^{-1} indicating weak Lewis acidity in the samples (Table 4, in Chapter 3).

The sulfur analysis data (Table 5, in Chapter 3) shows that the samples, synthesized by one-step and two-step method after calcination at 600 ºC, have the sulfur content in the range of 1.3- 1.6 wt.%.

4.1.2.2 Isomerization of longifolene to isolongifolene

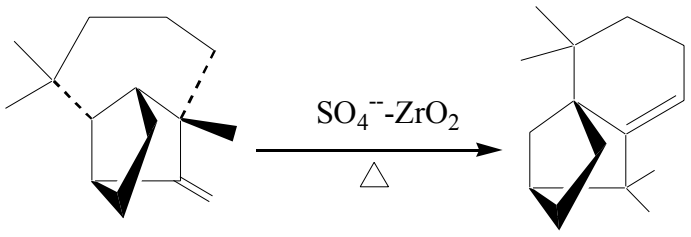

Longifolene Isolongifolene

The isomerization of longifolene was carried out with all four sulfated-zirconia catalysts, synthesized by one-step and two-step sol-gel methods, at 180 ºC taking substrate to catalyst weight ratio of 10. All catalysts show similar activity for isomerization of longifolene giving maximum conversion in range of 90- 93 % with ~100 % selectivity of isolongifolene, after 1 h (Table 1). The similar activity of all catalysts shows that the textural, structural and acidic properties of sulfated-zirconia catalysts do not show any remarkable effect on the catalytic activity for the isomerization of longifolene to isolongifolene. The catalysts are slightly different from each other in their textural and structural properties. The molecular size of longifolene and isolongifolene is very smaller (~ 7 Å) in comparison of the pore size of the catalysts (35- 62 Å). The smaller molecular size of longifolene and isolongifolene helps in proper diffusion through the pores of the catalysts and therefore, the structural, textural properties and slight variation in the acidity of the catalyst do not affect the activity of the catalysts. The

higher catalytic activity of the catalysts for dehydration of cyclohexanol and isomerization of longifolene reactions shows that isomerization of longifolene to isolongifolene is Bronsted acid catalyzed reaction.

The optical rotation [α] of diluted (1% in EtOH) longifolene before reaction and the reaction mixture was measured. The optical rotation [α] of diluted (1% in EtOH) reaction mixture was –23^{o}, while the optical rotation of longifolene before reaction was 32.6^{o}. The decrease in the optical rotation of the reaction mixture indicates the inversion of molecular geometry during isomerization of longifolene to isolongifolene.

Table 1. Conversion (wt.%) of longifolene and selectivity of isolongifolene (%) in isomerization of longifolene with sulfated-zirconia samples, synthesized by one-step and two-step sol-gel methods.

Sample	Conversion of longifolene (wt.%)	Selectivity of isolongifolene (wt.%)
SZO1	91	~ 100
SZO2	93	~ 100
SZTB	92	~ 100
SZTN	90	~ 100

(Longifolene = 2 g, Catalyst = 0.2 g, Reaction Temperature = 180 ºC, Reaction Time = 1 h)

4.1.2.2.1 Characterization of isolongifolene

The product was identified by FT-IR, ^{1}H NMR spectroscopy comparing with the reactant and GC-MS analysis of the reaction mixture.

FT-IR spectrum (Figure 1a) of longifolene shows the bands at 2948 and 2868 cm^{-1} for asymmetric and symmetric stretching modes of C-H bonds of saturated carbons respectively. The band at 1656 cm^{-1} is the stretching mode of C=C bond and at 1455 and 1375 cm^{-1} are the bending modes of C-H of methylene (-CH_2-) and methyl (-CH_3) groups respectively. The presence of the band at 873 cm^{-1} in longifolene (Figure 1a) indicates the presence of C-H bond of C=C-H outside the ring. FT-IR spectrum (Figure 1b) of the neat reaction mixture shows the bands at 2953 and 2872 cm^{-1} for asymmetric and symmetric stretching modes of C-H bonds of saturated carbons respectively. The band at 1684 cm^{-1} is the stretching mode of C=C bond and at 1456 and 1376 cm^{-1} are the bending modes of

C-H of methylene (-CH_2-) and methyl (-CH_3) groups respectively. The band at 815 cm^{-1} represents the bending mode of C-H bond of C=C-H inside the six membered ring.

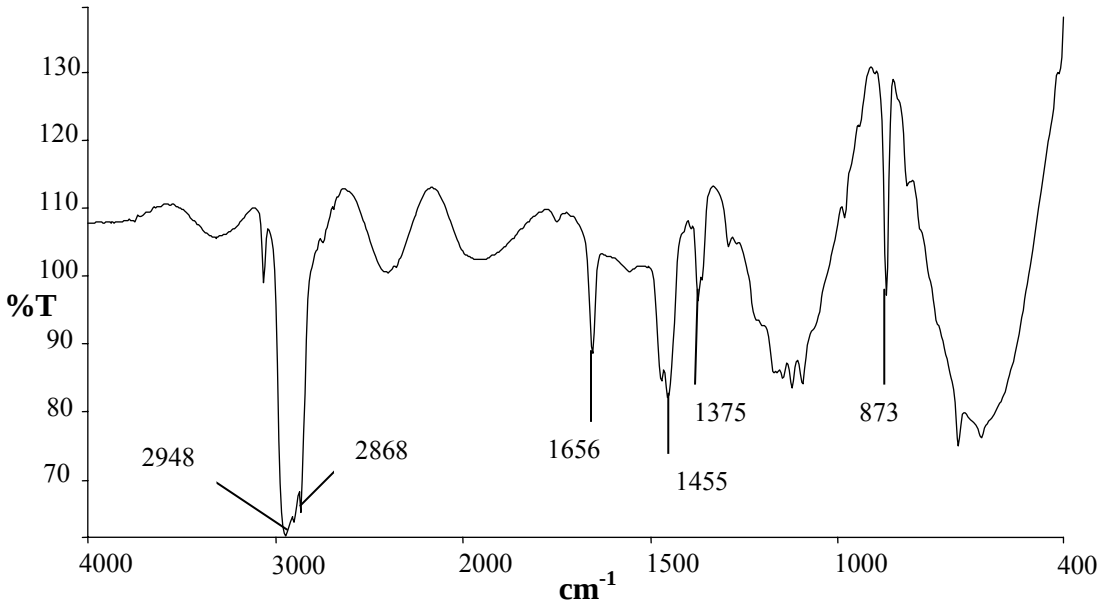

Figure 1(a). FT-IR spectra of longifolene.

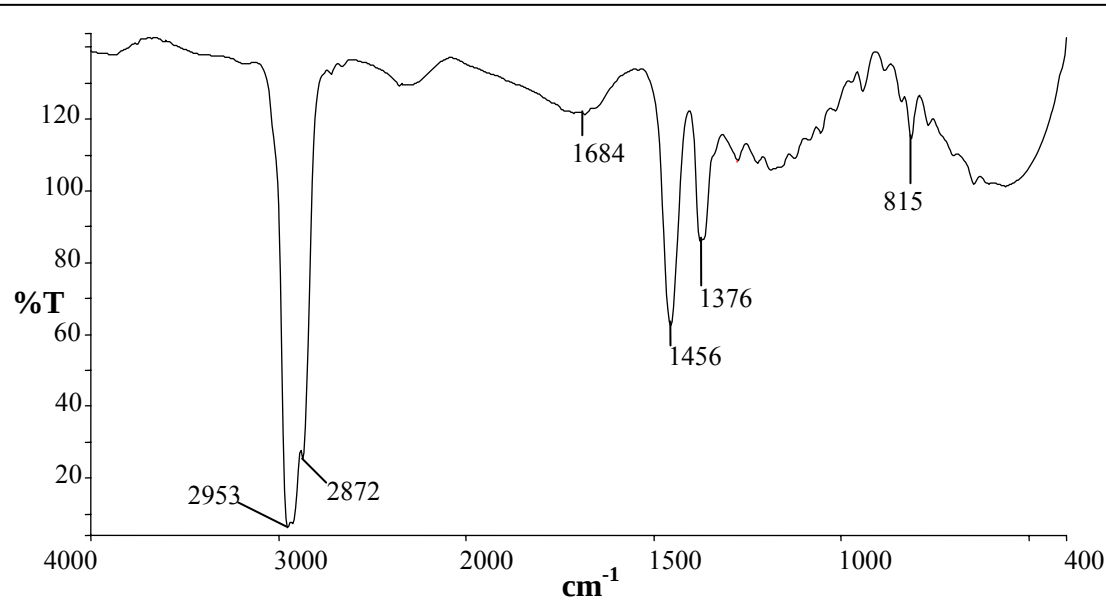

Figure 1(b). FT-IR spectra of isolongifolene.

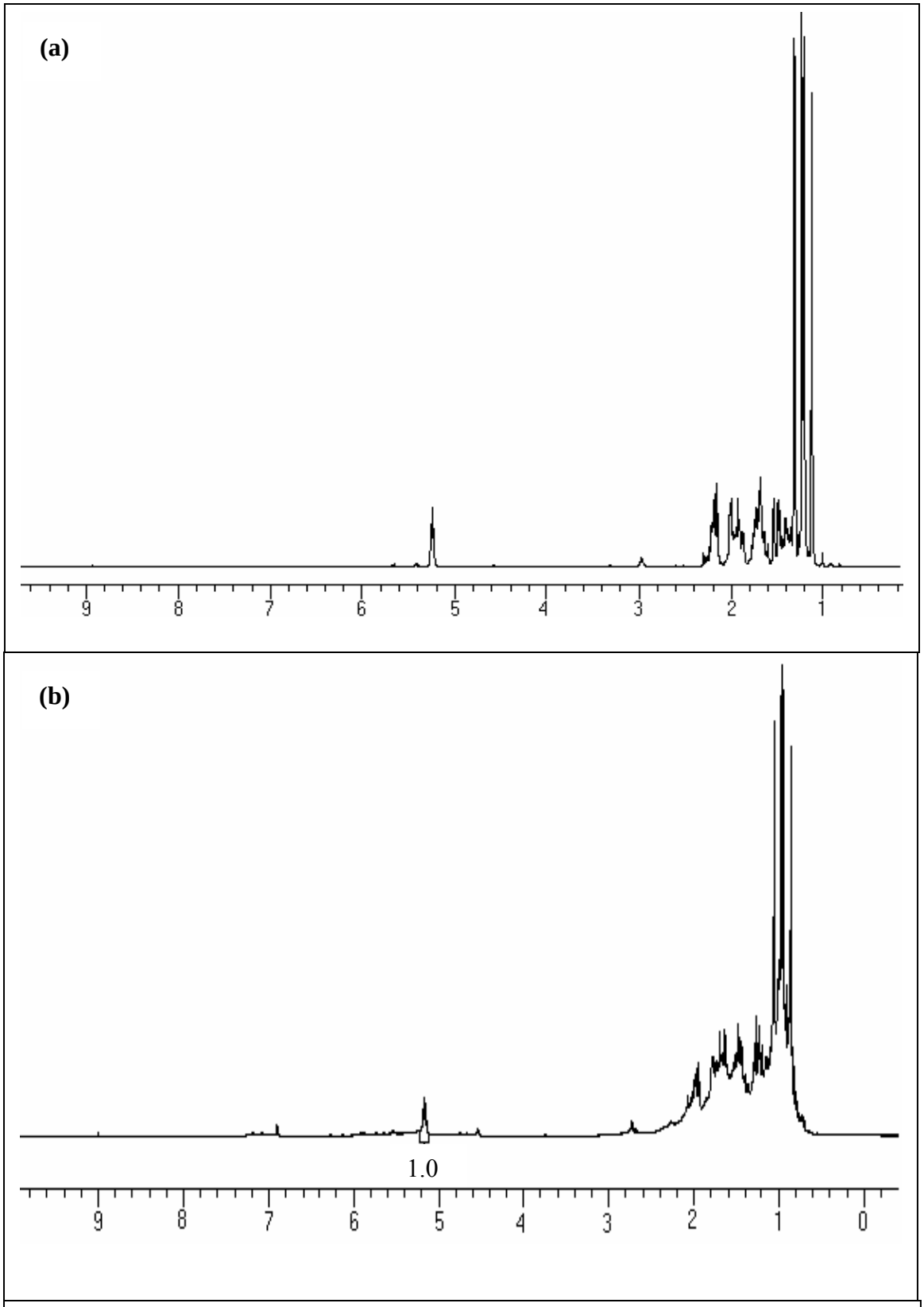

Figure 2 ^{1}H NMR spectra of **(a)** pure isolongifolene and **(b)** reaction mixture.

^{1}H NMR spectrum (Figure 2b) of the reaction mixture in $CDCl_3$ was taken and compared with ^{1}H NMR of pure isolongifolene showing the signals from 0- 2.0 ppm for aliphatic protons, which are not clear in the spectrum and a triplet, equivalent to one proton at 5.2 ppm for olefinic proton of isolongifolene.

The mass spectrum (GC-MS analysis of the reaction mixture) of the isolongifolene (Figure 3) shows the molecular ion peak [M^+] at 204 (m/z) for $C_{15}H_{24}$.

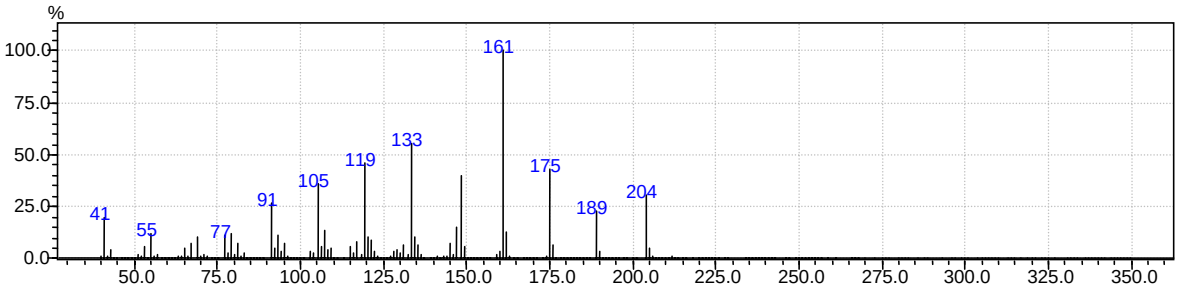

Figure 3. Mass spectra of isolongifolene.

4.1.2.2.2 Optimization of reaction temperature

The effect of reaction temperature on isomerization of longifolene to isolongifolene was studied to optimize the reaction temperature to achieve maximum conversion of longifolene to isolongifolene taking substrate to catalyst weight ratio of 10. The reaction was carried out with the sample SZO1, at different temperatures in the range of 120 to 200 ºC for 1 h. The data clearly show the effect of reaction temperature on isomerization of longifolene as the conversion gradually increases from 120 to 180 ºC and after that it remains steady till 200ºC (Figure 4). Therefore, 180ºC reaction temperature was selected for detail study.

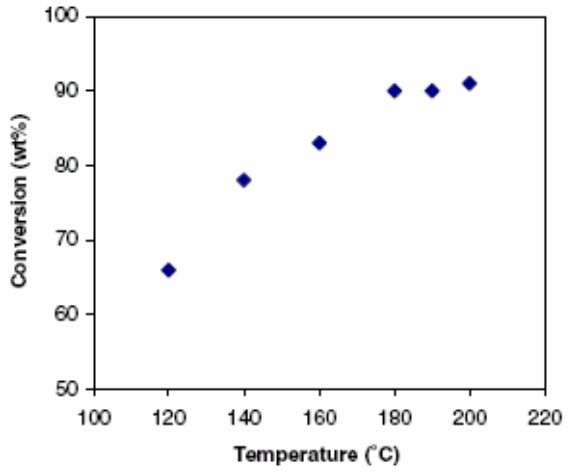

Figure 4. Conversion (wt%) of Longifolene to Isolongifolene at different temperatures (ºC) after 1 h.

4.1.2.2.3 Study of reaction time

The kinetic study was done on the catalyst SZO2 to determine the minimum reaction time required to achieve maximum conversion. The reaction was carried out at 180 ºC for 6 h taking substrate to catalyst ratio of 10. Kinetic study of isomerization of longifolene to isolongifolene (Figure 5a and 5b) shows that the maximum conversion (93 %) with ~100 % selectivity for isolongifolene was achieved within 15 min of the reaction after that it remains steady till 360 min. The fast kinetics of reaction reveals the higher activity of sulfated-zirconia catalyst for isomerization of longifolene to isolongifolene.

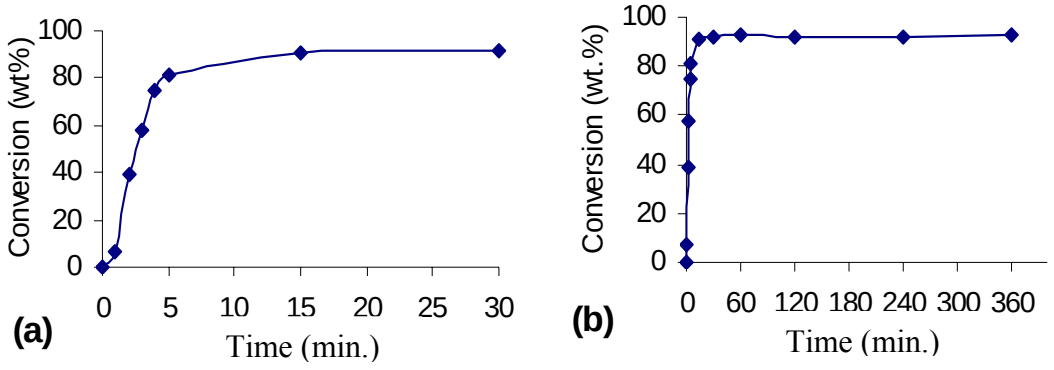

Figure 5. Conversion (wt%) of Longifolene to Isolongifolene at different reaction time (min); **(a)** for 30 min and **(b)** for 360 min.

4.1.2.2.4 Effect of substrate to catalyst weight ratio

The isomerization of longifolene to isolongifolene was also carried out at different substrate to catalyst ratio ranging from 10 to 100 at 180 ºC to get the minimal amount of catalyst required to achieve maximum conversion of longifolene. The reaction was carried out with SZO2 at 180 ºC for 1 h. The data (Table 2) shows that the conversion of longifolene to isolongifolene is in similar range (93- 95 %) with ~ 100 % selectivity of isolongifolene till substrate to catalyst weight ratio of 100 after 1 h. It shows that sulfated-zirconia catalyst is highly active catalyst for isomerization of longifolene and the minimal catalytic amount is sufficient to obtain maximum conversion.

Table 2. Conversion of longifolene (wt.%) and selectivity (%) of isolongifolene in isomerization of longifolene at different substrate to catalyst ratio.

Substrate/Catalyst weight ratio	Conversion of longifolene (wt.%)	Selectivity of isolongifolene (%)
10	93	~ 100
50	95	~ 100
70	95	~ 100
100	94	~ 100

(Reaction Temperature = 180 ºC, Reaction Time = 1 h)

However, the substrate to catalyst weight ratio was observed to affect the kinetics of the reaction. With increase in the ratio, the kinetics of the reaction was observed to be slower (Figure 6). The rate of the reaction at each substrate to catalyst ratio was calculated by differential method from the graph plotted between the time and the concentration (number of moles) of longifolene remained unreacted in the reaction mixture. The logarithm of concentrations (- log c) of longifolene was plotted with the negative logarithm of the rate of reaction (- log r) at different concentrations of longifolene. The slop of curve gives the order of reaction (n) and the intercept gives logarithm of rate constant (log k). The antilogarithm of the value of log k gives rate constant (k). Figure 6 shows the variation of conversion (wt.%) with reaction time and the graph plotted between log c and –log r at different substrate to catalyst weight ratios.

The observed order of reaction at different substrate to catalyst weight ratio (10 to 100) was in range of 0.6 to 0.8 (Table 3) showing the order of reaction to be of first order and the rate constant was found to be decreasing from 0.015 s^{-1} to 0.003 s^{-1} with increasing substrate to catalyst weight ratio from 10 to 100.

Table 3. Order of reaction and rate constant at different substrate to catalyst ratio at 180ºC.

Substrate/Catalyst weight ratio	Observed order	Observed rate constant (s^{-1})
10	0.8	0.015
50	0.8	0.008
70	0.6	0.003
100	0.6	0.003

The increase in the substrate to catalysts weight ratio increases the amount of substrate, which lowers the rate of reaction resulting to decrease in the rate constant. The

order of reaction is of first order; however, it slightly decreases from 0.8 to 0.6 with increasing the substrate to catalyst weight ratio due to increase in substrate amount.

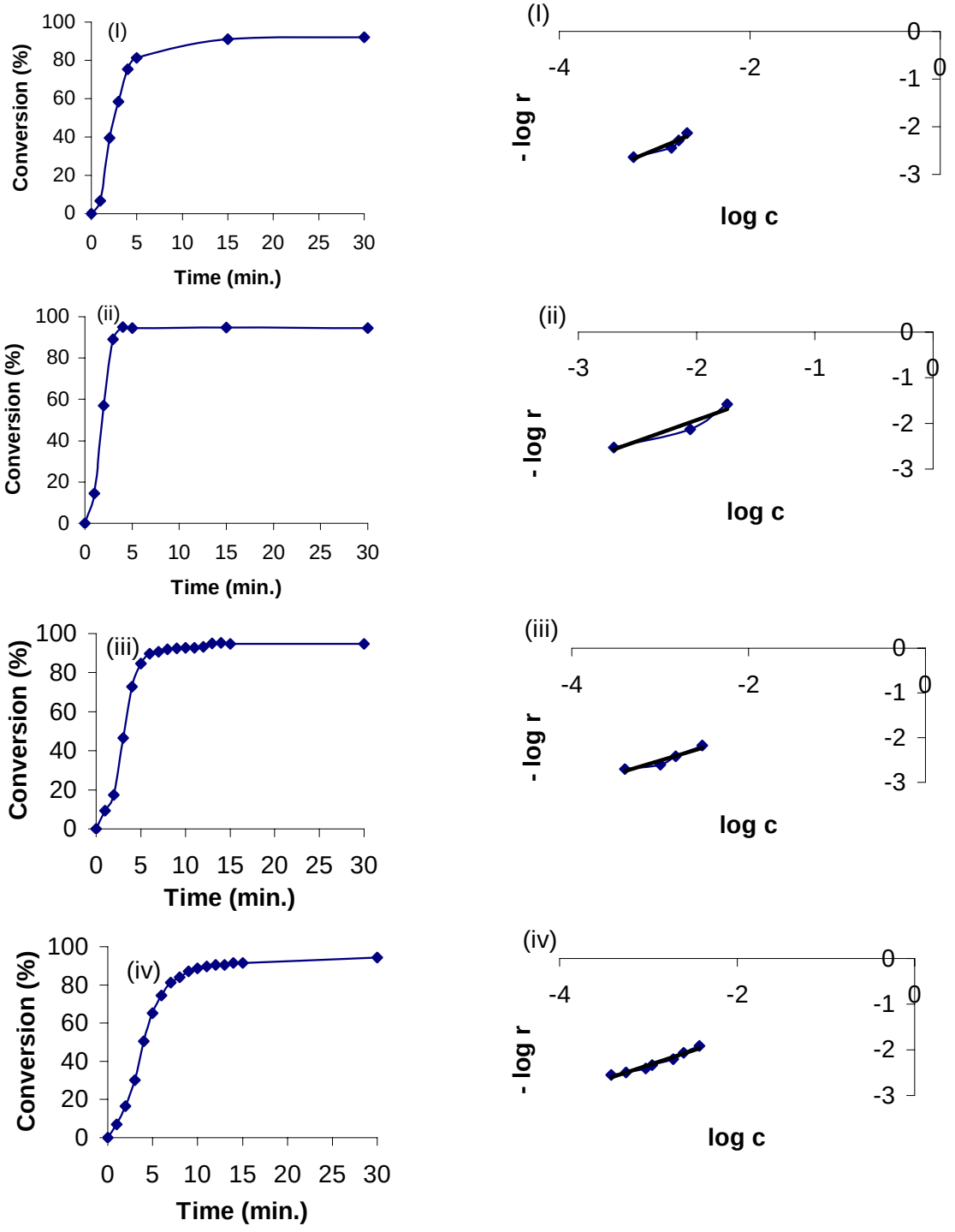

Figure 6. Conversion (wt%) of Longifolene to Isolongifolene at different reaction time (min) and kinetics for different substrate to catalyst ratio (i) 10, (ii) 50, (iii) 70, (iv) 100 at 180 ºC.

4.1.2.2.5 Activation energy of the reaction

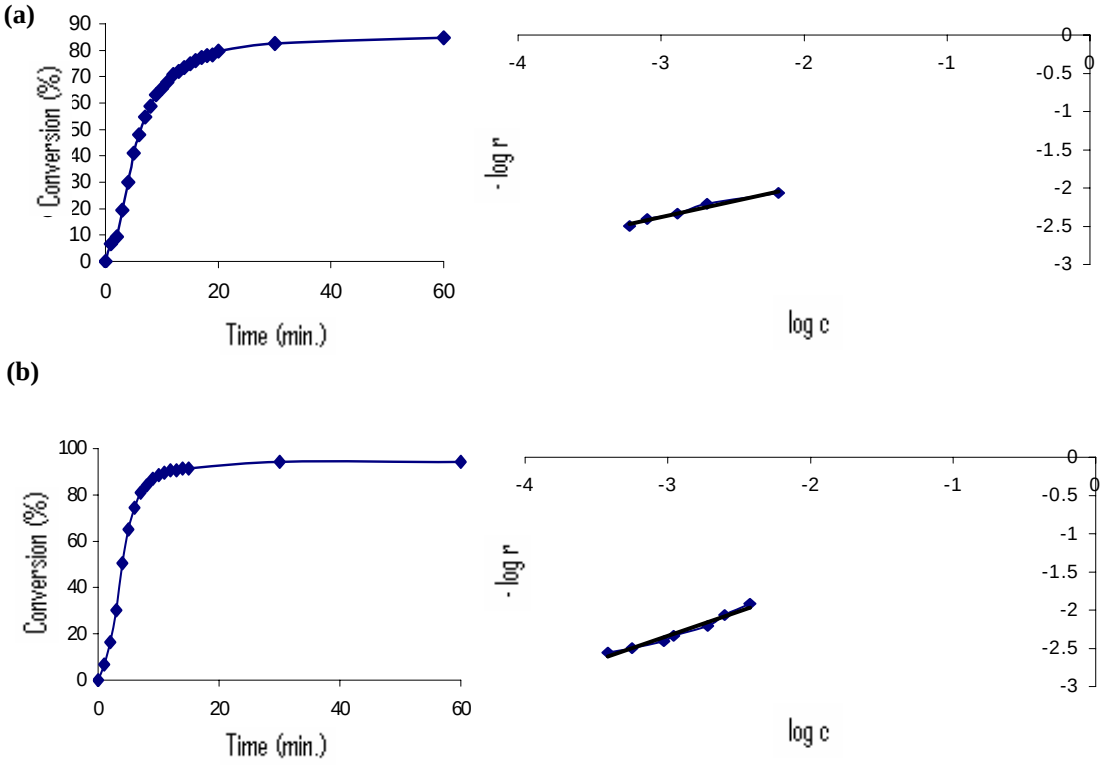

Figure 7. Conversion (wt%) of Longifolene to Isolongifolene at different reaction time (min) and kinetics at **(a)** 160 and **(b)** 180 ºC.

The activation energy of isomerization of longifolene to isolongifolene was calculated by determining the rate constants (Figure 7) at 160 and 180 ºC (substrate to catalysts ratio = 100). Substituting the values of rate constants obtained at 160 and 180 ºC in Arhinius equation, the activation energy of isomerization of longifolene was obtained.

$\ln (k_2/k_1) = Ea / R. (T_2 – T_1 / T_1.T_2)$

Where k_1 and k_2 are the rate constants at T_1 and T_2 respectively, Ea is the activation energy and R is gas constant (8.314 joule K^{-1} mol^{-1}).

The observed rate constants at 160ºC (433 K) and 180ºC (453 K)-

$k_1 = 0.001\ s^{-1}$

$k_2 = 0.003\ s^{-1}$

$T_1 = 433$ K

$T_2 = 453$ K

Therefore,

$Ea = R. \ln (0.003/0.001) (T_1.T_2 / T_2 – T_1)$

$= 8.314$ joule K^{-1} mol^{-1} X 1.1 (9807.45 K)

$= 89580$ joule $mol^{-1} = 89.6$ kjoule mol^{-1}

The calculated activation energy was 89.6 kjoule mol^{-1}, which shows the feasibility of isomerization of longifolene to isolongifolene with sulfated-zirconia at moderate reaction conditions. It also proves the higher reactivity of longifolene molecule for isomerization.

4.1.2.2.6 Isomerization of longifolene to isolongifolene at large scale

Isomerization of longifolene was also carried out at large scale of 100, 500 and 1000 gm in large volume liquid phase reactor with SZO2 sample taking substrate to catalyst ratio of 100 at 180 ºC for 6 h. The conversion of longifolene in all three batches was found to be 95 % with ~100 % selectivity of isolongifolene (Table 4) showing the consistency in conversion and selectivity at large batch.

Table 4. Conversion of longifolene to isolongifolene at large scale.

Longifolene amount (gm)	Conversion (%)	Selectivity (%)
5	95	~100
100	95	~100
500	95	~100
1000	95	~100

4.1.2.2.7 Regeneration of catalyst

The thermally regenerated catalyst (SZO2) showed similar conversion and selectivity as the fresh catalyst for isomerization of longifolene under similar reaction conditions. Table 5 shows that the regenerated catalyst do not show any decrease in the catalytic activity till 10^{th} reaction cycle. FT-IR spectra of the regenerated catalyst (Figure 8) is not showing any peak of adsorbed longifolene or isolongifolene on the surface of sulfated-zirconia and therefore, the acidic sites of the catalyst do not get deactivated. The presence of a peak at 1453 cm^{-1} shows a deposition of only small carbonaceous material,

which might be on the external surface of used catalyst and could be easily removed on activation resulting into the similar catalytic activity as the fresh catalyst.

Table 5. Conversion of longifolene with regenerated sulfated-zirconia catalyst in successive reaction cycles.

Regeneration Cycle	Conversion (wt.%)	Selectivity (%)
Ist	93	~100
IInd	92	~100
IIIrd	94	~100
IVth	97	~100
Vth	97	~100
VIth	93	~100
VIIth	94	~100
VIIIth	96	~100
IXth	96	~100
Xth	94	~100

(Substrate/ catalyst weight ratio = 10, Reaction Temperature = 180 ºC, Reaction Time = 1 h)

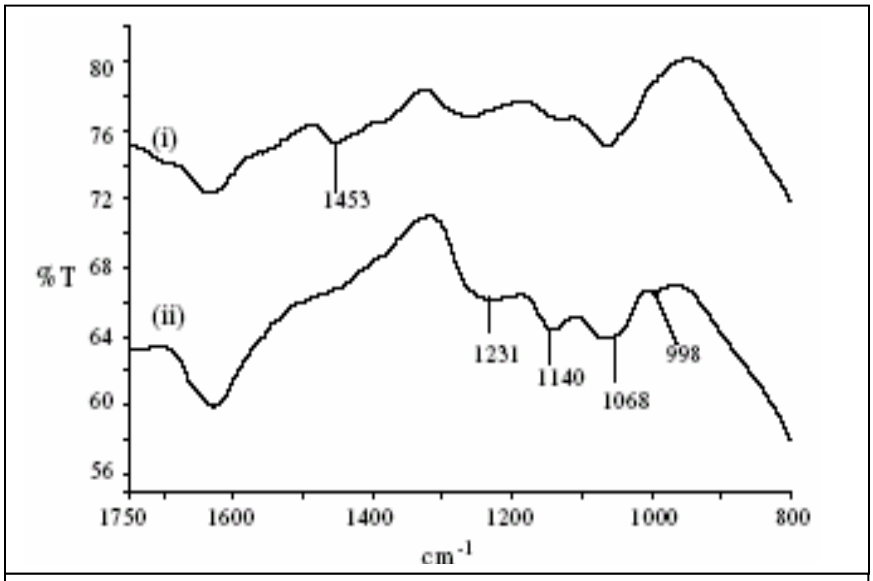

Figure 8. FT-IR spectra of: (i) used and (ii) regenerated catalyst.

Mechanism of isomerization of longifolene to isolongifolene

The Scheme 1 shows the mechanism of isomerization of longifolene to isolongifolene. The higher activity of sulfated-zirconia catalysts, prepared by one-step and two-step sol-gel method, for cyclohexanol dehydration reaction and the presence of

less Lewis acidity depicted from DRIFT study show that these catalysts have higher Bronsted acidity. The higher activity of sulfated-zirconia catalysts for isomerization of longifolene to isolongifolene indicates that the reaction is a Bronsted acid catalyzed reaction.

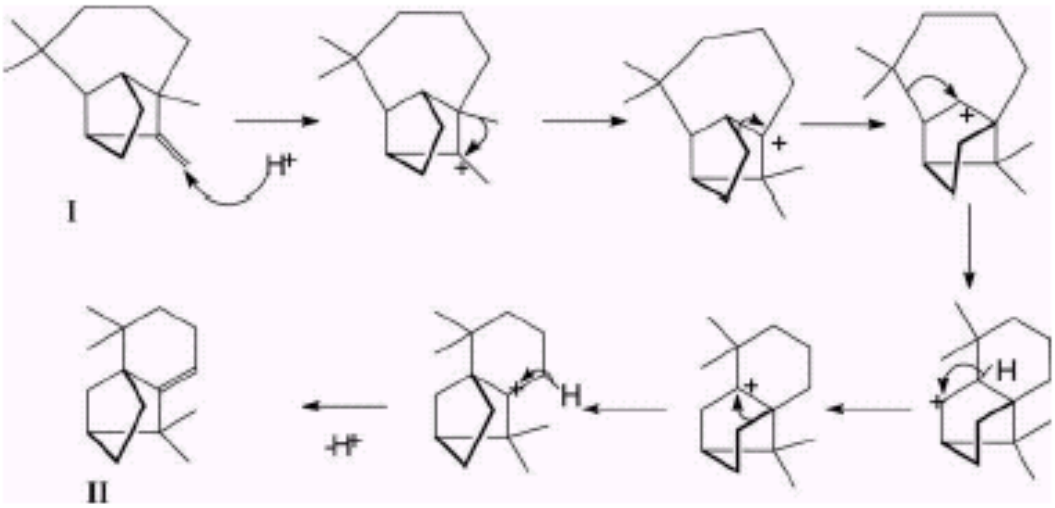

Scheme 1. Mechanism of isomerization of Longifolene (I) to Isolongifolene (II).

4.1.3 Conclusions

The nano-crystalline sulfated-zirconia catalysts prepared by one-step and two-step sol-gel methods are potential solid acid catalysts for liquid phase, single step and solvent free selective isomerisation of longifolene to isolongifolene with higher catalytic conversion and selectivity. The kinetics for isomerization of longifolene to isolongifolene over sulfated-zirconia catalysts is very fast and the maximum conversion can be achieved within 15 minutes by using very less amount of the catalyst (0.1 g catalyst/ 10 g substrate). The kinetics of the reaction is affected by the reaction temperature and the substrate to catalyst weight ratio. Kinetics was observed to be fast with increasing reaction temperature and decreasing the substrate to catalyst weight ratio. The calculated activation energy (89.6 kjoule mol^{-1}) of the reaction shows the feasibility of the reaction with sulfated-zirconia under moderate reaction conditions and higher reactivity of longifolene molecules towards isomerization reaction. The catalyst can be easily

regenerated and reused for several reaction cycles with similar activity as fresh catalyst. Isomerisation of longifolene is a Bronsted acid catalyzed reaction, taking place inside the pores of the sulfated-zirconia catalyst thus maintaining the maximum catalytic activity of the catalyst for a longer time. This study shows the higher activity of sulfated-zirconia catalyst for isomerization reactions and it can be applied for isomerization of other terpines giving valuable products.

Chapter 4

(II)

Isomerization of Isolongifolene to 7-isopropyl- 1, 1-dimethyl Tetraline with Nano-crystalline Sulfated Zirconia

4.2 Introduction

Longifolene, on treatment with acid catalyst, undergoes acid catalyzed isomerization forming an isomerized product, isolongifolene, of perfumery importance **[219, 227]**. In presence of acidic medium, longifolene rearranges to give different rearranged products, which depends on the acidic condition of the medium. The acid catalyzed rearrangement of longifolene (I) in presence of strong protic acids such as H_2SO_4 or Lewis acids such as BF_3-Et_2O to selectively isolongifolene (II) has been reported in literature **[219, 227]**. However, if the reaction is carried out under more severe conditions (excess acid), for example, the isomerization of longifolene in excess of BF_3-Et_2O or if isolongifolene is further treated with silica gel – H_3PO_4 at reflux temperature (scheme 1), a polymer (25- 30 %), the tetraline (III) and the octalin are formed **[228]**. It is evident that the excess acid concentration catalyzes the further isomerization of isolongifolene to tetraline. The strong acids give selectively isolongifolene (II) from longifolene (I), whereas excess amount of the strong acid can pursue the further isomerization of isolongifolene (II) to tetraline (III). Therefore, the product selectivity can be controlled by controlling the acid amount. The mechanistic pathway of isomerization of longifolene to tetraline via isolongifolene and direct to tetraline and further acid catalyzed isomerization of isolongifolene to tetraline has been explained by S. Dev **[223]**.

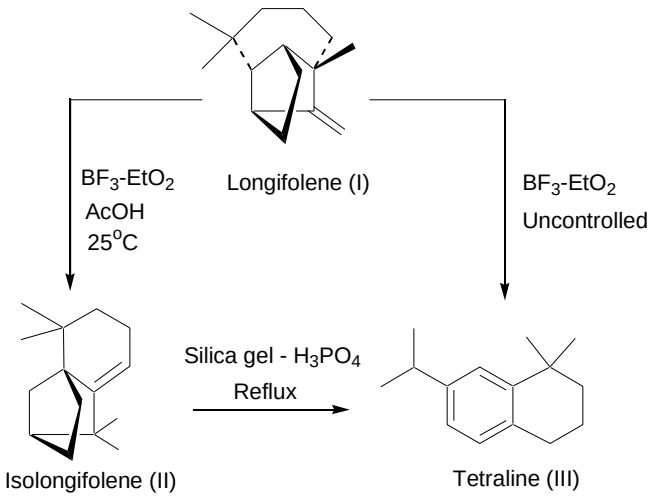

Scheme 1

Longifolene (I) is a strained higher energy molecule having an exo-olefinic double bond, which has strong affinity towards protons to form carbonium ion. The carbonium ion undergoes a series of 1, 2 shifts of methyl group, hydrogen and C-C sigma bonds to have a comparatively low energy configuration and finally results to isolongifolene (II). However, isolongifolene is still a high-energy molecule by virtue of the presence of the strained bicyclo [2.2.1] heptane system with an olefinic double bond in side the ring. Therefore, the molecule rearranges further under appropriate conditions (higher concentration of protic acid) to attain a stable molecular system **[224]**. The excess acidic condition propagates further isomerization of isolongifolene to attain a stable configuration resulting to mainly a tetraline derivative, 7-isopropyl 1, 1-dimethyl tetraline (III).

It has been discussed in chapter 4 (I) that the sulfated-zirconia catalysts, synthesized by one-step and two-step sol-gel methods, are highly active solid acid catalyst for isomerization of longifolene to isolongifolene. The nano-crystalline sulfated-zirconia catalysts showed excellent catalytic activity for the isomerization of longifolene to isolongifolene resulting > 90% conversion with ~100 % selectivity of isolongifolene. There was not observed the formation of any further isomerized products till 6 h (Figure 5b). Nano-crystalline sulfated-zirconia catalyst SZO2 (600), discussed in chapter 3 (I), synthesized by similar one-step sol-gel method, however with different water to alkoxide molar ratio, was studied for isomerization of longifolene. Interestingly, the catalyst was found active for further isomerization of isolongifolene to tetraline derivative (7-isopropyl 1, 1-dimethyl tetraline) as major product along with other isomerized products.

The present work is the study of the further isomerization of isolongifolene to tetraline derivative (7-isopropyl 1, 1-dimethyl tetraline) using nano-crystalline sulfated-zirconia, synthesized by one-step sol-gel method. Further, the investigation of the physicochemical and acidic properties responsible for the further isomerization of isolongifolene was done.

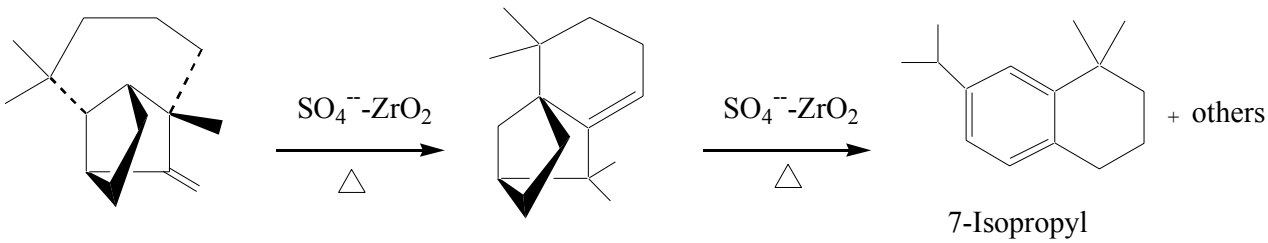

Longifolene Isolongifolene 7-Isopropyl 1,1-dimethyl tetralene

4.2.1 Experimental

4.2.1.1 Catalysts Synthesis

The synthesis of sulfated-zirconia samples SZO2 (600), SZO2 (700) and SZO2 (800) by one-step sol-gel method has been described in chapter 3 (I). These samples are different from the sample SZO2, which was also synthesized by one-step sol-gel method, described in chapter 4 (I), in terms of water to zirconium propoxide molar ratio, while other synthetic parameters were unchanged. The synthesis of the samples SZO2 (600), SZO2 (700) and SZO2 (800) was carried out using water to zirconium propoxide molar ratio of 2.7. The value in parenthesis denotes the calcination temperature. The sample SZO2 was synthesized by using water to zirconium propoxide ratio of 4.0 and was calcined at 600 ºC.

4.2.1.2 Catalyst Characterization

The sulfated-zirconia catalysts were characterized by X-ray Powder Diffraction studies, FT-IR Spectroscopic Studies, FT-IR Spectroscopic Studies of the samples adsorbed with pyridine, N_2 adsorption-desorption isotherm studies, Bronsted acidity by cyclohexanol dehydration and Sulfur Analysis. The description of the characterization techniques used to characterize the sulfated-zirconia samples is given in chapter 3 (I) and 4 (I).

4.2.1.3 Isomerization of longifolene

The isomerization of longifolene was carried out with substrate to catalyst wt. ratio ranging from 10 to 100 at 180 ºC for 1 min to 4 h. The reaction mixtures were taken out at different time intervals and analyzed with a Hewlett–Packard gas chromatogram (HP 6890). The conversion of longifolene was calculated on the basis of its weight percent; the initial theoretical weight percent of longifolene was divided by initial GC peak area percent to get the response factor. Final unreacted weight percent of longifolene remaining in the reaction mixture was calculated by multiplying response factor with the area percentage of the GC peak for longifolene obtained after the reaction.

The conversion was calculated as follows:

Response factor = Initial theoretical weight percent of longifolene/ Initial GC peak area percent of longifolene before reaction.

Final unreacted weight percent of longifolene = Response factor X Final GC peak area percent of longifolene after reaction.

$$\text{Conversion (wt \%) of longifolene} = \frac{100 \text{ X [Initial wt\% - Final wt\%]}}{\text{Initial wt\%}}$$

$$\text{Selectivity of isolongifolene (wt. \%)} = \frac{100 \text{ X [GC peak area\% of isolongifolene]}}{\sum \text{Total GC peak area \% for all the products}}$$

$$\text{Selectivity of tetraline derivative (wt. \%)} = \frac{100 \text{ X [GC peak area\% of tetraline derivative]}}{\sum \text{Total GC peak area \% for all the products}}$$

The products were identified by ^{1}H NMR spectroscopy (Bruker, Advance DPX 200MHz) and GC-MS analysis (Shimadzu GC MS-QP 2010).

4.2.1.4 Regeneration study

The regeneration study of sulfated-zirconia catalyst was done with the spent catalyst, which was recovered from the reaction mixture by filtration. The used catalyst was washed with acetone and activated at 550 ºC for 4 h in flow of air. The catalyst was used for further reaction cycles. After every reaction cycle, the recovered catalyst was thoroughly washed with acetone and activated at 550 ºC for 4 h in flow of air.

4.2.2 Results and Discussion

4.2.2.1 Physico-chemical properties of sulfated-zirconia catalysts

The characterization (described in Chapter 3) of the sulfated-zirconia samples SZO2, SZO2 (600), SZO2 (700) and SZO2 (800) shows that all samples are having purely tetragonal crystalline phase with crystallite size ranging from 9- 14 nm. The samples are highly crystalline, except the sample SZO2 (600), which was less crystalline with smaller crystallite size (9 nm). The less crystallinity and smaller crystallite size of

the sample SZO2 (600) is attributed to higher sulfur content (3.0 wt.%) after calcination at 600 ºC. The reduced sulfur content (0.6- 1.6 wt.%) in the samples SZO2, SZO2 (700) and SZO2 (800) results to higher crystallinity and comparatively higher crystallite size (11 and 14 nm respectively). With increasing calcination temperature from 600 to 800 ºC, the crystallinity and crystallite size increases. The surface area pore volume and pore size of the sample SZO2, is lesser than the sample SZO2 (600), although, both the samples were calcined at 600 ºC. The surface area of the samples SZO2 (600), SZ (700) and SZ (800) decrease from 150 to 58 m^2/g and the pore size increase from 89 to 170 Å with increasing the calcination temperature, however, the pore volume marginally varies (0.25- 0.33 cm^3/g). The sample SZO2 and SZO2 (600) were found to have significant variation in sulfur content. The higher sulfur content of SZO2 (600) may be attributed to difference in water to alkoxide molar ratio during hydrolysis and mode of addition of sulfuric acid during sulfation (described in Chapter 3).

4.2.2.2 Isomerization of longifolene to isolongifolene and further to tetraline derivative

The results of isomerization of longifolene with sulfated-zirconia samples SZO2, SZO2 (600), SZO2 (700) and SZO2 (800) are given in Table 6.

Table 6. Conversion (%) of longifolene and selectivity of isolongifolene, tetraline derivative and other products with sulfated-zirconia samples.

Catalyst	Conversion (%)	Selectivity (%)		
		Isolongifolene	Tetraline	Others
SZO2	92	~100	0	0
SZO2 (600)	92	3	56	41
SZO2 (700)	95	37	25	38
SZO2 (800)	94	~100	0	0

(Longifolene = 1.0 g, catalyst = 0.1 g, Reaction Temperature = 180 ºC, Reaction Time = 1 h)

The conversion of longifolene is almost in similar range (92- 95 %) after 1 h with all sulfated-zirconia samples but the selectivity of isolongifolene varies with the samples. The sample SZO2 gives selectively isolongifolene (~100 %), while the sample

SZO2 (600) shows significantly higher reduction in selectivity of isolongifolene (~3 %) due to formation of tetraline derivative (56 %) and other products (41 %). With the sample SZO2 (700), the selectivity of isolongifolene increases to 37 % and the selectivity of tetraline derivative and other products decreased to 25 % and 38 % respectively. The selectivity of isolongifolene was again achieved to ~100 % with the sample SZO2 (800), tetraline derivative and other products were not observed to be formed.

The formation of tetraline derivative by further isomerization of isolongifolene is reported in the literature in presence of excess amount of acids **[228]**. The stronger protic acids have been used for the selective isomerization of longifolene to isolongifolene **[219, 227]**, however, the use of stronger acids has not been found to give tetraline derivative. It shows that the stronger acid does not catalyze the further isomerization of isolongifolene. The excess amount of acid is responsible for further isomerization of isolongifolene. The higher sulfur content (3.0 wt.%) in the sample SZO2 (600) generates higher number of Bronsted acid sites, which results the further isomerization of isolongifolene to tetraline derivative. Calcination at higher temperature (700 ºC) decreases the sulfur content (1.1 wt.%), which affects the number and strength of Bronsted acid sites and therefore, the formation of tetraline derivative is decreased. The calcination at further higher temperature (800 ºC) significantly reduces the sulfur content (0.6 wt.%) generating less number of acid sites that are not sufficient for further isomerization of isolongifolene.

The samples SZO2 and also other samples SZO1, SZTB and SZTN, studied in Chapter 4 (I) for isomerization of longifolene, having optimum sulfur content (1.3- 1.6 wt.%) after calcination at 600 ºC, do not generate enough amount and strength of acid sites responsible for further isomerization of isolongifolene.

4.2.2.3 Kinetic study

The sulfated-zirconia catalysts have variation in the structural and textural properties in terms of sulfur content, surface area, pore volume and also surface acidity as shown by the cyclohexanol dehydration data. The textural properties do not affect the conversion and selectivity of isolongifolene as the molecular dimension of reactant and product molecules (~7 Å) are much smaller and diffuses much smoothly through the

large pores (58- 170 Å) of the catalyst. These properties of the catalyst do not show any remarkable effect on the catalytic activity as all samples showed the conversion of longifolene in similar range (92- 95 %). However, further isomerization of isolongifolene to tetraline derivatives and other products and selectivity of the products was found to be greatly influenced, which may be attributed to the sulfur content, nature, number and strength of acid sites. As the sample SZO2 (600) showed higher selectivity for tetraline derivative and other products, the kinetic study of the isomerization of longifolene to isolongifolene and further to tetraline derivative and other products was done with the sample SZO2 (600) taking substrate to catalyst ratio of 10 at 180 ºC. The data (Table 7) shows that the maximum conversion of longifolene (96 %) and selectivity of isolongifolene (~100 %) were obtained within 2 minutes of the reaction time. After 2 minutes, the selectivity of isolongifolene was observed to be successively decreasing with time and the selectivity of tetraline derivative and other products gradually increased giving ~56 % tetraline derivative and ~41 % other products with small amount (~3 %) of isolongifolene after 1 h. The selectivity of tetraline derivative, other products and isolongifolene remains constant up to 4 h.

Table 7. Conversion (%) of longifolene and selectivity of isolongifolene, tetraline and other products at different reaction time.

Time (min)	Conversion (%)	Selectivity (%)		
		Tetraline	Isolongifolene	Others
1	40	0	~100	0
2	96	0	~100	0
10	96	25	42	33
15	96	41	22	37
30	96	56	8	36
60	96	56	3	41
120	96	56	2	41
240	96	56	2	41

(Longifolene = 5 g, catalyst = 0.5 g, Reaction Temperature = 180 ºC, Reaction Time = 4 h)

The kinetic study clearly shows that longifolene initially isomerizes to isolongifolene and then further to tetraline derivative along with other products under the experimental conditions studied. The reaction may be proceeding according to first route as shown in Scheme 2. It was confirmed by recording ^{1}H NMR spectra of the reaction mixture after 1 minute, 10 minutes and 1 h. The ^{1}H NMR spectrum of the reaction

mixture after 1 minute (Figure 9a) shows an additional signal at 5.2 ppm (triplet) equivalent to one proton for an olefinic proton, which shows the presence of isolongifolene. The absence of the signals in aromatic region shows no formation of tetraline derivative. The ^{1}H NMR spectrum of the reaction mixture after 10 minutes (Figure 9b) shows three signals in aromatic region, two signals at 7.1- 7.2 ppm (doublets) equivalent to two protons and one at 7.0 ppm (singlet) equivalent to one proton, for tetraline derivative along with one signal at 5.2 ppm (triplet) for isolongifolene. It shows the presence of both isolongifolene and tetraline derivative in the reaction mixture after 10 minutes. The ^{1}H NMR spectrum of reaction mixture after 1 h (Figure 9c) shows the presence of signals only in aromatic region for tetraline derivative and absence of the signal at 5.2 ppm of isolongifolene. It confirms the formation of tetraline derivative by further isomerization of longifolene.

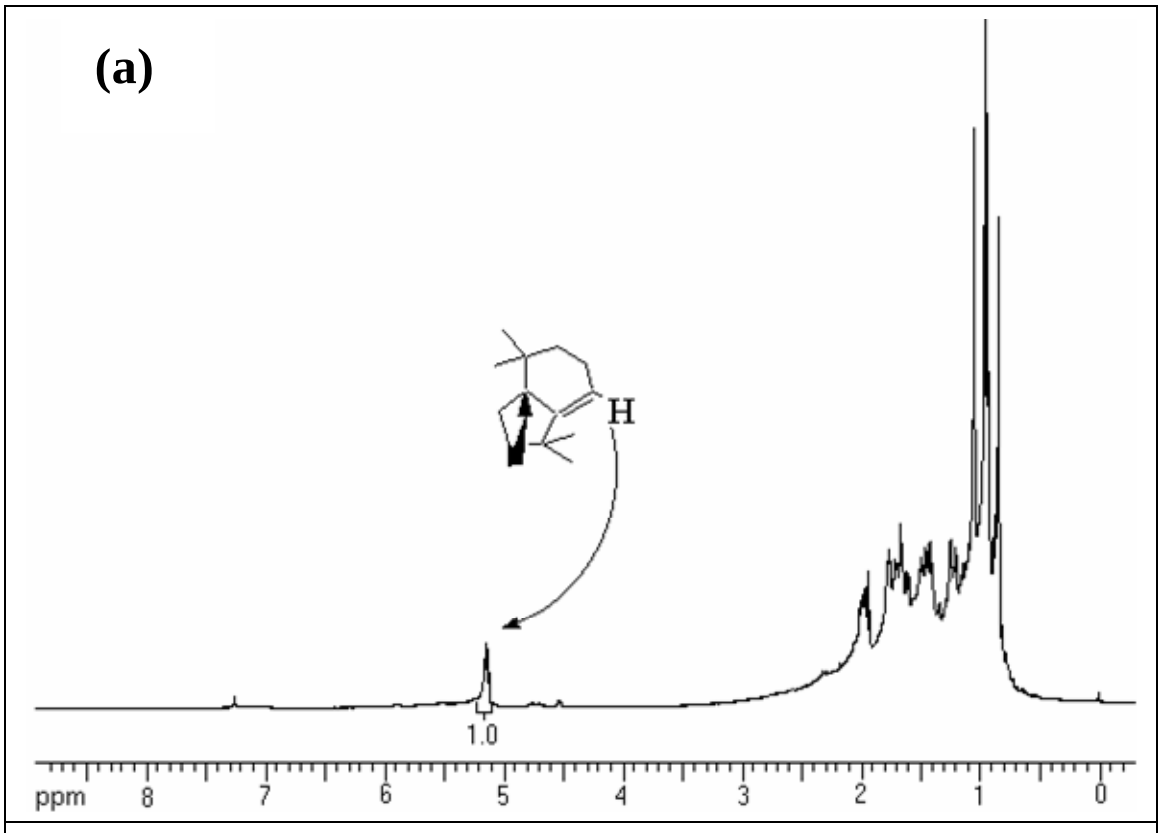

Figure 9a. ^{1}H NMR spectrum of reaction mixture after 1 minute.

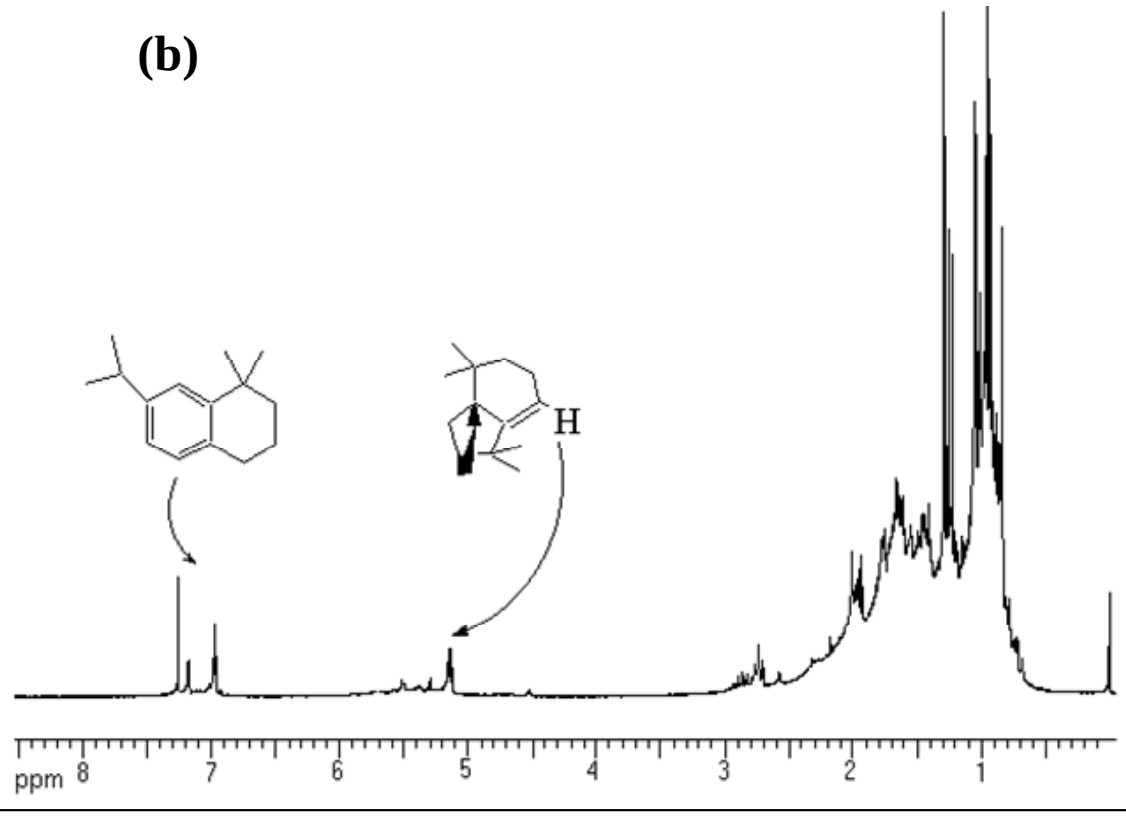

Figure 9b. ^{1}H NMR spectrum of reaction mixture after 10 minutes.

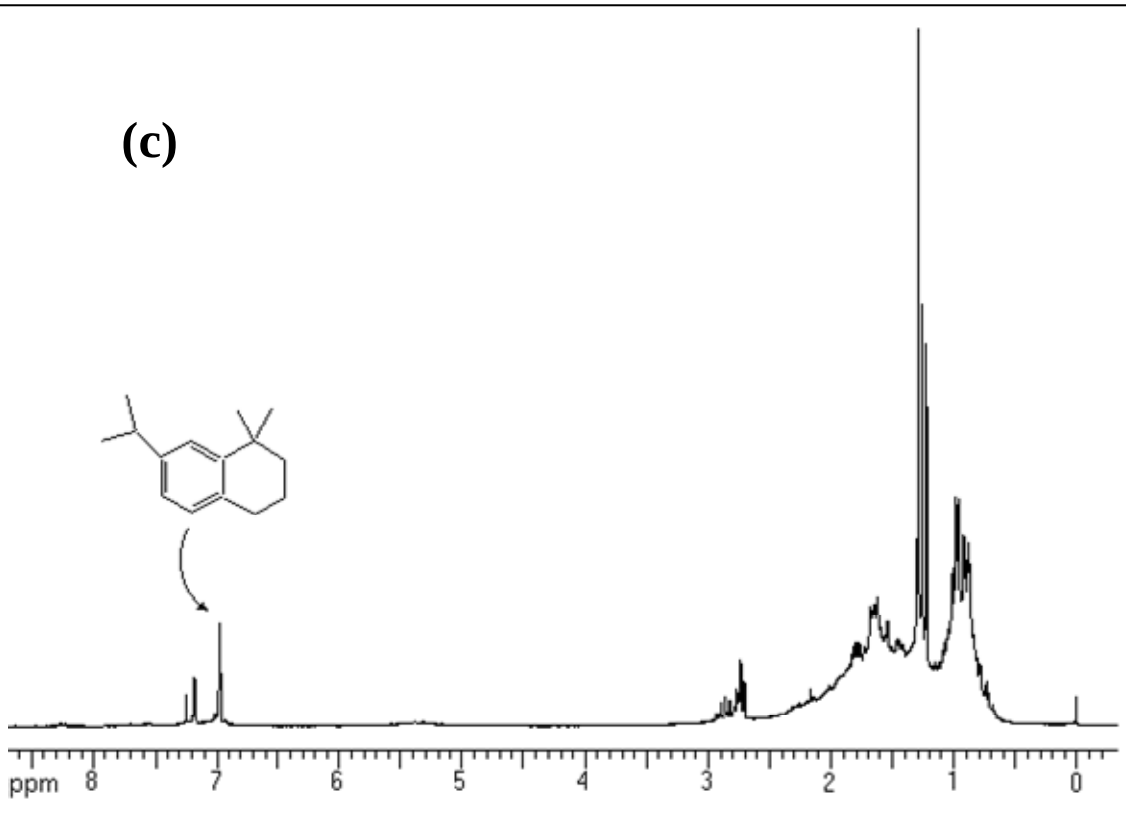

Figure 9c. ^{1}H NMR spectrum of reaction mixture after 1 h.

4.2.2.4 Effect of substrate to catalyst weight ratio

The effect of substrate to catalyst weight ratio on isomerization of longifolene was studied with the sample SZO2 (600) by carrying out the reaction at different substrate to catalyst weight ratio ranging from 10 to 100 at 180 ºC for 1 h. The data (Table 8) shows that with increasing the substrate to catalyst weight ratio from 5 to 100, the conversion of longifolene remains steady (94- 96 %), however, tetraline and other derivatives are formed only at lower substrate to catalyst weight ratio of 5 and 10. On increasing the substrate to catalyst weight ratio from 50 to 100, the isomerization results to the formation of isolongifolene with 100 % selectivity.

Table 8. Conversion (%) of longifolene and selectivity of isolongifolene after 1 h at different substrate to catalyst ratio.

Substrate/ Catalyst ratio	Conversion (%)	Selectivity (%)		
		Tetraline	Isolongifolene	Others
5	96	52	2	46
10	96	56	3	41
50	95	0	~100	0
70	95	0	~100	0
100	94	0	~100	0

(Reaction Temperature = 180 ºC, Reaction Time = 1 h)

It shows that the lower amount of the catalyst have Bronsted acidity to catalyze longifolene to isolongifolene with higher conversion and selectivity of isolongifolene. However, the lower catalyst amount has reduced number of acid sites, which are insufficient for further isomerization of isolongifolene.

4.2.2.5 Regeneration study

The regeneration study was done with the spent catalyst SZO2 (600) by carrying out the reaction under similar conditions as was done earlier with fresh catalyst. The thermally regenerated catalyst (550 ºC, 4 h in flow of air) showed similar conversion of longifolene but the selectivity of tetraline derivative was drastically decreased from 56 % to 10 % and the selectivity of isolongifolene was increased (46 %) while others were found in similar amount (44 %) (Table 9). In next cycle, the regenerated catalyst showed further decrease in selectivity of tetraline derivative (5 %) and others (37 %) and the selectivity of isolongifolene increased to 58 %, however, the conversion of longifolene

was similar. Third cycle shows similar selectivity data. The results showed that the selectivity of tetraline derivative is significantly decreased but the conversion of longifolene remains steady using the regenerated catalyst.

Table 9. Conversion of longifolene and selectivity of isolongifolene, tetraline derivative and other products.

Reaction Cycle	Conversion	Selectivity		
		Isolongifolene (%)	Tetraline derivative (%)	Others (%)
Fresh catalyst	92	3	56	41
I	94	46	10	44
II	94	58	5	37
III	94	58	5	37

(Substrate/ catalyst weight ratio = 10, Reaction Temperature = 180 ºC, Reaction Time = 1 h)

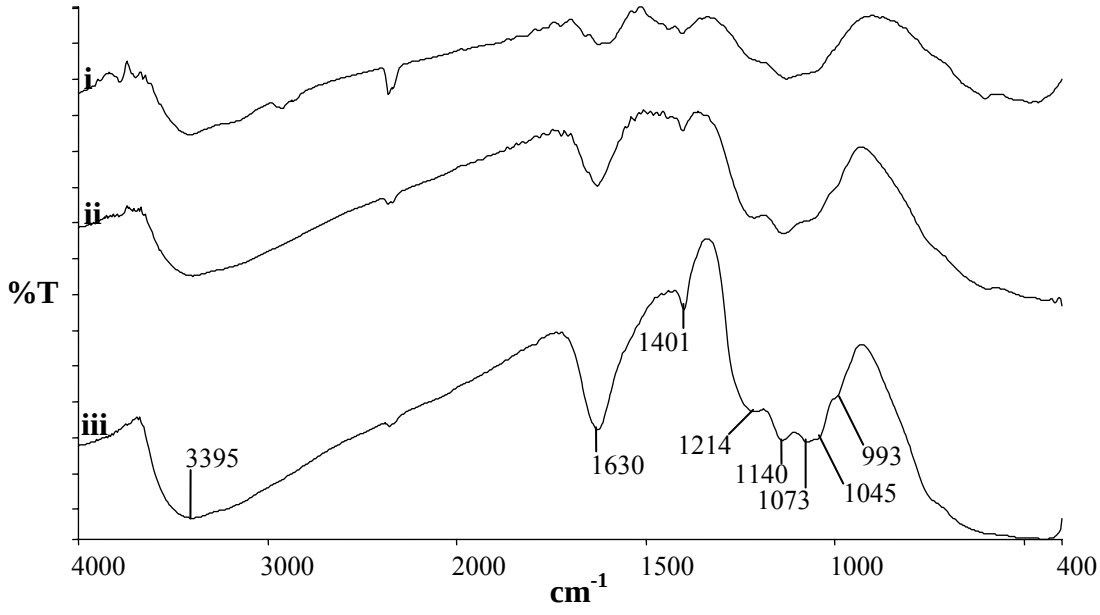

Figure 10. FT-IR spectra of: (i) used, (ii) regenerated catalyst at 550 ºC, 4 h in flow of air and (iii) regenerated catalyst at 550 ºC, 10 h in flow of air.

FT-IR spectrum of the regenerated catalyst (550 ºC, 4 h in flow of air) (Figure 10) does not show any peak of adsorbed substrate or products on the surface of sulfated-zirconia, however, the presence of a peak at 1401 cm^{-1} indicates the coke deposition on the some of the acid sites and therefore, few stronger sites of the catalyst, which may be

responsible for further isomerization of isolongifolene to tetraline derivative, get deactivated. The thermal regeneration of the catalyst at 550 ºC for longer time (10 h) in flow of air could also not remove the coke deposited on the acid sites as the FT-IR spectra of the regenerated catalyst shows the presence of the peak at 1401 cm^{-1} (Figure 10). It shows that the stronger acid sites are deactivated and could not be regenerated. The decrease in the selectivity of tetraline derivative with regenerated catalyst may be due to decrease in the number of sites lowering the activity of the catalyst for further isomerization of isolongifolene.

4.2.2.6 Characterization of the products

The major product, 7-isopropyl 1, 1-dimethyl tetraline, was separated from the reaction mixture by the column chromatography using silica gel (60- 120 mesh) with petroleum ether. It was characterized by ^1H NMR spectroscopy (Figure 11) and GC-MS analysis (Figure 12).

^1H NMR ($CDCl_3$): δ 7.10- 7.20 (d, 2H, ArH), 7.0 (s, 1H, ArH), 2.60- 2.90 (3H), 1.50- 1.90 (4H), 1.20- 1.40 (12H).

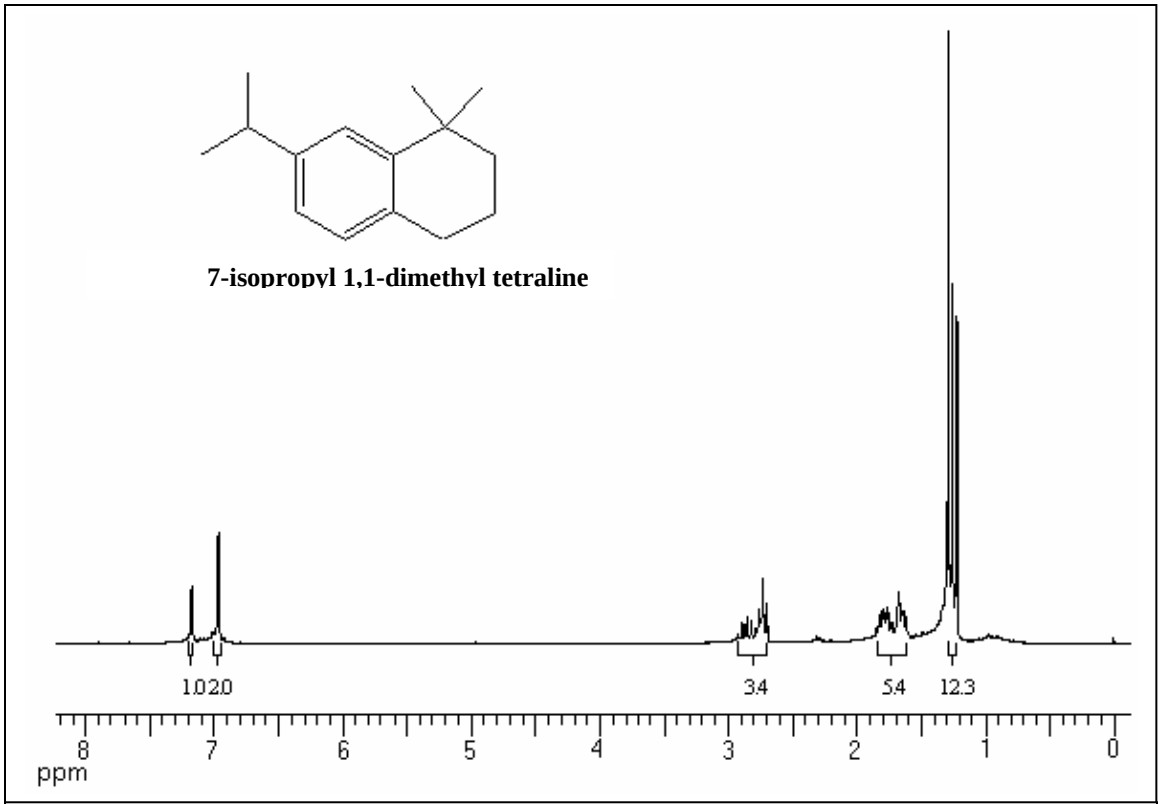

Figure 11. ^1H NMR spectrum of pure 7-isopropyl 1, 1-dimethyl tetraline.

The m/z for molecular ion $[M]^+$ at 202 is for 7-isopropyl 1,1-dimethyl tetraline ($C_{15}H_{22}$). The other major isomerized products were also identified by analyzing the reaction mixture by GC-MS. The mass spectra of the other products with their m/z values for molecular ions $[M]^+$ are given in figure 12.

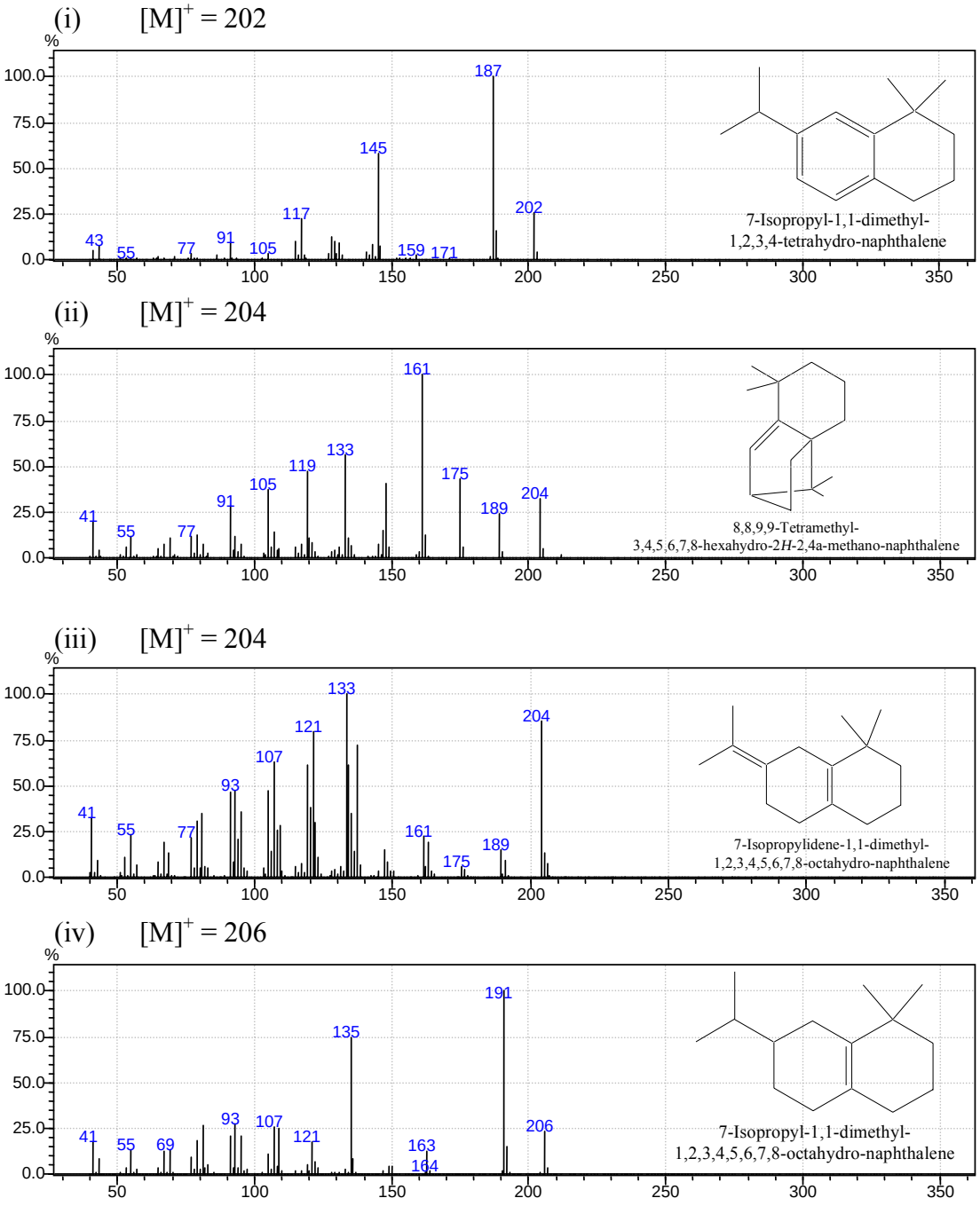

Figure 12. m/z $[M^+]$ of (i) 7-isopropyl 1,1-dimethyl tetraline (7-isopropyl- 1, 1-dimethyl- 1, 2, 3, 4-tetrahydro- naphthalene), (ii) & (iii) isomerized products and (iv) hydrogenated product.

Mechanistic pathway of isomerization of longifolene to isolongifolene and tetraline derivative

The isomerization of longifolene (I) results to isolongifolene (II) through given pathway, however, the formation of tetraline takes place by two pathways (Scheme 2). First route is the isomerization of longifolene to tetraline via isolongifolene and second is the direct isomerization of longifolene to tetraline. The isomerization of longifolene (I) involves the addition of proton to olefinic double bond resulting to carbonium ion intermediates (I.a – I.f) and finally isolongifolene (II). The double bond of isolongifolene (II) takes proton and forms carbonium ion (I.e), which undergoes C-C bond cleavage to form intermediate (I.g). The intermediate (I.g) isomerizes to different intermediates (I.h – I.j) and undergoes dehydrogenation to form tetraline (IV). Second route is the direct isomerization of longifolene (I) to tetraline (IV) via intermediate (I.e). In second route, the intermediate (I.e), without proceeding the rearrangement towards isolongifolene, forms the intermediate (I.g), which finally leads to tetraline derivative (III). The intermediate carbonium ion (I.e) is key intermediate of route 1 and 2 for the formation of tetraline derivative.

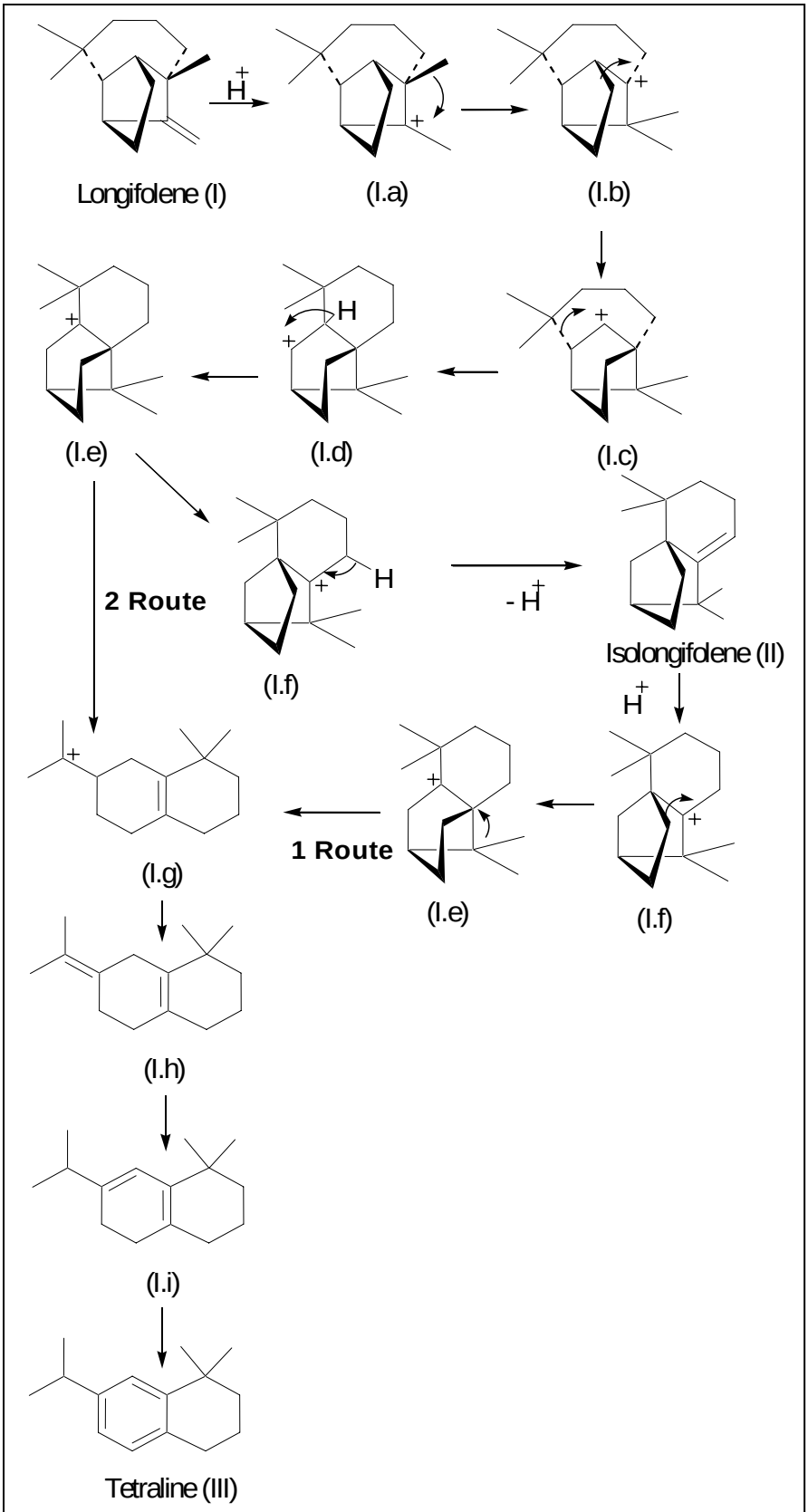
Longifolene (I)
(I.a)
(I.b)
(I.c)
(I.d)
(I.e)
(I.f)
Isolongifolene (II)
(I.f)
(I.e)
(I.g)
(I.h)
(I.i)
Tetraline (III)
2 Route
1 Route
- H+

Scheme 2 **[223]**

4.2.3 Conclusions

The sulfated-zirconia sample, synthesized by one-step sol-gel method using water to alkoxide molar ratio of 2.7, is nano-crystalline material having purely tetragonal phase but is less crystalline. The higher sulfur content in the sample is responsible for the variation in the physicochemical and acidic properties of the sample. The higher sulfur content generates higher number of Bronsted acid sites. The higher number of Bronsted acid sites on the surface catalyzes the further isomerization of isolongifolene to 7-isopropyl 1, 1-dimethyl tetraline as major product and other isomerized products. The substrate to catalyst weight ratio affects the selectivity of the isomerized products. At higher substrate to catalyst weight ratio, the isomerization of longifolene results to ~100 % isolongifolene, while at lower substrate to catalyst weight ratio, the formation of tetraline derivative along with other isomerized products takes place. The regenerated sample has similar activity for isomerization of longifolene to isolongifolene; however, the selectivity of the products varies.

Chapter 5

Synthesis of 7-Substituted 4-Methyl Coumarins by Pechmann Reaction using Nano-crystalline Sulfated Zirconia

5.1 Introduction

Sulfated-zirconia has been reported for a wide range of organic reactions such as isomerization **[43- 54, 84- 88]**, alkylation **[38- 42, 56- 66]**, acylation **[67- 74]**, esterification **[75- 81]**, etherification **[82- 83]**, nitration **[89]**, oligomerization **[90, 91]** etc. showing excellent activity. The catalytic application of sulfated-zirconia catalysts have been reviewed in detail in reviews **[92, 93]**. Various industrially important organic reactions have been aimed to replace conventional acids, toxic or expensive solvents and multistep process, with single step solvent-free ones by using environmentally benign solid acid catalysts. The Pachmann reaction is an important acid catalyzed reaction to synthesize the coumarin derivatives from activated phenols, mostly *m*-substituted phenol containing electron donating substituent at meta position and acetoacetic esters or an unsaturated carboxylic acid **[229- 231]**. The sulfated-zirconia has been studied for most of acid catalyzed reaction; however, the synthesis of coumarin derivatives using sulfated-zirconia is not studied in detail. The present chapter deals with the application of the nano-crystalline sulfated-zirconia for the synthesis of 7-amino 4- methyl coumarin and 7-hydroxy 4-methyl coumarin by acid catalyzed Pechmann reaction.

Coumarins are the benzo-2-pyrone derivatives. They are natural products and are mainly found in the plants of the family of Rutaceae and Umbelliferae. The coumarins have different interesting biological activities, for example, 'Decursin' extracted from *Angelica gigas* (Korean angelica) and 'Psoralidin' from *Psoralea coryfolia* (Psoralea seed) both exhibit toxic activity against various human cancer cell lines, Soulattrolide extracted from *Calophylum teysmanii* (Bintangor gading) shows a potent inhibitor of HIV-1 reverse transcriptase.

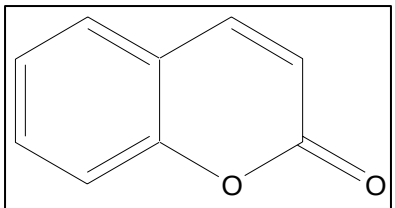

Benzo-2-pyrone

The coumarins find a broad range application, as drugs (anthelmintic, hypnotic, insecticidal, anticoagulant) drug intermediates, insecticides, fragrances, food additives,

cosmetic additive, optical brightening agent, dispersed fluorescents and laser dyes **[232-236]**. Coumarin and its derivatives are principal oral anticoagulants. Coumarins are having various bioactivities such as inhibitory of platelet aggregation, antibacterial, anticancer, inhibitory of steroid 5α-reductase and inhibitory of HIV-1 protease. 7-substituted coumarins are important group of coumarins showing various bioactivities and are medicinally important **[237]**.

7-hydroxy 4-methyl coumarin (β-methylumbelliferone) is used as fluorescent brightener, efficient laser dye, standard for fluorometric determination of enzymatic activity, as a starting material for the preparation of hymerocromone (insecticide), as precursor for furano coumarins and many other derivatives of substituted coumarins. 7-amino–4-methyl coumarin is mainly used as laser dyes.

The natural biosynthesis of the coumarins oxygenated at position 7 (7-hydroxy coumarin derivatives) involves the transformation of the trans-cinnamic acid derivative to cis-form by the help of glucose and the cyclization in presence of beta-glucosidase enzyme.

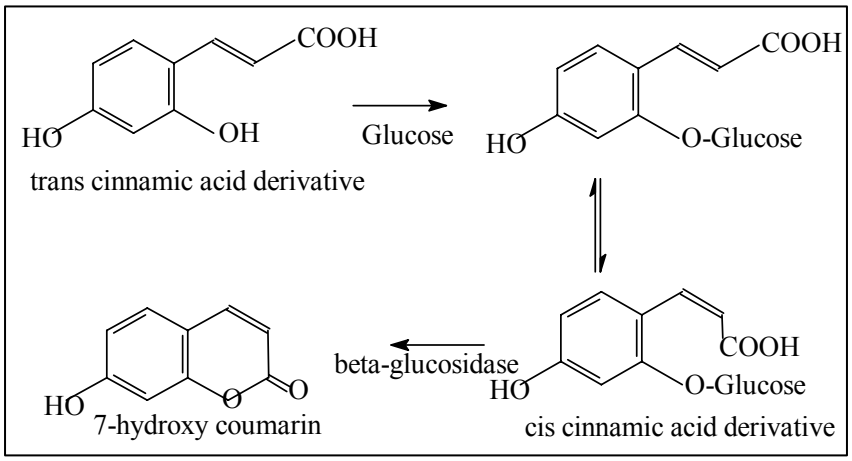

The natural source of coumarins are plants and are obtained by different extraction methods, for example, Maceration with solvent, under sonication, Infusion, Supercritical fluid extraction etc. **[238]**. Though, the plants are the natural sources of coumarins, the extraction from plants are time taking tedious job and needs sophisticated instrument based separation process to get pure product. Therefore, the chemical synthesis of coumarins and their derivatives has attracted the organic and medicinal

chemists to fulfill their requirements for wide range applications. Coumarins can be synthesized by various methods such as Claisen rearrangement **[239]**, Perkin reaction **[240- 242]**, Pechmann reaction **[229- 231]**, Wittig reaction **[243- 245]**, Knoevenagel condensation **[246- 248]**, Reformatsky reaction **[249]** and catalytic cyclization reactions **[250]**. However, most commonly coumarins are prepared by acid catalyzed Pechmann reaction from activated phenols, mostly *m*-substituted phenol containing electron donating substituent at meta position and acetoacetic esters or an unsaturated carboxylic acid **[229-231]**. The reaction involves two steps; the trans esterification of phenol derivative with acetoacetic ester to form phenyl acetoacetate followed by acid catalyzed electrophilic substitution at aromatic nucleus resulting to cyclization and elimination of water to form coumarin derivative (Scheme 1).

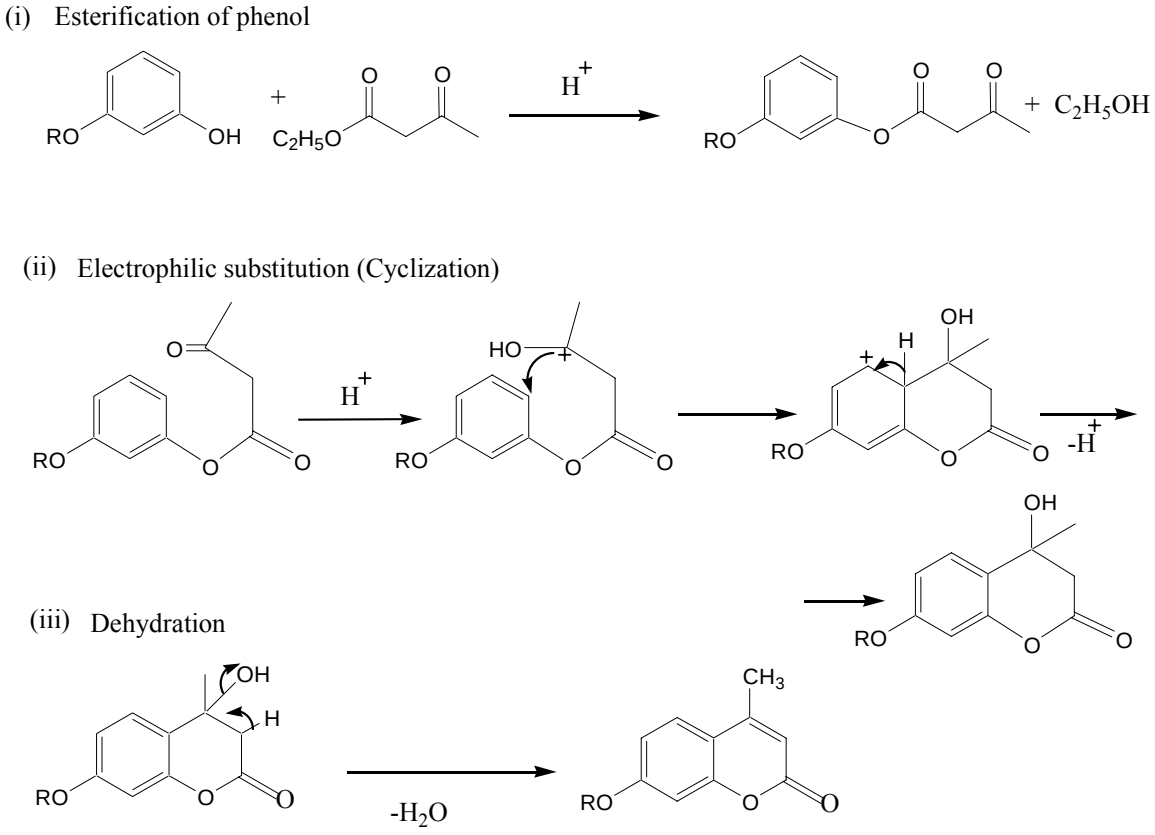

Scheme 1

Conventionally, the Pechmann reaction to synthesize coumarins is carried out in presence of concentrated sulfuric acid as a catalyst **[251, 252]**. Besides it, phosphorous

pentaoxide **[253]**, trifluoroacetic acid **[254]**, aluminum chloride **[255]**, zinc chloride **[256]** and alcoholic hydrochloric acid are also used. These mineral acids are corrosive, non-reusable and environmentally hazardous. These catalysts are required in excess amount; for example with H_2SO_4, reaction needs ten to twelve equivalents (1.1 liter H_2SO_4 to synthesize 1 mol of 7-hydroxy-4-methyl coumarin), with CF_3COOH three to four equivalents and with P_2O_5 five equivalents are required. In some cases, reaction takes place for a number of days to be completed depending on the reactivity of the substituted phenol **[257]**, e.g. the synthesis of 7-hydroxy 4-methyl coumarin takes 12- 24 h **[252]**, and higher reaction temperature (> 150 ºC) is required, which gives some undesired side products such as chromones. In order to overcome the above mentioned problems and to make economic process with better yield, some of the heterogeneous acid catalysts such as cation-exchanged resins **[258, 259]**, perfluorinated sulfuric acid resin (Nafion-H) **[260]**, zeolites **[261, 262]**, montmorillonite clays **[263, 264]**, Polyaniline sulfate salt **[265, 266]**, heteropoly acids **[267]**, Nafion resin/silica nanocomposites **[268]**, tungsten-zirconia **[269]**, sulfated-zirconia **[270]**, etc. have been reported to be as best alternative for coumarin synthesis by Pechmann reaction showing good activity for the same.

7-amino 4-methyl coumarin has been reported to be synthesized by Pechmann reaction using Graphite/K10 at 130 ºC yielding 66 % within 30 min and under microwave irradiation (60 W) 65% yield at 5 min **[263]**. 7-hydroxy-4-methyl coumarin has also been synthesized by Pechmann reaction using different solid acids such as Amberlyst ion-exchange resins **[259]**, zeolites **[261, 262]**, K-10 **[264]**, Polyaniline sulfate salt **[265, 266]**, WD Heteropoly acids **[267]**, Nafion resin/silica nanocomposites **[268]**, etc. either in presence of solvent or without solvent. Microwave irradiation has been found more useful for synthesis of 7-amino 4-methyl coumarin and 7-hydroxy 4-methyl coumarin using solid acids in order to minimize the reaction time **[263, 271]**.

The present chapter consists of the application of the nano-crystalline sulfated-zirconia, synthesized by one-step and two-step sol-gel method, for the synthesis of 7-amino 4-methyl coumarin and 7-hydroxy 4-methyl coumarin from activated phenols namely *m*-amino phenol and *m*-hydroxy phenol respectively with ethyl acetoacetate in presence of solvent as well as in solvent free condition. A detail study of the reaction to optimize the reaction parameters such as reaction temperature, reaction time,

substrate/catalyst weight ratio, reactants molar ratio and solvent effect has been carried out to obtain the maximum conversion and selectivity of respective products. The microwave assisted solvent free synthesis of 7-hydroxy 4-methyl coumarin has also been done to reduce the reaction time and temperature with better yield.

5.2 Experimental

5.2.1 Materials

Zirconium propoxide (70 wt.% solution in *n*-propanol) was procured from Sigma Aldrich, USA, *n*-propanol, aqueous ammonia (25%) and concentrate sulfuric acid were from s.d. Fine chemicals, India, *m*-amino phenol and ethyl acetoacetate were from Loba Chemei, India and *m*-hydroxy phenol was from Central Drug House, India.

5.2.2 Catalyst synthesis

The sulfated-zirconia catalysts were synthesized by sol-gel technique using one-step sol-gel method in acidic medium and two-step sol-gel method in basic as well as in neutral medium. The zirconium propoxide [$Zr(C_3H_7)_4$] was used as a precursor after dilution (30 wt%) with *n*-propanol, water or liquid ammonia as hydrolyzing agent and sulfuric acid as a sulfating agent. The detail of synthesis procedure has been described in chapter 3. The samples, synthesized by one-step sol-gel method, were designated as SZO1 and SZO2 (600) and the samples, synthesized by two-step sol-gel method in basic and neutral medium, were designated as SZTB and SZTN respectively.

5.2.3 Catalyst characterization

The sulfated-zirconia catalysts (SZO1, SZO2 (600), SZTB and SZTN) were characterized by X-ray Powder Diffraction study, FT-IR Spectroscopy, FT-IR study of the samples adsorbed with pyridine, N_2 adsorption-desorption isotherm study, dehydration of cyclohexanol to cyclohexene as model reaction for assessment of Bronsted acidity, CHNS/O and ICP (Inductive Couple Plasma) for Sulfur Analysis. The detail description of the characterization techniques used to characterize the sulfated-zirconia catalysts is given in chapter 3.

5.2.4 Catalytic activity

5.2.4.1 Synthesis of 7-substituted 4-methyl coumarins by Pechmann reaction using Sulfated-zirconia

The catalytic activity of the sulfated-zirconia catalysts, synthesized by one-step and two-step sol-gel methods, was studied to synthesize 7-substituted 4-methyl coumarins such as 7-amino 4-methyl coumarin and 7-hydroxy 4-methyl coumarin by acid catalyzed Pechmann reaction using activated phenols, *m*-amino phenol and *m*-hydroxy phenol respectively and ethyl acetoacetate. The synthesis of both coumarin derivatives was carried out in presence of nitrobenzene as a solvent as well as in solvent free conditions. The solvent free synthesis of 7-hydroxy 4-methyl coumarin was also done under microwave irradiation to reduce the reaction time and temperature as thermally, the reaction takes place at higher temperature (170 ºC) and for long time (3 h) to achieve maximum yield of 7-hydroxy 4-methyl coumarin. The thermal synthesis of 7-amino 4-methyl coumarin was observed to be very fast attaining 100 % conversion of meta-phenol to 7-amino 4-methyl coumarin with 100 % selectivity within 2 minutes at 110 ºC, therefore, microwave assisted synthesis was not needed.

5.2.4.1.1 Synthesis of 7-amino 4-methyl coumarin

m-amino phenol (10mmol) and ethyl acetoacetate (10mmol), in a 50 ml reaction tube of reaction station (12 Place Heated Carousel Reaction Station, RR99030, Radleys Discovery Technologies, UK), were taken in 1:1 molar ratio with nitrobenzene (3 g), as solvent and tridecane (0.1 g), as internal standard. When reaction was carried out in solvent free condition, *m*-amino phenol and ethyl acetoacetate were taken in 1:2 molar ratio to dissolve the phenol. The catalyst (*m*-amino phenol to catalysts ratio = 10) was activated at 450 ºC for 2 h in static air, was added in the reaction mixture. The reaction was carried out at different temperatures in the range of 90 to 150 ºC by heating the reaction mixtures in different reaction tubes on reaction station under stirring for 2 min to 3 h. The reaction tubes were taken out at different time intervals and dimethyl sulfoxide (2 ml) was added to dissolve the product, as the product is highly soluble in dimethyl sulfoxide compare to ethanol. The reaction mixture was analyzed by gas chromatography (HP6890) having a HP50 (30 miter long) capillary column with a programmed oven

temperature from 50 to 200 ºC, a 0.5 cm^3/min flow rate of N_2 as carrier gas and FID detector. The conversion of *m*-amino phenol was calculated by using weight percent method; the initial theoretical weight percent of *m*-amino phenol was divided by initial GC peak area percent to get the response factor. Final unreacted weight percent of m-amino phenol remaining in the reaction mixture was calculated by multiplying response factor with the area percentage of the GC peak for *m*-amino phenol obtained after the reaction.

The conversion was calculated as follows:

Response factor = Initial theoretical weight percent of *m*-amino phenol/ Initial GC peak area percent of *m*-amino phenol before reaction.

Final unreacted weight percent of *m*-amino phenol = Response factor X Final GC peak area percent of *m*-amino phenol after reaction.

$$\text{Conversion (wt \%) of } m\text{-amino phenol} = \frac{100 \text{ X [Initial wt\% - Final wt\%]}}{\text{Initial wt\%}}$$

$$\text{Selectivity of 7-amino 4-methyl coumarin (wt. \%)} = \frac{100 \text{ X [GC peak area\% of 7-amino 4-methyl coumarin]}}{\sum \text{Total GC peak area \% for all the products}}$$

The pure product was isolated and characterized by FT-IR (Perkin–Elmer GX), ^{1}H NMR spectroscopy (Bruker, Advance DPX 200MHz) and melting point. The reaction conditions such as reaction temperature, reaction time, molar ratio of reactants and phenol to catalyst weight ratio were studied in detail in presence of solvent and in solvent free condition to optimize the reaction conditions to achieve maximum conversion.

5.2.4.1.2 Synthesis of 7-hydroxy 4-methyl coumarin

In a 50 ml reaction tube of reaction station (12 Place Heated Carousel Reaction Station, RR99030, Radleys Discovery Technologies, UK), *m*-hydroxy phenol (10mmol) and ethyl acetoacetate (10mmol) were taken in 1:1 molar ratio with nitrobenzene, as solvent. The *m*-hydroxy phenol and ethyl acetoacetate were taken 1:2 molar ratio to dissolve the phenol, when the reaction was carried out in solvent free condition. The activated catalyst, at 450 ºC for 2 h in static air, was added in the reaction mixture. The reaction was carried out at different temperatures in the range of 150 to 170 ºC by heating

the reaction mixtures in different reaction tubes on reaction station under stirring for 30 min to 24 h. The reaction tubes were taken out at different time intervals. The hot reaction mixture was filtered to separate catalyst and catalyst was washed with ethanol to remove the product. The reaction mixture gets solidified on cooling the reaction mixture due to the fast crystallization of 7-hydroxy 4-methyl coumarin, therefore, the yield of the 7-hydroxy 4-methyl coumarin was obtained. The added ethanol was evaporated by rotavapour. The reaction mixture was kept for 12 h to completely crystallize the product. The crystals of product were filtered and washed with petroleum ether to remove unreacted reactants and nitrobenzene. The crystals were dried and recrystallized in ethanol-water system (10:1) under slow crystallization.

The yield of 7-hydroxy 4-methyl coumarin was calculated as follows,

$$\text{Yield \%} = \frac{100 \text{ X Obtained weight of Product}}{\text{Theoretical weight}}$$

The product was characterized by FT-IR, ^{1}H NMR spectroscopy and melting point. The reaction conditions such as reaction temperature, reaction time, molar ratio of reactants and phenol to catalyst weight ratio were studied in detail in presence of solvent as well as in solvent free condition to optimize the reaction parameters to achieve maximum yield of 7-hydroxy 4-methyl coumarin.

5.2.4.1.3 Microwave assisted solvent free synthesis 7-hydroxy 4-methyl coumarin

Solvent free synthesis of 7-hydroxy 4-methyl coumarin was also carried under microwave irradiation (250 W) at different temperatures ranging from 90 to 170 ºC for 5 to 20 min. In a 100 ml microwave reactor (Ethos 1600 microwave labstation), *m*-hydroxy phenol and ethyl acetoacetate (in molar ratio of 1:2) were taken and the activated catalyst, at 450 ºC for 2 h in static air, (substrate to catalyst ratio = 10) was added in the reaction mixture. The reaction mixture was kept in microwave reactor at required temperature for required time. The hot reaction mixture was filtered to separate the catalyst and the catalyst was washed with ethanol to remove the reactant and product. The ethanol added in the reaction mixture was evaporated by rotavapour and the reaction mixture was kept for 12 h to crystallize the product. The crystals of product were filtered and washed with petroleum ether to remove unreacted reactants. The crystals were dried and recrystallized

in ethanol-water system (10:1) under slow crystallization. The product was characterized by FT-IR, ^{1}H NMR spectroscopy and melting point.

5.2.4.2 Catalyst regeneration

The regeneration study was done with SZO2 (600) catalyst, used in the solvent free synthesis. The spent catalyst was filtered from reaction mixture and regenerated by washing the catalyst with hot ethanol and then with acetone to remove the adsorbed reactants and products from the catalyst and then activating the catalyst at 450 ºC for 2 h in flow of air. The reaction with regenerated catalyst was done under similar reaction conditions as done with fresh catalyst. After every reaction cycle, the catalyst was recovered from reaction mixture and regenerated as earlier.

5.3 Results and Discussion

5.3.1 Physicochemical properties of sulfated-zirconia catalysts

X-ray diffraction pattern of sulfated-zirconia samples after calcination at 600 ºC (Figure 1 and 2, in Chapter 3) showed the peaks at 2θ = 30.4, 35.3, 50.2 and 60.2, which indicates the presence of purely tetragonal crystalline phase in all the samples. The samples were highly crystalline except SZO2 (600), which was found less crystalline at 600 ºC due to higher sulfur content (3.0 wt.%) in the sample (Table 5, in Chapter 3). Crystallite size was determined from X-ray diffraction data using Scherer formula, which showed that the sulfated-zirconia catalysts were of nano-crystalline nature with crystallite size ranging from 9 to 16 nm (Table 1, in Chapter 3). The sample SZO2 (600) was having smaller crystallite (9 nm) size among four samples.

FT-IR spectrum of sulfated-zirconia sample (Figure 3, in Chapter 3) showed the IR bands at 1246-1220, 1142-1138, 1049-1044 and 996 cm^{-1}, which are characteristic of inorganic chelating bidentate sulfate group having partially ionized S=O double bonds **[98]**. FT-IR study of the pyridine adsorbed samples at 150 to 450 ºC showed the presence of significant amount of stronger Bronsted and Lewis acid sites in the samples (Figure 5a- 5g, in Chapter 3).

N_2 adsorption-desorption isotherms of the samples calcined at 600 ºC showed type IV isotherm (Figure 6a, 6b and 6c in Chapter 3), which is generally found in

mesoporous materials. The hysteresis in all three samples SZO1, SZTN and SZTB, except one-step sample SZO2 (600), shows type H2 hysteresis. While it is of type H3 in sample SZO2 (600), reflecting the presence of large mesopores. The surface area was in the range of 81- 150 m^2/g (Table 2, in Chapter3). The samples, synthesized by one-step sol-gel method, showed higher surface area, pore volume and pore size as compared to two-step samples. Among the samples, synthesized by one-step sol-gel method, the sample SZO2 (600) has the highest surface area, pore volume and pore size and in the samples, synthesized by two-step sol-gel method, the samples SZTB has higher surface area. The pore size distribution (Figure 7a, 7b and 7c, in Chapter 3) in SZO2 (600) was observed to be broader than other three samples.

The sulfur (wt.%) retained in the samples after calcination at 600 ºC (Table 5, in Chapter 3) was in the range of 1.4 to 3.0 wt.% (measured by CHNS/O). However, the sulfur content was higher in the samples (1.3- 3.0 wt.%), synthesized by one-step sol-gel method than the samples (1.3- 1.4 wt.%), synthesized by two-step sol-gel method. Sulfur retained in the sample SZO2 (600) after calcination at 600 ºC was highest (3.0 wt%).

The sulfated-zirconia samples, synthesized by one-step and two-step sol-gel methods showed good activity for dehydration of cyclohexanol giving conversion (wt%) of cyclohexanol in range of 78- 100 % with 100 % selectivity for cyclohexene (Table 3, in Chapter 3). It indicates that all four samples have higher Bronsted acidity.

5.3.2 Synthesis of 7-amino 4-methyl coumarin

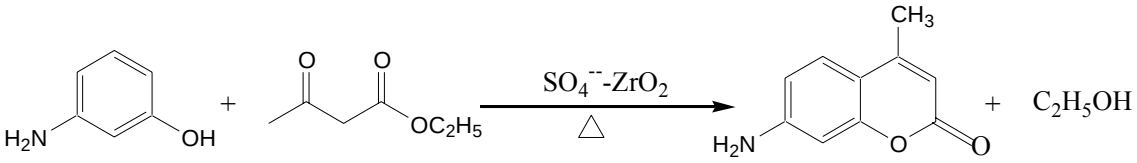

m- amino phenols Ethyl acetoacetate 7-amino 4-methyl coumarin

The synthesis of 7-amino 4-methyl coumarin, using nano-crystalline sulfated-zirconia catalysts, synthesized by one-step and two-step sol-gel methods, was carried out with nitrobenzene as a solvent as well as in solvent free condition at 150 ºC.

Table 1. Conversion (wt.%) of *m*-amino phenol and selectivity (%) of 7-amino 4-methyl coumarin with sulfated-zirconia catalysts, synthesized by one-step and two-step sol-gel methods.

Catalyst	With nitrobenzene		Solvent free	
	Conversion (wt.%)	Selectivity (%)	Conversion (wt.%)	Selectivity (%)
SZO1	100	100	100	100
SZO2 (600)	100	100	100	100
SZTB	100	100	100	100
SZTN	100	100	100	100

(With nitrobenzene- 10 mmol m-amino phenol, 10 mmol ethyl acetoacetate (1:1), 0.1 g tridecane (internal standard), 3 g nitrobenzene (solvent), 0.1 g catalyst, Reaction Temperature = 150 ºC, Reaction Time = 1 h)
(Without solvent- 10 mmol m-amino phenol, 20 mmol ethyl acetoacetate (1:2), 0.1 g tridecane (internal standard), 0.1 g catalyst, Reaction Temperature = 150 ºC, Reaction Time = 1 h)

All four catalysts were found highly active for synthesis of 7-amino 4-methyl coumarin and similar in activity showing 100 % conversion with ~100 % selectivity of 7-amino 4-methyl coumarin after 1 h in presence of solvent as well as in solvent free condition (Table 1). The detail kinetic study and effect of various reaction parameters such as reaction temperature, time, molar ratio of reactants and substrate to catalyst weight ratio, in presence of nitrobenzene as solvent as well as in solvent free condition for the synthesis of 7-amino 4-methyl coumarin was done over the sample SZO2 (600), synthesized by one-step sol-gel technique.

5.3.2.1 Optimization of reaction temperature and reaction time

The reaction temperature for maximum conversion of *m*-amino phenol to 7-amino 4-methyl coumarin was optimized by carrying out reaction at different temperatures ranging from 110 to 150 ºC for 1 h. The data (Table 2) shows that in presence of nitrobenzene, the conversion of *m*-amino phenol gradually increases from 110 to 150 ºC showing maximum conversion (100 %) with 99 % selectivity of 7-amino 4-methyl coumarin at 150 ºC after 1 h. Whereas the reaction in solvent free condition (Table 3) gives maximum conversion (100 %) of *m*-amino phenol with 100 % selectivity for 7- amino 4-methyl coumarin at comparatively much lower temperature (110 ºC) after 1 h. The kinetic study of the reaction in presence of nitrobenzene was studied at 150 ºC to

observe the effect of solvent on the reaction kinetics and to optimize the reaction time for achieving the maximum conversion. Table 2 shows that in presence of nitrobenzene, the maximum conversion (100 %) was observed within 45 min with ~ 98 % selectivity for 7-amino 4-methyl coumarin, which was further increased to 100 % after 2 h of the reaction and remained steady upto 3 h of the reaction. Therefore, further detail study of the reaction in presence of nitrobenzene was carried out at 150 ºC for 2 h.

Table 2. Effect of temperature on conversion (wt.%) of *m*-amino phenol and kinetic study with solvent.

Temperature (ºC)	Time (min.)	Conversion (wt.%)	Selectivity (%)
110		65	100
130	60	64	99
150		100	99
150	15	77	99
	30	91	98
	45	100	99
	60	100 (45)*	96 (100)*
	90	100	97
	120	100	100
	150	100	100
	180	100	100

(10 mmol m-amino phenol, 10 mmol ethyl acetoacetate (1:1), 0.1 g tridecane (internal standard), 3 g nitrobenzene (solvent), 0.1 g catalyst)
*(*In presence of toluene as solvent; 10 mmol m-amino phenol, 10 mmol ethyl acetoacetate (1:1), 0.1 g tridecane (internal standard), 3 g toluene (solvent), 0.1 gm catalyst, Reaction Temperature = 150 ºC, Reaction Time = 1 h)*

The synthesis of 7-amino 4-methyl coumarin was also carried out with SZO2 (600) in presence of toluene as solvent at 150 ºC for 1 h to observe the effect of non-polar solvent on the reaction. The conversion of *m*-amino phenol was found much lower (45 %) in presence of toluene as compared to nitrobenzene (100 %), however, the selectivity of the product was similar (100%). The kinetics was observed to be very fast when the reaction was carried out at 110 ºC in solvent free condition as shown in Table 3, showing 100 % conversion of *m*-amino phenol with 100 % selectivity of 7-amino 4-methyl coumarin within 2 minutes. Therefore, further detail study of the reaction in solvent free condition was done at 110 ºC for 15 min. It clearly shows the effect of solvent on the reaction temperature and the kinetics of the reaction.

Table 3. Effect of temperature on conversion (wt.%) of *m*-amino phenol and kinetic study in solvent free condition.

Temperature (ºC)	Time (min.)	Conversion (wt.%)	Selectivity (%)
90	60	95	100
110		100	100
130		100	100
150		100	100
110	2	100	100
	4	100	100
	6	100	100
	8	100	100
	10	100	100
	12	100	100
	15	100	100

(10 mmol m-amino phenol, 20 mmol ethyl acetoacetate (1:2), 0.1 g tridecane (internal standard), 0.1 g catalyst)

5.3.2.2 Effect of molar ratio of *m*-amino phenol and ethyl acetoacetate

The effect of molar ratio of *m*-amino phenol to ethyl acetoacetate was studied by carrying out the reaction at optimized conditions of temperature and time with different molar ratio of reactants from 1:1 to 1:2. With nitrobenzene, the conversion of *m*-amino phenol at 150 ºC after 2 h was 100 % but selectivity of 7-amino 4-methyl coumarin was observed to be slightly decreased with increase of amount of ester from 1:1 to 1:1.5 and 1:2 (Table 4). In solvent free condition, no effect of *m*-amino phenol to ethyl acetoacetate molar ratio was observed on the conversion and selectivity (Table 4).

Table 4. Effect of phenol to ester ratio on conversion (wt.%) of *m*-amino phenol and selectivity (%) of 7-amino 4-methyl coumarin, with solvent and in solvent free condition.

m-AP:EAA	With solvent		Without solvent	
	Conversion (wt.%)	Selectivity (%)	Conversion (wt.%)	Selectivity (%)
1:1	100	100	100	100
1:1.5	100	97	100	
1:2	100	97	100	

(10 mmol m-amino phenol, ethyl acetoacetate (according to molar ratio) 0.1 g tridecane (internal standard), 0.1 g catalyst,
With solvent - 3 gm nitrobenzene (solvent), Reaction Temperature = 150 ºC, Reaction Time = 2 h,
Without solvent - Reaction Temperature = 110 ºC, Reaction Time = 15 min)

5.3.2.3 Effect of phenol to catalyst weight ratio

In presence of nitrobenzene, the effect of *m*-amino phenol to catalyst weight ratio on the conversion of *m*-amino phenol was studied by carrying out the reaction of *m*-amino phenol and ethyl acetoacetate in 1:1 molar ratio at different *m*-amino phenol to catalyst weight ratio in the range of 10 to 80 at 150 ºC for 2 h. Table 5 shows that the conversion of *m*-amino phenol (100 %) remained steady with increasing the substrate to catalyst weight ratio from 10 to 80. It shows the higher catalytic activity of sulfated-zirconia catalyst, which is required in very small catalytic amount for the synthesis of 7-amino 4-methyl coumarin. However, the selectivity was observed to be decreased to 94 % with increasing the substrate to catalyst weight ratio from 10 to 80.

When the reaction was carried out in solvent free conditions at 110 ºC for 15 minutes, the conversion of *m*-amino phenol remained steady at maximum 100 % with increasing the substrate to catalyst weight ratio from 10 to 40, however, on further increase in the substrate to catalyst weight ratio (80), the conversion of *m*-amino phenol was observed to be slightly decreased to 96 % without affecting the selectivity of the product (Table 5).

Table 5. Effect of phenol to catalyst weight ratio on conversion (wt.%) of *m*-amino phenol and selectivity (%) of 7-amino 4-methyl coumarin, in presence of solvent and in solvent free condition.

Substrate/ Catalyst weight ratio	With solvent		Without solvent	
	Conversion (wt.%)	Selectivity (%)	Conversion (wt.%)	Selectivity (%)
10	100	100	100	100
20	100	96	100	
40	100	96	100	
80	100	94	96	

(With solvent - 10 mmol m-amino phenol, 10 mmol ethyl acetoacetate (1:1), 0.1 g tridecane (internal standard), 3 g nitrobenzene (solvent), catalyst amount has been taken according to substrate to catalyst ratio, Reaction Temp. = 150 ºC, Reaction Time = 2 h)
(Without solvent - 10 mmol m-amino phenol, 20 mmol ethyl acetoacetate (1:2), 0.1 g tridecane (internal standard) catalyst amount has been taken according to substrate to catalyst ratio, Reaction Temperature = 110 ºC, Reaction Time = 15 min)

It was observed that the reaction in presence of nitrobenzene resulted to lower selectivity of the product and slow kinetics. The presence of nitrobenzene resists the reactant molecules to approach the acid sites slowing the kinetics of the reaction. The decrease in the selectivity in the reaction under nitrobenzene may be due to the cleavage of the product, which has been reported to be taking place in polar solvent **[258]**.

5.3.3 Synthesis of 7-hydroxy 4-methyl coumarin

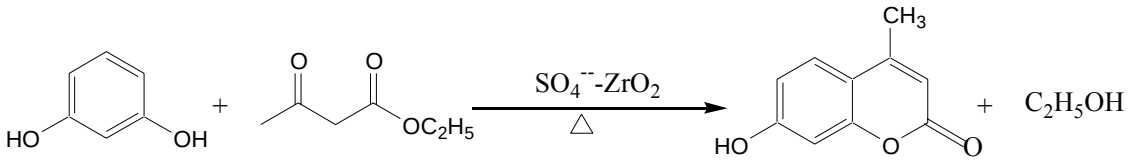

m- hydroxy phenols Ethyl acetoacetate 7-hydroxy 4-methyl coumarin

The synthesis of 7-hydroxy 4-methyl coumarin, using nano-crystalline sulfated-zirconia catalysts, synthesized by one-step and two-step methods, was carried out with nitrobenzene as a solvent as well as in solvent free conditions at 150 ºC for 1 h. All four catalysts showed similar catalytic activity for synthesis of 7-hydroxy 4-methyl coumarin. The yield of 7-hydroxy 4-methyl coumarin was found higher (40- 43 %) in solvent free synthesis than with solvent (21- 24 %) after 1 h (Table 6).

Table 6. Yield (wt.%) of 7-hydroxy 4-methyl coumarin with sulfated-zirconia catalysts, synthesized by one-step and two-step sol-gel methods.

Catalyst	Yield (wt.%)	
	With solvent	**Without solvent**
SZO1	23	42
SZO2 (600)	24	43
SZTB	21	43
SZTN	22	42

(With solvent- 10 mmol m-hydroxy phenol, 10 mmol ethyl acetoacetate (1:1), 3 g nitrobenzene (solvent), 0.1 g catalyst, Reaction Temperature = 150 ºC, Reaction Time = 1 h,
Without solvent- 10 mmol m-hydroxy phenol, 20 mmol ethyl acetoacetate (1:2), 0.1 g catalyst, Reaction Temperature = 150 ºC, Reaction Time = 1 h)

The detail kinetic study and effect of various reaction parameters such as reaction temperature, time, molar ratio of reactants and substrate to catalyst ratio in

nitrobenzene solvent as well as in solvent free condition for the synthesis of 7-hydroxy 4-methyl coumarin was done over SZO2 (600) sample prepared by one-step sol-gel technique.

5.3.3.1 Optimization of reaction temperature and reaction time

The synthesis of 7-hydroxy 4-methyl coumarin was done by carrying out reaction at 150 and 170 ºC for different time ranging from 30 min to 24 h to select the appropriate reaction temperature for achieving maximum yield of 7-hydroxy 4-methyl coumarin. The data (Table 7) show that the synthesis of 7-hydroxy 4-methyl coumarin in presence of nitrobenzene gives yield in the range of 35- 43 % and takes longer time (12-24 h) to achieve maximum yield at 150 and 170 ºC. Whereas the solvent free synthesis of 7-hydroxy 4-methyl coumarin was found to give higher yield (76- 78 %) in comparatively lesser time (3- 6 h).

Table 7. Yield (wt.%) of 7-hydroxy 4-methyl coumarin with solvent and without solvent at 150 and 170 ºC.

Time (hours)	Yield (%)			
	With solvent		Without solvent	
	At 150 ^{o}C	At 170 ^{o}C	At 150 ^{o}C	At 170 ^{o}C
0.5	-	-	-	43
1	24	30	43	72
3	24	32 (15%)*****	56	78
6	27	34	74	77
12	33	38	76	78
18	34	-	74	-
24	35	43	74	-

(With solvent- 10 mmol m-hydroxy phenol, 10 mmol ethyl acetoacetate (1:1), 3 g nitrobenzene (solvent), 0.1 g catalyst)
(Without solvent- 10 mmol m-hydroxy phenol, 20 mmol ethyl acetoacetate (1:2), 0.1 g catalyst)
*(*In presence of toluene as solvent- 10 mmol m-hydroxy phenol, 10 mmol ethyl acetoacetate (1:1), 3 g toluene (solvent), 0.1 g catalyst)*

The higher temperature was observed to decrease the reaction time to achieve maximum yield of 7-hydroxy 4-methyl coumarin in nitrobenzene as well as in solvent free condition. The solvent free synthesis of 7-hydroxy 4-methyl coumarin gives higher

yield (78 %) after 3 h at 170 ºC; therefore, the detail study was carried out at 170 ºC. For the comparison, the detail study of the synthesis of 7-hydroxy 4-methyl coumarin was also done in presence of nitrobenzene at 170 ºC for 3 h. The presence of solvent was found to be affecting the yield of 7-hydroxy 4-methyl coumarin and reaction time.

The synthesis of 7-hydroxy 4-methyl coumarin was also carried out in presence of toluene at 170 ºC to observe the effect of polarity of the solvent on the reaction. The yield of 7-hydroxy 4-methyl coumarin was much low (15 %) after 3 h. The synthesis of 7-hydroxy 4-methyl coumarin in presence of nitrobenzene as well as toluene resulted to lower yield. The lower yield of 7-hydroxy 4-methyl coumarin is associated with the slow rate of reaction in presence of solvent due to inhibitory effect of solvent molecules. The solvent molecules resist the approach of reactant molecules with acid sites slowing the kinetics of the reaction. The effect of solvent on the reaction with sulfated-zirconia is not associated with the polarity of the solvent. Toluene is a non-polar solvent and has been most commonly used in the synthesis of coumarins **[259, 260, 268]**. Polar solvents are reported to result the cleavage of coumarin ring **[258]**.

The study with sulfated-zirconia catalyst showed better results in terms of higher conversion or yield and short reaction time in presence of nitrobenzene, a polar solvent. In solvent free condition, conversion/yield is very high in short reaction time. The presence of toluene should have given higher conversion/yield due to non-polar effect, however, toluene results to lower conversion/ yield. It shows that the polarity of the solvent is not responsible for slow kinetics and lower conversion/yield. The presence of solvent molecules resists the interaction of reactant molecules with the acid sites on the surface resulting to slow reaction with lower yield of 7-hydroxy 4-methyl coumarin. The effect of the nature (polar or non-polar) of a solvent is observed in the reaction, which takes place in solution. However, with sulfated-zirconia, a heterogeneous catalyst, the reaction takes place at the surface by adsorbing the reactant molecules followed by reaction of reactants at the surface in adsorbed form. The mechanistic pathway of coumarin formation with sulfated-zirconia is shown in scheme 2. The reacting species are in adsorbed form on the surface, not free in the solution; therefore, the polarity of solvent has no influence on the reaction. The presence of the solvent delays the approach of the reactants with sites resulting to slow reaction rate and lower yield.

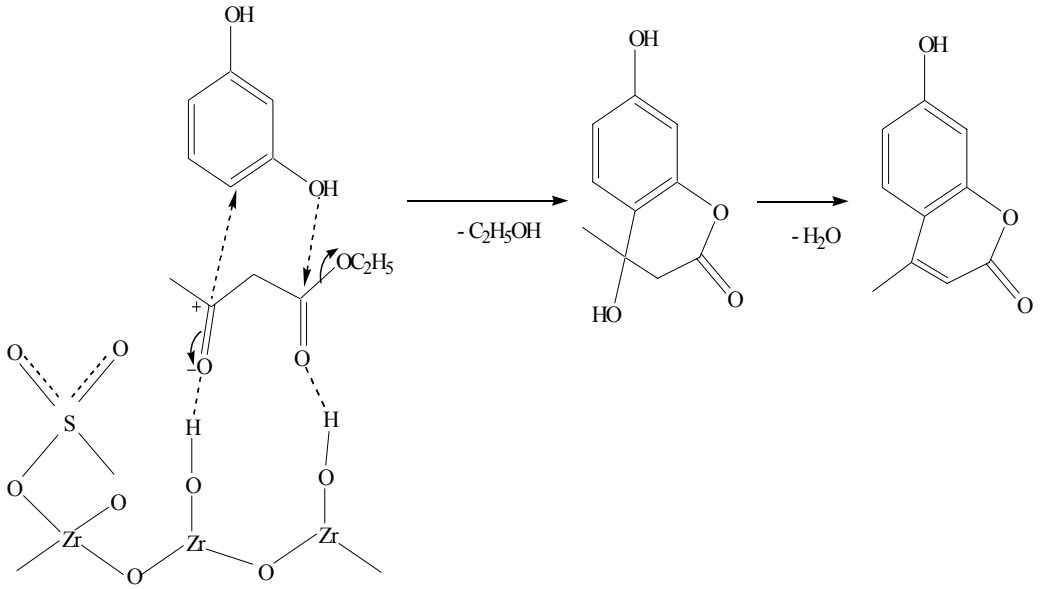

Scheme 2

5.3.3.2 Effect of *m*-hydroxy phenol to ethyl acetoacetate molar ratio

The effect of molar ratio of *m*-hydroxy phenol to ethyl acetoacetate was studied at different molar ratio from 1:1 to 1:3 by carrying out the reaction in presence of solvent as well as in solvent free condition at 170 ºC for 3 h. There was not observed any significant effect of phenol to ester molar ratio on the yield of 7-hydroxy 4-methyl coumarin with solvent (31- 32 %) and also in solvent free condition (76- 78 %) after 3 h (Table 8).

Table 8. Effect of phenol to ester molar ratio on yield (wt.%) of 7-hydroxy 4-methyl coumarin, with solvent and without solvent.

***m*-HP:EAA**	**Yield (%)**	
	With solvent	**Without solvent**
1:1	32	76
1:1.5	31	78
1:2	32	78
1:3	32	77

(With solvent- 10 mmol m-hydroxy phenol, ethyl acetoacetate (according to molar ratio), 3 g nitrobenzene (solvent), 0.1 g catalyst, Reaction temperature = 170 ºC, Reaction time = 3 h,
Without solvent- 10 mmol m-hydroxy phenol, ethyl acetoacetate (according to molar ratio), 0.100 gm catalyst, Reaction temperature = 170 ºC, Reaction time = 3 h)

5.3.3.3 Effect of phenol to catalyst weight ratio

The effect of phenol to catalyst weight ratio on the yield of 7-hydroxy 4-methyl coumarin was studied by carrying out the synthesis at different weight ratio of substrate and catalyst in presence of solvent as well as in solvent free condition at optimized temperature and time i.e., 170 ºC for 3 h. The reaction was carried out at substrate to catalyst ratio ranging from 2 to 80.

In presence of solvent, the yield of 7-hydroxy 4-methyl coumarin was observed to be decreasing with increasing the substrate to catalyst weight ratio (Figure 1). But surprising results were found in case of solvent free synthesis on increasing the substrate to catalyst weight ratio (Figure 1). In solvent free condition, the yield of 7-hydroxy 4-methyl coumarin successively increased from 57 to 94 on increasing the substrate to catalyst ratio from 2 to 80. At the ratio of 80, the yield of 7-hydroxy 4-methyl coumarin was 94%.

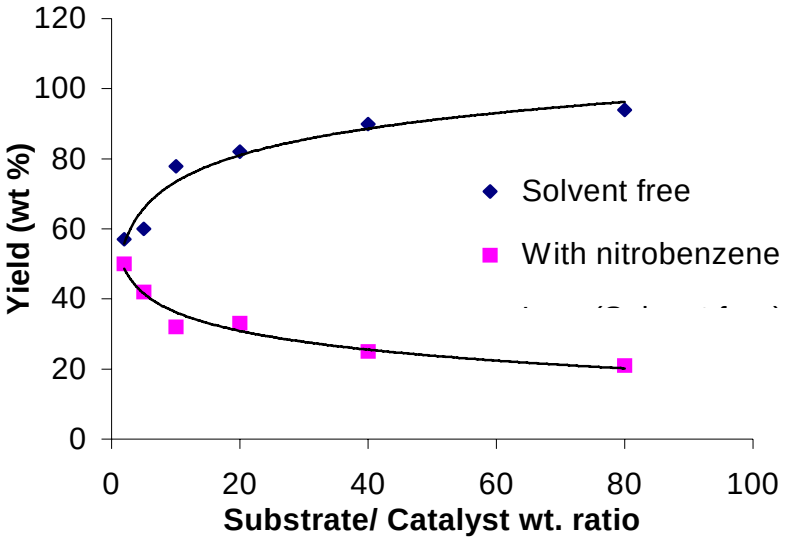

Figure 1. Effect of substrate to catalyst ratio on yield (wt.%) of 7-hydroxy 4-methyl coumarin with nitrobenzene and without solvent.

The increasing trend of the yield of 7-hydroxy 4-methyl coumarin with increase in the substrate to catalyst weight ratio is attributed to better dispersion of the less quantity of the catalyst in the large amount of reaction medium, which provides more catalytic sites to reactant molecules. The presence of solvent suppresses the approach of

reactants to acidic sites, thus lowering the yield of 7-hydroxy 4-methyl coumarin. The use of less catalytic amount of the sulfated-zirconia catalyst giving higher yield (94%) shows the higher activity of the catalyst for Pechmann reaction.

5.3.4 Regeneration of catalyst

The catalyst was thermally regenerated at 450 ºC for 4 h in flow of air in tubular furnace. The regenerated catalyst showed similar conversion/ yield and selectivity as the fresh catalyst for the synthesis of both 7-amino 4-methyl coumarin and 7-hydroxy 4-methyl coumarin. The catalyst did not show any decrease in the catalytic activity till 6th reaction cycle showing similar conversion or yield. FT-IR spectra of regenerated catalyst of both reactions (Figure 2a and 2b) do not show any peak of adsorbed reactants and products on the surface of sulfated-zirconia, which shows that the acid sites of the catalyst are not deactivated.

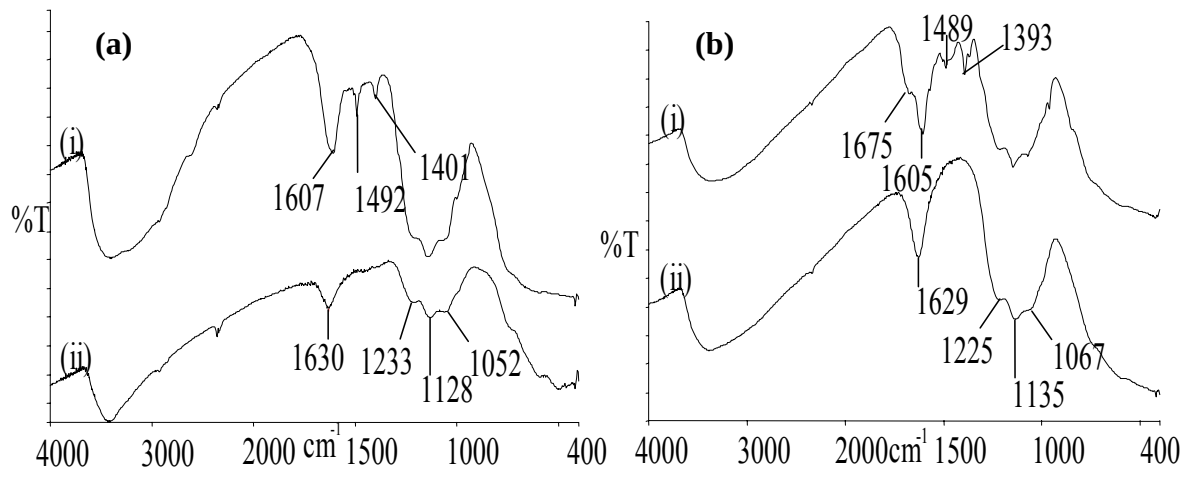

Figure 2. FT-IR spectra of (i) used and (ii) regenerated sulfated-zirconia catalyst, which was separated from reaction mixture of **(a)** 7-amino 4-methyl coumarin and **(b)** 7-hydroxy 4-methyl coumarin.

5.3.5 Microwave assisted synthesis of 7-hydroxy 4-methyl coumarin

Microwave assisted synthesis of 7-hydroxy 4-methyl coumarin using nano-crystalline sulfated-zirconia was carried out by irradiating the reaction mixture of *m*-hydroxy phenol and ethyl acetoacetate (1:2) with microwave (250W) in a microwave reactor at different temperatures ranging from 90 to 170 ºC for 5 to 20 min.

The microwave assisted synthesis of 7-hydroxy 4-methyl coumarin was found to be decreasing the reaction time as well as reaction temperature required to achieve maximum yield of coumarin in comparison to thermal heating. The yield increases with temperature from 110 to 150 ºC (Figure 3), while there is no formation of 7-hydroxy 4-methyl coumarin at lower temperature (90 ºC). Similarly, the yield increases with time from 5 min to 20 min at each temperature (Figure 3). Maximum yield (99%) of 7-hydroxy 4-methyl coumarin was found in 15 min at 150 ºC without any other side product, which was confirmed by GC-MS analysis (Shimadzu GC MS-QP 2010 having Petrocol capillary column of 50 meter length and 0.2 mm diameter with a programmed oven temperature from 40 to 250 ºC, at 1.2 cm^3/min flow rate of He as carrier gas and ion source at 473 K) of the mother liquor.

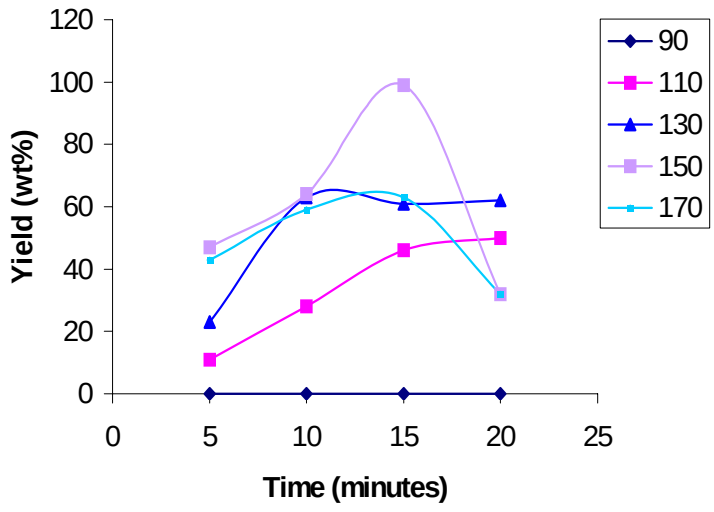

Figure 3. Yield (w%) of 7-hydroxy 4-methyl coumarin with time under solvent free microwave irradiation (250W) at different temperatures.

At higher temperature (170 ºC), the yield is low. Further, the yield of the coumarin was found to be decreased at higher time. The lower yield of 7-hydroxy 4-methyl coumarin at higher temperature and higher reaction time was found to decrease due to formation of side products such as chromones, the products from self condensation of ethyl acetoacetate, isomerization and cleavage of 7-hydroxy 4-methyl coumarin (Figure 4). The formation of these side products was confirmed by GC-MS analysis of the residue remained after separation of the crystals of 7-hydroxy 4-methyl coumarin. The residue was dissolved in dimethyl sulfoxide for GC-MS analysis.

(i) $[M]^+ = 176$

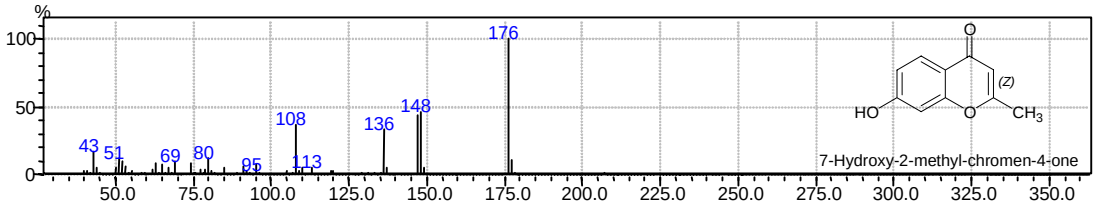

(ii) $[M]^+ = 158$

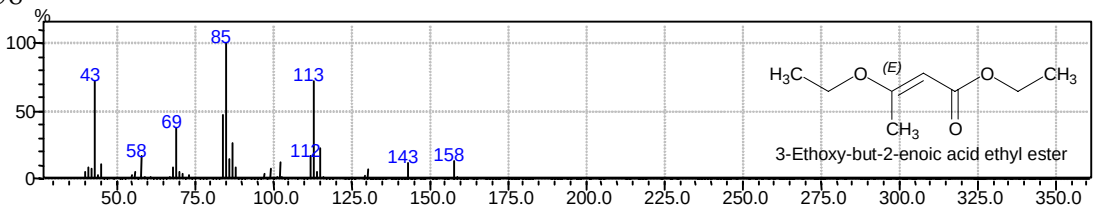

(iii) $[M]^+ = 168$

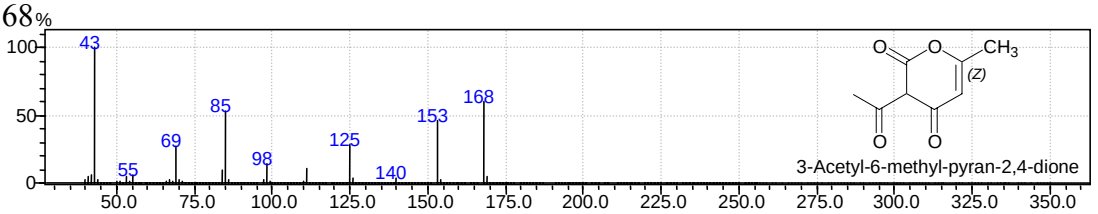

(iv) $[M]^+ = 196$

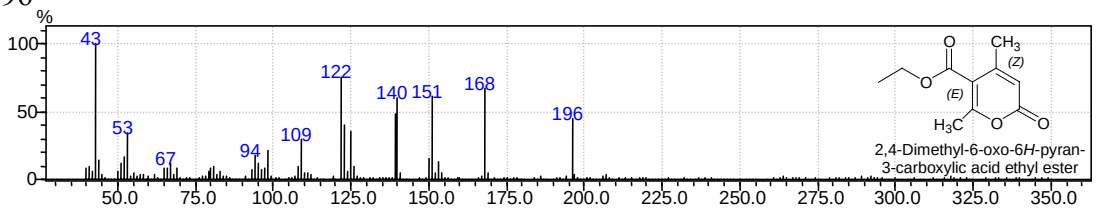

(v) $[M]^+ = 176$

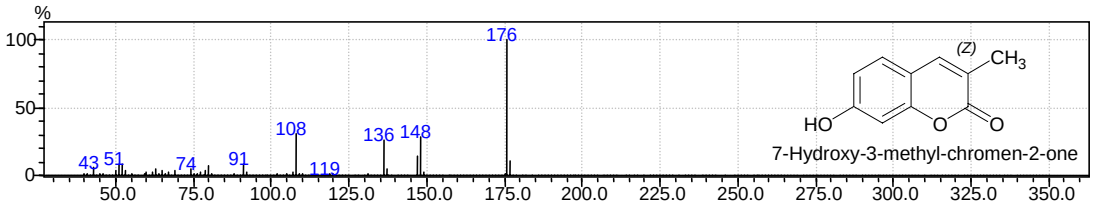

(vi) $[M]^+ = 222$

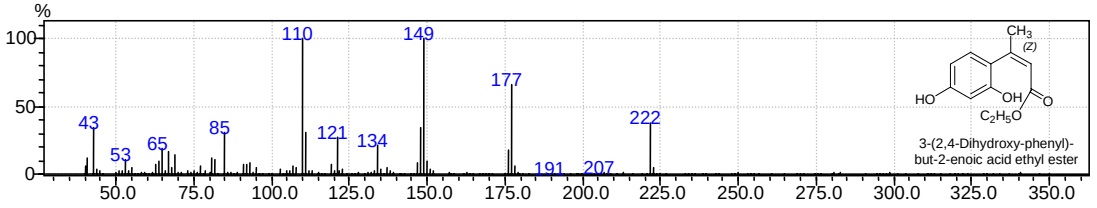

Figure 4. Side products with their $[M]^+$ and mass spectra, formed in microwave assisted synthesis of 7-hydroxy 4-methyl coumarin at higher time and temperature [(i) is Chromone, (ii), (iii) and (iv) are the products formed by self condensation of ethyl acetoacetate, (v) is isomerized product and (vi) is cleaved products from 7-hydroxy 4-methyl coumarin].

5.3.6 Characterization of 7-amino 4-methyl coumarin and 7-hydroxy 4-methyl coumarin

The products (7-amino 4-methyl coumarin and 7-hydroxy 4-methyl coumarin) synthesized were characterized by FTIR (Figure 5), H^1 NMR (Figure 6) and melting point and compared with the literature data reported for known products.

7-amino 4-methyl coumarin:

Melting point: 225-230^oC; IR (KBr): ~3000 cm^{-1} (ν_{NH2}), 1653 cm^{-1} ($\nu_{C=O}$); ^1H NMR (DMSO-d_6): δ 10.06 (s, 2H, -NH_2), 7.49 (d, 1H, ArH), 6.60 (s, 1H, ArH and d, 1H, ArH), 6.14 (s, 1H, C=CH), 2.34 (s, 3H, -CH_3).

7-hydroxy 4-methyl coumarin:

Melting point: 185-190^oC; IR (KBr): 3159 cm^{-1} (ν_{OH}), 1674 cm^{-1} ($\nu_{C=O}$); ^1H NMR (DMSO-d_6): δ 10.54 (s, 1H, -OH), 7.56 (d, 1H, ArH), 6.79 (d, 1H, ArH), 6.72 (s, 1H, ArH), 6.12 (s, 1H, C=CH), 2.36 (s, 3H, -CH_3).

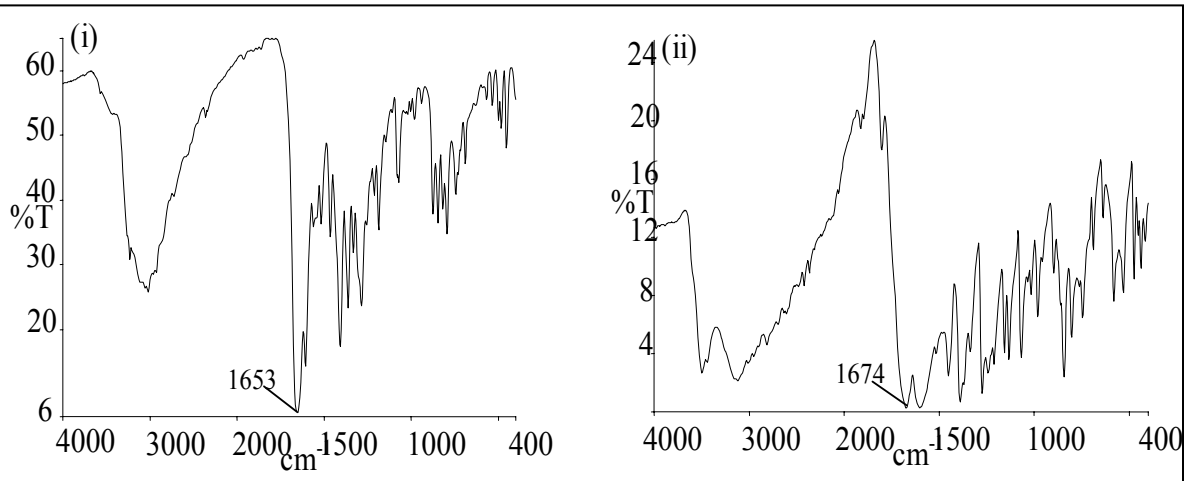

Figure 5. FT-IR spectra of (i) 7-amino 4-methyl coumarin and (ii) 7-hydroxy 4-methyl coumarin.

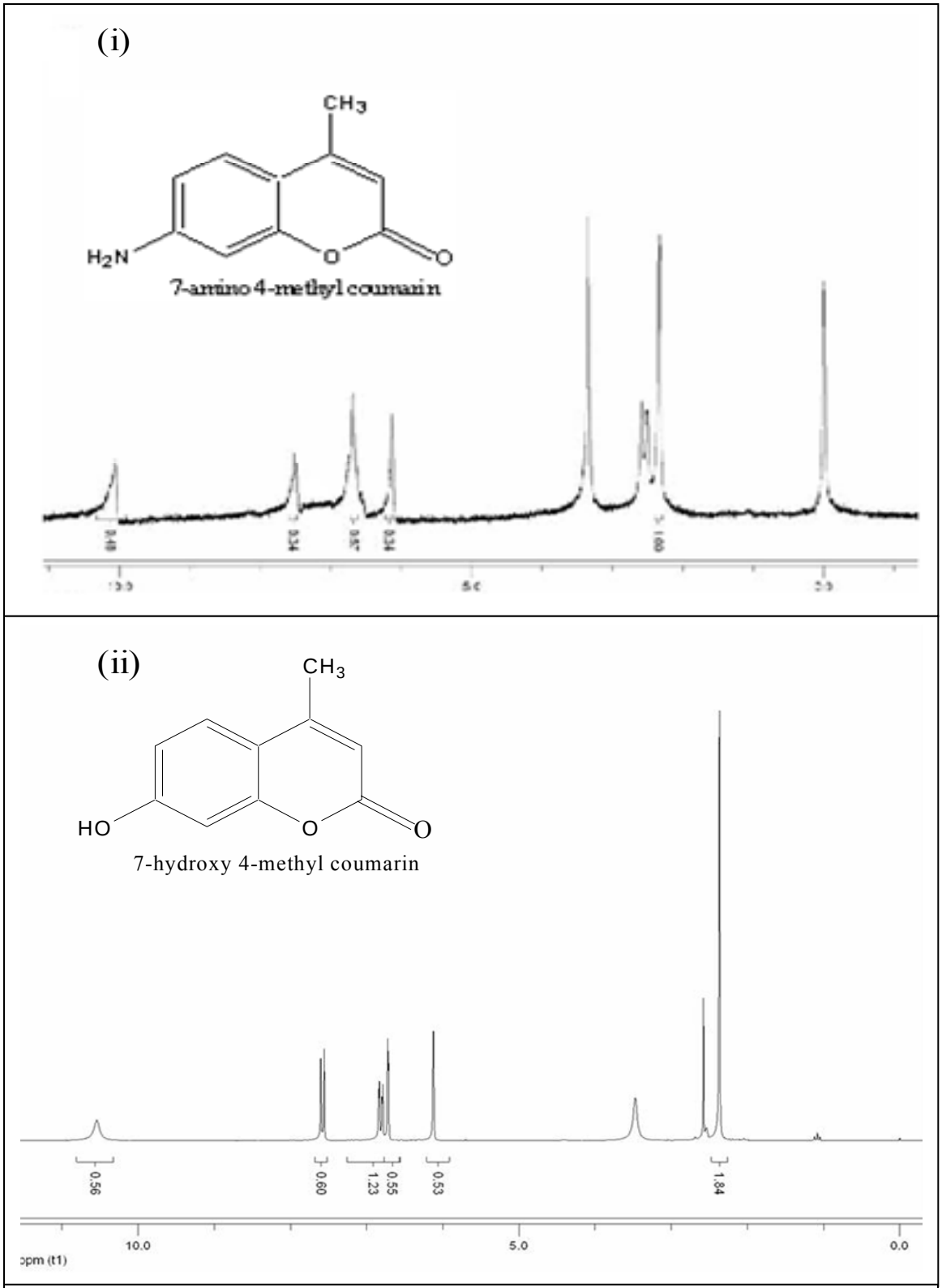

Figure 6. ^{1}H-NMR spectra of (i) 7-amino 4-methyl coumarin and (ii) 7-hydroxy 4-methyl coumarin.

5.4 Conclusions

The nano-crystalline sulfated-zirconia catalysts, synthesized by one-step and two-step sol-gel methods, are highly active solid acid catalyst for Pechmann reaction to synthesize 7-substituted 4-methyl coumarins with excellent yield and purity replacing the use of the conventional homogenous acids. The *m*-amino phenol is more reactive towards Pechmann reaction catalyzed by sulfated-zirconia catalyst than *m*-hydroxy phenol. For synthesis of 7-amino 4-methyl coumarin, the sulfated-zirconia catalyst gives 100 % conversion with ~ 100 % selectivity in presence of nitrobenzene as well as in solvent free condition. However, in solvent free condition, the reaction is very fast showing complete conversion at comparatively lower temperature within 2 min. For 7-hydroxy 4-methyl coumarin, the yield is less and takes longer time to attain maximum yield in presence of solvent. However, solvent free synthesis results higher yield and takes less time to achieve maximum yield. The use of very small catalytic amount of sulfated-zirconia catalyst for the synthesis of 7-amino 4-methyl coumarin and 7-hydroxy 4-methyl coumarin and the reusability of the sulfated-zirconia catalyst after simple activation for several times with similar activity are advantageous properties of the catalyst. The solvent free microwave assisted synthesis of 7-hydroxy 4-methyl coumarin is efficient way of synthesis giving excellent yield decreasing the reaction time as compared to thermal heating.

Summary and Conclusions

Acid catalysis is an important area in organic synthesis and is of fundamental industrial importance. The acid catalyzed reactions are largely carried out by using homogeneous liquid acids like HF, H_2SO_4, $AlCl_3$ and $FeCl_3$ etc. These homogeneous catalysts, however, have some disadvantages such as they are required in more than stoichiometric amount to attain maximum conversion, corrosive to reaction system and a very careful handling is required, not recoverable from reaction mixture and thus not reusable. After reaction, either they form complex molecule with product or they are highly soluble in reaction mixture resulting into the hazardous waste influent. This also leads to the formation of hazardous inorganic acids as by-products. The disadvantages of homogeneous catalysts, environmental restrictions and requirement of non-polluting, atom-efficient and economic catalytic process inspired the need to find the alternative of the liquid acids.

Solid acids were found to be alternative to the homogeneous acids as they are non-corrosive, required in small catalytic amount, easy to separate, reuse and eco friendly. Solid acid catalysts such as transition metal oxides when treated with sulfuric acid showed enhanced acidity than their pure oxides. Among the various transition metal oxides **Sulfated Zirconia** is a well-known solid super acid ($-H_0$ = 16.1) having both Bronsted as well as the Lewis acid sites (Figure 1) on its surface. The sulfate species are bonded with zirconium atom as bidentate chelating ligand and in presence of water molecule the sulfate group behaves like ionic sulfate and generates Bronsted acid sites on the surface. The desorption of water molecule converts the ionic sulfate to covalently bonded sulfate group, which generates Lewis acid sites on zirconium atom by reducing the electronic density at zirconium atom. The required site can be predominantly populated by changing the reaction conditions, so it is capable to conduct both Bronsted and Lewis acid catalyzed reactions.

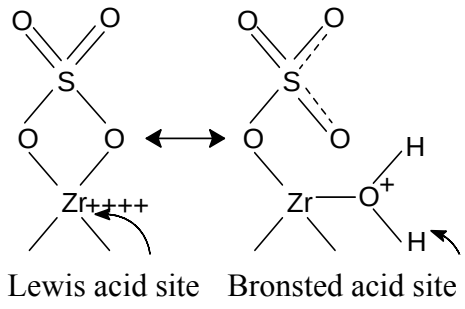

Figure 1. The Bronsted and Lewis sites on the surface of the sulfated-zirconia.

Furthermore, nano-crystalline materials have improved catalytic activity because of large surface-to-volume ratio and also more corners and edges, which provides increased number of active sites available for a catalytic reaction.

Therefore, in view of above, the present thesis is focused on the synthesis and characterization of nano-crystalline sulfated-zirconia solid acid catalyst and its catalytic application for various organic transformations such as benzylation, acylation, isomerization and Pechmann reaction. The work done in the present thesis is summarized as below:

Nano-crystalline sulfated-zirconia solid acid catalyst was synthesized using one-step and two-step sol-gel techniques using zirconium propoxide as a precursor, water and/or aqueous ammonia as hydrolyzing agent and concentrated H_2SO_4 (1N) as sulfating agent. A number of samples have been synthesized with varying synthetic parameters such as concentration of precursor, mode of physical perturbation, drying temperature, the way of addition of sulfuric acid in alkoxide solution, water to alkoxide molar ratio, pH of the synthesis medium during hydrolysis and calcination temperature. The effect of various synthetic parameters was correlated with the structural, textural and catalytic properties of sulfated-zirconia catalysts.

The samples were characterized by X-ray Powder Diffraction study, FT-IR Spectroscopy, DRIFT study, FT-IR study of the samples adsorbed with pyridine, N_2 adsorption-desorption isotherm study, CHNS/O elemental analyzer and ICP (Inductive Couple Plasma) for Sulfur Analysis. The identification of crystalline phase and the measurement of the crystallite size of the phase in sulfated-zirconia samples were carried out by X-ray Powder Diffraction study using Scherrer formula. The nature of surface sulfates in the samples was studied by FT-IR spectroscopic study. The Lewis acidity in the samples was quantified by DRIFT study and the Bronsted and Lewis acidity were measured by FT-IR study of the samples adsorbed with pyridine at different temperatures from 150 to 450 ºC. The textural properties such as surface area, pore volume, pore size and pore size distribution of the sulfated-zirconia samples were characterized by N_2 adsorption-desorption isotherm study at liquid nitrogen temperature (77K). The Bronsted acidity of the samples was also assessed by dehydration of cyclohexanol to cyclohexene as a model test reaction. The catalytic evaluation of the sulfated-zirconia samples was

done for various acid catalyzed organic transformations such as benzylation, acylation, isomerization and Pechmann reaction.

Both one step as well as two-step sol-gel techniques were found to be an appropriate route to synthesize nano-crystalline zirconia and sulfated-zirconia having crystallite size in range of 10- 17 nm having predominantly tetragonal crystalline phase.

During the two-step sol-gel technique the zirconium hydroxide gel formed after the hydrolysis and condensation of zirconium propoxide precursor and dried at 110 ºC was found to be amorphous in nature. The crystallinity was developed on thermal treatment at higher temperatures. The zirconia gel, after calcination at 400 ºC, was observed to be crystalline having purely tetragonal phase and crystallite size of 13 nm. Calcination at higher temperatures results into the transformation of tetragonal to monoclinic crystalline phase and also increase in the crystallite size of tetragonal phase. The crystallite size of tetragonal phase of pure zirconia samples (ZrO_2) increases progressively from 13 to 23 nm with an increase in calcination temperature (400- 600 ºC), which shows the sintering of zirconia crystallites with temperature forming larger crystallites. The monoclinic phase gradually increased from 4 to 29 % with an increase in the calcination temperature from 450 to 600 ºC. The transformation of tetragonal to monoclinic phase occurs due to the loss of hydroxyl groups by the dehydroxylation.

The sulfated zirconium hydroxide sample, calcined at 450 ºC, was amorphous. The samples, calcined at 500 ºC, were crystalline and had predominantly the tetragonal phase. With increase of calcination temperature, the monoclinic phase started to increase. In sulfated-zirconia, crystallization of an amorphous sample to a crystalline phase occurs at higher temperature (450 ºC) than that of pure sample (400 ºC). The reason of increase in crystallization temperature in sulfated-zirconia samples is the presence of SO_4^{--} ions, which requires higher thermal energy for the removal of hydroxyl groups for dehydroxylation during crystallization. Dehydroxylation of the amorphous phase at 500 ºC generated mainly tetragonal zirconia. The transformation of tetragonal to monoclinic phase in sulfated-zirconia samples has been found at higher temperature, which is attributed to the presence of sulfate groups resisting the dehydroxylation of the sample.

The effect of synthetic parameters such as physical perturbation during the hydrolysis and condensation of the precursor and drying temperature for the gel showed

remarkable effect on the formation of crystalline phase and crystallinity of the phase. The sulfated-zirconia samples, prepared using sonication, shows the presence of predominantly tetragonal phase even after calcination at 600 ºC. While, at same calcination temperature (600 ºC), the samples prepared using magnetic stirring, shows monoclinic phase also (22 %) along with tetragonal phase. The higher thermal stability of the tetragonal phase in samples prepared using ultrasonication as compared to conventional stirring probably is due to higher loading and proper dispersion of sulfate ions on zirconium oxide surface during ultrasonication, which is also confirmed by a higher sulfur content retained (0.78- 1.91 wt.%) in these samples. The duration of ultrasonication was also found to be affecting the sulfur loading. In the samples, prepared by ultrasonication, the retained sulfur after calcination increased from 0.78 to 1.77 wt.% with increasing the ultrasonication time from 30 to 120 min keeping other conditions same.

Effect of drying temperature of gel, before calcination, was also found to be affecting the calcination temperature and formation of phase. The samples initially dried, before calcination, at 80 or 110 ºC have only tetragonal phase after calcination at 600 ºC, whereas the sample initially dried at room temperature, showed predominantly a monoclinic phase (89 %) after calcination at 600 ºC. The drying of gel at room temperature could not remove the solvent (*n*-propanol) completely, which is present with precursor and also formed during the hydrolysis of the alkoxide. The presence of *n*-propanol filled inside the gel pores affected sulfate loading, as sulfate ions could not go inside the pores during the sulfation process and therefore, forms the monoclinic phase at lower calcination temperature.

The surface sulfates species in the prepared sulfated-zirconia samples were found to be present as inorganic chelating bidentate sulfate groups on the surface of zirconia. The presence of water molecules adsorbed

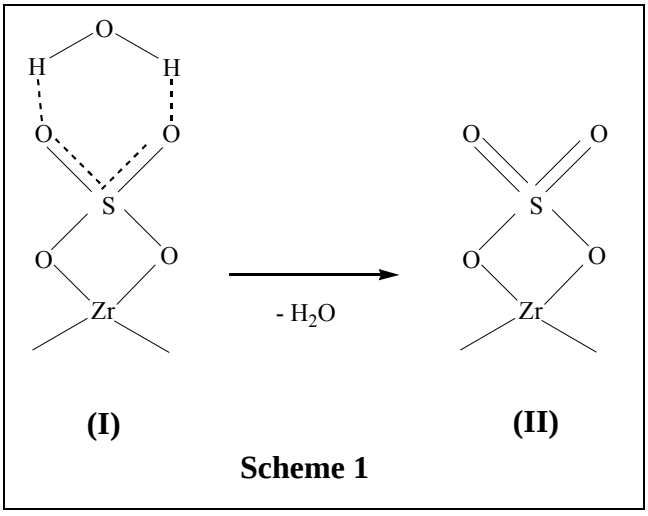

Scheme 1

with surface sulfates by hydrogen bonding gives the ionic form (I). The desorption of water molecule converts the ionic sulfate to covalently bonded sulfate having S=O double bonds, which is evident from the presence of a weak to medium band at around 1401 cm^{-1}, attributed to asymmetric stretching ($\nu_{S=O}$) of S=O double bond. This structure (II) is responsible for the formation of the Lewis acid sites on the surface by attracting the electron density from the zirconium atom (Scheme 1). The peak area of the $\nu_{S=O}$ band (~1400 cm^{-1}) was used to quantify the amount of Lewis acidity of the sample, which gradually increases on *in-situ* heating from 150 ºC to 450 ºC and shows the sensitivity of sulfated-zirconia samples towards moisture.

The total sulfur content was correlated with covalently bonded sulfur, which represents Lewis acid sites and quantified by peak area of the $\nu_{S=O}$ band, which shows that the samples having < 1.0 wt.% sulfur content (< 0.8 S atoms/ nm^2) have higher Lewis acid sites, whereas the samples with 1.0- 2.0 wt.% or > 2.0 wt.% sulfur content (> 0.8 S atoms/ nm^2) have less Lewis acid sites and higher Bronsted acid sites.

The catalytic activity of the sulfated zirconia samples was tested by carrying out the benzylation of toluene with benzyl chloride in liquid phase batch reactor taking toluene and benzyl chloride in 1:1 molar ratio, substrate to catalyst weight ratio of 10 at 450 ºC for 2 h. The sample, synthesized by ultrasonication method showed higher catalytic activity giving maximum conversion of toluene (68 %) after 4 h with 100 % selectivity of the *p*-benzyl toluene. The higher catalytic activity of the sample is attributed to higher sulfur content (1.91 wt.% or 1.4 S atoms/ nm^2) in the sample, which results to higher Bronsted acid sites. However, the concentration of the precursor used for the synthesis of sulfated-zirconia, was also observed to be affecting the activity of the samples. The samples, synthesized by using higher concentration (70 wt.%) of the precursor showed higher activity (61- 68 %) in comparison to samples prepared by using a lower (10 wt.%) concentration of the precursor (17- 53 % conversion). The catalytic activity of the sulfated zirconia samples increases with increasing total sulfur content of the sample, which is attributed to the increase in Bronsted acidity.

During the one-step sol-gel technique the synthetic parameters such as the way of addition of sulfuric acid in alkoxide, water to alkoxide molar ratio, and calcination

temperature were observed to influence the physicochemical and catalytic properties of the sulfated-zirconia catalysts.

By one-step sol-gel method, three samples were synthesized. One sample (SZO1) was synthesized by adding sulfuric acid and water mixture (water to alkoxide molar ratio = 4) to zirconium propoxide precursor to hydrolyze the zirconium propoxide to zirconium hydroxide. The gel was dried and calcined at 600 ºC for 2 h in static air atmosphere. The second sample (SZO2) was synthesized by adding concentrated sulfuric acid in zirconium propoxide followed by addition of distilled water (water to alkoxide molar ratio = 4) to hydrolyze the zirconium propoxide to zirconium hydroxide. The gel was dried and calcined at 600 ºC for 2 h in static air atmosphere. The third sample (SZO2-600) was synthesized by following the similar procedure as used for the synthesis of second sample, however, by using lesser quantity of water (water to alkoxide molar ratio = 2.7) just sufficient to form the gel. The sample was further calcined at higher temperatures of 700 and 800 ºC for 2 h in static air atmosphere to study the effect of calcination temperature on the structural, textural and catalytic properties of the sample.

The X-Ray Diffraction study of sulfated-zirconia samples calcined at 600 ºC show the presence of purely tetragonal crystalline phase in all samples. The sample (SZO2-600) was observed to be less crystalline after calcination at 600 ºC and the crystallinity of the sample increases with increasing the calcination temperature from 600 to 800 ºC. However, only tetragonal crystalline phase was observed even after calcination at 800 ºC. The less crystalline nature of this sample was observed to be related to higher sulfur content (3 wt.%). The sulfate ions attached with hydroxyl groups resist the crystallization process. The higher thermal energy is required for the removal of hydroxyl groups for crystallization. It results into increase in calcination temperature required for crystallization. The crystallite size of this sample increases from 9 to 14 nm with increase of calcination temperature from 600 to 800 ºC.

The sulfated-zirconia samples, calcined at 500- 600 ºC, are mesoporous in nature as they show isotherms of type IV with hysteresis of H2 or H3 type. The crystalline sulfated-zirconia samples show higher surface area (71- 116 m^2/g) than amorphous sulfated-zirconia (25- 41 m^2/g) and pure zirconia (6- 9 m^2/g). The surface area increases with increasing calcination temperature but after certain calcination temperature

it decreases, which may be due to sintering of pores at higher temperature. The pore size distribution in all the samples was found to be broad, ranging from 20 to 100 Å.

Among the one-step and two-step sol-gel method, sulfated zirconia samples prepared by one-step method were observed to have better structural and textural properties in terms of lower crystallite size, higher sulfur loading, higher surface area , pore volume and pore size as compared to the samples synthesized by two-step sol-gel method. Further, among the samples prepared by one-step method, the sulfated zirconia sample (SZO2-600) showed maximum surface area (150 m^2/g), pore volume (0.33 cm^3/g) and pore size (89 Å). The surface area of the sample decreases with increasing calcination temperature (600 to 800 ºC) due to increase of crystallite size and sintering but the pore volume increased due to formation of larger pores due to collapse of micropores.

The sulfated-zirconia catalysts are having higher Bronsted acidity as they were found highly active for dehydration of cyclohexanol to cyclohexene giving conversion of cyclohexanol from 78- 100 % with ~100 % selectivity of cyclohexene, however, the method of activation (in air or nitrogen atmosphere) plays an important role in order to attain maximum activity.

The nano-crystalline sulfated-zirconia samples, synthesized by one-step and two-step sol-gel methods, were found active for acylation reaction showing the conversion of anisole and veratrole in the range of 25- 36 % and 29- 42 % respectively at 110 ºC after 3 h, with substrate to catalyst weight ratio of 10. The sample, synthesized by two-step sol-gel method in alkaline medium, showed higher conversion of anisole (36 %) and veratrole (42 %).

The conversion of anisole and veratrole was found to be significantly increased from 19 to 35 % and 22 to 60 % respectively at 110 ºC after 3 h with increase of calcination temperature from 600- 700 ºC, which was observed to be dependent of the sulfur content. However, the sample, calcined at higher temperature (800 ºC) showed the decrease in the conversion of both anisole and veratrole due to very less sulfur content (0.6 wt.%) in the sample, which generates less and very weak Bronsted and Lewis acid sites. The optimum amount of sulfur (~1 wt.%) is required to generate reasonable amount

of stronger Bronsted and Lewis sites and thus higher catalytic activity of the sulfated-zirconia.

The conversion of anisole as well as veratrole was also found to be gradually increased with increase in reaction temperature and showed maximum conversion of anisole (46 %) and veratrole (60 %) at 150 ºC after 3 h, while selectivity remained constant.

The time study of the reaction showed that the acylation reaction is very fast with sulfated-zirconia catalyst. The maximum conversion of anisole was achieved within 30 min. with 46 % conversion and 98 % selectivity of 4-methoxy acetophenone while veratrole showed maximum conversion (60 %) within 10 min. with 100 % selectivity of 3, 4-dimethoxy acetophenone.

With decreasing the substrate to catalyst weight ratio from 10 to 5, the conversion of anisole and veratrole was increased from 32 to 52 % after 1 h and 48 to 66% after 30 minutes respectively at 150 ºC, while the selectivity of the acylated products remains steady.

The spent catalyst can be easily regenerated by simple thermal treatment showing similar activity and selectivity for the desired product of acylation of anisole and veratrole as fresh catalyst.

The nano-crystalline sulfated-zirconia catalysts, synthesized by one-step and two-step sol-gel methods, were studied for solvent free single step isomerization of longifolene to isolongifolene. The isomerization of longifolene to isolongifolene is an important reaction finding applications as perfumery agent and intermediate compound for the synthesis of other perfumery chemicals. The sulfated-zirconia catalysts were found potential for selective isomerization of longifolene to isolongifolene with higher catalytic conversion in range of 90- 93 % with ~100 % selectivity of isolongifolene, within 15 min at 180 ºC by using small catalytic amount (0.1 g catalyst/ 10 g longifolene) of the catalyst. Kinetic study shows that the maximum conversion and selectivity for isolongifolene was achieved within 15 min of the reaction after that it remains steady till 360 min.

The effect of substrate to catalyst weight ratio on isomerization of longifolene to isolongifolene was carried out at different substrate to catalyst ratio ranging from 10 to

100 at 180 ºC for 1 h. The conversion of longifolene to isolongifolene is in similar range (93- 95 %) with ~ 100 % selectivity of isolongifolene till substrate to catalyst weight ratio of 100 after 1 h. It shows that sulfated-zirconia catalyst is highly active catalyst for isomerization of longifolene and the minimal catalytic amount is sufficient to obtain maximum conversion.

Isomerization of longifolene was also carried out at large scale of 100, 500 and 1000 gm in large volume liquid phase reactor taking substrate to catalyst ratio of 100 at 180 ºC for 6 h. The conversion of longifolene in all three batches was found to be 95 % with ~100 % selectivity of isolongifolene.

The catalyst was easily regenerated by simple thermal regeneration and reused for several reaction cycles (10^{th}) with similar activity as fresh catalyst. Isomerisation of longifolene was found a Bronsted acid catalyzed reaction.

The sulfated-zirconia catalysts having optimum sulfur content (1.3- 1.6 wt.%, after calcination at 600 ºC) showed selectivity (~100 %) isolongifolene from the isomerization of longifolene, however, one of the catalyst (SZO2-600) having higher sulfur content (3 wt.%) resulted further isomerization of isolongifolene to tetraline derivative (7-isopropyl 1, 1-dimethyl tetraline) and other products. The further isomerization of isolongifolene is an acid catalyzed reaction, reported to be carried out under excess acidic condition. The catalyst SZO2-600 showed 92 % conversion of longifolene with ~3 % selectivity of isolongifolene, 56 % selectivity of tetraline derivative and 41 % of other products at 180 ºC for 1 h. The catalyst SZO2-700, calcined at 700 ºC, showed the increase in the selectivity of isolongifolene to 37 % and the selectivity of tetraline derivative and other products decreased to 25 % and 38 % respectively. The catalyst SZO2-800, calcined at 800 ºC, showed further increase in the selectivity of isolongifolene ~100 % and tetraline derivative and other products were not observed to be formed. Calcination at higher temperature (700 ºC) decreased the sulfur content (1.1 wt.%) reducing the number and strength of Bronsted acid sites and therefore, the formation of tetraline derivative was decreased. The calcination at further higher temperature (800 ºC) significantly reduced the sulfur content (0.6 wt.%) generating less number of acid sites that are not sufficient for further isomerization of isolongifolene.

The kinetic study of the isomerization of longifolene to isolongifolene and further to tetraline derivative (taking substrate to catalyst ratio of 10 at 180 ºC) showed that the maximum conversion of longifolene (96 %) and selectivity of isolongifolene (~100 %) were obtained within 2 minutes of the reaction time. After 2 minutes, the selectivity of isolongifolene was observed to be successively decreasing with time and the selectivity of tetraline derivative and other products gradually increased giving ~56 % tetraline derivative and ~41 % other products with small amount (~3 %) of isolongifolene after 1 h. The selectivity of tetraline derivative, other products and isolongifolene remains constant up to 4 h. The kinetic study clearly shows that longifolene initially isomerizes to isolongifolene and then further to tetraline derivative along with other products, which was also confirmed by recording ^{1}H NMR spectra of the reaction mixture after 1 minute, 10 minutes and 1 h.

The regenerated catalyst has similar activity for isomerization of longifolene to isolongifolene; however, the selectivity of the products varies showing the decrease in the selectivity of tetraline derivative.

The nano-crystalline sulfated-zirconia catalysts, synthesized by one-step and two-step sol-gel methods, were found highly active solid acid catalyst for the synthesis of 7-amino 4- methyl coumarin and 7-hydroxy 4-methyl coumarin by acid catalyzed Pechmann reaction replacing the use of the conventional homogenous acids. 7-substituted 4-methyl coumarins such as 7-hydroxy 4-methyl coumarin (β-methylumbelliferone) and 7-amino–4-methyl coumarin are important coumarins finding applications as fluorescent brightener, efficient laser dye, standard for fluorometric determination of enzymatic activity, synthesis of insecticides, as precursor for furano coumarins and many other derivatives of substituted coumarins.

The sulfated-zirconia catalysts showed excellent conversion or yield for the synthesis of 7-substituted 4-methyl coumarins in solvent and solvent free conditions. The *m*-amino phenol is more reactive towards Pechmann reaction. The catalysts, synthesized by one-step and two-step sol-gel methods, were found highly active for synthesis of 7-amino 4-methyl coumarin and similar in activity showing 100 % conversion with ~100 % selectivity of 7-amino 4-methyl coumarin at 150 ºC after 1 h in presence of solvent as well as in solvent free condition. Solvent free synthesis of 7-amino 4-methyl coumarin

gives 100 % conversion with 100 % selectivity of 7-amino 4-methyl coumarin at comparatively low temperature, i.e., 110 ºC within 2 minutes. The presence of solvent was observed to be slowing the kinetics and lowering the selectivity in presence of polar solvent.

The yield of 7-hydroxy 4-methyl coumarin was found higher (40- 43 %) in solvent free synthesis than with solvent (21- 24 %) at 150 ºC after 1 h. The synthesis of 7-hydroxy 4-methyl coumarin in presence of solvent gives low yield (43 %) at higher temperature (170 ºC) after 24 h. Solvent free synthesis of 7-hydroxy 4-methyl coumarin gives higher yield (78 %) at 170 ºC within 3 h. The lower yield in presence of solvent is attributed to inhibitory effect of the solvent molecule, resisting the approach of reactant molecules with acid sites. The nature of solvent i.e., polarity, does not affect the reaction but makes the reaction slower due to the resisting effect of solvent molecules. In presence of solvent, the yield of 7-hydroxy 4-methyl coumarin was observed to be decreasing with increasing the substrate to catalyst weight ratio, but in solvent free synthesis, the yield of 7-hydroxy 4-methyl coumarin successively increases from 57 to 94 on increasing the substrate to catalyst ratio from 2 to 80. The maximum yield of 7- hydroxy 4-methyl coumarin under solvent free condition is 94 % at optimized reaction conditions (at 170 ºC for 3 h) using substrate to catalyst weight ratio of 80. The use of very small catalytic amount of sulfated-zirconia catalyst for the synthesis of coumarins and the reusability of the sulfated-zirconia catalyst after simple activation for several times with similar activity are advantageous properties of the catalyst. The solvent free microwave assisted synthesis of 7-hydroxy 4-methyl coumarin was found more effective way of coumarin synthesis giving excellent yield (99 %) decreasing the reaction time (15 minutes) compare to thermal heating.

- The present study shows that the sulfated-zirconia is highly active solid acid catalyst for acid catalyzed organic transformations such as benzylation of toluene, acylation of anisole and veratrole, isomerization of longifolene and for synthesis of 7-hydroxy 4-methyl coumarins by Pechmann reaction.
- The use in small catalytic amount, fast reaction kinetics, easy separation from reaction mixture and simple regeneration method with retention of

catalytic activity after several reaction cycles makes the sulfated-zirconia an efficient heterogeneous catalyst of industrial application. However, the catalytic activity of sulfated-zirconia was observed to be affected by the method of synthesis and synthetic parameters. The different synthetic parameters of sol-gel technique were observed to be affecting the structural, textural and acidic properties and therefore, the catalytic activity of the catalyst.

- The presence of both type of acidity, i. e., Bronsted and Lewis, in the sulfated-zirconia provides a wide scope of application in Bronsted and Lewis acid catalyzed organic transformations.
- The higher Bronsted acidity of the sulfated-zirconia catalyst shows higher activity for Bronsted acid catalyzed reactions.
- The sulfated-zirconia can also be applied for several other acid catalyzed reactions such as electrophilic addition reactions, cycloaddition reactions, cyclization reactions, etc. giving valuable products to replace the conventional homogeneous acid catalysts.

References

[1] G. Heinrich, M. Valais, M. Passot, B. Chapotel, 13th World Pet. Congress, Buenos Airs, October 20–25, 1991.

[2] http://en.wekipedia.org/polymerization.

[3] H. Hennell, Philosophical Transaction, 118 (1828) 365.

[4] J. E. Lodgsdon "Ethanol" In J. I. Kroschmitz (Ed.) Encyclopedia of Chemical Technology, New York: John Wiley & Sons, 4th ed. Vol. 9, p. 820.

[5] http://www.britannica.com/eb/article-49254/acidbasereaction.

[6] I. V. Kozhevinikov, In Catalysts for Fine Chemical Synthesis, vol. 2, Catalysis by Polyoxometalates (2002) Culinary and Hospitality Industry Publication Services.

[7] J. A. Horseley, CHEMTECH (1997) 45.

[8] Bauer, D. Garbe, H. Surburg, Common Fragrance and Flavor Materials, VCH Verlagsgesellschaft, Weinheim, 1990, p. 83.

[9] P. H. Gore, In: G.A. Olah Ed., Friedel Crafts and Related Reactions, Vol. III, Wiley Interscience, New York, 1964, p.64.

[10] (a) M. Hino, S. Kobayashi, K. Arata, J. Am. Chem. Soc. 101 (1979) 6439, (b) K. Tanabe, W. F. Holderich, Appl. Catal. A: Gen. 181 (1999) 399.

[11] T. Yamaguchi, Appl. Catal. A: Gen. 61 (1990) 1.

[12] G. A. Olah, G. K. S. Prakash, J. Sommer, Superacids, Wiley, New York, 1985.

[13] K. Arata, H. Matsuhashi, M. Hino, H. Nakamura, Catal. Today, 81 (2003) 17.

[14] K. Arata, Appl. Catal. A: Gen. 146 (1996) 3.

[15] K. Sayama, H. Arakawa, J. Phys. Chem. 97 (1993) 531.

[16] Bo-Q. Xu, Shi-B. Cheng, S. Jiang, Qi-M. Zhu, App. Catal. A: Gen. 188 (1999) 361.

[17] J. R. Sohn, S. G. Ryut, Langmuir, 9 (1993) 126.

[18] Wei-P. Dow, Ta-J. Huang, J. Catal. 160 (1996) 171.

[19] http://www.accuratus.com/zirc.html.

[20] S. Somiya, N. Yamamoto, H. Yanagina (Eds.), Advances in Ceramics, vols. 24A and 24B, American Ceramic Society, Westerville, OH, 1988.

[21] C. Piconi, G. Maccauro, Biomaterials, 20 (1999) 1.

[22] N. Q. Minh, J. Am. Ceram. Soc. 76 (1993) 563.

[23] T. Habino, A. Hashimoto, S. Kakimoto, M. Sano, J. Electrochem. Soc. 148 (2001) H1.

[24] V. Fiorentini, G. Gulleri, Phys. Rev. Lett. 89, 266101 (2002) 4.

[25] M. Ozawa, J. Alloys Compd. 275-277 (1998) 886.

[26] A. Khodakov, J. Yang, S. Su, E. Iglesia, A. T. Bell, J. Catal. 177 (1998) 343.

[27] M. E. Manriquez, T. Lopez, R. Gomez, J. Navarrete, J. Mol. Catal. A: Chem. 220 (2004) 229.

[28] C. Palazzi, L. Oliva, M. Signoretto, G. Strukul, J. Catal. 194 (2000) 286.

[29] W. Sun, L. Xu, Y. Chu, W. Shi, J. Coll. Inter. Sci. 266 (2003) 99.

[30] Y. Sun, P. A. Sermon, Catal. Lett. 29 (1994) 361.

[31] J. A. Anderson, M. M. Khader, J. Mol. Catal. A: Chem. 105 (1996) 175.

[32] Y. Okamoto, H. Gotoh, Catal. Today, 36 (1997) 71.

[33] K. Shimizu, T. N. Venkatraman, W. Song, Appl. Catal. A: Gen. 224 (2002) 77.

[34] E. Zhao, Yu. Isaev, A. Sklyarov, J. J. Fripiat, Catal. Lett. 60 (1999) 173.

[35] P. T. Patil, K. M. Malshe, P. Kumar, M. K. Dongare, E. Kemnitz, Catal. Commun. 3 (2002) 411.

[36] V. C. F. Holm, G. C. Baily, U.S. Patent 3032599 (1962).

[37] M. Hino, K. Arata, J. Chem. Soc. Chem. Commun. (1980) 851.

[38] C. Guo, S. Yao, J. Cao, Z. Qian, Appl. Catal. A: Gen. 107 (1994) 229.

[39] D. Das, D. K. Chakrabarty, Energy Fuels, 12 (1998) 109.

[40] M. C. Clark, B. Subramaniam, Ind. Eng. Chem. Res. 37 (1998) 1243.

[41] R. B. Gore, W. J. Thomson, Appl. Catal. A: Gen. 168 (1998) 23.

[42] X. Xiao, J. W. Tierney, I. Wender, Appl. Catal. A: Gen. 183 (1999) 209.

[43] M. R. Gonzalez, K. B. Fogash, J. M. Kobe, J. A. Dumesic, Catal. Today, 33 (1997) 303.

[44] A. Sayari, Y. Yang, X. Song, J. Catal. 167 (1997) 346.

[45] A. Ghenciu, D. Farcasiu, Catal. Lett. 44 (1997) 29.

[46] D. R. Milbum, R. A. Keogh, R. Srinivasan, B. H. Davis, Appl. Catal. A: Gen. 147 (1996) 109.

[47] K. B. Fogash, R. B. Larson, M. R. Gonzalez, J. M. Kobe, J. A. Dumesic, J. Catal. 163 (1996) 138.

[48] H. Matsuhashi, H. Shibata, H. Nakamura, K. Arata, Appl. Catal. A: Gen. 187 (1999) 99.

[49] M. Y. Wen, I. Wender, J. W. Tierney, Energy Fuels, 4 (1990) 372.

[50] J. M. Grau, J. M. Parera, Appl. Catal. A: Gen. 162 (1997) 17.

[51] D. Farcasiu, J. Q. Li, S. Cameron, Appl. Catal. A: Gen. 154 (1997) 173.

[52] Y. -W. Suh, J. -W. Lee, H. -K. Rhee, Appl. Catal. A: Gen. 274 (2004) 159.

[53] T. Funamoto, T. Nakagawa, K. Segawa, Appl. Catal. A: Gen. 286 (2005) 79.

[54] X. Li, K. Nagaoka, R. Olindo, J. A. Lercher, J. Catal. 238 (2006) 39.

[55] A. Sassi, J. Sommer, Appl. Catal. A: Gen. 188 (1999) 155.

[56] G. D. Yadav, T. S. Thorat, Tetra. Lett. 37 (1996) 5405.

[57] G. D. Yadav, T. S. Thorat, P. S. Kumbhar, Tetra. Lett. 34 (1993) 529.

[58] G. D. Yadav, T. S. Thorat, Ind. Eng. Chem. Res. 35 (1996) 721.

[59] G. D. Yadav, A. A. Pujari, A. V. Joshi, Green Chem. 1 (1999) 269.

[60] G. D. Yadav, P. K. Goel, A. V. Joshi, Green Chem. 3 (2001) 92.

[61] G. D. Yadav, M.S.M. M. Rahuman, Appl. Catal. A: Gen. 253 (2003) 113.

[62] A. Sakthivel, N. Saritha, P. Salvam, Catal. Lett. 72 (2001) 225.

[63] R. A. Rajadhyaksha, D. D. Chaudhari, Ind. Eng. Chem. Res. 26 (1987) 1743.

[64] D. M. Ginosar, K. Coates, D. N. Thompson, Ind. Eng. Chem. Res. 41 (2002) 6537.

[65] J. Hu, K. R. Venkatesh, J. W. Tierney, I. Wender, Appl. Catal. A: Gen. 114 (1994) L179.

[66] R. Suresh, R. A. Rajadhyaksha, P. S. Kumbhar, J. Chem. Tech. Biotechnol. 62 (1995) 268.

[67] G. D. Yadav, A. A. Pujari, Green Chem. 1 (1999) 69.

[68] M. Hino, K. Arata, J. Chem. Soc. Chem. Commun. (1985) 112.

[69] J. Deutsch, V. Quaschning, E. Kemnitz, A. Auroux, H. Ehwald, H. Lieske, Catal. Lett. 88 (2003) 9.

[70] J. Deutsch, A. Trunschke, D. Muller, V. Quaschning, E. Kemnitz, H. Lieske, Top. in Catal. 13 (2000) 281.

[71] A. Trunschke, J. Deutsch, D. Muller, H. Lieske, V. Quaschning, E. Kemnitz, Catal. Lett. 83 (2002) 271.

[72] K. Biro, F. Figueras, S. Bekassy, Appl. Catal. A: Gen. 229 (2002) 235.

[73] J. Deutsch, A. Trunschke, D. Muller, V. Quaschning, E. Kemnitz, H. Lieske, J. Mol. Catal. A: Chem. 207 (2004) 51.

[74] G. D. Yadav, A. V. Pujari, Clean Techn. Environ. Policy, 4 (2002) 157.

[75] S. Ardizzone, C.L. Bianchi, V. Ragaini, B. Vercelli, Catal. Lett. 62 (1999) 59.

[76] C. L. Bianchi, S. Ardizzone, G. Cappelletti, Surf. Inter. Anal. 36 (2004) 745.

[77] C. Morterra, G. Cerrato, S. Ardizzone, C. L. Bianchi, M. Signoretto, F. Pinna, Phys. Chem. Chem. Phys. 4 (2002) 3136.

[78] Y. Sun, S. Ma, Y. Du, L. Yuan, S. Wang, J. Yang, F. Deng, F. -S. Xiao, J. Phys. Chem. B 109 (2005) 2567.

[79] G. D. Yadav, P. H. Mehta, Ind. Eng. Chem. Res. 33 (1994) 2198.

[80] T. S. Thorat, V. M. Yadav, G. D. Yadav, Appl. Catal. A: Gen. 90 (1992) 73.

[81] F. T. Sejidov, Y. Mansoori, N. Goodarzi, J. Mole. Catal. A: Chem. 240 (2005) 186.

[82] M. E. Quiroga, N. S. Figoli, U. A. Sedran, Chem. Eng. J. 67 (1997) 199.

[83] B. M. Reddy, P. M. Sreekanth, Synth. Commun. 32 (2002) 3561.

[84] G. D. Yadav, D. V. Satoskar, J. Am. Oil Chem. Soc. 74 (1997) 397.

[85] G. D. Yadav, J. J. Nair, J. Chem. Soc. Chem. Commun. (1998) 2369.

[86] G. K. Chuah, S. H. Liu, S. Jaenicke, L. J. Harrison, J. Catal. 200 (2001) 352.

[87] K. Tanabe, H. Hattori, T. Yamaguchi, Crit. Rev. Surf. Chem 1 (1990) 1.

[88] L. Grzona, N. Comelli, O. Masini, E. Ponzi, M. Ponzi, React. Kinet. Catal. Lett. 69 (2000) 271.

[89] G.D. Yadav, K.A. Bhirud, paper presented at the 49th Indian Chemical Engineering Congress, CHEMCON-96, Indian Institute of Chemical Engineers, Bharuch, Ankleshwar, 18- 21 Dec. 1996.

[90] T. Akio, H. Suzuka, Chem. Lett. 2 (1987) 423.

[91] A. de Klerk, Ind. Eng. Chem. Res. 44 (2005) 3887.

[92] X. Song, A. Sayari, Catal. Rev. Sci. Eng. 38 (1996) 329.

[93] G. D. Yadav, J. J. Nair, Micropor. Mesopor. Mater. 33 (1999) 1.

[94] K. Arata, Adv. Catal. 37 (1990) 165.

[95] J. R. Sohn, H. W. Kim, J. Mol. Catal. A: Chem. 52 (1989) 361.

[96] A. Clearfield, G.P.D. Serrete, A.H. Khazi-Syed, Catal. Today, 20 (1994) 295.

[97] T. Jin, T. Yamaguchi, K. Tanabe, J. Phys. Chem. 90 (1986) 4794.

[98] T. Yamaguchi, T. Jin, K. Tanabe, J. Phys. Chem. 90 (1986) 3148.

[99] W. R. Moser, U. S. Patent 5,466,646 (1995).

[100] W. R. Moser, J. Find, S. C. Emerson, I. M. Krausz, In Nanostructured Material, Ed. By J. Y. Ying, Academic Press, p.4.

[101] E. O. Hall, Proc. Phys. Soc. B, 64 (1951) 747.

[102] N. J. Petch, J. Iron Steel Inst. 174 (1953) 25.

[103] M. F. Ashby, Philos. Mag. A, 46 (1982) 737.

[104] R. Wurschum, S. Herth, U. Brossmann, Adv. Eng. Mater. 5 (2003) 365.

[105] P. Courty, C. Marcilly, B. Delmon, P.A. Jacobs, G. Poncelet (Eds.), Preparation of Catalysts, Elsevier, Amsterdam, 1976.

[106] T. Yamaguchi, K. Tanabe, Y. C. Kung, Mater. Chem. Phys. 16 (1986) 67.

[107] D. Farcasiu, J. Q. Li, Appl. Catal. A: Gen. 128 (1995) 97.

[108] A. Corma, V. Fornes, M. I. Juan-Rajadell, J. M. Lopez Nieto, Appl. Catal. A; Gen. 116 (1994) 151.

[109] J. M. Parera, Catal. Today, 15 (1995) 481.

[110] M. T. Tran, N. S. Gnep, G. Szapo, M. Guisnet, Appl. Catal. A: Gen. 171 (1998) 207.

[111] D. A. Ward, E. I. Ko, J. Catal. 150 (1994) 18.

[112] D. A. Ward, E. I. Ko, J. Catal. 157 (1995) 321.

[113] D. Tichit, B. Coq, H. Armendariz, F. Figueras, Catal. Lett. 38 (1996) 109.

[114] M. Signoretto, F. Pinna, G. Strukul, G. Cerrato, C. Morterra, Catal. Lett. 36 (1996) 129.

[115] C. Morterra, G. Cerrato, S. DiCiero, M. Signoretto, F. Pinna, G. Strukul, J. Catal., 165 (1997) 172.

[116] B. Li, R. D. Gonzalez, Ind. Eng. Chem. Res. 35 (1996) 3141.

[117] A. F. Bedilo, K. J. Klabunde, J. Catal., 176 (1998) 448.

[118] H. Armendariz, B. Coq, D. Tichit, R. Dutartre, F. Figueras, J. Catal. 173 (1998) 345.

[119] V. Parvulescu, S. Coman, P. Grange, V. I. Parvulescu, Appl. Catal. A: Gen. 176 (1999) 27.

[120] M. Signoretto, L. Oliva, F. Pinna, G. Strukul, J. Non-Crystalline Solids, 290 (2001) 145.

[121] S. Melada, M. Signoretto, S. A. Ardizzone, C. L. Bianchi, Catal. Lett. 75 (2001) 199.

[122] S. Melada, S. A. Ardizzone, C. L. Bianchi, Micropor. Mesopor. Mater. 73 (2004) 203.

[123] K. Arata, M Hino, N. Yamagata, Bull. Chem. Soc. Jpn. 63 (1990) 244.

[124] E. E. Platero, M. P. Mentruit, Mater. Lett. 14 (1992) 318.

[125] E. E. Platero, M. P. Mentruit, Catal. Lett. 30 (1995) 31.

[126] J. A. Wang, M. A. Valenzyela, J. Salmons, A. Vazques, A. Gracia-Ruiza, X. Bokhimi, Catal. Today, 68 (2001) 21.

[127] X. Bokhimi, A. Morales, O. Novaro, T. Lopez, R. Gomez, Polyhedron, 19 (2000) 22.

[128] S. Ardizzone, C. L. Bianchi, G. Cappelletti, F. Porta, J. Catal. 227 (2004) 470.

[129] R. Srinivasan, B.H. Davis, Catal. Lett. 14 (1992) 165.

[130] R.A. Comelli, C.R. Vera, J.M. Parera, J. Catal. 151 (1995) 96.

[131] K. Arata, M. Hino, in: M.J. Philips, M. Ternan (Eds.), Proceedings of the Ninth International Congress on Catalysis, Calgary, Vol. 4, 1988, p. 1727, Chemical Institute of Canada, Ottawa.

[132] Y. Sun, S. Ma, Y. Du, L. Yuan, S. Wang, J. Yang, F. Deng, F. - S. Xiao, J. Phys. Chem. 109 (2005**)** 2567.

[133] B.H. Davis, R.A. Keogh, R. Srinivasan, Catal. Today, 20 (1994) 219.

[134] B. Tyagi, K. Sidhpuria, B. Shaik, R. V. Jasra, Ind. Eng. Res. Chem. 45 (2006) 8643.

[135] C. Morterra, G. Cerrato, V. Bolis, Catal. Today 17 (1993) 505.

[136] C. Zhang, R. Miranda, B.H. Davis, Catal. Lett. 29 (1994) 349.

[137] G. Morterra, G. Cerrato, C. Emanuel, V. Bolis, J. Catal. 142 (1993) 349.

[138] M. Bensitel, O. Saur, J. C. Lavalley, B. A. Morrow, Mater. Chem. Phys. 19 (1988) 147.

[139] G. Morterra, L. Orio, V. Bolis, P. Ugliengo, Mater. Chem. Phys. 29 (1991) 457.

[140] F. R. Chen, G. Coudurier, J. F. Joly, J. C. Vedrine, J. Catal. 143 (1993) 616.

[141] C. Morterra, G. Cerrato, F. Pinna, M. Signoretto, G. Strukul, J. Catal. 149 (1994) 181.

[142] C. J. Brinker, G. W. Scherer, Sol-Gel Science: The Physics and Chemistry of Sol-Gel processing, Academic Press, Boston, 1990.

[143] D. A. Ward and E. I. Ko, Langmuir, 11 (1995) 369.

[144] N. T. Nga, V. T. Son, H. D. Chinh, L. T. Ngugen, Proceedings of the Eighth German- Vietnamese Seminar on Physics and Engineering, Erlangen, 03–08, April, 2005.

[145] J. Livage, M. Henry, C. Sanchez, Prog. Solid St. Chem. 18 (1988) 259.

[146] H. D. Gresser, P. C. Goswami, Chem. Rev. 89 (1989) 765.

[147] http://www.psrc.usm.edu/mauritz/solgel.html.

[148] E. Matijevic, Langmuir, 10 (1994) 8.

[149] A. Minesso, F. Genna, T. Finotto, A. Baldan, A. Benedetti, J. Sol-Gel Sci. and Tech. 24 (2002) 197.

[150] L. L. Hench, J. K. West, Chem. Rev. 90 (1990) 33.

[151] L. B. Hamouda, A. Ghorbel, J. of Sol-Gel Sci. Technol. 19 (2000) 413.

[152] A. A. Kline, T. N. Rogers, M. E. Mullins, B. C. Cornilsen, Lj. M. Sokolov, J. Sol Gel Sci. Tech. 2 (1994) 269.

[153] J. S. Park, H. J. Hah, S. M. Koo, Y. S. Lee, J. Ceramic Process. Res. 7 (2006) 83.

[154] J. Optoelectron. Adv. Mater. 7 (2005) 2727.

[155] K. Parida, V. Quaschning, E. Lieske, E. Kemnitz, J. Mater. Chem. 11 (2001) 1903.

[156] M. G. Cutrufello, U. Diebold, R. D. Gonzalez, Catal. Lett. 101 (2005) 5.

[157] R. Gomez, T. Lopez, J. Sol-Gel Sci. Technol.11 (1998) 309.

[158] P. S. Kumbhar, V. M. Yadav, G. D. Yadav, in: D. E. Leyden, W. T. Collins (Eds.), Chemically Modified Oxide Surfaces, Gordon and Breach, 1989, p. 81.

[159] K. Arata, M. Hino, Appl. Catal. 59 (1990) 197.

[160] L.M. Kustov, V.B. Kazansky, F. Figueras, D. Tichit, J. Catal. 150 (1994) 143.

[161] W. Hertl, Langmuir, 5 (1989) 96.

[162] F. Babou, G. Coudurier, J.C. Vedrine, J. Catal. 152 (1995) 341.

[163] T. Yamaguchi, T. Jin, T. Ishida, K. Tanabe, Mater. Chem. Phys. 17 (1987) 3.

[164] M. Waqif, T. Bachelier, O. Saur, J. C. Lavalley, J. Mol. Catal. A: Chem. 72 (1992) 127.

[165] P. Nascimento, C. Akratopoulon, M. Oszagyan, G. Coudurier, C. Travers, J. F. Joly, J. Vedrine, Stud. Surf. Sci. Catal. 75 (1993) 1185.

[166] S. Ardizzone, C.L. Bianchi, W. Cattagni, V. Ragaini, Catal. Lett. 49 (1997) 193.

[167] J. M. Kobe, M. R. Gonzalez, K. B. Fogash, J. A. Dumesic, J. Catal. 164 (1996) 459.

[168] F. Pinna, N. Signoretto, G. Strukul, G. Cerrato, C. Morterra, Catal. Lett. 26 (1994) 339.

[169] K.B. Fogash, G. Yaluris, M.R. Gonzalez, P. Ouraipry- van, D.A. Ward, E.I. Ko, J.A. Dumesic, Catal. Lett. 32 (1995) 241.

[170] J. H. Lunsford, H. Sang, S.M. Campbell, C. -H. Liang, R.G. Anthony, Catal. Lett. 27 (1994) 305.

[171] J. C. Lavalley, R. Anquetil, J. Czyzniewska, M. Ziolek, J. Chem. Soc., Faraday Trans. 92 (1996) 1263.

[172] H. Knozinger, in Handbook of Heterogeneous Catalysis, ed. G. Ertl, H. Knozinger and J. Weitkamp Weinheim, VCH, 1997, p. 707.

[173] R. W. Stevens Jr., Steven S. C. Chuang, B. H. Davis, Appl. Catal A: Gen. 252 (2003) 57.

[174] K. Shimizu, N. Kounami, H. Wada, T. Shishido, H. Hattori, Catal. Lett. 54 (1998) 153.

[175] Z. Hong, K.B. Fogash, J.A. Dumesic, Catal. Today 51 (1999) 269.

[176] C. Morterra, G. Cerrato, V. Bolis, S. D. Ciero, M. Signoretto, J. Chem. Soc., Faraday Trans. 93 (1997) 1179.

[177] C. Morterra, G. Cerrato, Phys. Chem. Chem. Phys. 1 (1999) 2825.

[178] S. X. Song, R. A. Kydd, J. Chem. Soc., Faraday Trans. 94 (1998) 1333.

[179] V. Adeeva, H.- Y. Liu, B.- Q. Xu, W. M. H. Sachtler, Top. in Catal., 6 (1998) 61.

[180] W. H. Bragg, W. L. Bragg, Proc. Roy. Soc. London, Ser. A, 88, 605 (1993) 428.

[181] Caili. Su, Junrong. Li, Dehua. He, Zhengxing. Cheng, Qiming. Zhu, Appl. Catal. A: Gen. 202 (2000) 81.

[182] B. D. Cullity, S. R. Stock, Elements of X-ray Diffraction, 3rd ed.; Prentice Hall: Upper Saddle River, NJ, 2001, p 388.

[183] S. J. Gregg, K. S. W. Sing, Adsorption, Surface Area and Porosity, 2nd ed; Academic Press: New York, 1982.

[184] W. K. Hall in Handbook of Heterogeneous Catalysis, Vol. 2, Ed. By G. Ertl, H. Knozinger, J. Weitkamp, Weinheim: VCH, p 692.

[185] O. Johnson, J. Phys. Chem. 52 (1955) 827.

[186] H. A. Benesi, J. Phys. Chem. 61 (1957) 970.

[187] R. Barthos, F. Lonyi, G. Onyestyak, J. Valyon, Solid State Ionics, 141 (2001) 253.

[188] V. Quaschning, A. Auroux, J. Deutsch, H. Lieske, E. Kemnitz, J. Catal. 203 (2001) 426.

[189] K. T. Wan, C. B. Khoun, M. E. Davis, J. Catal. 158 (1996) 311.

[190] B. H. Li, R. D. Gonzalez, Catal. Today, 46 (1998) 55.

[191] V. Adeeva, J. W. Haan, J. Janchen, G. D. Lei, G. Schunemann, L. J. M. van de Ven, W. M. H. Sachtler, R. A. van Santen, J. Catal. 151 (1995) 364.

[192] D. J. Coster, A. Bendada, F. R. Chen, J. J. Fripiat, J. Catal. 140 (1993) 497.

[193] H. Armendariz, C. S. Sierra, F. Figueras, B. Coq, C. Mirodatos, F. Lefebvre, D. Tichit, J. Catal. 171 (1997) 85.

[194] T. Riemer, D. Spielbauer, M. Hunger, G. A. H. Mekhemer, H. Knozinger, J. Chem. Soc. Chem. Commun. (1994) 1181.

[195] T. Riemer, H. Knözinger, J. Phys. Chem., 100 (1996) 6739.

[196] K. Zhang, C. Huang, H. Zhang, S. Xiang, S. Liu, D. Xu and H. Li, Appl. Catal. A: Gen. 166 (1998) 89.

[197] N. Kirthivasan, Heterogeneous Catalysis: Preparation, Characterisation and Application, Ph.D. (Chemistry) Thesis, University of Bombay, Bombay (Mumbai), Dec. 1995.

[198] K. Zhang, C. Huang, H. Zhang, S. Xiang, S. Liu, D. Xu, H. Li, Appl. Catal. A: Gen. 166 (1998) 89.

[199] A. Sakthivel, S.K. Badamali, P. Selvam, Micropor. Mesopor. Mater. 39 (2000) 457.

[200] S.K. Badamali, A. Sakthivel, P. Selvam, Catal. Lett. 65 (2000) 153.

[201] D. Farcasiu, J.Q. Li, Appl. Catal. A 175 (1998) 1.

[202] C. Su, J. Li, D. He, Z. Cheng, Q. Zhu, Appl. Catal. A: Gen. 202 (2000) 81.

[203] L. H. Thompson, L. K. Doraiswamy, Ind. Eng. Chem. Res. 38 (1999) 1215.

[204] C. P. Bezouhanova, Appl. Catal. A: Gen. 229 (2002) 127.

[205] T. Raja, A. P. Singh, A. V. Ramaswamy, A. Finiels, P. Moreau, Appl. Catal. A: Gen. 211 (2001) 31.

[206] Q. L. Wang, M. Yudao, Ji. Xingdong, Y. Hao, Q. Qin. J. Chem. Soc., Chem. Commun. 22 (1995) 2307.

[207] Q. L. Wang, M. Y. Dao, J.X. Dong, Y. Lio, Q. Qim, Chem. Lett. 7 (1996) 99.

[208] G. Kristin; A. Duncan. J. Mol. Catal. A: Chem. 109 (1996) 177.

[209] J. Kaur, K. Griffin, B. Harrison, I.V. Kozhevnikov., J. Catal. 208 (2002) 448.

[210] B. M. Choudary, M. Sateesh, M. L. Kantam, K. V. R. Prasad, Appl. Catal. A: Gen. 171 (1998) 155.

[211] M. A. Harmer, Q. Sun, Appl. Catal. 221 (2001) 45.

[212] R. V. Jasra, Y. Badheka, S. Muthusamy, Clay based catalytic process for the preparation of acylated aromatic ethers, US Patent application 10/341606, 2003.

[213] M. H. Valkenberg, C. de Castro, W.F. Holderich, Appl. Catal. 215 (2001) 185.

[214] http://www.thegoodscentscompany.com/data/rw10200031.html.

[215] A Fragrant Introduction To Terpenoid Chemistry, by Charles S. Sell, RSC publishing.

[216] C. Sell, in: D.H. Pybus, C.S. Sell (Eds.), The Chemistry of Fragrances, Royal Society of Chemistry, Cambridge, 1999, p. 81.

[217] J. Panten, H. - J. Bertram, H. Surburg, Chem. Biodivers. 1 (2004) 1936.

[218] H. H. Zeiss, M. Arakawa, J. Am. Chem. Soc. 76 (1954) 1653.

[219] R.E. Beyler, G. Ourisson, J. Org. Chem. 30 (1965) 2838.

[220] R. Ranganathan, U.R. Nayak, T.S. Santhanakrishnan, S. Dev, Tetrahedron 26 (1969) 621.

[221] J. Kula, A. Masarweh, J. Flavour Frag. 13 (1998) 277.

[222] R.R. Sobti, S. Dev, Tetrahedron 26 (1970) 649.

[223] S. Dev, Acc. Chem. Res. 14 (1981) 82.

[224] S.C. Bisarya, U.R. Nayak, S. Dev, Tetrahedron Lett. 28 (1969) 2323.

[225] A.R. Ramasha, Organic Preparation Procedure Int. 31 (1999) 227.

[226] X. Jingshi, Z. Guobin, C. Huizong, L. Yuelong, W. Hongming, Huaxue Tongbao (Chinese) 10 (2001) 647.

[227] U. R. Nayak, S. Dev, Tetrahedron, 8 (1960) 42.

[228] S. C. Bisarya, U. R. Nayak, S. Dev, B. S. Pandey, J. S. Yadav, H. P. S. Chawla, J. Indian Chem. Soc. 55 (1978) 1138.

[229] H. von Pechmann, C. Duisberg, Chem. Ber. 16 (1883) 2119.

[230] H. von Pechmann Chem. Ber. 17 (1884) 929.

[231] V. Singh, J. Singh, K. P. Kaur, G. L. Kad, J. Chem. Res. (S), 1997, 58-59.

[232] R. O'Kennedy, R. D. Thornes, Biology, Applications and mode of Action, John Wiley & Sons, Chichester, 1997.

[233] E. A. Gunnewegh, A. J. Hoefnagel, R. S. Downing, H. van Bekkum, Recl. Trav. Chim. Pays-Bas 115 (1996) 226.

[234] W. C. Sun, K. R. Gee, R. P. Haugland, Bioorg. Med. Chem. Lett. 8 (1998) 3107.

[235] J. Oyamada, C. Jia, Y. Fujiwara, T. Kitamura, Chem. Lett. (2002) 380.

[236] R. D. H. Murray, J. Medez, S.A. Brown, The Natural Coumarins: Occurrence, Chemistry and Biochemistry, Wiley, New York, 1982.

[237] A. E. Braun, A. G. Gonzalez, Nat. Prod. Rep. 14 (1995) 465.

[238] R. M. S. Celeghini, J. H. Y. Vilegas, F. M. Lancas, J. Braz. Chem. Soc. 12 (2001) 706.

[239] N. Cairns, L. M. Harwood, D. P. Astles, J. Chem. Soc. Perkin Trans. 1 (1994) 3101.

[240] W. H. Perkin, W. Sr. Henry, J. Chem. Soc. 28 (1875) 10.

[241] W.H. Perkin, J. Chem. Sot. 31 (1887) 388.

[242] J. R. Johnson, Org. React. 1 (1942) 210.

[243] A. Maercker, Org. Synth. 14 (1934) 270.

[244] I. Yavari, R. Hekmat-shoar, A. Zonouzi, Tetra. Lett. 39 (1998) 2391.

[245] A. Shockravi, H. Valizadeh, M. M. Heravi, H. A. Ghadim, J. Chem. Res. (S) (2003) 718.

[246] E. Knoevenagel, Chem. Ber. 29 (1896) 172.

[247] E. Knoevenagel, Ber. Dtsch. Chem. Ges. 37 (1904) 446.

[248] A. Song, X. Wang, K. S. Lam, Tetrahedron Lett. 44 (2003) 1755.

[249] R. L. Shriner, Org. React. 1 (1942) 1.

[250] M. R. Saidi, K. Bigdeli, J. Chem. Res. (S) (1998) 800.

[251] A. Russell, J. R. Frye, Org. Synth. 21 (1941) 22.

[252] E. C. Horning, in: Organic Synthesis Vol. III. Wiley, New York, 1955, p.281.

[253] F. W. Canter, F. H. Curd and A. Robertson, J. Chem. Soc. (1931) 1255.

[254] L. L. Woods, J. Sapp, J. Org. Chem. 27 (1962) 3703.

[255] A. K. Das Gupta, R. M. Chatterje, K. R. Das, B. Green, J. Chem. Soc. C (1969) 29.

[256] H. Appel, J. Chem. Soc. (1935) 1031.

[257] H. Valizadeh, A. Shockravi, Tetra. Lett. 46 (2005) 3501.

[258] E. V. O. John, S. S. Israelstam, J. Org. Chem. 26 (1961) 240.

[259] R. Sabou, W. F. Hoelderich, D. Ramprasad, R. Weinand, J. Catal. 232 (2005) 34.

[260] D. A. Chaudhari, Chem. Ind. (1983) 569.

[261] E. A. Gunnewegh, A. J. Hoefnagel, Herman van Bekkum, J. Mol. Catal. A: Chem. 100 (1995) 87.

[262] A. J. Hoefnagel, E. A. Gunnewegh, R. S. Downing, H. van Bekkum, J. Chem. Soc. Chem. Commun. (1995) 225.

[263] S. Frere, V. Thiery, T. Besson, Tetra. Lett. 42 (2001) 2791.

[264] T. S. Li, Z. H. Zhang, F. Yang, C. G. Fu, J. Chem. Res. (S) (1998) 38.

[265] S. Palaniappan, R. C. Shekhar, J. Mol. Catal. A: Chem. 209 (2004) 117.

[266] S. Palaniappan, C. Saravanan, V. J. Rao, Polym. Adv. Technol. 16 (2005) 42.

[267] G. P. Romanelli, D. Bennardi, D. M. Ruiz, G. Baronetti, H. J. Thomas, J. C. Autino, Tetra. Lett. 45 (2004) 8935.

[268] M. C. Laufer, H. Hausmann and W. F. Holherich, J. Catal. 218 (2003) 315.

[269] B. M. Reddy, V. R. Reddy, D. Giridhar, Synth. Commun. 31 (2001) 3603.

[270] J. C. R. Dominguez, G. Kirsch, Tetra. Lett. 47 (2006) 3279.

[271] A. de la Hoz, A. Moreno, E. Vazquez, Syn. Lett. (1999) 608.

Appendix

List of Papers published/ communicated

[1] Effect of Synthetic Parameters on Structural, Textural, and Catalytic Properties of Nano-Crystalline Sulfated Zirconia Prepared by Sol-Gel Technique.

Manish K. Mishra, Beena Tyagi and Raksh V. Jasra, *Industrial Engineering Chemistry Research,* 2003, 42, 5727-5736.

[2] Synthesis and Characterization of Nano-Crystalline Sulfated Zirconia by Sol-Gel method.

Manish K. Mishra, Beena Tyagi and Raksh V. Jasra, *Journal of Molecular Catalysis A: Chemical,* 223, 2004, 61-65.

[3] Solvent free Isomerisation of Longifolene with Nano-Crystalline Sulfated-Zirconia.

Beena Tyagi, **Manish K. Mishra** and Raksh V. Jasra, *Catalysis Communications,* 7, 2006, 52–57.

[4] Solvent Free Synthesis of 7-Substituted 4-Methyl Coumarins using Nano-Crystalline Sulfated-Zirconia. (Manuscript under preparation)

[5] Acylation of Aromatic Ethers using Nano-Crystalline Sulfated-Zirconia. (Manuscript under preparation)

[6] Solvent Free Isomerization of Longifolene to Tetraline Derivative using Nano-Crystalline Sulfated-Zirconia. (Manuscript under preparation)

Patents

[1] A catalytic process for the preparation of Isolongifolene.

R. V. Jasra, Beena Tyagi and **M. K. Mishra,**

US Patent No. – US 7,132,582 B2

Indian Patent No.- 0759/DEL/2003

US Application No.- 10/448457, PCT No.- PCT/IN03/00200

[2] A Process for Preparation of Sulfated Zirconia Catalyst.

R. V. Jasra, Beena Tyagi and **M. K. Mishra,**

Indian Patent No.- 1530/DEL/2003

Patent Appl. Field for US and PCT

[3] Green Catalytic Process for the Synthesis of Acetyl Salicylic acid.

R. V. Jasra, Beena Tyagi and **M. K. Mishra,**

Patent Appl. Field for US, PCT and India

Papers and posters presented in National and International Conferences

[1] Correlation of synthetic strategy with Structural and Textural features of Sulfated Zirconia.

Beena Tyagi, **M. K. Mishra** and R. V. Jasra

Paper presented at National Symposium on New Horizons in Heterogeneous Catalysis, (Chemical Engineering Department, Banaras Hindu University, Varanasi), February 22- 23, 2002

[2] Synthesis and Characterization of Nano-Crystalline Sulfated Zirconia by Sol-Gel method.

M. K. Mishra, Beena Tyagi and R. V. Jasra

Paper presented at 16^{th} National Symposium and 1^{st} Indo-German Conference on Catalysis, (Indian Institute of Chemical Technology, Hyderabad)**,** February 6- 8, 2003

[3] Nano-Crystalline Sulfated Zirconia for Catalytic Acylation of Anisole.

M. K. Mishra, B. Tyagi and R. V. Jasra

Paper presented at Third All Gujarat Research Scholars Meet 2003, Indian Chemical Society, (Chemistry Department, M.S. University, Vadodara)**,** February 23, 2003

[4] Structural and Textural properties of Nano-Crystalline Sulfated Zirconia prepared by Sol-gel technique at different pH.

M. K. Mishra, B. Tyagi and R. V. Jasra

Poster presented at Modern Trend In Inorganic Chemistry-2003, (Indian Institute of Technology-Bombay), December 15- 17, 2003

[5] Nano-Crystalline Zirconia using Sol-Gel Technique.

Beena Tyagi, **Manish K. Mishra** and R. V. Jasra

Paper presented at Seminar on Nano-materials and Nano-technology- The current scenario, (Department of Material Science, S.P. University, V. V. Nagar), March 11-12, 2005

[6] Greener Route for Isomerisation of Longifolene to Iso-longifolene using nano-crystalline Sulfated-zirconia solid acid catalyst.

Beena Tyagi, **Manish K. Mishra** and Raksh V. Jasra

Poster presented at Fourth All Gujarat Research Scholars Meet 2006, Indian Chemical Society, (Chemistry Department, M.S. University, Vadodara)**,** 23 January 2006

[7] Single step, Solvent free, Green Catalytic route for Coumarin synthesis using Nano-crystalline Sulfated-Zirconia.

Beena Tyagi, **M. K. Mishra** and R. V. Jasra

Paper presented at International Conference on Green Chemistry, organized under the series of Malaysian Chemical Congress (MCC 2006), (The Institut Kimia Malaysia (IKM, Malaysian Institute of Chemistry), Kuala Lumpur, Malaysia), September 19-21, 2006

[8] Single step, Solvent free, synthesis of 7-substituted 4-methyl coumarins over nano-crystalline sulfated-zirconia catalyst.

Beena Tyagi, **Manish K. Mishra** and Raksh. V. Jasra

Poster presented at International Conference on Materials for the new Millennium (MatCon 2007), (Department of Applied Chemistry, Cochin University of Science and Technology, Kochi, India), 1- 3 March 2007

[9] Isomerization of Longifolene to Tetraline Derivative over Nano-Crystalline Sulfated-Zirconia Prepared by One-Step Sol-Gel Method.

Beena Tyagi, **Manish K. Mishra** and Raksh. V. Jasra

Poster to be presented at 18^{th} National Symposium & Indo-US Seminar on Catalysis, organized by Catalysis Society of India, (Indian Institute of Petroleum, Dehradun), 16- 18 April 2007